Optimal Congestion Management

in

Deregulated Power System

A THESIS

Submitted in fulfillment of the requirement for the award of the degree of

DOCTOR OF PHILOSOPHY

in

ELECTRICAL ENGINEERING

By

Indu Batra

(901104002)

Under the Supervision of

Dr. Smarajit Ghosh

Professor, EIED

Electrical and Instrumentation Engineering Department

Thapar Institute of Engineering and Technology,

Patiala-147004, INDIA

Certificate

I hereby certify that the research work which is being presented in the thesis entitled "Optimal Congestion Management in Deregulated Power System" in partial fulfillment of the requirement for the award of degree of "Doctor of Philosophy" submitted in Department of Electrical and Instrumentation Engineering of Thapar Institute of Engineering and Technology, Patiala is an authentic record of my own work carried out under the supervision of Dr. Smarajit Ghosh and refers other research work, which are duly listed in the reference section.

The work presented in the thesis has not been submitted for the award of any other degree of this or any other university.

28-4-2021

(Indu Batra)
901104002

This is to certify that the above statement made by the candidate is correct and true to the best of my knowledge.

S. Ghosh
28-04-2021

(Dr. Smarajit Ghosh)
Professor
Department of Electrical and Instrumentation Engineering
Thapar Institute of Engineering and Technology,
Patiala-147004, INDIA

i

Dedicated to my family

Abstract

The structural arrangement and the operation of electric power industry have been completely changed since last few decades. This restructuring of the power industry has been done to initialize market competition among the various participants to enhance market profits. In a deregulated utility system the generation, transmission and distribution systems work as independent entities and it becomes hard for a system operator to maintain the synchronism among all the systems especially when congestion or line outage occurs. If the congestion persists for a long time, it may harm system security and reliability. Optimal congestion management must be done to alleviate the congestion so that market efficiency, stability and reliability do not alter. Numerous methods are available in art of literature to relieve the congestion. These are broadly classified as convention methods and optimization methods. The conventional optimization methods of congestion management perform perfectly if the objective function has good continuity and differentiability. As the congestion management is a nonlinear complex problem, the conventional optimization methods are not well suited as tuning of assessment weighing factors is a laborious task. The solution of nonlinear optimization problems completely confine on the weights, so the optimization methods are more appropriate for congestion management.

The main objective of the thesis is to develop an optimized congestion management methodology in restructured transmission system in order to optimize the congestion cost in deregulated environment. Thesis also aims to determine the optimized location of Unified Power Flow Controller (UPFC) device under severe line outages conditions.

The main purpose of the thesis is to develop the hybrid optimization algorithms, which can yield only the feasible solutions of congestion management cost over the entire searching area. To achieve this, two evolutionary chaotic particle swarm optimization algorithms namely; Improved Tent Map Adaptive Chaotic Particle Swarm Optimization (ITM-CPSO) and Twin Extremity Chaotic Mapped Particle Swarm Optimization (TECM-PSO) have been framed. The proposed algorithms; ITM-CPSO and TECM-PSO have been implemented to evaluate congestion management cost and rescheduled generation cost respectively. Required load management has also been incorporated

while evaluating overall congestion management cost in order to make the approach more robust, secure and reliable. Furthermore, ITM-CPSO has also been explored for finding suitable locations and parameter settings of Unified Power Flow Controller (UPFC) device for the most severe line outage cases of two test systems.

Till date sensitivity factor based approach has been widely used to decide the number of participating generators for the rescheduling process, but this sensitivity factor based approach requires a rigorous system operator efforts and computational time. To get rid of this, a modified Upstream Real Capacity Tracing (URCT) algorithm has been formulated and implemented in the thesis for deciding the number of participating generators for the rescheduling process. Use of URCT algorithm has an advantage of handling less and specific generator information resulting in less computational efforts and time. Furthermore, implementation of TECM-PSO algorithm to achieve near global optimal solution of rescheduled generation cost function has remarkably enhanced the profile of congestion management in terms of reduced amount of rescheduled generation with high computational efficiency rate and decreased rescheduled generation cost.

The main attribute of proposed algorithms are that these have evolved near global optimum solutions in every independent trial run which remain consistent even for large system as well. Rapid and consistent convergence, improved voltage profile, increased computational proficiency and best quality solutions are the major achievements of the research. Decrease in Net Generation Rescheduled (NGR) using proposed approach lies in the broad scale range of 1.15 to 1.61 and the percentage decrease in Rescheduled Generation Cost (RGC) has been achieved up to 32.4 % for most severe line outage cases. Also the percentage Convergence Mobility Rate (CMR) is found to be the highest among all comparative algorithms for each line outage case.

Acknowledgements

Firstly, I would offer my sincere and deepest gratitude to Almighty God for everything I achieved in my life.

I would like to express my sincere appreciation to my supervisor, **Dr. Smarajit Ghosh**, for his support and encouragement throughout my research work. His experience, strength, tenderness and willfulness, has taught me the ways, which are of immense help to me to take the decisions in my every endeavor.

I would like to express my gratitude to the Director of the Institute, **Professor Prakesh Gopalan** for his constant motivation and encouragement.

I am thankful to my doctoral committee members, **Dr. S. S. Bhatia**, Professor (School of Mathematics) and Dean of Academic Affairs (DoAA), **Dr. Maninder Singh**, Professor and Head Department of Computer Science and Engineering and **Dr. Gagandeep Kaur**, Associate Professor, Department of Electrical and Instrumentation Engineering, Thapar Institute of Engineering and Technology, Patiala, for their constructive comments and regularly ensuring the progress of my research work. I am also thankful to Dean of Research and Sponsored Projects (DoRSP) **Dr. Rafat Siddique** for his valuable guidance and blessing during this thesis work.

I am thankful to the chairman of Doctoral committee (HEIED, Ex-officio). I am also thankful to **Professor P. K. Bajpayee** and **Dr. O. P. Pandey** (Ex-DoRSP) for their cordial behavior.

I offer deepest regards to my family members for their love and moral support.

(Indu Batra)

Table of Contents

List of Figures

List of Tables

List of Acronyms

AAA	Artificial Algae Algorithm
AF	Auxiliary Function
ALO	Ant Lion Optimization
ATC	Available Transfer Capacity
CBM	Capacity Benefit Margin
CM	Congestion Management
CMR	Convergence Mobility Rate
CV	Cumulative Violation
DE	Differential Evaluation
FACT	Flexible Alternating Current Transmission
FFA	Firefly Algorithm
FPA	Flower Pollination Algorithm
GA	Genetic Algorithm
ITM-CPSO	Improved Tent Map Adaptive Chaotic Particle Swarm Optimization
LMP	Locational Marginal Price
LODF	Load Outage Distribution Factor
LSA	Load shedding amount
LUF	Line Utilization Factor
MFE	Main Function Evaluation
NGR	Net Generation Rescheduled
NOLL	Number of Overloaded Lines
NOVB	Number of Voltage Violated Buses
OPF	Optimal Power Flow
OTCDF	Outage Transfer Congestion Distribution Factor
PSO	Particle Swarm Optimization
PTCDF	Power Transfer Congestion Distribution Factor
RGC	Rescheduled Generation Cost

RGCF	Rescheduled Generation Cost Function
RPCF	Real Power Contribution Factor
SBO	Satin Bird Optimization
SOS	Symbiotic Organisms Search
TECM-PSO	Twin Extremity Chaotic Map Adaptive Particle Swarm Optimization
TGR	Total Generation Rescheduled
TRM	Transmission Reliability Margin
TTC	Total Transfer Capability
UPFC	Unified Power Flow Controller
URCT	Upstream Real Capacity Tracing
VSI	Voltage Stability Index

List of Variables and Symbols

P_{ij}^{0}	Base case real power flow between buses $i-j$
$P_{ij}^{\max}$	Maximum allowed real power flow between buses $i-j$
ΔP_{ij}	Change in real power flow between buses $i-j$
ΔP_{sb}	Change in real power transaction between seller and buyer buses
$P_{\max(ij-sb)}$	Maximum allowable transaction amount between seller (s) and buyer (b) bus constrained by line flow limits from bus i to j
P_i	Real power of the i^{th} bus
Q_i	Reactive power of the i^{th} bus
P_{ij}	Real power flow between buses $i-j$
Q_{ij}	Reactive power flow between buses $i-j$
V_i	Voltage magnitude at bus i
V_j	Voltage magnitude at bus j
Y_{ij}	Magnitude of the ij^{th} element of Y_{bus} matrix
Y_{sh}	Shunt admittance
δ_i	Load angle at bus i
δ_j	Load angle at bus j
θ_{ij}	Angle of the ij^{th} element of Y_{bus} matrix
$P_{gi}^{\min}$	Lower bound on the active power output from the i^{th} generator
$P_{gi}^{\max}$	Upper bound on the active power output from the i^{th} generator
$Q_{gi}^{\min}$	Lower bound on the reactive power output from the i^{th} generator
$Q_{gi}^{\max}$	Upper bound on the reactive power output from i^{th} generator

$V_{gi}^{\min}$	Lower voltage magnitude bounds for the i^{th} bus
$V_{gi}^{\max}$	Upper voltage magnitude bounds for the i^{th} bus
$\Delta P_n^{k\max}$	maximum allowable transaction from bus i to j
P_{mn}^0	Pre outage power flows from bus $m-n$
P_{nm}^0	Pre outage power flows from $n-m$
$P_{ij,mn}$	Post outage line flows between buses $m-n$
$\Delta P_{ij,mn}$	Change in the line flows $i-j$ due to outage of line $m-n$
$\Delta P_{ij}^{\max}$	Change in the post contingency maximum flow limit on the line $i-j$ due to outage of line $m-n$
$\Delta P_n^{ij,mn}(\max)$	Maximum value of change in post outage line flows between buses $i-j$ due to outage of line $m-n$
$C_{g_{ip}}\left(\Delta P_{gi}{}_p\right)$	Incremented or decremented bids submitted by i_p^{th} generator or generator company, willing to adjust real power outputs to relieve the congestion
$\Delta P_{gi}{}_p$	Adjustment in real power by i_p^{th} generator in MW
Npg	Total number of participating generators which are decided using URCT algorithm
Ng	Total number of generators
Ns	Total number of load buses selected for load shedding
$C_{j_{lb}}^{bid}$	Load shedding bids submitted by j_{lb}^{th} load or distribution company, willing to shed the load
$\Delta P_D^{j_{lb}}$	Adjustment in the load at j_{lb}^{th} bus
i_p	Participating generator number
k_g	Non-participating generator number
m_{l_b}	Individual load at each bus

j_{lb}	Load shed bus number
$P^0_{gi_p}$	Active power generated by i_p^{th} generator as determined by the system operator
$P^0_{Dm_{lb}}$	Active power consumed by the determined $m_{l_b}{}^{th}$ load by the system operator
$P_{gi_p}{}^{resh}$	Active power generated by the i_p^{th} generator after the process of rescheduling
P_{gk_g}	Active power generated by the k_g^{th} generator
$P^0_{Dm_{lb}}$	Active power consumed by the m_{lb}^{th} load as determined by the system operator
ND	Number of loads
P_L	Power Loss in MW
Nsv	Number of specified inequality constraints on state variables
S_{Li}	MVA power flow of PQ buses
$S_{Li\max}$	Maximum MVA limit of PQ buses
N_{PQ}	Number of PQ buses
V_{Li}	Load bus voltage of i^{th} PQ bus
$V_{Li\min}$	Minimum value of voltages at i^{th} PQ bus
$V_{Li\max}$	Minimum value of voltages at i^{th} PQ bus
Q_{Gi}	Reactive power generation limit of i^{th} PV bus in MVAR
$Q_{Gi\min}$	Minimum reactive power generation of i^{th} PV bus in MVAR
$Q_{Gi\max}$	Maximum reactive power generation limit of i^{th} PV bus
P_{Gi}	Real power generation of i^{th} PV bus in MW
$P_{Gi\min}$	Minimum real power generation of i^{th} PV bus in MW

$P_{Gi\max}$	Maximum real power generation of i^{th} PV bus in MW
P_{DLi}	Load bus power of i^{th} PQ bus
$P_{DLi\min}$	Minimum value of load bus power of i^{th} PQ bus
$P_{DLi\max}$	Maximum value of load bus power of i^{th} PQ bus
N_B	Number of buses
N_{B-1}	Number of buses except slack bus
P_{ij}	Real power flow in the line $i-j$
P_j	Real power of j^{th} bus at receiving end
Q_j	Reactive power of j^{th} bus at receiving end
X	Line reactance
u	Control variable
x	State variable
$u_{\min}$	Minimum value of control variable
$u_{\max}$	Maximum value of control variable
$\left\|P_{i-j}^{gross}\right\|$	Total power flow from through node $i-j$
α_i^u	Set of nodes supplying power directly to node i
P	Vector of nodal power flows
P_G	Vector of nodal power generations
α_i^d	Set of nodes supplied directly from node i
A_u	Upstream distribution matrix
$CF_{i-j,k}^G$	Real power contribution factor (RPCF) and is the flow in the line $i-j$ due to k^{th} generator
ΔP_k	Change of power flow change on the target branch k
ΔP_j	Change in load power at bus j
S_{kj}	Sensitivity factor of target branch k due to change in load power at bus j

ΔP_d	Minimum reduction of power flow on the congested branch
$u_{cL}^{\max}$ and $u_{cL}^{\min}$	Acceptable ranges of load curtailment expressed by the customer
u_{CLj}^{req}	Required amount of load adjustment at bus j
η	Number of iterations for which stopping criterion applies
μ_S	Sensitivity index
μ_{cL}	Load curtailment index
μ_{IC}	Incentive cost index
ω_L	Overall index
P_{besti}	Local best position of the i^{th} particle
G_{best}	Global best position
$r_1,\ r_2$	Random variables between 0 and 1
w	Inertia weight
$w_{\max}$	Maximum value of the inertia weight and is chosen 0.9
$w_{\min}$	Minimum value of the inertia weight and is chosen 0.4
V_F	Final value of velocity for each particle
$V_{\max}$	Maximum value of velocity
$V_{\min}$	Minimum value of velocity
k	Current iteration
$k_{\max}$	Maximum number of iterations
$r_1(k), r_2(k),$ $C_r(k)$	Deterministic variables displaying chaotic dynamics for k^{th} iteration
c_1	Cognitive acceleration coefficient
c_2	Social acceleration coefficient
$C_r x_i^k$	i^{th} chaotic sequence variable for k^{th} iteration and has been distributed in range [0, 1]
$C_r x_i^0$	Initial value of chaotic sequence and is chosen 0.01

λ	Driving parameter which controls the behavior of chaotic sequence and $0 \le \lambda \le 4$.
x_i^k	Position of the i^{th} particle at k^{th} iteration among intervals $(x_{\min,i}, x_{\max,i})$
x_{best}^g	Best optimal solution attained until iteration ends
Xc_{ri}^k	Chaotic local search point
$\in$	Constraint handling the linear combination of x_i^k and x_{best}^g and lies between [0,1]
$x_{best,d}^k$	The best individual in the k^{th} iteration for d^{th} dimension
$\bar{x}_{best,d}$	Mean value of the best individuals
X_{opt}	Global optimal solution
f_{opt}^g	Global optimal fitness
I_c	Iteration count
$I_c^{\max}$	Maximum iteration count
E_{sh}	Ideal shunt voltage source magnitude
E_{se}	Ideal series voltage source magnitude
V_{se}	Series voltage source magnitude
V_{sh}	Shunt voltage source magnitude
I_{se}	Current injections of series branch
I_{sh}	Current injections of shunt branches
Z_{se}	Impedances of the series branch
Z_{sh}	Impedances of the shunt branch
P_k, P_m	Active powers at bus k and bus m terminal respectively
Q_k, Q_m	Reactive powers at bus k and bus m terminal respectively

P_{dk} , Q_{dk}	Active and reactive power load at bus k respectively
P_{dm} , Q_{dm}	Active and reactive power load at bus m respectively
P_{gk} , Q_{gk}	Active and reactive power generation at bus k respectively
P_{gm} , Q_{gm}	Active and reactive power generation at bus m respectively
θ_{se}	Series voltage source angle
θ_{sh}	Shunt voltage source angle
θ_{ij}	Angle of the ij^{th} element of Y_{bus} matrix
P_{sh}	Real power delivered to shunt converter
P_{se}	Real power required by the series converter
ΔP_g	Power mismatch between the shunt and series converters
V_k , V_m	Voltages at bus k and m respectively
G_{kk}	Self-conductance of bus k
G_{km}	Mutual conductance between buses k and m
B_{km}	Mutual susceptance between buses k and m
G_{sh}	Shunt conductance
B_{sh}	Shunt susceptance
B_{kk}	Self susceptance of bus k
G_{mm}	Self-conductance of bus m
G_{mk}	Mutual conductance between buses m and k
B_{mk}	Mutual susceptance between buses m and k
B_{mm}	Self susceptance of bus m
Nl	Number of transmission lines
S_l	Apparent power in the line l
$S_{l\max}$	Maximum apparent power in the line l
p , q	Coefficients to compensate more or less the overloaded transmission lines

	and voltage variations of buses and are chosen 2
w_l, w_m	Weight coefficients and have index values for 10% voltage difference and 100% branch loading respectively
V_m, V_m^{ref}	Existing voltage magnitude and reference voltage magnitude of m^{th} bus respectively
C_g^+	Incremented bids submitted by generators to adjust their loads in \$/MWh
C_g^-	Decremented bids submitted by generators to adjust their loads in \$/MWh
V_i^{k+1}	Velocity of the i^{th} particle at $k+1^{th}$ iteration
V_i^k	Velocity of the i^{th} particle at k^{th} iteration
P_i^k	Position of the i^{th} particle at k^{th} iteration
P_i^{k+1}	Position of the i^{th} particle at $k+1^{th}$ iteration
ΔP_{Dj}	Amount of load shedding at j^{th} bus
RGC_i	Rescheduling generation cost of generator i
$\in_T$	Threshold value for the standard deviation at which stopping criterion applies
n_P	Total number of particles
n_D	Total number of dimensions

Chapter 1: Introduction

1.1 Background

Power industries across the world are subjected to a rapid and radical change in their operational model since last few decades. This power sector market transformation was driven due to many reasons. Among them political factors, financial crises, rapid technological advancement and the globalization of the world economy were the main reasons. Most of the traditional vertical utility system has now been restructured and replaced by generator companies, transmission companies and distribution companies, which work independently to achieve higher efficiency and better utilization of power. Initiation of restructuring process has been done by uncoupling of traditional vertical utility system. As a result, transmission and distribution activities have been separated from the generation and transmission activities respectively. Re-establishment of rules and economic incentives set by governing authorities to manage and drive the electric power industry is basically the deregulation. Deregulation is done to improve the public finances through sale of state assets and elimination of subsidies gradually. Moreover, improved performance of power entities, lower consumer tariffs can be achieved by restructured power sectors. Independent system operator, generation companies, transmission companies, distribution companies, retail energy service companies and customers are the main entities of deregulated environment. The structures of vertical utility system and deregulated power system and the interconnection between various entities of both the systems and regarding power, money and information flow is shown in Fig.1.1.

The earlier vertical arrangement of the power industry had a single utility control on generation, transmission and distribution of electrical energy. So, vertical integrated utilities were in fact the monopoly utilities in their area of operation. This monopoly scenario was unable to offer any incentive for its efficient operation. While in government linked public utilities, over manning and bad resource management were the main reasons of their poor performance. Therefore, the economic reformers encouraged the need of competitive market world for electric energy with an aim that the new restructured world of electrical power would offer a good range of benefits for both customers and private entities. Reductions in electricity prices, good service quality and more choices for the

customers for choosing retailers were considered as the major benefits for promoting the necessity of restructuring of traditional market structure.

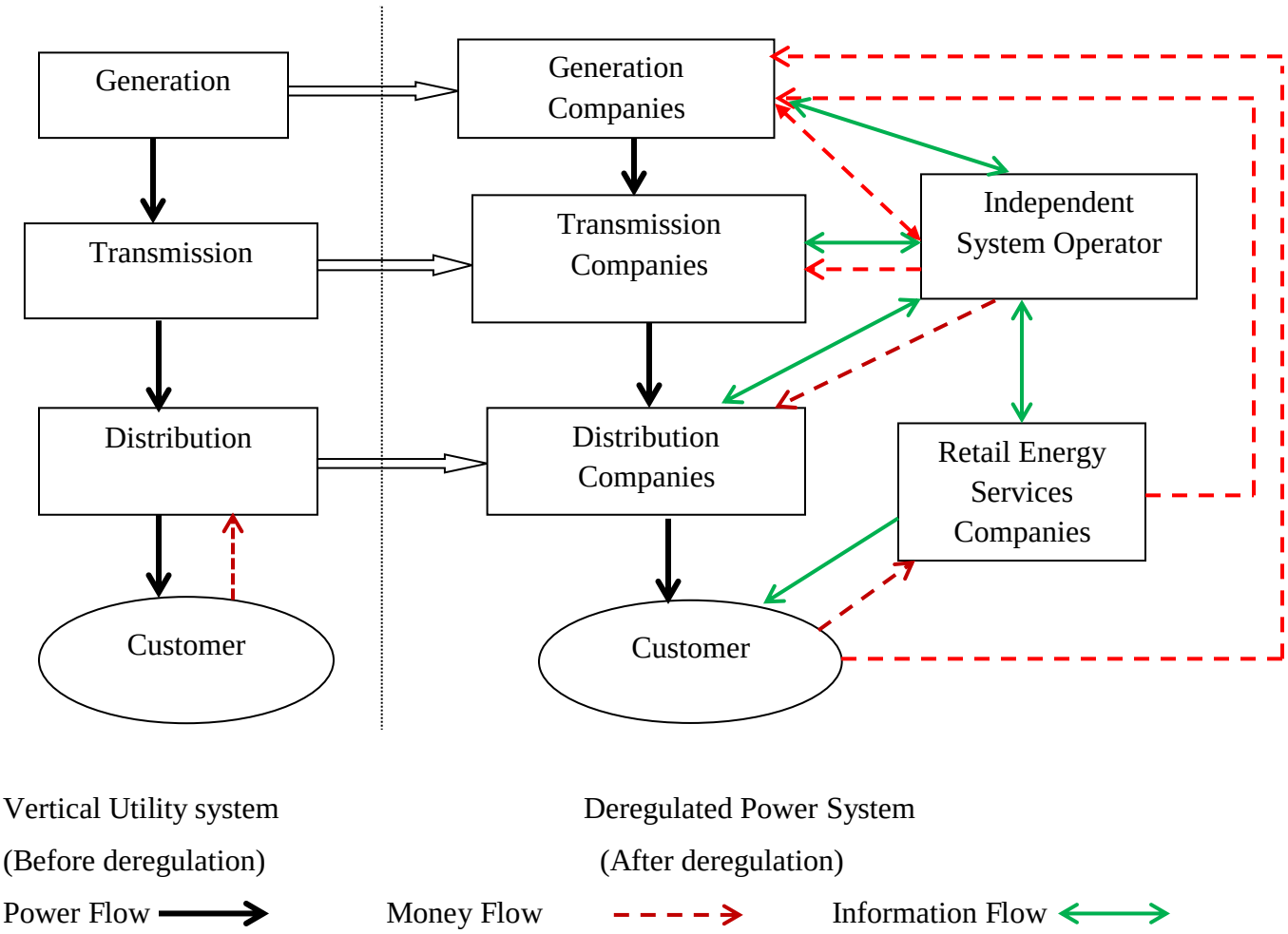

Figure 1.1: Structure and interconnection between various entities of vertical utility system and deregulated power system regarding power, money and information flow

From Fig. 1.1, it is clear that individual entity in deregulated power system work independently and independent system operator has to take care of overall deregulated system security, power delivery, pricing, quality assurance and economic efficiency. In deregulated power system, every company operates near its physical limits to increase the economic benefits due to which chances of voltage violations and overloading increase to a great extent. The existence of such violations results in congestion. If congestion persists for long duration, it may cause cascade outages with uncontrolled load loss. Hence, it becomes important for service operation to manage congestion with proper time

management. In real time scenario of deregulated environment, lack of required available transmission capacity to deal with all committed purposes simultaneously is actually the congestion. Congestion Management (CM) system basically involves the determination of suitable generation patterns, which do not violate the line flow limits. In deregulated power system, efficient congestion management system is mandatory to work regularly and efficiently as it directly affects the profit of market participants.

1.2 Objectives of Research

The research aims to derive a novel and optimized methodology towards CM cost problem in deregulated power system. The following objectives have been fulfilled in the research.

- To study various aspects in connection with power system deregulation and congestion management techniques.
- To develop an optimized congestion management methodology in restructured transmission system.
- To optimize the congestion cost in deregulated environment and to determine the optimized location of FACTS devices.
- To compare the developed technique with the existing techniques.

1.3 Scope of the Research

To meet the above four objectives, optimized research has been carried out and is detailed below:

1. Under first objective intensive and laborious literature survey has been carried out to deeply analyze the concepts of deregulation and CM methodologies, which are detailed in Chapter 2.
2. To meet second objective, a dual objective sensitivity based algorithm has been developed to measure both the static and dynamic ATC values and is described in Chapter 3. The evaluated sensitivity factors have been further utilized to allocate the optimal location of UPFC.
3. A novel approach of congestion cost management (including load management) employing Improved Tent Map adaptive Chaotic PSO (ITM-CPSO) algorithm has been introduced and applied to two test systems, as discussed in Chapter 4. Modified formulation of URCT

algorithm has also been done in Chapter 4 to determine the exact and accurate number of participating generators for alleviating contingencies.

4. Furthermore, ITM-CPSO (introduced in Chapter 4) has also been explored for evaluating optimal line locations of UPFC to achieve third objective as mentioned in Chapter 5.
5. To achieve fourth objective introduction and implementation of a novel hybrid TECM-PSO algorithm has been introduced to solve complex rescheduling generation cost problem, which has been designed to yield only feasible solutions over the entire searching area. The developed technique has also been compared with various algorithms stated in literature as explained in Chapter 6.

1.4 Contribution of the Research

The thesis contributes essentially to optimize the CM cost problem in the deregulated power system for its near global optimal solution. This thesis is significant in many aspects. Firstly, a deep and rigorous study of various aspects of deregulation and CM has been done. Secondly, deterministic approach has been used to determine the ATC values of various lines of the test system. Optimal placement of UPFC has also been done for security enhancement of power system. The most significant aspect of the thesis is that two intelligently trained chaotic PSO optimization based algorithms have been introduced, implemented and compared for their performance to optimize the overall CM. The main feature of the proposed developed optimization methodologies is that there is a need of optimizing very few control parameters and even out of them, some are adaptive, which has made the optimization procedures best suited for the nonlinear problems like congestion relieving.

1.5 Organization of Thesis

Chapter 1 has demonstrated the reasons behind the need of deregulated power system. Structures of both vertical utility and deregulated power system have also been illustrated showing interconnection between various entities of respective systems. Objectives, scope, overview and contribution of the research have also been highlighted in the chapter.

Chapter 2 presents an extensive literature review on deregulation and CM methodologies. The literature review presents both the conventional and evolutionary optimization methods of CM.

Sufficient and important discussions are made under both methods. Literature analysis, research gaps and contribution of thesis is described in detail.

Chapter 3 presents a deterministic and sensitivity based approach towards evaluation of static and contingency ATC values for different types of transactions. Sensitivity curves obtained are further utilized to identify most suitable location for placing UPFC for the respective transactions.

Chapter 4 demonstrates a novel hybrid approach using Improved Tent Map adaptive Chaotic PSO (ITM-CPSO) algorithm toward security constraint optimal CM cost evaluation. Load management has also been incorporated. Novel formulation for estimating participation factors of the various generators using Upstream Real Capacity Tracing (URCT) algorithm has been introduced and implemented. This chapter examines the performance of proposed approach quantitatively and qualitatively. Security constraints have been incorporated while evaluating overall congestion cost function.

Chapter 5 presents the implementation of ITM-CPSO algorithm (detailed in Chapter 4) for allocating UPFC optimally for stability enhancement. $N-1$ Contingency ranking process has also been done for different line outage cases of chosen test systems. Improved voltage profiles of most severe line outage cases after UPFC placement for both the test systems have also been found. Simulation results have been compared with various evolutionary algorithms which are stated in art of literature.

Chapter 6 introduces a novel hybrid chaotic PSO algorithm. The novel algorithm has also been applied to evaluate overall rescheduled generation cost function to optimally manage the congestion. The algorithm has been designed in such a manner that only feasible solutions are obtained over the entire search region. Three test systems have been used for results validation.

Chapter 7 summarizes the thesis by concluding all the important findings. Information and suitable suggestions about future scope of the research are also illustrated in the chapter.

Chapter 2: Literature Survey

This chapter describes the literature analysis of the research methods carried out by the various researchers so far in the field of deregulation and congestion management in power system. An exhaustive literature survey has been done on two areas: a) Power System Deregulation and b) Congestion Management (CM) as shown in subsequent section/subsections. The observations from the work done by the researchers have also been illustrated separately.

2.1 Survey on Power System Deregulation

Ferrero ***et al.*** (1997) demonstrated that in deregulated environment all power transactions are made on the basis of price rather than cost. Optimization in their work was done using game theory to simulate the decision making process of price in deregulated environment. Guan and Luh (1999) proposed two promising bidding strategies for power suppliers in deregulated power industry. In the first approach, game theoretic method was proposed to aim at bidding and self-scheduling of a utility company. In the second approach, utility problem was solved using Lagrangian relaxation. Arrillaga ***et al.*** (2000) provided the illustration of various methods available to achieve power quality solutions in deregulated environment. Voltage sags and harmonic distortion were the main factors which were considered in the approach. Donde ***et al.*** (2001) introduced the concept of path sensitivities and the main contribution of their work was to illustrate the importance of automatic generation control in deregulated environment. Bhattacharya ***et al.*** (2001) provided the details of deregulation of the electricity supply industry, overview of economic power system operation, power system operation in private competitive environment, open access transmission and issues related to pricing and ancillary services management in their book chapters**.** Details of cost of energy nationwide and region wise in deregulated power system were illustrated by Campbell (2001). Lal (2001) illustrated detailed information of deregulation and related performance issues. Rashidi-Nejad ***et al.*** (2002) investigated a combined deterministic and stochastic criterion for assessing operating reserve in deregulated power system. Shikoski ***et al.*** (2003) introduced new infra technologies in the deregulated power sector. They proved that infra technologies could potentially increase the benefits or decrease the operational costs. The importance of potential economic impact

and measurement standardization were also discussed. Various key issues related to deregulated power market judging function were illustrated by Rahimi and Sheffrin (2003).

Ni ***et al.*** (2004) presented an integrated algorithm incorporated with risk management for deregulated environment. They proved the risk management procedure as an effective way to reduce profit variances and bidding risks. Androulidakis ***et al.*** (2005) analyzed the technical considerations and main trends required for the power system restructuring by focusing on the design of local and wide area controls supported by suitable information systems. They proved that deregulation certainly affect the normal operation of a power system in accordance to market requirements. Hira ***et al.*** (2005) tried to improve the participation levels in regulatory decision making through a large variety of institutional mechanisms for participation. Aggarwal ***et al.*** (2009) reviewed many price forecasting methodologies in deregulated power system. Applications of various models to different electricity market structures were also presented. Quantification of various research price forecasting models were also considered. Vijay and Verma (2010) discussed the technical and economic issues related to reliability of a restructured power system. They advocated that power flow tracing algorithm is a powerful approach for reliable operation of restructured power system.

Georgilakis and Vernados (2011) proved that the operation of transmission network is always near to its physical limits under deregulated environment. They demonstrated advanced power electronics based technique to evaluate transmission capability of the transmission system. Dhanalakshmi ***et al.*** (2011) emphasized on Price Based Unit Commitment (PBUC) approach for generators scheduling in deregulated power system. They also presented a survey on various unit commitment based market models. Shukla and Tampy (2011) presented a review on the structural arrangement and competitiveness of the wholesale power market. They suggested that market power of firms may be part of the reason for the increase in electricity prices. Karthikeyan ***et al.*** (2013) presented a detailed review on market power and related indices, which were used in market power analysis. They also illustrated various aids and software tools for analyzing the market power. Kumar and Ramana (2013) reviewed the different control techniques on design of load frequency controllers in deregulated environment. Both classical and modern feedback controllers along with their relative advantages and disadvantages were discussed. FACT devices and energy storage devices in the investigation of load frequency control problem were also analyzed. Pal ***et al.*** (2016) highlighted the

major challenge faced by developing countries for the requirement of constant power supply for deregulation purpose. They demonstrated the need, driving principles and prospectus of deregulation in developing nations. Hota ***et al.*** (2016) explained the detailed procedure for obtaining power tracing for the real and reactive power transmitted between generators and loads in the deregulated environment. They utilized the proportional sharing method to trace out the individual power drawn by the different load in a common loss line.

Iqbal ***et al.*** (2018) provided a comprehensive survey about the reliability of generation, transmission and distribution system in deregulated power system. Moreover, various reliability indices and related soft computing tools were also illustrated in detail. Gultom (2019) examined the effect of the governance structures on the technical efficiency of investor-owned utilities. The results indicated that the use of market transactions had a significant negative effect on technical efficiency of investor-owned utilities.

2.2 Survey on Congestion Management (CM)

Transmission CM is referred to the deeds that the transmission system operator should perform to maintain all system constraints within their specified limits as mentioned by Shahidehpour ***et al.*** (2002). Bompard ***et al.*** (2003) provided details of different CM techniques used in various market structures across the world. Pillay ***et al.*** (2015) and Yusoff ***et al.*** (2017) described various approaches and algorithms related to congestion relieving in overhead lines. Based on literature studies, it has been analyzed that the CM methods have been broadly divided into two categories namely; a) conventional methods and b) optimization/expert methods and both are explained in following subsections.

2.2.1 Survey on Conventional Methods of CM

- **ATC based CM**

ATC measurement is the basic and traditional method of CM. The amount of surplus power over all committed usages is ATC. Mathematical expression of ATC is shown in Eq. (2.1).

$$ATC = TTC - TRM - (ETC + CBM) \quad (2.1)$$

OPF (Kumar ***et al.***, 2004; Hur ***et al.***, 2003; Hamound,2000), Continuation power method (Ejebe ***et al.***, 1998; Ou ***et al.***, 2002; Flueck ***et al***.,1996), PTCDF and LODF (Ilic ***et al.,***1997; Yadav and Sharma, 2013; Yuan-Kang, 2007) are the main methods used for ATC computation. Tuglie ***et al.*** (2000) demonstrated dynamic ATC evaluation using static approach under deregulated environment. Ou and Singh (2002) evaluated ATC along with its various margins. ATC enhancement using FACT devices was demonstrated by (Xiao ***et al.*** 2003; Mustafa and Bawazir, 2013). ATC evaluation along with energy transaction scheduling under open market environment was demonstrated by Yu ***et al.*** (2003). Selvi ***et al.*** (2007) implemented Genetic Algorithm (GA) for total transmission capacity evaluation. Liu ***et al.*** (2007) presented a CM approach using optimal resource allocation methodology. The main feature of the approach was that it always allocated the near feasible solution during the iterations and required very small transaction information. Shayesteh ***et al.*** (2009) proposed contingency incentive-based demand response programs for ATC enhancement. Rao ***et al.*** (2016) had presented a current based modeling method for evaluation of ATC values. FACT controllers had also been optimally located for ATC enhancement and they proved that UPFC was the most effective device for the ATC enhancement as compared to the remaining FACTS controllers.

- **Nodal Pricing based CM**

Nodal prices are also called Locational Marginal Prices (LMP). Four methods were demonstrated by Pillay ***et al.*** (2015) to compute LMP. In the first method, the system could be made to operate after 1 MW use and before 1 MW use. The difference in the two costs of operation then gave the LMP. Secondly, LMP was computed on the basis of sensitivity factors of the marginal generators. Thirdly, LMP was evaluated from Lagrange multipliers from the OPF. In fourth method, LMP was obtained from transposed Jacobian matrix. Yamin and Shahidehpour (2003) achieved the optimal CM and power balancing control scheme by utilizing nodal prices. Milano ***et al.*** (2003) proposed a novel voltage security constraint OPF incorporated with LMP approach for CM. Overbye ***et al.*** (2004) proposed both DC and AC, OPF methods for LMP computation. Alomoush (2005) had introduced some performance indices in the social welfare problem to compare different dispatch options to obtain the considerable increase in welfare and remarkable reduction in overall congestion cost. Sood ***et al.*** (2007) had proposed a novel model which dispatched the pool demand combined with contracts. Price (2007) worked on redesigning, implementation of unit commitment and LMP

approaches for CM. Orfanogianni and Gross (2007) proposed a general formulation for LMP by making explicit use of the ATC at various nodes.

- **Sensitivity Methods based CM**

Bompard ***et al.*** (2003) presented various sensitivity CM schemes for short term operation. They also compared the techniques used for short term operation. Niimura ***et al.*** (2003) introduced simple and transparent indices for CM and load curtailment was also carried to get the complete congestion relieving solution. Kumar ***et al.*** (2004) proposed power rescheduling processes for CM. Congestion costs in all of the cases in the proposed method were found to be quite less compared with those obtained with DC models. Chung ***et al.*** (2004) proposed a novel sensitivity approach to improve ATC. Most sensitive generators for rescheduling and loads for load curtailment were chosen by Singh ***et al.*** (2006) for CM. Conejo and Bertrand (2006) proposed an OPF based constraints approach to alleviate voltage instability, which was demonstrated on IEEE 24 bus system. Voltage stability index based CM was demonstrated by (Yesuratnam ***et al.,*** 2007; Yang ***et al.,*** 2012). A novel voltage stability index based load shedding approach was demonstrated by Kanimozhi ***et al.*** (2014).

- **FACT Devices based CM**

Singh and David (2001) demonstrated the importance of series controllers as well as the shunt controllers for CM. Verma ***et al.*** (2001) developed an efficient method for the determination location of UPFC with static features for CM. Soto and Green (2002) compared the topologies of high power rated converters for implementation of FACT controllers. From the comparison, it had been observed that the chain converter was most suitable for the implementation of a static synchronous series compensator. They also showed the impact of FACT controllers on the total energy consumption of the system. Fernandez ***et al.*** (2002) studied the impact of social economic factors on energy consumption of optimization systems. Song ***et al.*** (2004) demonstrated the security index based optimization methodology for allocating FACT devices. Reddy ***et al.*** (2006) applied GA for suitable positions of FACT devices for CM. Verma and Gupta (2006) evaluated nodal spot prices and also studied the impact of UPFC on spot prices. Besharat and Taher (2008) proposed a performance index based sensitivity methodology to allocate series compensators. Fang ***et al.*** (2009) introduced sensitivity methods for dispatch and optimal setting of FACTS controllers. Zeraatzade (2010) focused on OPF framework for CM in real time balancing market. That

framework was based on generation re-dispatch and FACTS devices. Wibowo ***et al.*** (2011) presented a simulation of dynamic state transitions caused by specified contingencies using FACT devices allocation method. Blanco ***et al.*** (2011) proposed an investment valuation approach based on the least square Monte Carlo method for FACTS investments. Shaheen ***et al.*** (2011) presented a Differential Evaluation (DE) based optimization technique for finding suitable UPFC placement positions for different $N-1$ contingencies. Lashkar ***et al.*** (2012) developed a mathematical programming formulation based model for installation of shunt-series controllers. Ghahremani and Kamwa (2013) proposed a GA based graphical user interface to find suitable of multi-type FACTS locations. Alamelu ***et al.*** (2015) demonstrated the implementation of various evolutionary algorithms for sizing and placement of UPFC.

2.2.2 Survey on Optimization based Methods of CM

As, CM is a nonlinear problem subjected to various constraints as well as involving a lot of variables; therefore, the optimization techniques are the best suited for such problem. Particle Swarm Optimization (PSO) (Saravanan ***et al.,*** 2007; Hazara and Sinha, 2008; Dutta and Singh, 2008; Baskar and Mohan, 2009; Boonyaritdachochai ***et al.,*** 2010; Balaraman and Kamaraj, 2011; Chen ***et al.,*** 2014; Sarwar and Siddiqui, 2015), Genetic Algorithm (Surender ***et al.,*** 2010; Balaraman and Kamaraj 2010), Neural Network (Luo et al., 2000; Pandey ***et al.*** 2010; Balaraman 2013), Bacterial Foraging Optimization (Venkaiah and Kumar, 2011), Ant Colony (Liu ***et al.,*** 2011), Hybrid Evolutionary (Taher and Amooshahi, 2012; Pandiarajan and Babulal, 2014), Firefly Algorithm (Verma and Mukherjee, 2016b), Symbiotic Organisms Search (Verma *et al.*, 2017), Firefly Algorithm (Verma and Mukherjee, 2016a), Ant Lion Optimizer (Verma and Mukherjee, 2016 b), Flower Pollination Method (Verma and Mukherjee, 2016c), Satin Bowerbird Optimization (Chintam and Daniel, 2018) algorithms are the few heuristics methods implemented by the various researchers for alleviating congestion. Importance of soft computing techniques and their applications in research areas have been demonstrated by Thampi ***et al.*** (2018). In another research areas, the contribution of smart optimization techniques such as PSO (Patel and Trivedi, 2010; Tekchandani and Trivedi, 2011), hybrid PSO with neural (Chatterjee ***et al.,*** 2017), fuzzy with chaos (Lin ***et al.,*** 2011), hybrid algorithm (Thomas and Chaudhari, 2013) in designing perfect decision making procedure for global optimal solutions clearly indicate their superiority and precision over traditional methods.

Hazara and Sinha (2008) evaluated the optimal solutions to alleviate overloads and minimized the operation cost using multi objective PSO algorithm. Baskar and Mohan (2009) proposed an improved PSO algorithm with novel velocity strategy equation for economic load dispatch problem for security enhancement. Boonyaritdachochai ***et al.*** (2010) presented an implementation of novel algorithm based on PSO with modified acceleration coefficients for optimal CM. Venkaiah and Kumar (2011) demonstrated the hybrid algorithm using fuzzy PSO for the CM. Balaraman and Kamaraj (2011) proposed an effective PSO algorithm to reduce line overloads with minimum deviations in generations. Panida ***et al.*** (2010) modified PSO with new acceleration coefficients and implemented the same for optimal CM. The results were compared with other PSO algorithms and found effective in terms of computational time. Liu ***et al.*** (2011) handled the congestion cost problem by transforming it into a nonlinear programming problem, and was solved using ant colony algorithm. Taher and Amooshahi (2012) introduced a hybrid algorithm using immune GA and immune PSO to locate UPFC. Phadke ***et al.*** (2012) as well as Kumar and Srikant (2017) presented the hybrid algorithms for suitable placements of FACT devices. Esmaili ***et al.*** (2013) illustrated benders decomposition approach for CM in hybrid electricity market for different transactions. Salehizadeh ***et al.*** (2014) proposed a multi attribute decision approach for power generation planning to manage the transmission congestion problem. Hybrid group search optimization was demonstrated by Hagh ***et al.*** (2014). Hybrid DEPSO algorithm was proposed for transmission CM by Pandiarajan and Babulal (2014). Sarwar and Siddiqui (2015) presented an efficient PSO optimizer to solve the nonlinear congestion cost problem, and the results were compared with other types of PSO optimizers to prove the superiority. Many optimization algorithms like GA (Arabkhaburi ***et al.*** 2006), Differential Evolution (Shaheen ***et al.,*** 2011; Roselyn ***et al.***, 2013), Cat Swarm Optimization (Kumar and Kalavathi, 2014), Gravitational Search Algorithm (Sarker and Goswami, 2014), Artificial Algae Algorithm (Zahid ***et al.,*** 2017), Krill Herd (Mukherjee and Mukherjee, 2016), Grey Wolf (Behera and Mohanty, 2019) had also been implemented to allocate the optimal position of UPFC device. Transmission Power loss minimization had been achieved using optimal placements of UPFC using Krill Herd Algorithm (Mukherjee and Mukherjee, 2016). Verma and Mukherjee (2016 a, b, c) implemented various nature-inspired approaches such as Flower Pollination Algorithm (FPA), Firefly Algorithm (FFA), Ant Lion Algorithm (ALO) towards optimal rescheduling of generators for CM. Verma ***et al.*** (2017) introduced and proposed the Symbiotic Organisms Search (SOS) optimization algorithm for CM. Hosseini ***et al.*** (2016) presented

the normalized normal constraint optimized mathematical programming based solution approach towards CM. Behera and Mohanty (2019) proposed an Improved Grey Wolf Optimization technique to solve CM problems. The improvement in Grey Wolf Optimization technique was made by an appropriate balance among the exploitation and exploration phases of the technique.

2.3 Literature Survey Analysis

- After meticulous literature studies of conventional methods of CM, sensitivity based approaches have been found to be the best suited for various objectives of CM. Sensitivity based ATC measurement is found to be the most appropriate way for CM. If accurate ATC value is known to the system operator, the congestion among various lines can be relived to a great extent. AC Power Transfer Congestion Distribution Factor (AC-PTCDF) approach has been found to be the most efficient towards ATC measurement; therefore, there is a need to develop AC-PTCDF based sensitivity approach, which can evaluate both the static and contingency ATC values for all types of transactions.
- The conventional optimization methods of CM works satisfactorily if the function to be optimized has good continuity and differentiability, which may further lead to local optimal solution. Hence, the CM conventional optimization methods are not well suited in case of multi objective optimization and nonlinear problems where tuning of weighting factor and constraint handling is a difficult task. The solutions of such problems depend on the weights; therefore, the conventional methods may not be suitable.
- Literature studies also reveal that the optimization methods have the ability to overcome the drawback of conventional methods in terms of lesser convergence time, higher convergence rate and lesser computational efforts and very few number of control parameters. It has also been observed that the incorporation of evolutionary optimization techniques in nonlinear congestion cost problem not only reduces the overall rescheduling cost to a greater extent, but also reduces the computational time and efforts of a system operator.
- PSO with certain improvements is a productive evolutionary optimization tool for solving the non-convex optimization problems as compared to other optimization tools due to its excellent searching capability through individual improvement, cooperation and competition of population (Venkaiah and Kumar, 2011; Sarwar and Siddiqui, 2015; Tanweer ***et al.,*** 2015; Uriarte ***et al.,*** 2016). Moreover, the searching capability of PSO can be further enhanced and

optimized by incorporation of search behavior of chaos (Liu ***et al.,*** 2005, Yang ***et al.,*** 2012; Chen ***et al.,*** 2014). Chaotic sequences have been chosen and proven to be very easily generated, fast, reliable and best suited for implementation on nonlinear problems (Yang ***et al.,*** 2012; Chen ***et al.,*** 2014). Moreover, chaotic maps can generate uniform distributed sequences due to their periodicity and uniform randomness (Jiao ***et al.,*** 2008; Liu ***et al.,*** 2005; Xiang ***et al.,*** 2007; Yaoyao ***et al.,*** 2008). Basic need of an optimization algorithm is to avoid the entrapment of final solution in local optima, which can be easily achieved with chaotic maps (Lu and Chen, 2006). The flat distribution and steady chaotic behavior of the improved tent map can extract best iterative results to obtain the global optimal solution (Yaoyao ***et al.,*** 2008) in case of complex optimization problems.

- Moreover, security constraints for both the load bus voltages and the line loadings are efficiently handled with the PSO techniques in case of complex problems (Chanda and De, 2011).
- Determination of number of participating generators had been done using sensitivity approach in literature, which may requires rigorous system operator efforts and generator information (Bompard ***et al.***, 2003; Venkaiah and Kumar, 2011; Boonyaritdachochai ***et al.,*** 2010; Balaraman and Kamaraj, 2011; Sarwar and Siddiqui, 2015; Verma and Mukherjee, 2016 a, b. c; Verma ***et al.***, 2017).
- In proclaimed literature, generally penalty function method had been widely used to deal with constraints in CM problem. In penalty function approach, optimization becomes inefficient due to addition of penalty to the objective function for constraint violations. **(**Iwan ***et al.,*** 2012**)**.

2.4 Research Gaps

Scrupulous literature analyses pronounced the subsequent areas as scope of further research and are also highlighted in this thesis.

- Lack of dynamic algorithm evaluating both the static and contingency ATC values for all types of transactions.
- Non-availability of advanced and intelligently trained chaotic PSO algorithms to deal with security constraint nonlinear CM problem incorporated with load management.

- Lack of robust algorithm requiring less information of generator units (with ease of data handling) for evaluation of number of participating generators for rescheduling purpose, as the sensitivity-based approach available in literature requires a rigorous system operator efforts.
- Deficiency of constraint handling procedures to yield only feasible solutions. Till date, generally penalty function method has been widely used to deal with constraints in CM problem.

2.5 Research Excellence

To overcome the above mentioned research gaps, the research excellence and contribution of the thesis is discussed below:

- To overcome the first research gap, a dual objective sensitivity based algorithm has been developed to measure both static and dynamic ATC values and is detailed in Chapter 3. Furthermore, the evaluated sensitivity factors have been utilized to allocate the optimal location of UPFC.
- To meet second research gap, a novel approach of congestion cost management (including load management) employing Improved Tent Map adaptive Chaotic PSO algorithm (ITM-CPSO) has been introduced and applied to nonlinear security constraint CM problem, which is given in detail in Chapter 4. Moreover, the same algorithm has also been explored to find the optimal location of UPFC device, which is illustrated in detail in Chapter 5.
- To meet third research gap, modified formulation and implementation of URCT algorithm has been done and mentioned in Chapter 4 to determine the exact and accurate number of participating generators for alleviating contingencies, which has further resulted in easy handling of data for a system operator.
- To overwhelm fourth research gap, a novel and dynamic constraint optimized Twin Extremity Chaotic Map Adaptive Particle Swarm Optimization (TECM- PSO) algorithm has been introduced and implemented to solve complex rescheduling generation cost problem. This approach has the capability to achieve only feasible solutions over all the searching area as explained in Chapter 6.

Based upon the above work, the objectives of this study have been derived and listed in section 1.2.

Chapter 3: Deterministic Approach towards Static and Dynamic ATC Evaluation

3.1 Introduction

Due to large number of transactions in deregulated environment, chances of congestion in the network increase to great extent. The system operator should know the values of Available Transfer Capacity (ATC) before carrying out any transaction to overcome the adverse effects of congestion. In this chapter, a multi objective deterministic approach has been applied to evaluate linear and contingency ATC values of various lines of IEEE 30 bus system for three types of transactions namely a) simultaneous, b) bilateral and c) single. The fast and dynamic results obtained are useful to reduce the congestion at various lines by utilizing the evaluated ATC values for various types of transactions. AC Real Power Transfer Congestion Distribution Factors (AC-PTCDFs) are needed to be determined prior to ATC evaluation. Therefore, the entire mathematical procedure has been divided into two main broad categories; a) the congestion distribution factors determination, and b) ATC evaluation.

In the proposed work, AC-PTCDFs have been derived using sensitivity based approach. PTCDF is defined as the change in real power flow (ΔP_{ij}) in a transmission line 'k' connected between buses 'i' and 'j', due to unit change in power injection (ΔP_n) at bus 'n'. In deregulated environment let, 's' be the seller bus and 'b' be the buyer bus. For a change in the real power transaction ΔP_{sb} and for a change in real power transmission line quantity ΔP_{ij}, the real power transmission distribution factors can be mathematically represented by Eq. (3.1).

$$PTCDF = \frac{\Delta P_{ij}}{\Delta P_{sb}} \tag{3.1}$$

Moreover, if $P_{\max(ij-sb)}$ is the maximum allowable transaction amount between seller and buyer bus constraint by the line flow limits from bus i to j, the ATC is determined by the relation using Eq.(3.2).

$$ATC = \min\left(P_{\max(ij-sb)} \right) \tag{3.2}$$

3.2 Mathematical Formulation for Determining Congestion Distribution Factors

The complex power flow equation is nonlinear and is expressed in the form as given by Eq. (3.3) at i^{th} bus.

$$S_i = P_i - jQ_i = V_i^* \sum_{k=1}^{n} Y_{ik} V_k \tag{3.3}$$

for $i = 1,2,3.....n$, These n complex equations represent $2n$ real and $2n$ reactive power flow equations represented by Eq.(3.4) and Eq.(3.5) respectively.

$$P_{ij} = V_i V_j Y_{ij} \cos\left(\theta_{ij} + \delta_j - \delta_i\right) - V_i^2 Y_{ij} \cos\left(\theta_{ij}\right) \tag{3.4}$$

$$Q_{ij} = V_i V_j Y_{ij} \sin\left(\theta_{ij} + \delta_j - \delta_i\right) - V_i^2 Y_{ij} \sin\left(\theta_{ij}\right) - V_i^2 \frac{Y_{sh}}{2} \tag{3.5}$$

Using Taylor's series and neglecting higher order terms of Eq. (3.4) and Eq. (3.5) can be expressed by Eq. (3.6) and Eq. (3.7) respectively.

$$\Delta P_{ij} = a_{ij} \Delta\delta_i + b_{ij} \Delta\delta_j + c_{ij} \Delta v_i + d_{ij} \Delta v_i \tag{3.6}$$

$$\Delta Q_{ij} = a_{ij}' \Delta\delta_i + b_{ij}' \Delta\delta_j + c_{ij}' \Delta v_i + d_{ij}' \Delta v_i \tag{3.7}$$

Where, $a_{ij} = V_i V_j Y_{ij} \sin\left(\theta_{ij} + \delta_j - \delta_i\right)$, $b_{ij} = -V_i V_j Y_{ij} \sin\left(\theta_{ij} + \delta_j - \delta_i\right)$

$c_{ij} = V_j Y_{ij} \cos\left(\theta_{ij} + \delta_j - \delta_i\right) - 2V_i Y_{ij} \cos\left(\theta_{ij}\right)$, $d_{ij} = V_i Y_{ij} \cos\left(\theta_{ij} + \delta_j - \delta_i\right)$

$$a_{ij}^{'} = V_i V_j Y_{ij} \cos(\theta_{ij} + \delta_j - \delta_i), \qquad b_{ij}^{'} = V_i V_j \cos(\theta_{ij} + \delta_j - \delta_i)$$

$$c_{ij}^{'} = -V_j Y_{ij} \sin(\theta_{ij} + \delta_j - \delta_i) + 2V_i Y_{ij} \sin(\theta_{ij}) - V_i Y_{sh}, \qquad d_{ij}^{'} = V_j Y_{ij} \sin(\theta_{ij} + \delta_j - \delta_i)$$

According to Jacobian relationship and neglecting P-V and Q-δ coupling, the change in real and reactive power can be expressed by Eq. (3.8) and Eq. (3.9) respectively.

$$\Delta P = [J_{11}]\Delta\delta \tag{3.8}$$

$$\Delta Q = [J_{22}]\Delta V \tag{3.9}$$

From Eq. (3.8) and Eq. (3.9), Eq. (3.10) and Eq. (3.11) can be derived.

$$\Delta\delta = [J_{11}]^{-1}\Delta P \tag{3.10}$$

$$\Delta V = [J_{22}]^{-1}\Delta Q \tag{3.11}$$

For the i^{th} bus, Eq. (3.12) and Eq. (3.13) are obtained.

$$\Delta\delta_i = \sum_{l=1}^{n} X_{il}\Delta P_l, \quad i = 1,2,3.....n \tag{3.12}$$

$$\Delta V_i = \sum_{l=1}^{n} Y_{il}\Delta Q_l, \; i = 1,2,3.....n \tag{3.13}$$

Substituting values of Eq. (3.12) and Eq. (3.13) in Eq. (3.6) and Eq. (3.7) respectively, Eq. (3.14) and Eq. (3.15) are obtained.

$$\Delta P_{ij} = a_{ij}\sum_{l=1}^{n} X_{il}\Delta P_l + b_{ij}\sum_{l=1}^{n} X_{jl}\Delta P_l \tag{3.14}$$

$$\Delta Q_{ij} = c_{ij}^{'}\sum_{l=1}^{n} Y_{il}\Delta Q_l + d_{ij}^{'}\sum_{l=1}^{n} Y_{jl}\Delta Q_l \tag{3.15}$$

Expanding Eq. (3.14) and Eq. (3.15), Eq. (3.16) and Eq. (3.17) are obtained.

$$\Delta P_{ij} = a_{ij}[X_{i1}\Delta P_1 + X_{i2}\Delta P_2 + ...] + b_{ij}[X_{ji}\Delta P_1 + X_{j2}\Delta P_2 + ...] \tag{3.16}$$

$$\Delta Q_{ij} = c_{ij}^{'}[Y_{i1}\Delta Q_l + Y_{i2}\Delta Q_2 + ...] + d_{ij}^{'}[Y_{j1}\Delta Q_1 + Y_{j2}\Delta Q_2 + ...] \tag{3.17}$$

Considering only the real power transfer congestion distribution factor, Eq. (3.18) is obtained.

$$\Delta P_{ij} = PTCDF_1^k \Delta P_1 + PTCDF_2^k \Delta P_2 + ... + PTCDF_n^k \Delta P_n \quad (3.18)$$

Here, $PTCDF_n^k = a_{ij} X_{in} + b_{ij} X_{jn}$

3.2.1 Static Available Transfer Capacity (ATC) Formulation

Once the PTCDF values have been determined, the maximum allowable transaction from bus i to j can be given by Eq. (3.19).

$$\Delta P_n^{k\,\max} = \frac{P_{ij}^{\max} - P_{ij}^0}{PTCDF_n^k} \quad (3.19)$$

Then, static ATC can be evaluated using Eq. (3.20).

$$ATC_n = \min(\Delta P_n^{k\,\max}) \quad (3.20)$$

The maximum limit can be evaluated by incorporating the thermal limits and the various inequality constraints of the above system are given by Eq. (3.21) to Eq. (3.23).

$$P_{gimin} \le P_{gi} \le P_{gimax} \quad (3.21)$$

$$Q_{gimin} \le Q_{gi} \le Q_{gimax} \quad (3.22)$$

$$V_{gimin} \le V_{gi} \le V_{gimax} \quad (3.23)$$

3.2.2 Contingency Available Transfer Capacity (ATC) Formulation

ATC evaluation during contingency cannot be accurately measured alone with PTCDF determination. Load outage distribution factor (LODF) has to be incorporated along with PTCDF to compute the exact value of ATC. LODF is a factor, which indicates the effect of any line outage to the power flows on the remaining lines in the system. The line outage between the buses 'm' and 'n' is considered having pre-outage power flows P_{mn}^0 and P_{nm}^0 from bus 'm' to 'n' and from to 'n' to 'm' respectively. Considering $P_{ij,mn}$ be the post-outage line flows between buses 'm' to 'n', then the change in the power flows between line $i-j$ due to outage of line $m-n$ can be evaluated from Eq. (3.24).

$$\Delta P_{ij,mn} = P_{ij,mn} - P_{mn}^0 \quad (3.24)$$

The LODF of line $i-j$ due to outage of line $m-n$, is defined as the ratio of change in the power flows between line $i-j$ due to outage of line $m-n$ to the pre-outage power flows between $m-n$ as expressed by Eq. (3.25).

$$LODF_{ij,mn} = \frac{\Delta P_{ij,mn}}{P^0_{mn}} \tag{3.25}$$

The PTCDFs for the contingency cases are called Outage Transfer Congestion Distribution Factors (OTCDFs). Outage Transfer Congestion Distribution Factor (OTCDF) on line $i-j$ due to outage of $m-n$ can be expressed by Eq. (3.26).

$$OTCDF_{ij,mn} = \left[PTCDF_{ij} + LODF_{ij,mn} * PTCDF_{mn}\right] \tag{3.26}$$

OTCDF on line $i-j$ due to outage of $m-n$ can also be defined as the ratio of change in post outage line flows between buses m and n to the change in power injection at n^{th} bus expressed by Eq. (3.27).

$$\Delta P_{ij,mn} = OTCDF_{ij,mn} * \Delta P_n \tag{3.27}$$

Maximum allowable transaction from bus $i-j$ due to outage of line $m-n$ can be expressed as the ratio of the difference between post outage change in maximum real power flow limit from bus i to j and base case real power flow buses to OTCDF on line $i-j$ due to outage of $m-n$, as expressed by Eq. (3.28). Where $P^{\max}_{ij}$ is the post contingency flow limit on the line $i-j$ due to outage of line m to n and P^0_{ij} is the base case real power flow between $i-j$.

$$\Delta P^{ij,mn}_n(\max) = \frac{P^{\max}_{ij} - P^0_{ij}}{OTCDF_{ij,mn}} \tag{3.28}$$

Then, contingency ATC value can be expressed by Eq. (3.29).

$$ATC_{n,mn} = \min\left(\Delta P^{ij,mn}_n(\max)\right) \tag{3.29}$$

3.3 Algorithm for Static and Contingency ATC Measurements

The steps of the proposed algorithm are presented below:

- Enter the line data and bus data.
- Formulate Y bus matrix.
- Initialize system conditions such as base MVA, bus voltages, bus angles, type of buses, minimum and maximum power limits and power flows.
- Compute power flows and check for P and Q limit violations.
- Obtain the change of powers from their specific values.
- Obtain the Jacobin matrix from the load flow solution.
- Update the state vectors; voltage magnitude, voltage angle and tolerance values.
- Compute new transmission quantities i.e., system voltages and angles using updated state vectors.
- For the specified transaction, compute the sensitivity factors and line flows for all the lines after running Newton-Raphson method, provided that the in equality constraints represented by Eq. (3.21) to Eq. (3.23).
- *If* any line outage or generator outage exists, *then* do the contingency analysis by finding LODF, OTCDF and ATC values for the corresponding outages using Eq. (3.25), Eq. (3.26) and Eq. (3.29) respectively. *Else*, if no contingencies occur then after completing all the transfers for the specified transaction, compute ATC using Eq. (3.20).
- Repeat the above steps for all the transactions.

Figure 3.1 presents the flow chart of proposed approach.

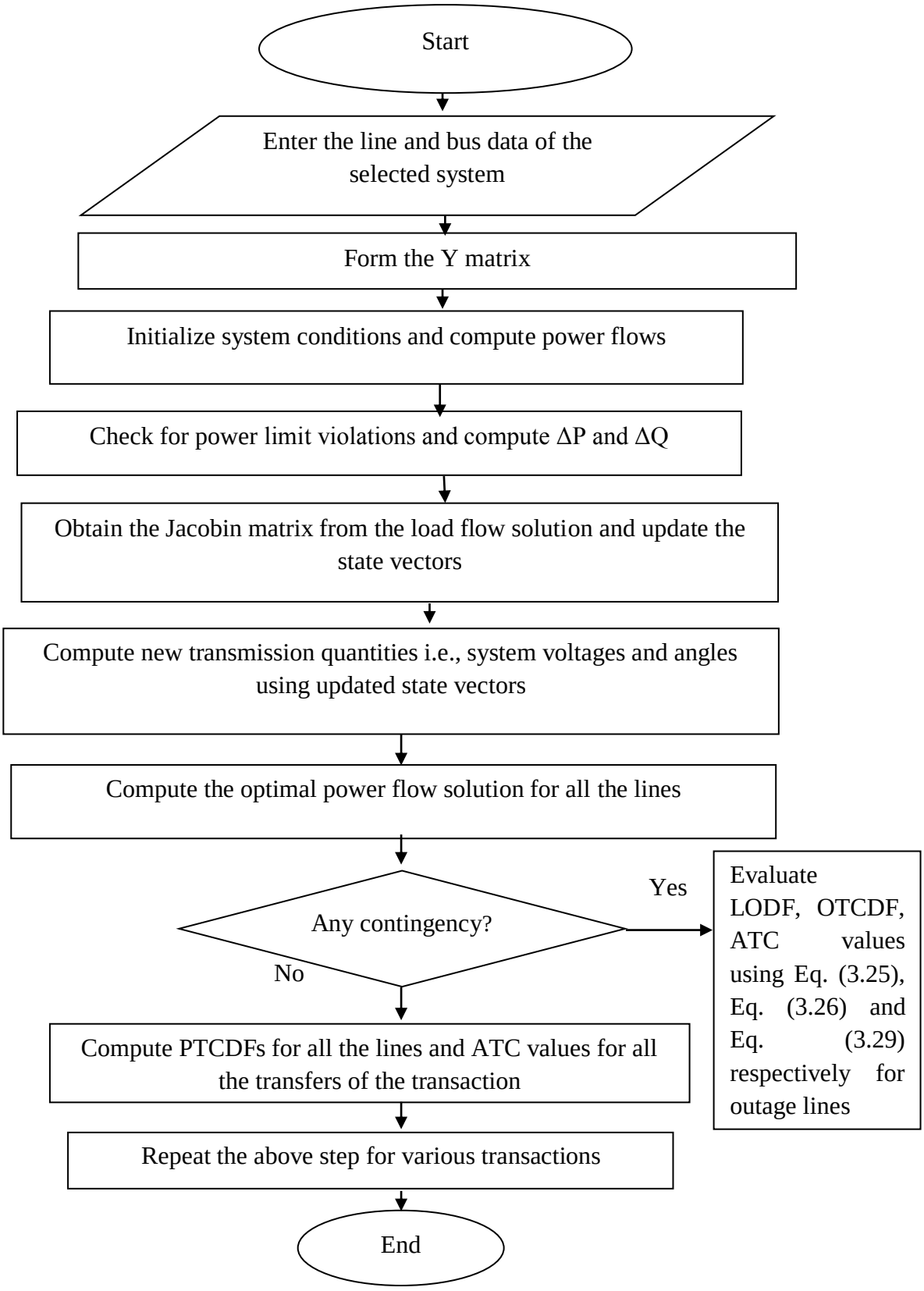

Figure 3.1: Flow chart of the proposed methodology

The above mentioned mathematical formulation has been simulated for IEEE 30 bus system using MATLAB sequential programming. Data details of IEEE 30 bus system are depicted in **Appendix A1.**

3.4 Static ATC Evaluation

Three types of transactions; single, multiple and simultaneous have been carried out. The simulation results of these transactions represent the ATC and congestion distribution factors for the respective transactions as shown in Table 3.1 and Table 3.2 respectively.

Table 3.1: Static ATC variations for single, bilateral and simultaneous transactions among different buses of IEEE 30 bus system

Simultaneous Transactions (T1) From 14-21 buses		**Over All ATC (MW)**	**Bilateral Transactions (T2)**		**Over All ATC (MW)**	**Single Transactions (T3)**		**Transaction Number**	**ATC (MW)**
From Bus	**To Bus**		**From Bus**	**To Bus**		**From Bus**	**To Bus**		
14	12	19.4768	23	25	20.5296	12	23	T3′	22.9742
12	15		25	27		30	11	T3″	27.2178
15	11		25	29		4	23	T3‴	26.9766
11	19		29	27		7	12	T3⁗	83.8532
19	21		28	24		7	23	T3⁗′	27.5988
21	30		24	25		2	12	T3⁗″	88.9025
30	25		25	24		6	21	T3⁗‴	53.9099
25	21		29	30		21	30	T3⁗⁗	26.9829
21	19		30	28		23	12	T3⁗⁗′	23.7545

Table 3.1 shows the linear ATC values for three types of transactions i.e. simultaneous, bilateral and single. The number of transfers for simultaneous and bilateral transactions is 9. From the Table 3.1, it has been observed that the transfer capabilities are less for simultaneous and bilateral transactions

as compared to single transactions. Moreover, the sensitivity factors (PTCDFs) for the above said transactions have also been evaluated and are shown in Table 3.2. From the evaluated values of PTCDFs, it has been observed that the type of transaction directly impact on variation of PTCDF for various lines of the system. For simultaneous transactions, the variation of PTCDF values of system lines is small as compared to bilateral and single transactions. Positive and negative values of PTCDFs indicate the overloading directions of the lines.

Table 3.2: Real power transfer congestion distribution factors variations among various lines of IEEE 30 bus system for different types of transactions

Line No	**Real Power Transfer Congestion Distribution Factors (PTCDF)**										
	(T1)	**(T2)**	**(T3′)**	**(T3′′)**	**(T3′′′)**	**(T3′′′′)**	**(T3′′′′′)**	**(T3′′′′′′)**	**(T3′′′′′′′)**	**(T3′′′′′′′′)**	**(T3′′′′′′′′′)**
1	0.014	0.01	0.01	-0.003	0.032	-0.07	-0.06	-0.21	-0.01	0.008	-0.01
2	-0.01	0	-0.011	0.0027	-0.03	0.07	0.062	0.215	0.01	-0.008	0.011
3	-0.02	0	-0.017	0.0043	-0.05	0.113	0.096	0.335	0.02	-0.013	0.017
4	-0.01	0	-0.011	0.0027	-0.03	0.072	0.061	0.215	0.01	-0.008	0.011
5	0.011	0.01	0.008	-0.002	0.025	-0.2	-0.19	0.138	-0.01	0.006	-0.01
6	0.025	0.02	0.019	-0.005	0.057	0.017	0.036	0.312	-0.03	0.014	-0.02
7	0.203	0.16	0.153	-0.039	0.463	-0.4	-0.25	-0.06	-0.21	0.114	-0.15
8	0.011	0.01	0.008	-0.002	0.025	-0.2	-0.19	0.138	-0.01	0.006	-0.01
9	-0.01	-0	-0.009	0.0022	-0.03	-0.8	-0.81	-0.14	0.01	-0.006	0.009
10	0.001	0.1	0.037	-0.255	0.056	0.023	0.06	0.033	0.04	0.235	-0.04
11	0.158	0	0.063	0.4916	0.256	0.217	0.28	0.204	0.41	-0.275	-0.06
12	0.09	0	0.036	0.0847	0.145	0.123	0.159	0.116	0.23	-0.156	-0.04
13	0	0	0	1	0	0	0	0	0	0	0
14	0.158	0	0.063	-0.508	0.256	0.217	0.28	0.204	0.41	-0.275	-0.06
15	-0.24	-0.2	-0.181	0.0458	0.454	0.589	0.408	0.612	0.25	-0.135	0.181
16	0	0	0	0	0	0	0	0	0	0	0
17	-0.62	-0.1	0.136	-0.005	0.098	-0.04	0.093	-0.04	0.03	-0.008	-0.14

18	-0.43	-0.2	0.541	-0.021	0.384	-0.18	0.364	-0.17	0.11	-0.028	-0.54
19	0.817	0.08	0.142	0.0713	-0.03	-0.19	-0.05	-0.18	0.11	-0.099	-0.14
20	0.378	-0.1	0.136	-0.005	0.098	-0.04	0.093	-0.04	0.03	-0.008	-0.14
21	-0.18	0.08	0.142	0.0713	-0.03	-0.19	-0.05	-0.18	0.11	-0.099	-0.14
22	0.711	0.1	-0.008	0.0579	-0.1	-0.11	-0.11	-0.1	0.06	-0.068	0.008
23	0.71	0.1	-0.008	0.0579	-0.1	-0.11	-0.11	-0.1	0.06	-0.068	0.008
24	-0.29	0.1	-0.008	0.0579	-0.1	-0.11	-0.11	-0.1	0.06	-0.068	0.008
25	0.29	-0.1	0.008	-0.058	0.101	0.105	0.113	0.099	-0.06	0.068	-0.01
26	0.183	-0.1	-0.142	-0.071	0.028	0.192	0.05	0.181	-0.11	0.099	0.142
27	-0.14	0.07	0.141	-0.178	0.164	0.026	0.167	0.025	0.59	-0.457	-0.14
28	-0.09	0.05	0.092	-0.116	0.107	0.017	0.109	0.016	0.22	-0.141	-0.09
29	-0.14	0.07	0.141	-0.178	0.164	0.026	0.167	0.025	-0.42	0.543	-0.14
30	0.233	-0.4	0.685	-0.084	0.583	-0.11	0.57	-0.11	0.07	0.032	-0.68
31	-0.22	0.12	0.233	-0.294	0.272	0.043	0.276	0.041	-0.19	0.402	-0.23
32	0.233	0.63	-0.316	-0.084	-0.42	-0.11	-0.43	-0.11	0.07	0.032	0.316
33	0.009	-0.3	-0.082	-0.378	-0.15	-0.07	-0.15	-0.07	-0.12	0.434	0.082
34	0	0	0	0	0	0	0	0	0	0	0
35	0.009	0.75	-0.082	-0.378	-0.15	-0.07	-0.15	-0.07	-0.12	0.434	0.082
36	-0.01	0.25	0.082	-0.623	0.145	0.072	0.154	0.068	0.12	0.567	-0.08
37	0	-0.7	0	-0.41	0	0	0	0	0	0.41	0
38	0	-0.3	0	-0.59	0	0	0	0	0	0	0
39	0	0.28	0	-0.41	0	0	0	0	0	0.41	0

40	0.001	0.1	0.037	-0.256	0.056	0.023	0.06	0.034	0.04	0.236	-0.04
41	-0.01	0.15	0.045	-0.367	0.09	0.049	0.094	0.034	0.08	0.33	-0.04

Table 3.2 shows that PTCDF values have positive, negative and zero values. The positive values of PTCDFs indicate that the corresponding lines have been overloaded in positive direction and the lines having negative values of PTCDFs have been overloaded in negative direction. The zero values of PTCDFs indicate that the corresponding lines have infinite $P_{\max ij-sb}$ values. The system operator will have to look the overloading directions accordingly. From the evaluated PTCDF values, the sensitivity curves for different types of transactions have been drawn for above mentioned transactions and are shown in Fig. 3.2 to Fig. 3.12.

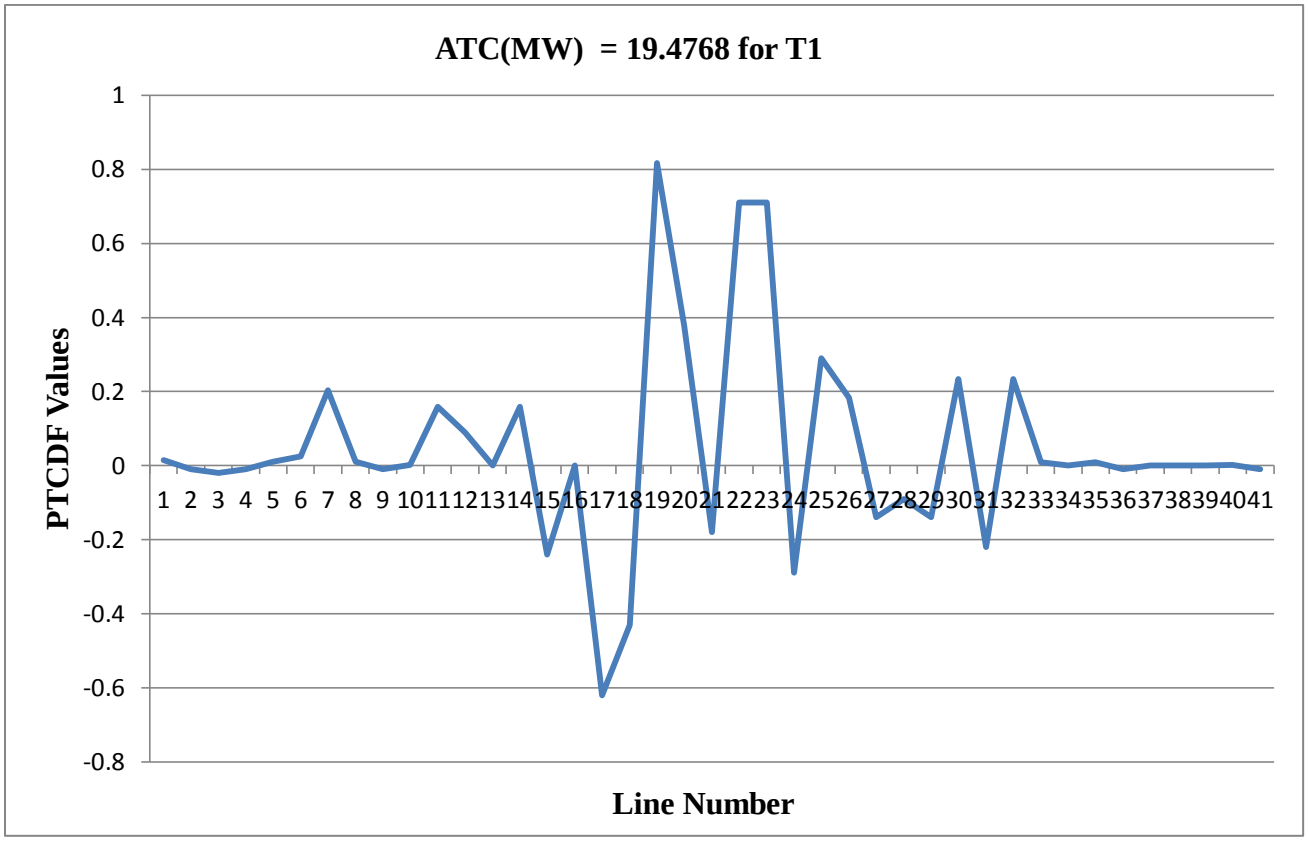

Figure 3.2: Distribution of sensitivity factors among various lines of IEEE 30 bus system for transaction (T1)

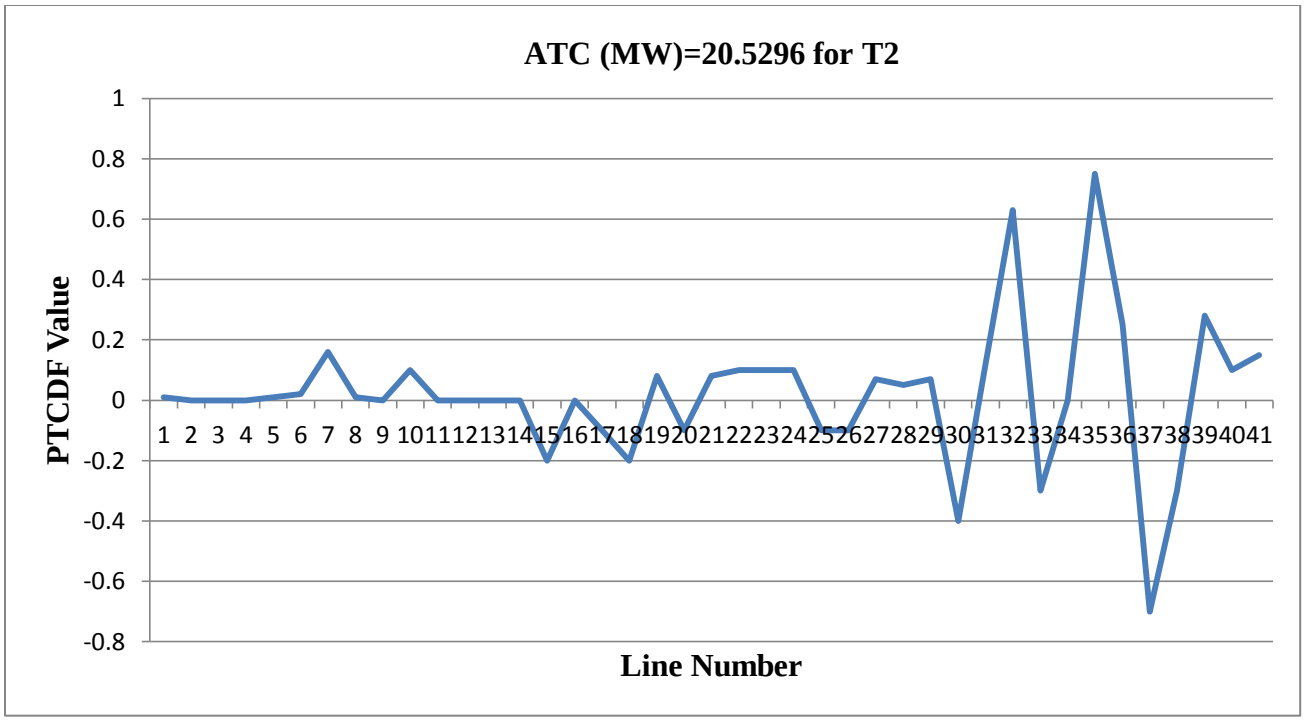

Figure 3.3: Distribution of sensitivity factors among various lines of IEEE 30 bus system transaction (T2)

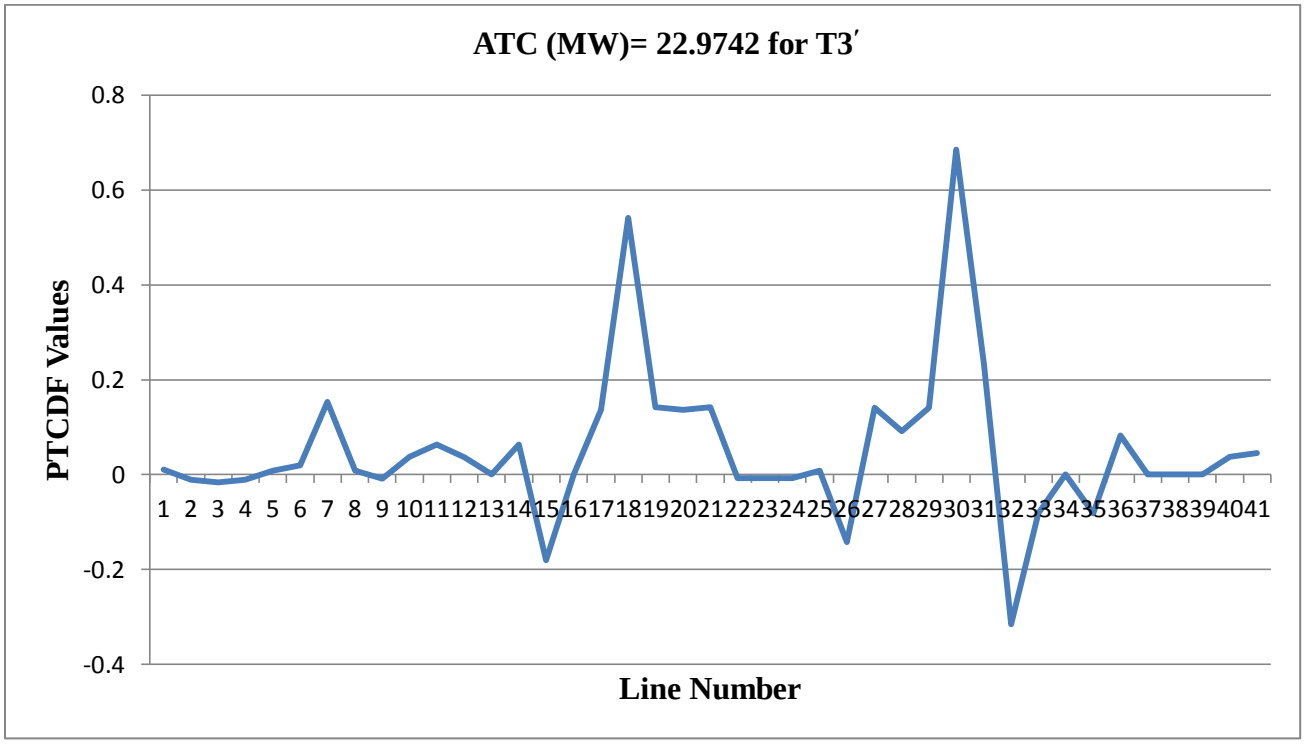

Figure 3.4: Distribution of sensitivity factors among various lines of IEEE 30 bus system for transaction (T3′)

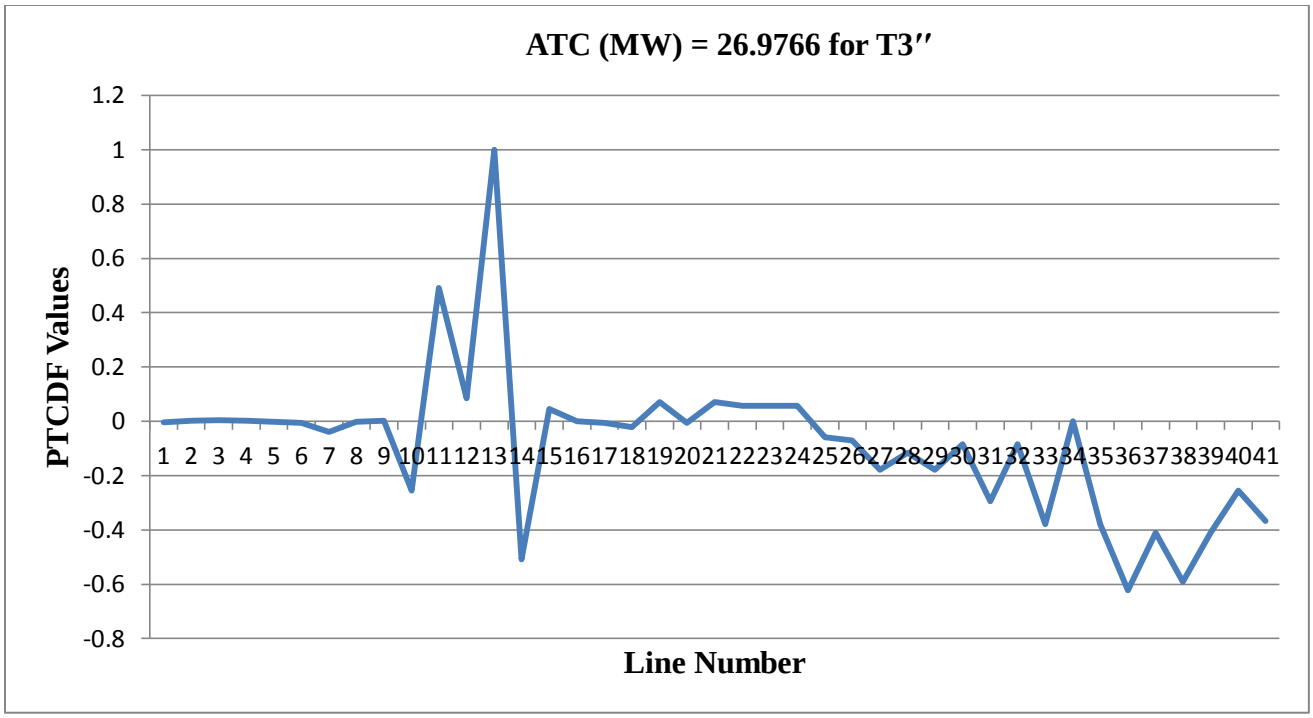

Figure 3.5: Distribution of sensitivity factors among various lines of IEEE 30 bus system for transaction (T3′′)

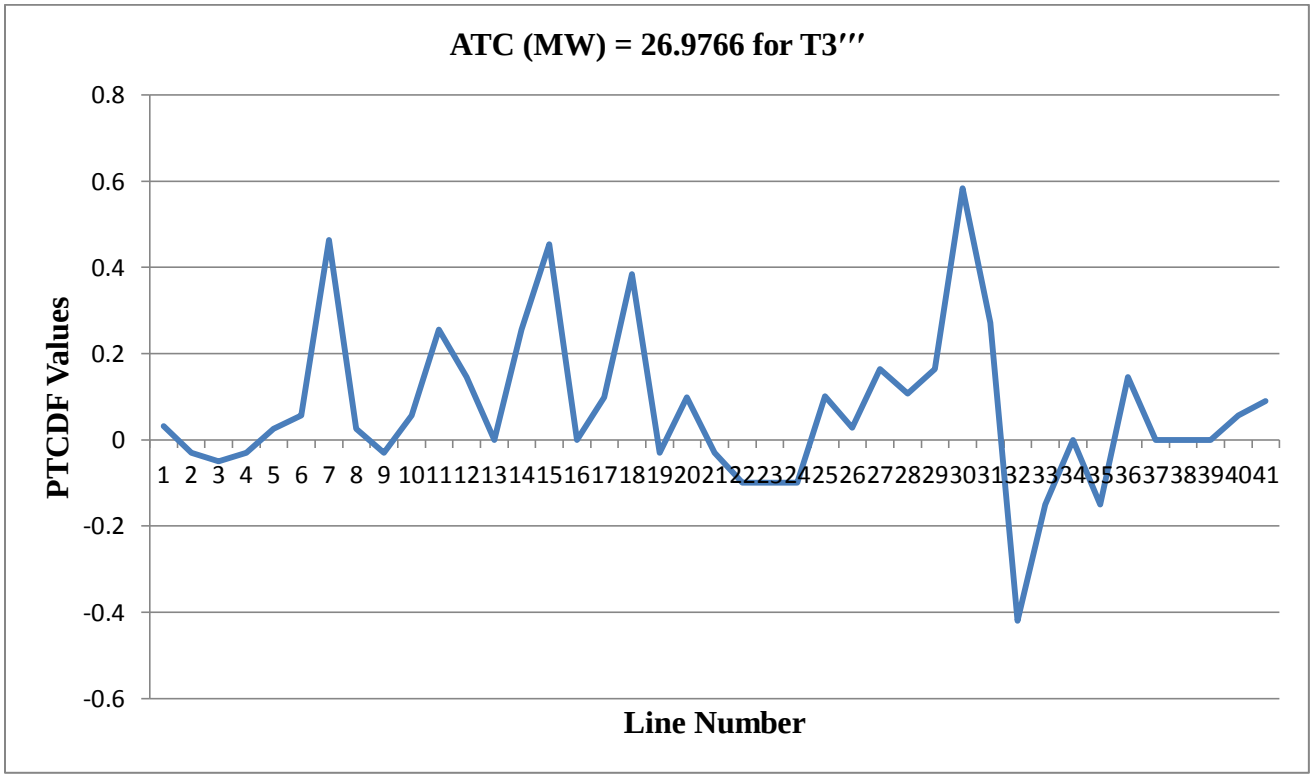

Figure 3.6: Distribution of sensitivity factors among various lines of IEEE 30 bus system for transaction (T3′′′)

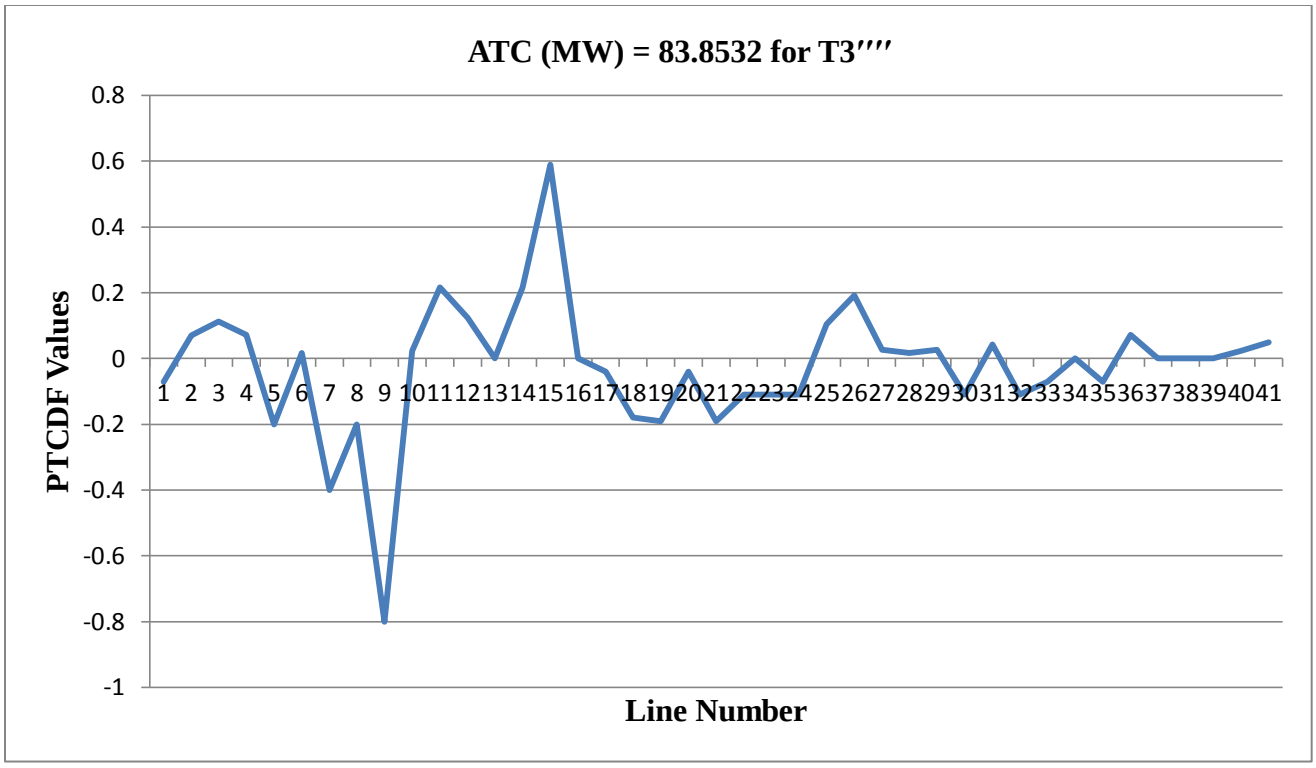

Figure 3.7: Distribution of sensitivity factors among various lines of IEEE 30 bus system for transaction (T3′′′′)

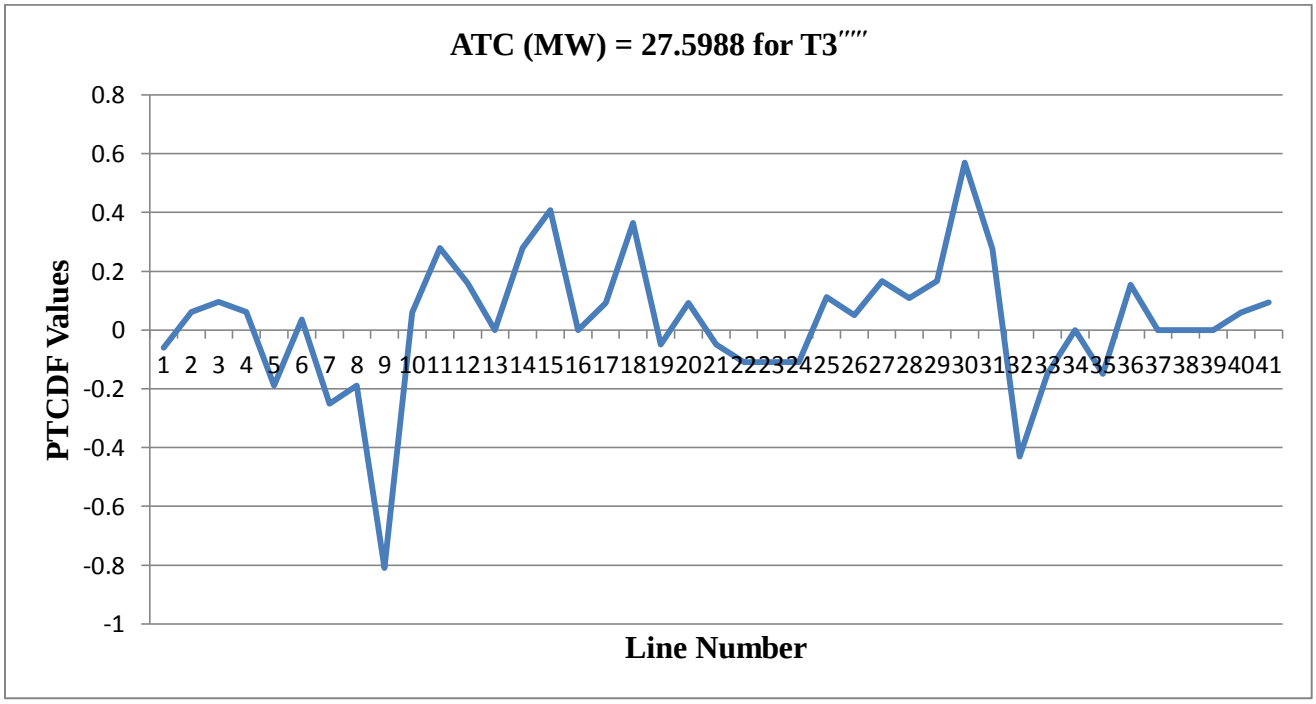

Figure 3.8: Distribution of sensitivity factors among various lines of IEEE 30 bus system for transaction (T3′′′′′)

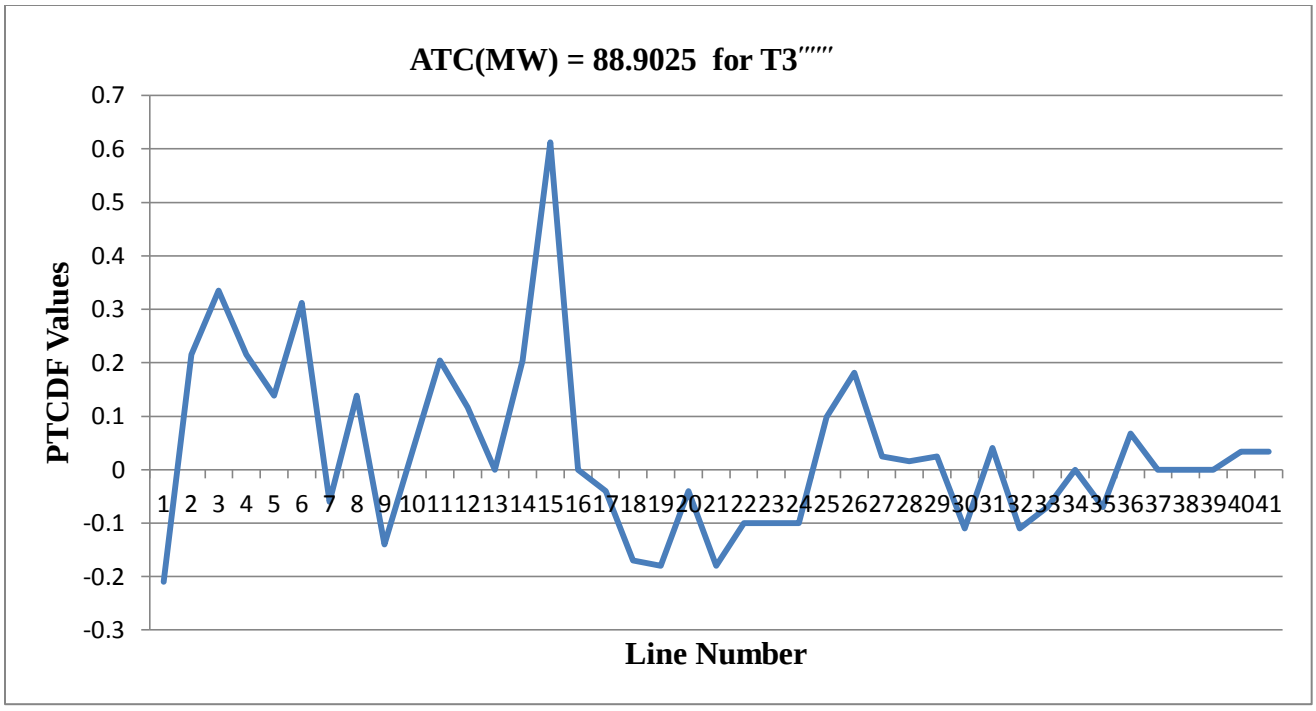

Figure 3.9: Distribution of sensitivity factors among various lines of IEEE 30 bus system for transaction (T3′′′′′′)

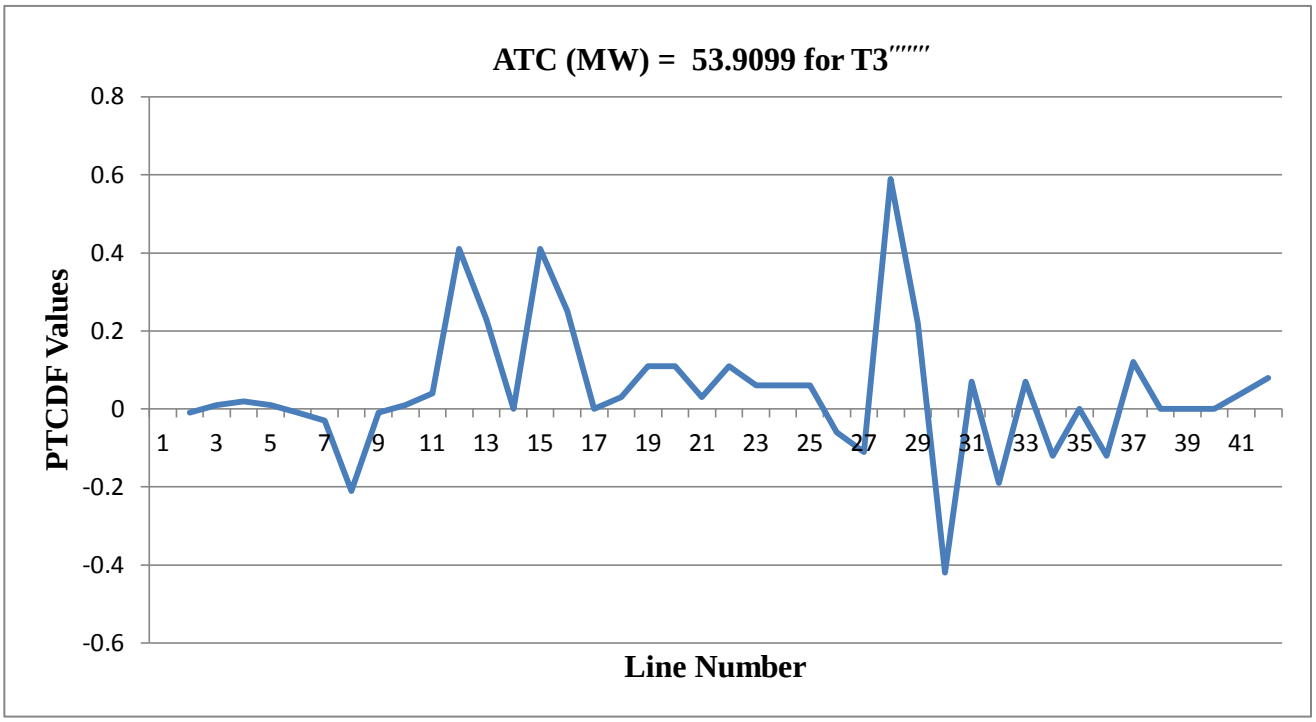

Figure 3.10: Distribution of sensitivity factors among various lines of IEEE 30 bus system for transaction (T3′′′′′′)

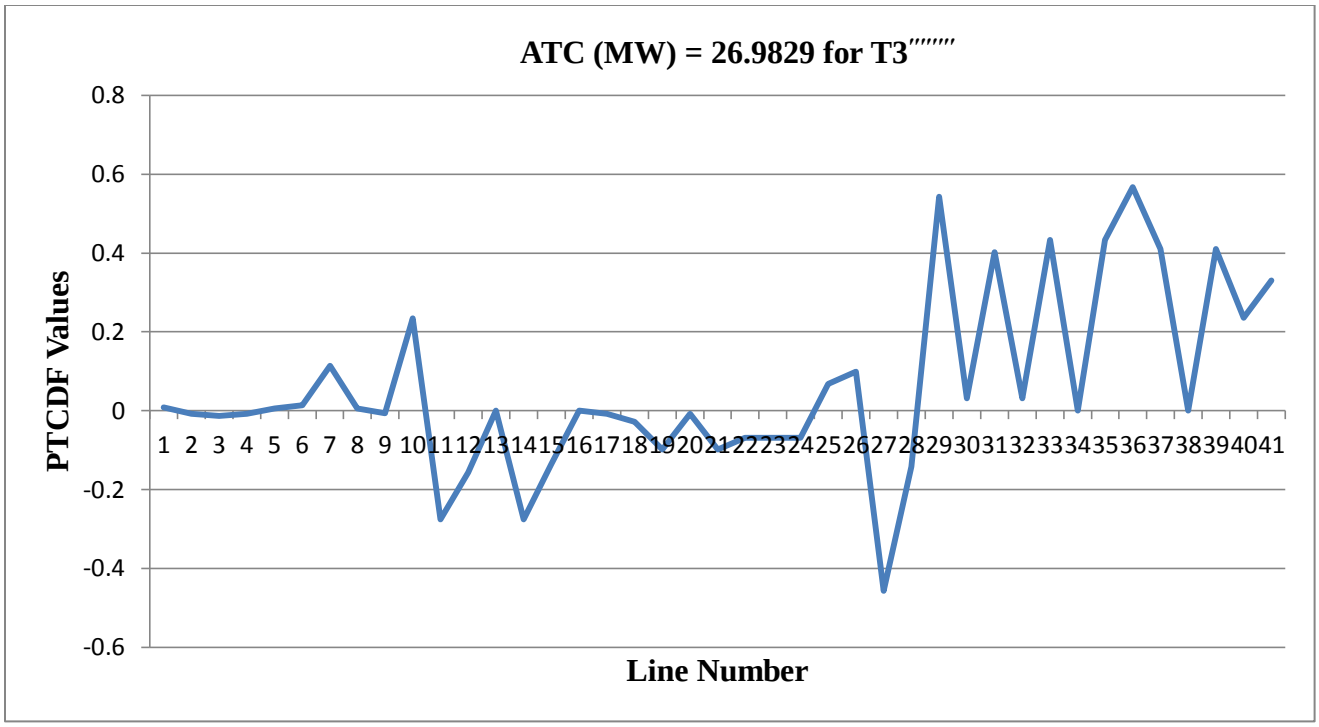

Figure 3.11: Distribution of sensitivity factors among various lines of IEEE 30 bus system for transaction (T3′′′′′′′)

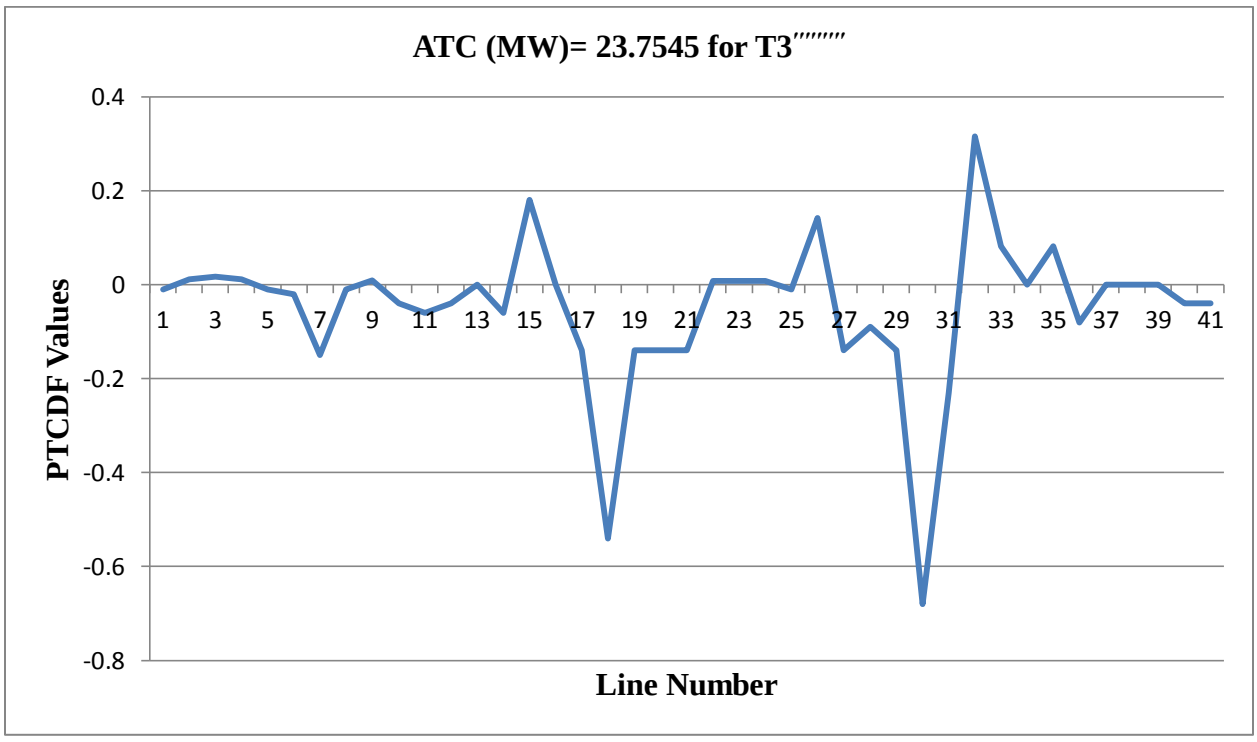

Figure 3.12: Distribution of sensitivity factors among various lines of IEEE 30 bus system for transaction (T3′′′′′′′)

The sensitivity curves obtained for various specified transactions clearly depict the variations of real power transfer congestion distribution factors among various lines of 30 bus system. The lines with higher variations of the sensitivities can be the best optimally located lines for the FACT devices because even small perturbation in the power injection bus will cause large change in the power flows. If installation of UPFC device for ATC enhancement is considered, the lines with lowest magnitude of PTCDF and highest slope of sensitivity curve are best chosen for its installation, which are shown in Table 3.3.

Table 3.3: Optimal line location of UPFC placement for different types of transactions

Transaction Number	**Optimal Line Location for UPFC**
T1	23-24
T2	36-37
T3′	32-33
T3″	35-36
T3″	32-33
T3‴	9-10
T3⁗	8-9
T3⁗′	1-2
T3⁗″	28-29
T3⁗‴	26-27
T3⁗⁗	29-30

3.5 Contingency ATC Evaluation

In this section the ATC values for various line outages of the bilateral transaction have been evaluated and are shown in Table 3.4.

Table 3.4: Dynamic/Contingency ATC evaluation for various bilateral transactions

Contingency ATC Evaluation				
Transaction Type	**Outage Line**	**Limiting Line**	**ATC (MW) Newton -Raphson Method (Yuan Kang Wu, 2007)**	**ATC (MW) Proposed Method**
Bilateral Transactions	6-28	8-28	19.12	20.98
	10-22	23-24	13.035	13.98
	15-23	10-21	21.714	21.985
	5-30	24-25	10.34	10.989
	12-15	22-24	13.84	14.87
	22-24	15-23	12.023	12.987
	2-4	2-6	15.05	16.034
	8-28	6 -8	40.23	41.87
	9-11	12-15	42.78	43.57

Table 3.4 shows that during contingency conditions the ATC values have been decreased for various transactions. Here, the bilateral transactions have been chosen for dynamic ATC evaluation. Moreover, the line having minimum ATC during line outage contingencies is taken as the limiting element.

3.6 Comparison of ATC Values with Existing Algorithm

In this section, the comparison of ATC values for various buses of IEEE 30 bus system has been done with the existing algorithm in the literature. Three different cases have been chosen for the comparison. In case 1, the transactions are carried out from bus 14 to buses 15,17,20,23,24,26,29 and 30. In case 2, bus 23 has been chosen as reference bus and from this bus the transactions are carried out to buses 16, 17, 20, 21,24,26,29 and 30. In case 3, transactions are carried out from bus 24 to 14, 16, 20, 21, 23, 26, 29 and 30 number buses

Table 3.5: Comparison of ATC values for various types of transactions of IEEE 30 bus system

Case 1: Bus 14 to specified buses								
From Bus	14	14	14	14	14	14	14	14
To Bus	15	17	20	23	24	26	29	30
ATC (MW) (Yuan Kang Wu, 2007)	25.6	31.96	23.4	16.7	22.8	12.3	13.6	14.8
ATC Proposed Method	27.58	34.41	31.33	21.69	31.76	15.96	22.2	26.98
Case 2 : Bus 23 to specified buses								
From Bus	23	23	23	23	23	23	23	23
To Bus	16	17	20	21	24	26	29	30
ATC (MW) (Yuan Kang Wu, 2007)	31.6	33.8	25.2	29.9	22.5	12.3	13.6	14.8
ATC Proposed Method	33.43	35.78	27.56	32.7	25.98	15.67	15.89	19.89
Case 3: Bus 24 to specified buses								
From Bus	24	24	24	24	24	24	24	24
To Bus	14	16	20	21	23	26	29	30
ATC (MW) (Yuan Kang Wu, 2007)	33.9	34.6	32.3	30.2	24.5	12.3	13.6	14.8
ATC (MW) Proposed Method	38.98	39.76	35.76	34.78	27.8	15.98	17.89	18.97

Table 3.5 shows that actual evaluated values of ATC with proposed methodology is much higher than the ATC values mentioned in literature.

3.7 Concluding Remarks

The proposed approach in the chapter contributes to extract the exact values of static and dynamic available transfer capacities under normal and line outage conditions. The basic factors on which value of ATC depends such as recognition of the time variant power flow conditions, power injections nodes, direction of power transfers and nodes of power extraction have been taken into consideration while evaluating the ATC values and congestion distribution factor values in each case. In this approach, the incorporation of OPF and ACPTCDFs has led to the static and dynamic ATC determination with faster convergence rate. From the results, it has been cleared that there is a wider and precise range of ATC values for various lines of the system as per the operator convenience. Moreover, the ATC results obtained can be further used to find better generation locations and transactions. Application of this method to evaluate ATC values effectively and speedily even under outage conditions indicates that the proposed analysis would surely decrease the security risks and increase the economic benefits. The main feature of the proposed methodology is that the distribution of sensitivity factors (PTCDF) among various line for different types of transactions have been analyzed for finding the optimal location of UPFC for respective transactions. These optimal line locations for UPFC placement can further improve the ATC values for all types of transactions.

Chapter 4: An Improved Tent Map Adaptive Chaotic Particle Swarm Optimized Approach towards Security Constraint Optimal Congestion Management

4.1 Introduction

Deregulation into the electric utility industry has led the transmission dispatch and congestion problem more severe and complex to manage. This chapter presents the implementation of an Improved Tent Map Embedded Chaotic Particle Swarm optimization (ITM-CPSO) algorithm to the security constraint nonlinear congestion management cost problem including load management. ITM-CPSO is a hybrid evolutionary algorithm, whose search procedure performs within a normalized plane of search space for all the chosen optimization variables for population based procedures. The dual and full benefits of the characteristics of chaotic variables (i.e., periodicity and randomness) and tent map (i.e., more flat distribution than logistic maps) have been taken while formulating the congestion management cost problem. Furthermore, to preserve the diversity of the proposed algorithm, inequality constraints have been handled by constraint prior optimal dominance method, which is more efficient than the traditional penalty function method. Main contributions of this chapter are twofold: firstly, participating generators are selected using Upstream Real Capacity Tracing (URCT) algorithm which is much superior to sensitivity based approach stated in literature. Secondly, the implementation of proposed algorithm to the nonlinear CM cost problem further minimizes the deviations of the rescheduled generator outputs from the scheduled levels as well as reduces the overall load shedding amount and cost.

4.2 Problem Formulation

The proposed CM problem formulation is comprised of "the minimization of active power rescheduling cost" as well as "minimization of load shedding cost" and can be expressed by Eq. (4.1).

Minimization of Congestion Management Cost (CMC)

$$Minimize(CMC) = \left(\sum_{i_p=1}^{Npg} C_{g\,ip}\left(\Delta P_{gi_p} \right) \Delta P_{gi_p} + \sum_{j_{lb}=1}^{Ns} C_{j_{lb}}^{bid} \Delta P_D^{j_{lb}} \right) (\$/h) \qquad (4.1)$$

4.2.1 Equality Constraints

The Equality Constraints can be generalized as

$g(x,u) = 0$,

Where x represent state variables and u indicates control variables.

(i) Power Equilibrium Constraint

Power Equilibrium Constraint is governed by nonlinear equation between total generation and total loads as given by Eq. (4.2).

$$\sum_{i_p=1}^{Npg} (P_{gi_p}^0 + \Delta P_{gi_p}) + \sum_{k_g, k_g \neq i_p}^{Ng} P_{gk_g} = \sum_{m_{lb}=1}^{ND} P_{Dm_{lb}}^0 + P_L \qquad (4.2)$$

Equation (4.2) can be rewritten by Eq. (4.3).

$$\sum_{i_p=1}^{Npg} P_{gi_p}^{resh} + \sum_{k_g, k_g \neq i_p}^{Ng} P_{gk_g} = \sum_{m_{lb}}^{ND} P_{Dm_{lb}}^0 + P_L \qquad (4.3)$$

Where $P_{gi_p}^{resh} = P_{gi_p}^{0} + \Delta P_{gi_P}$

Active power loss P_L has been evaluated using basic loss coefficients formulas.

(ii) Real and Reactive Power Balance Equations

Equation (4.4) and Eq. (4.5) represent real and reactive power balance equations respectively.

$$P_i - V_i \sum_{j=1}^{N_B} V_j (G_{ij} Cos\theta_{ij} + B_{ij} Sin\theta_{ij}) = 0, i = 1,2,\ldots. N_{B-1} \qquad (4.4)$$

$$Q_i - V_i \sum_{j=1}^{N_B} V_j (G_{ij} Sin\theta_{ij} - B_{ij} Cos\theta_{ij}) = 0, i = 1,2,\ldots N_{PQ} \quad (4.5)$$

4.2.2 Inequality Constraints

These constraints can be generalized by Eq. (4.6).

$$h_{\min} \le h(x,u) \le h_{\max} \quad (4.6)$$

(i) Inequality Constraints on State Variables

(a) Transmission line apparent power flow limit constraint is given by Eq. (4.7).

$$S_{Li} \le S_{Li\max}, \qquad Li \in N_{PQ} \quad (4.7)$$

(b) PQ bus voltage limit constraint is given by Eq. (4.8).

$$V_{Li\min} \le V_{Li} \le V_{Li\max}, \; Li \in N_{PQ} \quad (4.8)$$

(c) Generation reactive power constraint is given by Eq. (4.9).

$$Q_{Gi\min} \le Q_{Gi} \le Q_{Gi\max}, G_i \in N_{PV} \quad (4.9)$$

(i) Inequality Constraints on Control Variables

(a) Generation voltage limit constraint is given by Eq. (4.10).

$$V_{Gi\min} \le V_{Gi} \le V_{Gi\max}, \qquad G_i \in N_{PV} \quad (4.10)$$

(b) Generation real power limit constraint is given by Eq. (4.11).

$$P_{Gi\min} \le P_{Gi} \le P_{Gi\max}, \quad G_i \in N_{PV} \quad (4.11)$$

(c) Load management constraint is given by Eq. (4.12).

$$P_{DLi\min} \le P_{DLi} \le P_{DLi\max}, \; Li \in N_{PQ} \quad (4.12)$$

4.2.3 Security Constraints

(i) Line Utilization Factor LUF Constraint

Line Utilization Factor Constraint is given by Eq. (4.13).

$$LUF_{ij} = \left(\frac{P_{ij}}{P_{ij}^{\max}} \right) \leq 1 \tag{4.13}$$

(ii) Voltage Stability Index VSI Constraint

Voltage Stability Index Constraint is given by Eq. (4.14).

$$VSI_{ij} = \frac{2\sqrt{\left(P_j^2 + Q_j^2\right)}}{2Q_j X - V_i^2} \leq 1 \tag{4.14}$$

4.3 Constraint Handling

There are two types of constraints governing the CM cost problem.

4.3.1 Equality Constraint Handling

The handling violation in equality constraints has been done through Newton-Raphson load flow calculation method.

4.3.2 Inequality Constraint Handling

(a) Handling Constraints on Control Variables

If any control variable (u) of an individual violates its constraints, the individual's position has been adjusted according to the relation given by Eq. (4.15).

$$u = \begin{Bmatrix} u_{\min} \rightarrow if \quad u \prec u_{\min} \\ u_{\max} \rightarrow if\, u \succ u_{\max} \end{Bmatrix} \tag{4.15}$$

(b) Handling Constraints on State Variables

For this purpose, constraint-prior optimal dominance method has been implemented to preserve the diversity of the algorithm, which has been explained below:

If any state variable x violates its inequality constraints, the cumulative constraint violations have been calculated by Eq. (4.16).

$$\text{Cumulative Violation } (CV(X)) = \sum_{N=1}^{Nsv} \max(h_N(x,u),0) \tag{4.16}$$

To obtain the non-dominated solutions for the entire search space, cumulative violation has to be crossed checked for the conditions as expressed by Eq. (4.17), Eq. (4.18) and Eq. (4.19).

(i) **If** $CV(X_1) = CV(X_2)$ (4.17)

$$X_1 \text{ dominates } X_2 \Leftrightarrow \begin{pmatrix} X_1 \text{ is not worse than } X_2 \text{ for all objective evaluation} \\ X_1 \text{ is strictly better than } X_2 \text{ at least in one objective} \end{pmatrix}$$

(ii) **If** $CV(X_1) < CV(X_2)$ (4.18)

X_1 dominates X_2.

(iii) **If** $CV(X_1) > CV(X_2)$ (4.19)

X_2 dominates X_1.

X_1 is called as the optimal solution if X_1 dominates the solution X_2 and vice-versa. The implementation of constraint prior optimal dominance methodology has been done to attain non-dominated solutions within the entire search space. These non-dominated solutions are actually the global optimal solutions.

4.4 Mathematical Formulation of Upstream Real Capacity Tracing (URCT) Algorithm for Deciding Number of Participating Generators

Basic Upstream Real Capacity Tracing (URCT) algorithm has been illustrated by (Bialek, 1996; Malaki *et al.,* 2001) in which power flow tracing and proportional sharing principle had been explained.

Here, the modified mathematical formulation of URCT algorithm has been done as follows.

Considering a system having n number of nodes and k number of generators

The gross power inflow P_i through node i can be expressed by Eq. (4.20).

$$P_i^{gross} = \sum_{j \in \alpha_i^u} \left| P_{i-j}^{gross} \right| + P_{Gi} \quad i = 1,2,3.....,n \tag{4.20}$$

$\left|P_{i-j}^{gross}\right|$ is the total power flow from through node $i-j$, α_i^u is set of nodes supplying power directly to node i and P_G is vector of nodal power generations.

P_{Gi} is expressed by Eq. (4.21).

$$P_{Gi} = P_i^{gross} - \sum_{j \in \alpha_i^u} \frac{\left|P_{i-j}\right|}{P_j} P_j \tag{4.21}$$

Upstream tracing is the best way to allocate the level of participation of each generator to each overloaded transmission line in the transmission network. The upstream distribution matrix A_u of the order $n \times n$ can be derived from Eq. (4.20) and is expressed by Eq. (4.22).

$$A_u P = P_G \tag{4.22}$$

The $(i-j)^{th}$ element of A_u can be expressed by Eq. (4.23).

$$[A_u]_{i-j} = \begin{pmatrix} 1 & for\, i = j \\ -\frac{\left|P_{i-j}\right|}{P_j} & for\, j \in \alpha_i^u \\ 0 & else \end{pmatrix} \tag{4.23}$$

If the inverse of upstream distribution matrix exists, Eq. (4.22) can be written as

$$P = A_u^{-1} P_G \tag{4.24}$$

The i^{th} element of P can be written as $P_i = A_u^{-1} P_G$ for $i = 1,2,3.....n$ and this shows the contribution of the k^{th} generator to the i^{th} nodal power. Using proportional sharing principle, line outflow in line $i-j$ can be expressed using Eq. (4.25) to Eq. (4.27).

$$\left|P_{i-j}\right| = \frac{\left|P_{i-j}\right|}{P_i} P_i \tag{4.25}$$

$$\left|P_{i-j}\right| = \frac{\left|P_{i-j}\right|}{P_i} \sum_{k=1}^{n} \left[A_u\right]_{ik}^{-1} P_{GK} \tag{4.26}$$

$$\left|P_{i-j}\right| = \sum_{k=1}^{n} CF_{i-j,k}^{G} P_{GK} \forall j \in \alpha_i^d \tag{4.27}$$

Here , $CF_{i-j,k}^{G}$ denotes Real Power Contribution factor (RPCF) and is the flow in the line $i-j$ due to k^{th} generator and α_i^d is set of nodes supplied directly from node i.

4.5 Criterion of Load Management

If any of the security constraint is violated or some physical congestion persists even after the rescheduling of generation, there is a need of load management to restore the complete healthy system. In this section; various indexes governing the load management have been described for the necessary load shedding.

4.5.1 Sensitivity Index (μ_S)

The ratio of change of power flow ΔP_k on the target branch k , due to a change in load power ΔP_j , at bus j gives the sensitivity factor (S_{kj}) of the target branch k as given by Eq. (4.28).

$$\Delta P_k = S_{kj} \Delta P_j \tag{4.28}$$

The index which ranks the sensitivity factors of different locations of the system is called sensitivity index and is given by Eq. (4.29).

$$\mu_{Sj} = \begin{cases} 1 & (S_{kj} \geq S^{\max}) \\ \dfrac{S_{kj} - S^{\min}}{S^{\max} - S^{\min}} & (S^{\min} \leq S_{kj} \leq S^{\max}) \\ 0 & (S_{kj} \leq S^{\max}) \end{cases} \tag{4.29}$$

$S^{\max}$ indicates maximum sensitivity in the system. $S^{\min}$ shows the dead band minimum sensitivity in the system below index μ_S is 0.

4.5.2 Load Curtailment Index (μ_{cL})

If ΔP_d is the minimum reduction of power flow on the congested branch, the required amount of adjustment at bus j is given by Eq. (4.30).

$$u_{CLj}^{req} = \frac{\Delta P_d}{S_{kj}} \tag{4.30}$$

The acceptable range of curtailment must be expressed by the customer as $u_{cL}^{\max}$ and $u_{cL}^{\min}$. The acceptable level can be measured by the index μ_{cLj} given by Eq. (4.31).

$$\mu_{cLj} = \begin{cases} 1 & (u_{cLj} \le u_{cL}^{\min}) \\ \dfrac{u_{cL}^{\max} - u_{cLj}}{u_{cL}^{\max} - u_{cL}^{\min}} & (u_{cL}^{\min} \le u_{cLj} \le u_{cL}^{\max}) \\ 0 & (u_{cLj} \ge u_{cL}^{\max}) \end{cases} \tag{4.31}$$

Index $\mu_{cLj} = 1$, indicates the acceptable range of load curtailment for the customers, and $\mu_{cLj} = 0$, depicts the non-acceptable range of load curtailment for the customers.

4.5.3 Incentive Cost Index (μ_{IC})

This index measures the level of incentive offered to customer to curtail the load and is given by Eq. (4.32) for j^{th} bus.

$$\mu_{ICj} = \begin{cases} 1 & (\lambda_j \ge \lambda_{\max}) \\ \dfrac{\lambda^{\max} - \lambda_j}{\lambda^{\max} - \lambda^{\min}} & (\lambda^{\min} \le \lambda_j \le \lambda^{\max}) \\ 0 & (\lambda_j \le \lambda^{\max}) \end{cases} \tag{4.32}$$

where $\lambda_{\max}$ is the highest locational price, and $\lambda_{\min}$ gives the dead band below which the incentive is zero for load cutback.

4.5.4 Overall Index (ω_L)

The overall index for load management is given by Eq. (4.33).

$$\omega_{Lj} = \mu_{Sj} \cdot \mu_{CLjj} \cdot \mu_{IC\,j} \tag{4.33}$$

As all individual's indexes are scaled between 0 and 1; therefore, the overall index also falls between 0 and 1. The feasibility of CM option by load management is possible by evaluating the overall index for all the buses.

Load shedding amount LSA can be evaluated using the relation given by Eq. (4.34).

$$LSA = (1 - w_L)\sum_{j=1}^{Ns}(-\Delta P_{Dj})\forall j \tag{4.34}$$

4.6 PSO Algorithms

In the following subsections various PSO algorithms and proposed ITM-CPSO has been explained.

4.6.1 Modified PSO

PSO is a stochastic algorithm generally used for nonlinear optimization and was first proposed by Kennedy and Eberhart (1995). A swarm consists of N particles moving around in a D-dimensional search space. If each particle is represented in two dimensional planes with position (P_x, P_y) and velocity (V_x and V_y), equations for computing the velocity and position are given by Eq.(4.35) and Eq. (4.36).

$$V_i^{k+1} = wV_i^k + c_1 * r_1 * (P_{besti} - P_i^k) + c_2 * r_2 * (G_{best} - P_i^k) \tag{4.35}$$

$$P_i^{K+1} = P_i^K + V_i^{K+1} \tag{4.36}$$

To prevent algorithm divergence, the final value of velocity for each particle is limited, which is given by Eq. (4.37).

$$V_F \in [-V_{\max}, V_{\min}] \tag{4.37}$$

Fast convergence is achieved by properly selecting the inertia weight (w), which is defined by Eq. (4.38).

$$w = w_{\max} - \frac{w_{\max} - w_{\min}}{k_{\max}} \times k \tag{4.38}$$

4.6.2 Chaotic Particle Swarm Optimization (C-PSO)

Chaos is basically regular randomness of a simple deterministic, nonlinear, bounded and non-converging dynamical system. The random variables and chaotic sequence based on logistic maps are given by Eq. (4.39) and Eq. (4.40).

$$r_1(k) = \lambda \times r_1(k-1) \times [1 - r_1(k-1)] \quad (4.39)$$

$$r_2(k) = \lambda \times r_2(k-1) \times [1 - r_2(k-1)] \quad (4.40)$$

If the logistic map is taken into consideration then, the chaotic sequence is given by the Eq. (4.41).

$$c_r(k) = \lambda * C_r(k-1) * [1 - C_r(k-1)] \quad (4.41)$$

$$rand_1(0), rand_2(0) and C_r(0) \notin \{0, 0.25, 0.5, 0.75, 1\}$$

When $\lambda = 4$, the logistic map is ergodic in (0, 1), but if the value of λ is given, the distribution of logistic map is not flat as indicated by Liu ***et al.*** 2005. Values in [0, 0.1] and [0.9, 1] distribution are more frequent than the rest range of [0, 1], when is equal to $\lambda = 4$. The velocity equation for C-PSO is modified and given by Eq. (4.42).

$$V_i^{k+1} = w * V_i^k + C_1 * C_r * (P_{besti} - P_i^k) + C_2 * (1 - C_r) * (G_{best} - P_i^k) \quad (4.42)$$

4.6.3 Improved Tent Map based Chaotic PSO (ITM-CPSO)

The tent maps have more flat distributions than logistic maps and are insensitive to selection of initial values. Improved tent map chosen here has been defined by Eq. (4.43).

$$C_r x_i^{k+1} = \begin{cases} \dfrac{C_r x_i^k}{\lambda}, C_r x_i < \lambda \\ \dfrac{1 - C_r x_i^k}{1 - \lambda}, C_r x_i \geq \lambda \end{cases} \quad \text{, for } \lambda = 0.8 \quad (4.43)$$

Here $C_r x_i^0$ is chosen 0.01. The tent map with driving parameter $\lambda = 0.5$ is simple tent map and there exit minor periodic cycle points (0.2, 0.4, 0.6, 0.8) and unstable periodic cycle points (0.25, 0.5, 0.75). In order to come out of these limitations, λ has been chosen 0.8 as recommended by Yaoyao ***et al.*** (2008) to evenly distribute the chaotic sequence among all the iterations.

4.7 Mapping of the Chaotic Variables to Decision Variables

1. Initialize chaotic variables randomly. Check for any stuck of chaotic variables into periodic cycles, if there is any plugs of these variables into fixed points; insert a small positive random perturbation.

2. If there is no stuck of chaotic variables, remap the variables directly by Eq. (4.43).

3. For $k = 0$, Mapping of the decision variables x_i^k, among interval $(x_{\min,i}, x_{\max,i})$, $i = 1,2,3,.....n$, to chaotic variables $C_r x_i^k$ distributed in range (0, 1) has been done using relationship given by Eq. (4.44).

$$C_r x_i^k = \frac{x_i^k - x_{\min,i}}{x_{\max,i} - x_{\min,i}}, \; i = 1,2,3,.....n. \tag{4.44}$$

4. Determination of chaotic variables for the next generation is done using Eq. (4.43).

5. Mapping the chaotic variables $C_r x_i^{k+1}$ to decision variables x_i^{k+1} is done using Eq. (4.45).

$$x_i^{k+1} = x_{\min,i} + C_r x_i^{k+1}(x_{\max,i} - x_{\min,i}) \tag{4.45}$$

6. Evaluate new solutions with decision variables x_i^{k+1}.

7. If the obtained swarm is better than $X^{(0)} = [x_1^0, x_2^0, ..., x_n^0]$, update particle swarm using new solution.

8. Repeat the steps 3 to 7.

The adaptation of chaotic variables to decision variables has been shown in Table 4.1.

Table 4.1: Adaptation of the chaotic variables to decision variables

1. Set iteration count of chaotic search $k = 0$, Initialize chaotic variables $C_r^0 = (c_{r0}^0, c_{r1}^0, ..., c_{rn}^0)$ randomly. Map the variables directly by Eq. (4.43) for subsequent iteration. Also initialize the best function value set as X_{best}^0 for all the particles in the population. If X_{best}^g be the best optimal solution attained until generation ends, replace this by X_{opt} and the corresponding fitness as f_{opt}.
2. Mapping of the decision variables x_i^k, among intervals $(x_{\min,i}, x_{\max,i})$, $i = 1,2,3,.....n$ to chaotic variables $C_r x_i^k$ distributed in range (0,1) has been done using relationship given by Eq.

(4.44).

$$C_r x_i^k = \frac{x_i^k - x_{\min,i}}{x_{\max,i} - x_{\min,i}}, i = 1,2,3\ldots,n \quad (4.44)$$

3. Determine chaotic variables for the next generation using Eq. (4.43).

4. Map chaotic variables $C_r x_i^{k+1}$ to decision variables x_i^{k+1} using Eq. (4.45).

$$x_i^{k+1} = x_{\min,i} + C_r x_i^{k+1}(x_{\max,i} - x_{\min,i}) \quad (4.45)$$

5. Generate chaotic local search point $\left(Xc_{ri}^k\right)$ using linearly varying combination of above decision variables as given by Eq. (4.46).

Attain best solution until generation ends (X_{best}^g).

$$Xc_{ri}^k = (1-\in)x_i^k + \in x_{besti}^g, \text{ for } i = 1,2,3,.....n \quad (4.46)$$

where $\in$ is a constraint handling the linear combination of x_i^k and x_{best}^g and lies between [0,1].

The fitness value of Xc_r^k is calculated, if this is better than X_{opt}, replace the current Xc_r^k with X_{opt} and the corresponding fitness with f_{opt}^g.

6. Evaluate new solutions with variables X_i^{k+1}.

If the obtained swarm is better than $X^{(0)} = [x_1^0, x_2^0, ..., x_n^0]$, update particle swarm using new solution. Repeat the steps 2 to 6.

4.8 Application of Proposed Algorithm to Congestion Management Cost Problem

The building steps of the proposed algorithm have been shown in Table 4.2.

Table 4.2: Building steps for the proposed algorithm

(a) Set $k = 0$, Initialize the position and velocity of each particle, and also initialize the personal best position for each particle.
(b) Evaluate the objective function for each particle.
(c) Compare the evaluated values of the objective function for all the particles and obtain the

best value of objective function.
(d) Obtain the global best solution among all the particles by comparing their fitness value.
(e) See stopping criterion, *if* it met, *then* declare the output the current generation result, *else* update particles velocities and positions according to Eq. (4.35) and Eq. (4.36).
(f) Evaluate fitness of the updated particles and update personal best (P_{best}) and (G_{best}).
(g) Repeat the steps 1 to 6 from Table 4.1. Implement the mapping of chaotic variables to decision variables and update the best particle with variables $x_{best,i}^{k}, i = 1,2,3.....,n.$
(h) Check the two stopping criterions, First is to see whether the maximum number of iterations ($k = k_{\max}$) have reached and second is to check if congestion is completely relieved. *If* both the criterions are met *then* output the solution as global best so far, *else* $k = k + 1$ to meet first stopping criterion and perform the possible load curtailment to meet second stopping criterion.

Figure 4.1 presents the flow chart for proposed approach.

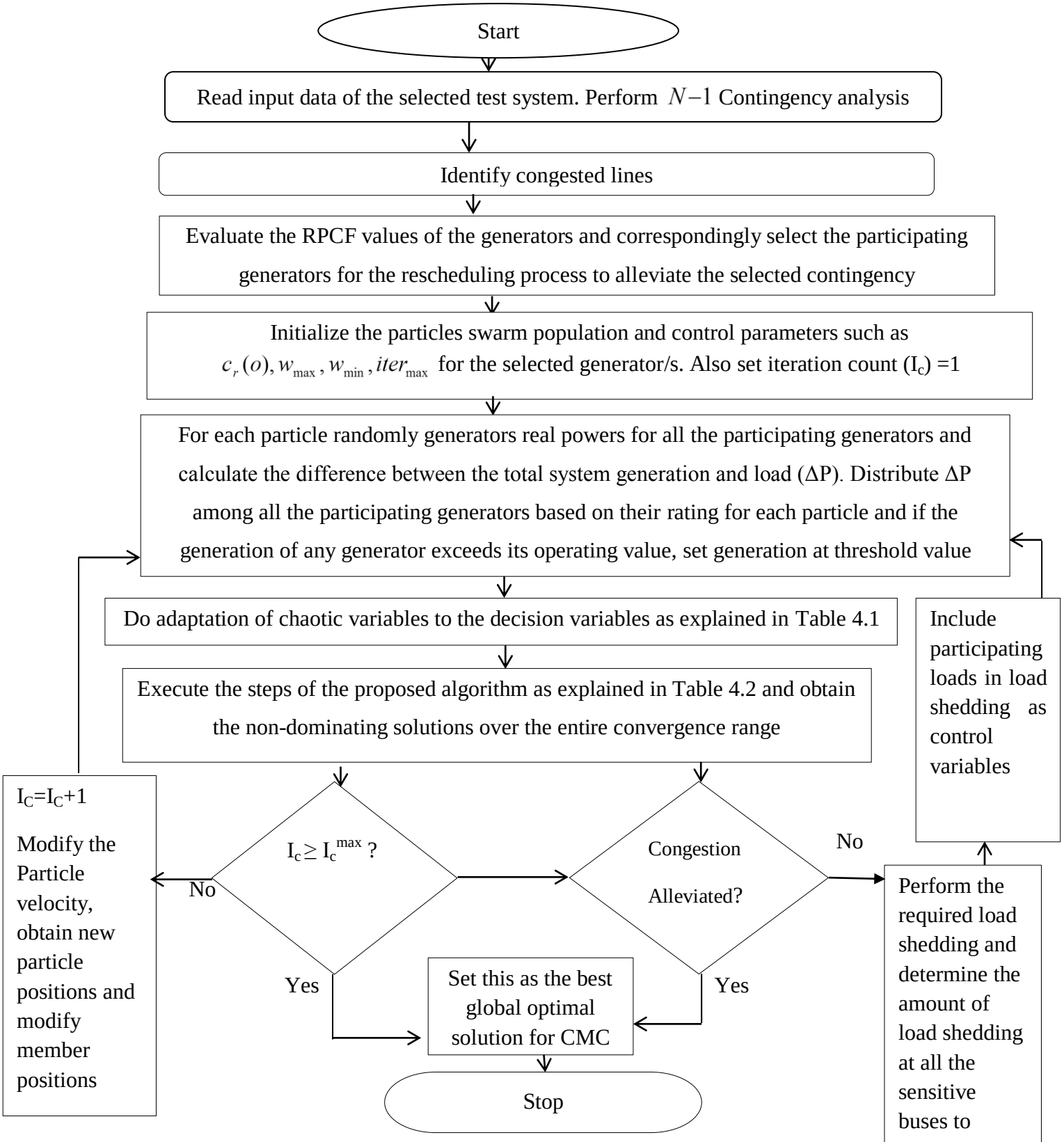

Figure 4.1: Flow chart of the proposed approach

4.9 Simulation Results and Discussions

The proposed algorithm has been demonstrated for various contingencies of two test systems. The parameter selection for the proposed algorithm has been done as shown in Table 4.3.

Table 4.3: Parameters of the ITM-CPSO

Specification	Value	Specification	Value
Total number of generations	150 (IEEE 30 & IEEE 57 bus systems)	w_{min}	0.4
Population Size	60	C_1	2
w_{max}	0.9	C_2	2

A large of weight factor facilitates global exploration while small weight factor facilitates local exploration. To make a balance between both global and local exploration, w_{min} has been chosen as 0.4 and w_{max} has been selected as 0.9. C_1, C_2 have been chosen 2 since this will make the weights for social and cognition parts to be 1.

In this work, line outage cases of two test systems have been chosen to demonstrate the implementation of CM with load shedding approach using proposed algorithm.

4.9.1 IEEE 30 Bus System

This system has 6 generator buses, 24 load buses and 41 transmission lines. Data details of bus data and line data of the system are given in **Appendix A1**.

The description of two line outage cases, their respective congested lines, line flow limits, line flows (during congestion and after rescheduling) and % line utilization factors has been shown in Table 4.4. Amount of line flows in the congested lines, before and after rescheduling process decide the necessity of load management for the respective line outage cases.

Table 4.4: Description of line outage cases, line flows and line utilization factor

Description of Test Case	**Congested Line**	**Line Flow During congestion (MVA)**	**Line flow limit (MVA)**	**Line Flow after Rescheduling (MVA)**	**% Line Utilization Factor after rescheduling**	**Line Flow after CM**
Case 1A: Outage of line 6-10	4-12	69.887	65	66.574	102.4	64.78
Case 1B: Outage of line 4-6	1-2 2-6	191.78 93.884	130 65	136.78 64.9	105.2 99.84	129 64

In above mentioned line outage cases, it has been observed that there is a violation of security constraint *LUF* after rescheduling process of generators. Therefore, there is a need of load management for the complete restoration of the system within permissible limits. As the line utilization factor of the congested lines has been found to be above 1 after rescheduling process as shown in Table 4.4, so there is a need of load curtailment for the overall congestion relieve.

The generators participation factors for the said outage cases (case 1A and 1B) have been found using URCT algorithm and are plotted in Fig. 4.2 and Fig. 4.3 respectively. Figure 4.2 and Fig. 4.3 show the distribution of RPCF values of individual generators among various lines of the system for the described contingencies. The bar distribution of RPCF of generators among congested lines is shown with red color. From this distribution of RPCF of generators among congested lines, it is observed that G2, G5 and G8 are the participating generators for the rescheduling process for case 1A and G2, G8 and G11 are the contributing generators for case 1B. The evaluated numbers of participating generators are exact and accurate.

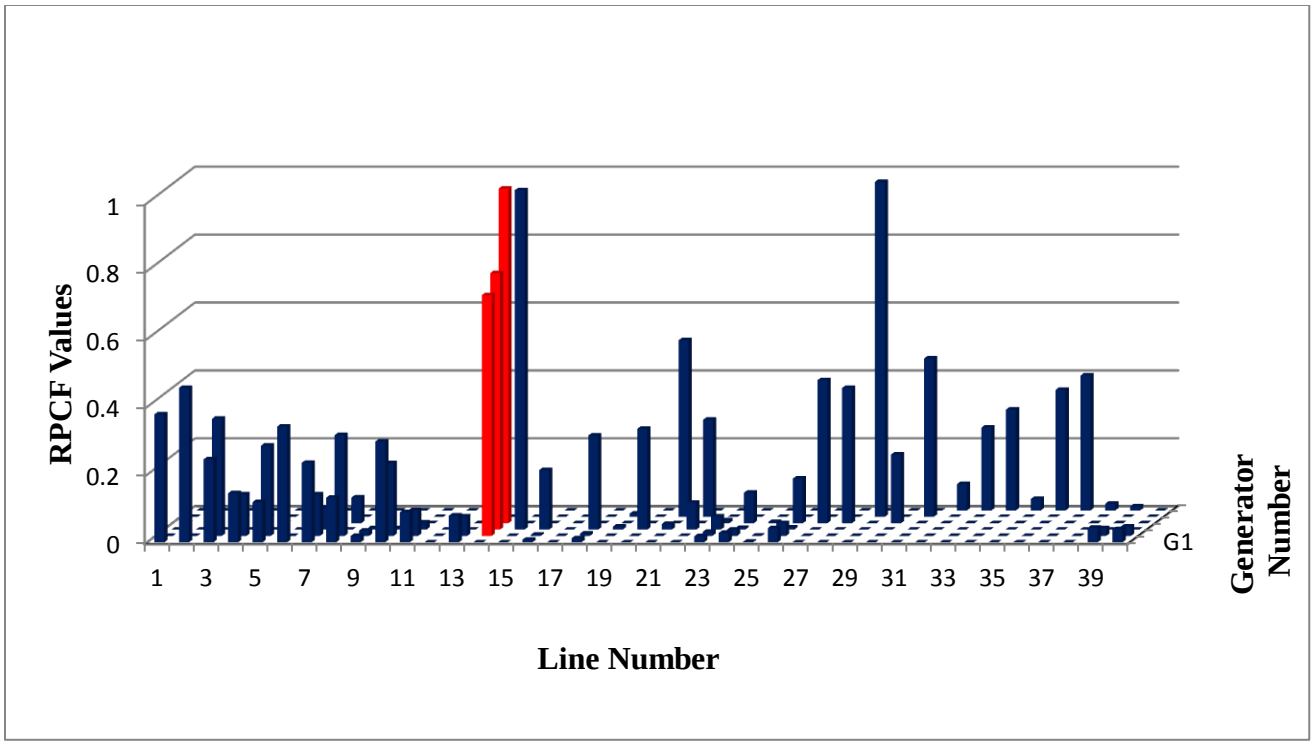

Figure 4.2: Distribution of generators contribution factors among various lines for line contingency case 1A

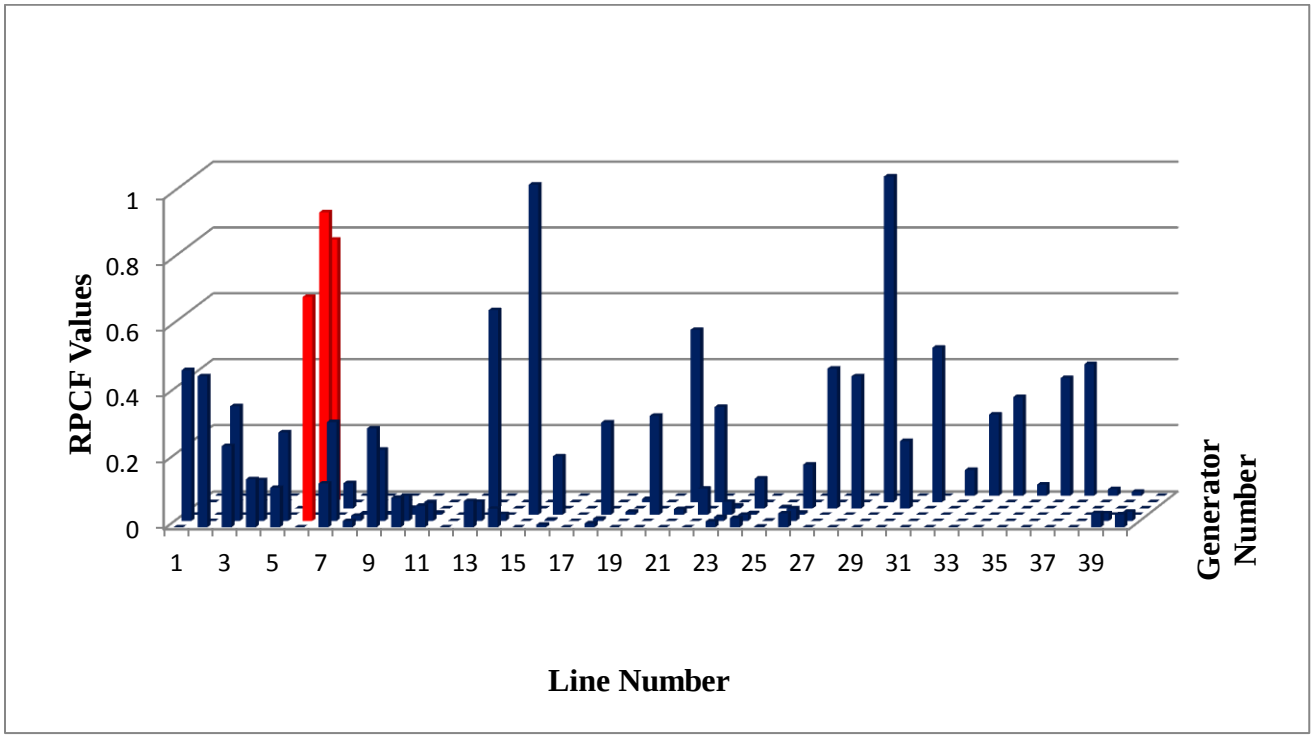

Figure 4.3: Distribution of generators contribution factors among various lines for line contingency case 1B

The load shed buses have been selected on the basis of *VSI* values; high value of *VSI* indicates the week buses and need load shedding. Top most 5 buses have been selected on the basis of *VSI* for case 1A and 6 buses have been ranked for case 1B for load shedding process, which is shown in Table 4.5. Various performance indexes for the selected week buses have been evaluated for both the contingency cases and are also shown in Table 4.5. Keeping in considerations the errors of the optimal power flow results, ΔP_d is set at 3% of the congested power flows, also, $u^{\max}$ and $u^{\min}$ are chosen as 30% and 5% of the scaled load respectively at each bus and for index μ_{cLj} loading margin is chosen 0.1.

Table 4.5: Performance indices for the most sensitive buses for both test cases

Case 1A **Bus No**	**VSI (Rank)**	**Sensitivity (S)**	**Sensitivity index** μ_S	**Incentive cost index** μ_{IC}	**Load Curtailment** u_{cL} **(MW)**	**Load Curtailment Index** μ_{cL}	**Overall Index** ω_L
4	0.124 (4)	0.4023	0.5678	0.345	2.67	0	0
12	0.345 (2)	0.6796	0.4965	0.8775	3.13	0.2399	0.1045
18	0.078 (5)	0.3578	0.3125	0.3237	2.12	0	0
24	0.476 (1)	0.7935	1	0.2878	3.35	0.82130	0.2363
29	0.145 (3)	0.3678	0.0568	0.567	1.78	0.1456	0.014
Case 1B **Bus No**	**VSI (Rank)**	**Sensitivity (S)**	**Sensitivity index** μ_S	**Incentive cost index** μ_{IC}	**Load Curtailment** u_{cL} **(MW)**	**Load Curtailment index** μ_{cL}	**Overall Index** ω_L
2	0.214	0.8634	1	0.9758	2.3875	0.6502	0.6345

	(3)						
3	0.124 (5)	0.4389	0.000	0.4567	2.47008	0	0
4	0.134 (4)	0.5288	0.2115	0.4537	3.7762	0	0
5	0.345 (1)	0.8367	0.9364	0.9988	4.0768	1	0.9544
7	0.279 (2)	0.8209	0.8993	0.6244	2.4767	0.6357	0.5615
30	0.098 (6)	0.7723	0.7848	0.3456	1.5882	0	0

From the results of the overall index and the amount of load curtailment needed to alleviate congestion, the necessary load shedding has been performed and is shown in Fig. 4.4 and Fig. 4.5 respectively for both cases.

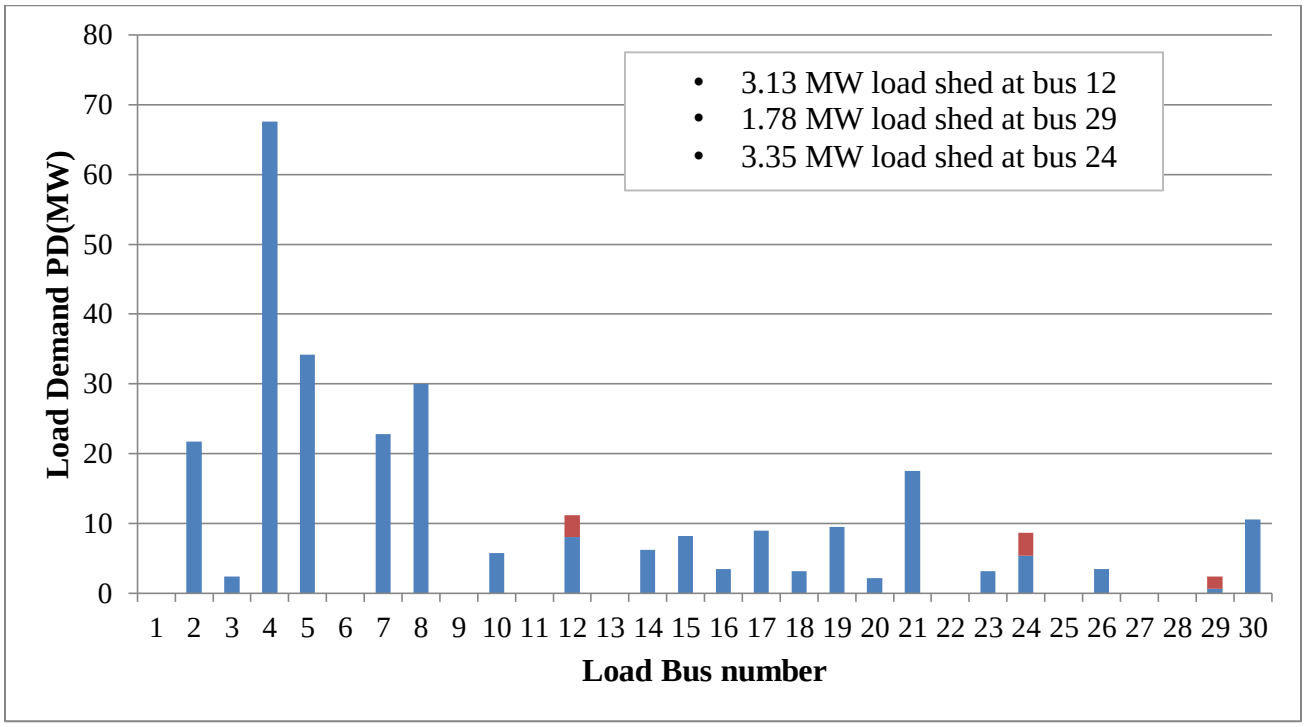

Figure 4.4: Amount of necessary load shedding needed at three buses for complete congestion relieve for case 1A

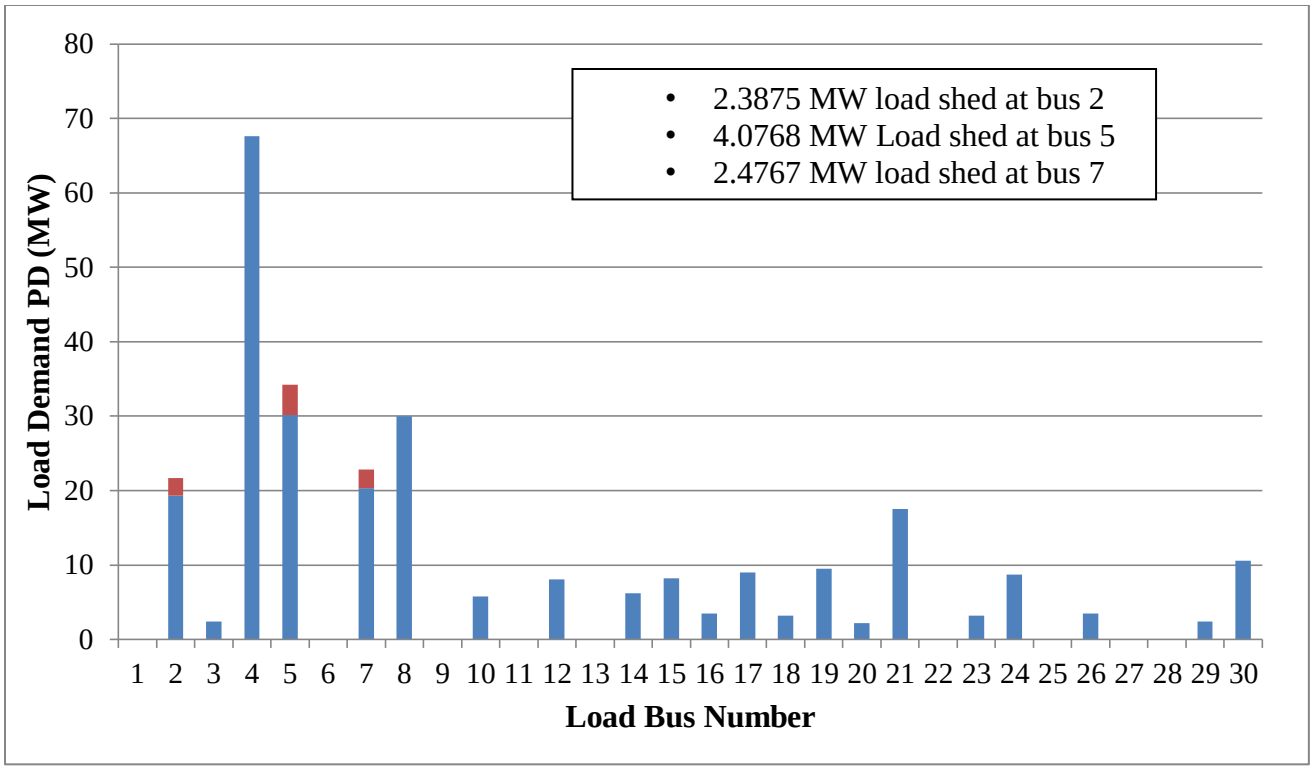

Figure 4.5: Amount of necessary load shedding needed at three buses for complete congestion relieve for case 1B

The simulation results of the re-dispatch of generators, load shedding cost, net power loss and overall congestion management cost to relieve the contingencies of both the test cases have been elaborated in Table 4.6.

Table 4.6: Simulation results of generation re dispatch, load shedding cost, rescheduling cost and net congestion management cost for cases 1A and 1B

Bus No	**Case 1A**			**Case 1B**		
	Generator Output (MW) When congested	**Amount of Rescheduling (MW)**	**Generator Output (MW) After Congestion Removal**	**Generator Output (MW) When congested**	**Amount of Rescheduling (MW)**	**Generator Output (MW) after Congestion Removal**
1	85.8	NP*	85.8	69.97	NP*	69.97
2	115.4	-40	79.4	48.97	-10.0120	38.2980

			(re-dispatched)			(re-dispatched)
5	71.4	-18.6	52.8 (re-dispatched)	91.6	NP*	91.6
8	43	-10.52	32.48 (re-dispatched)	21.5	+6.3312	27.8312 (re-dispatched)
11	26	NP*	26	12.24	+3.1614	15.4010 (re-dispatched)
13	32	NP*	32	56	NP*	56
TGR	69.12 MW			-0.5194 MW		
Total load shedding amount (MW)	8.28 MW			8.941 MW		
Load shedding cost ($/h)	23.56			58.67		
Rescheduling cost($/h)	229.78			274.5		
Net CMC ($/h)	253.34			333.17		

NP*- Not Participating

Total load shedding is approximately 3% and 3.5% of the total load demand for case 1A and case 1B respectively, which is sufficient to relieve the congestion for both the systems. The overall congestion management costs (including rescheduling and load shedding costs) for case 1A and case B are found to be 253.34 $/h and 333.17 $/h respectively, which is found to be minimum for the said outages. The voltage profiles before and after load shedding for both the test cases have been plotted and are shown in Fig. 4.6 and Fig. 4.7 respectively.

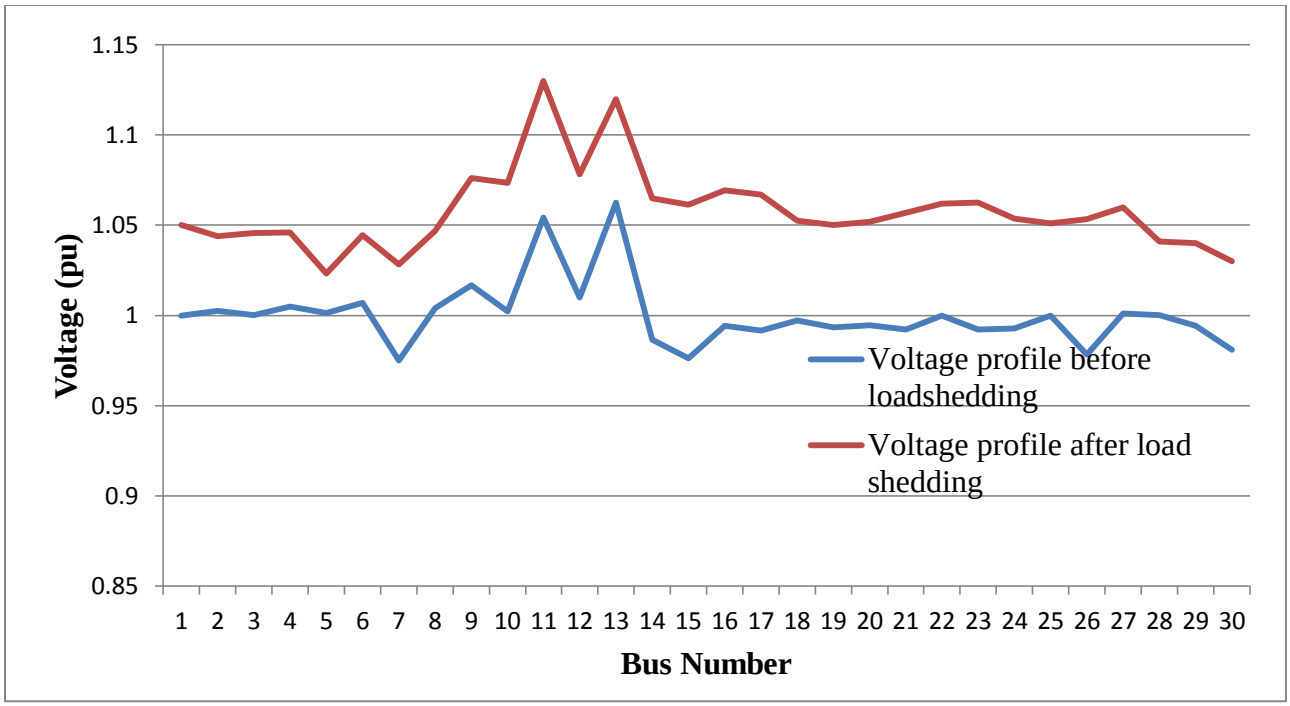

Figure 4.6: Voltage profiles of various buses before and after load shedding for case 1A line outage

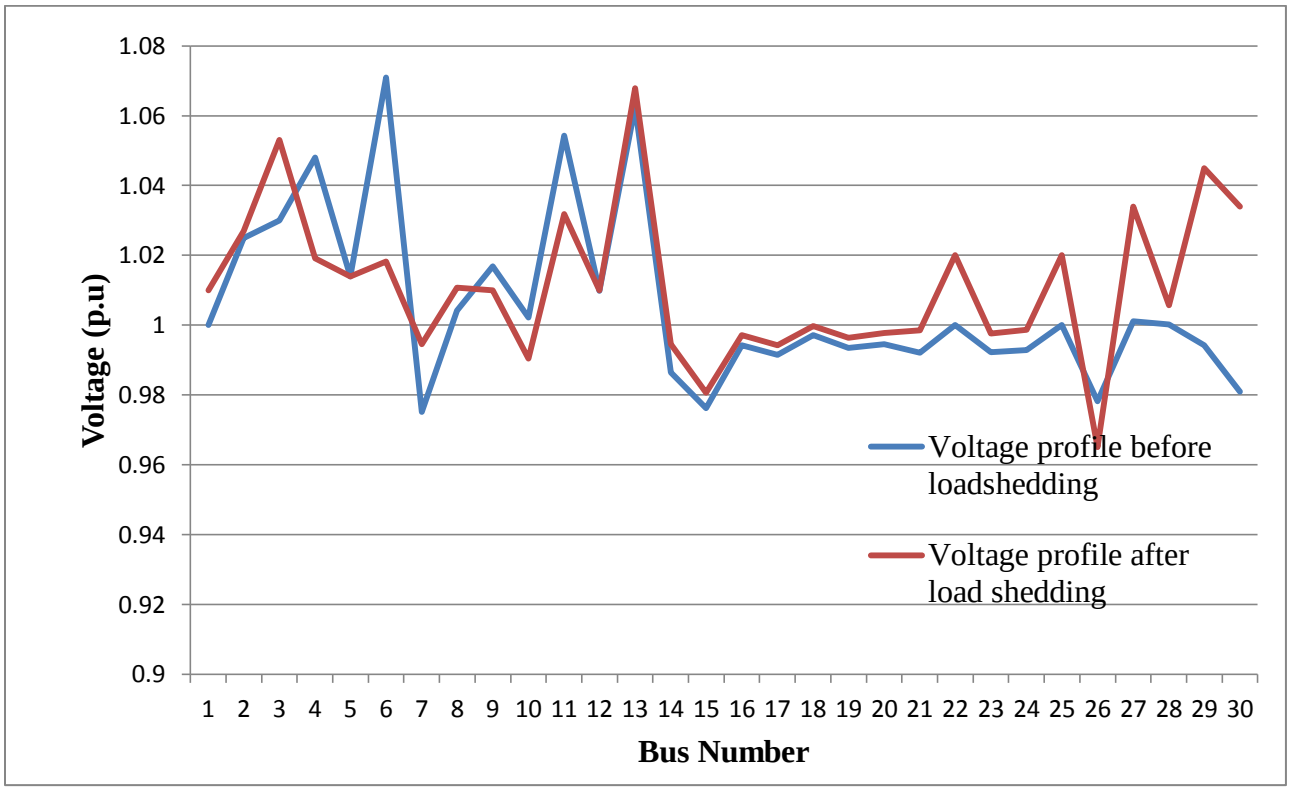

Figure 4.7: Voltage profiles of various buses before and after load shedding for case 1B line outage

4.9.2 IEEE 57 Bus System

Details of the bus system can be found in **Appendix A1**. Description of the multiple line contingency case has been shown in Table 4.7. There are six congested lines corresponding to outage of line 1-15.Overloading of the congested lines has to be minimized or the line flows need to come under specified limits for complete congestion removal.

The contributing generators for the rescheduling process have been found using URCT algorithm and the distribution of RPCF values of all the generators among various lines of the system has been shown in Fig. 4.8. Red bars in the figure represent the RPCF values of generators corresponding to the contingency lines. This distribution clearly indicates that 6 generators are actually participating in rescheduling process. After carrying rescheduling process, it has been observed that there is no complete congestion relieve as there are three congested lines, which are having $LUF > 1$. So, this necessitates the load management for the complete congestion relieve of the said case.

Table 4.7: Description of line outage cases, line flows and line utilization factor

Description of Test Case	**Congested Line**	**Line Flow before CM (MVA)**	**Line flow limit (MVA)**	**Line Flow After Rescheduling (MVA)**	**% Line Utilization Factor after rescheduling**	**Line Flow After CM (MVA)**
Case 2: Outage of line 1-15	1-2	123.87	99	105.23	106.29	98.23
	2-3	114.34	99	98.89	99.98	98.89
	1-16	115.67	99	98.65	99.64	98.65
	3-15	107.75	99	109.56	110.66	96.83
	12-17	108.44	99	108.56	109.65	95.367
	12-16	154.78	99	94.89	95.84	94.89

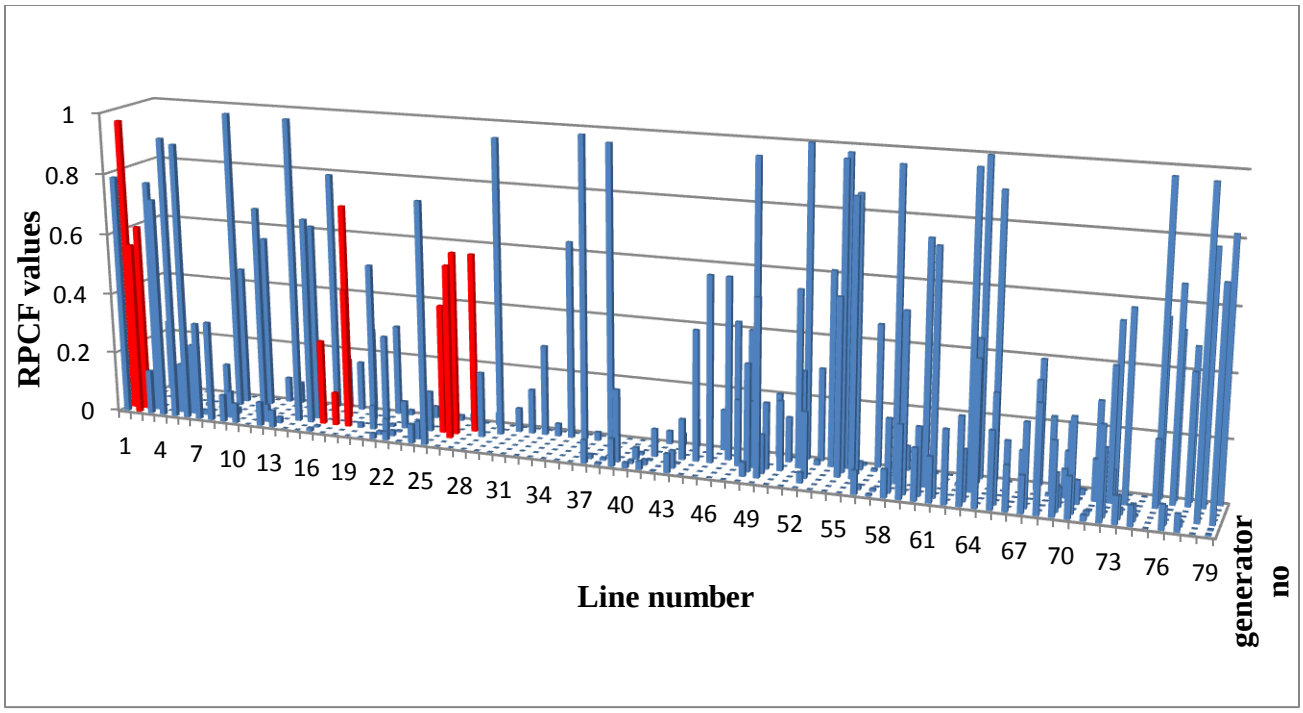

Figure 4.8: Distribution of generators contribution factors among various lines for line contingency case 2

Top most sensitive 15 buses have been selected on the basis of *VSI* for load shedding process. All the performance indexes governing the load management procedure have been evaluated and are shown in Table 4.8.

Table 4.8: Performance indices for the most sensitive buses of the system for case 2

Case 2 **Bus No.**	**VSI (Rank)**	**Sensitivity (S)**	**Sensitivity index** μ_S	**Incentive cost index** μ_{IC}	**Load Curtailment** u_{cL} **(MW)**	**Load Curtailment index** μ_{cL}	**Overall Index** ω_L
5	0.599(11)	1	0.4564	0.2354	7.834	0.0675	0.0072
6	0.729(3)	0.8756	0.3456	0.6778	13.956	0.4565	0.1069
13	0.687(7)	0.8789	0.5643	0.3456	10.878	0.5678	0.1107
15	0.702(4)	0.9865	0.5678	0.5667	13.26	0.6789	0.2184
18	0.754(2)	1	0.6785	0.4523	16.54	0.7653	0.2348

27	0.523(13)	0.8209	0.8993	0.6244	5.7967	0.9674	0.5432
29	0.632(9)	0.8965	0.7895	0.1254	10.634	0.3556	0.035
38	0.604(10)	0.9214	0.8990	0.6778	8.6756	0.3452	0.2103
42	0.457(15)	0.7647	0.6789	0.5456	4.678	0.7895	0.2924
44	0.587(12)	0.3546	0.7856	0.2378	7.6256	0.3567	0.0666
47	0.787 (1)	0.9468	0.8956	0.5467	17.8975	0.7895	0.3865
49	0.689(6)	0.8567	0.8675	0.7890	10.978	0.3450	0.2361
50	0.699(5)	0.9126	0.8690	0.6778	12.78	0.3456	0.2035
51	0.654(8)	0.8975	0.8967	0.6789	10.687	0.6789	0.4132
56	0.497(14)	0.3246	0.7890	0.3456	4.6789	0.54678	0.5467

From the statistical results, it has been shown that there is a need of 152.124 MW load shedding to completely relieve the congestion. Load demand and load shedding amount at various identified buses are plotted in Fig. 4.9.

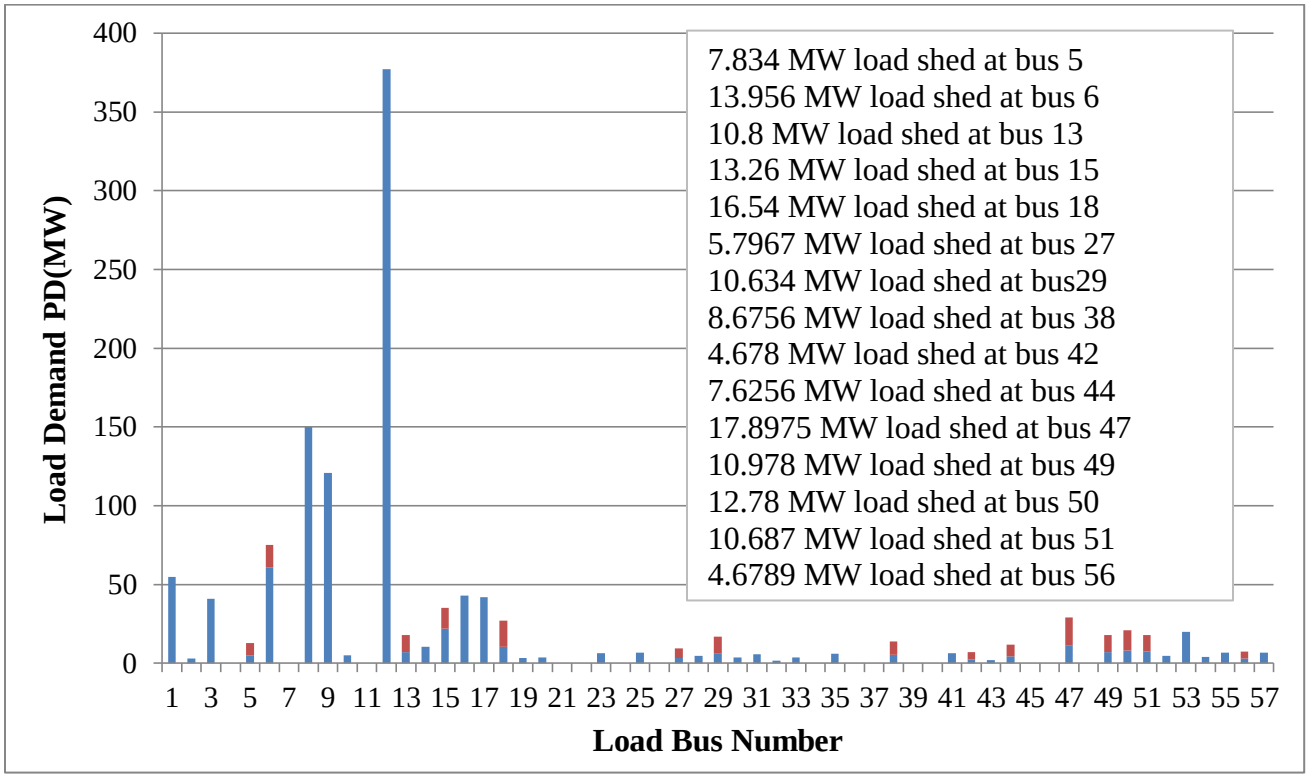

Figure 4.9: Amount of necessary load shedding needed at three buses for complete congestion relieve for case 2

Amount of load re-dispatch after congestion relief has been found to be about 1107.963 MW. Amount of load shedding and rescheduling costs for the test case 2 have been evaluated and are given in Table 4.9.

Table 4.9: Simulation results of generation re-dispatch, load shedding cost, rescheduling cost and net congestion management cost for case 2

Bus Number	**Case 2**		
	Generator Output (MW) When congested	**Amount of Rescheduling (MW)**	**Generator Output (MW) After Congestion Removal**
1	45.78	26.13	71.91 (re-dispatched)
2	65.67	19.44	85.11 (re-dispatched)
3	76.56	8.49	85.05 (re-dispatched)
4	89.67	−78.38	11.19 (re-dispatched)
5	92.56	−49.21	43.35 (re-dispatched)
6	75.34	NP*	75.34
7	74.78	19.03	93.81 (re-dispatched)
TGR	-54.5 (MW)		
Total load shedding amount (MW)	186.0882		
Load shedding cost ($/h)	545.67		
Rescheduling cost ($/h)	278.56		
Net CMC ($/h)	824.23		

NP*- Not Participating

System loss has been reduced to 20.9886 MW after congestion relief from 23.45 MW during congestion. Voltage improvement profile after load management of the test system is plotted in Fig. 4.10.

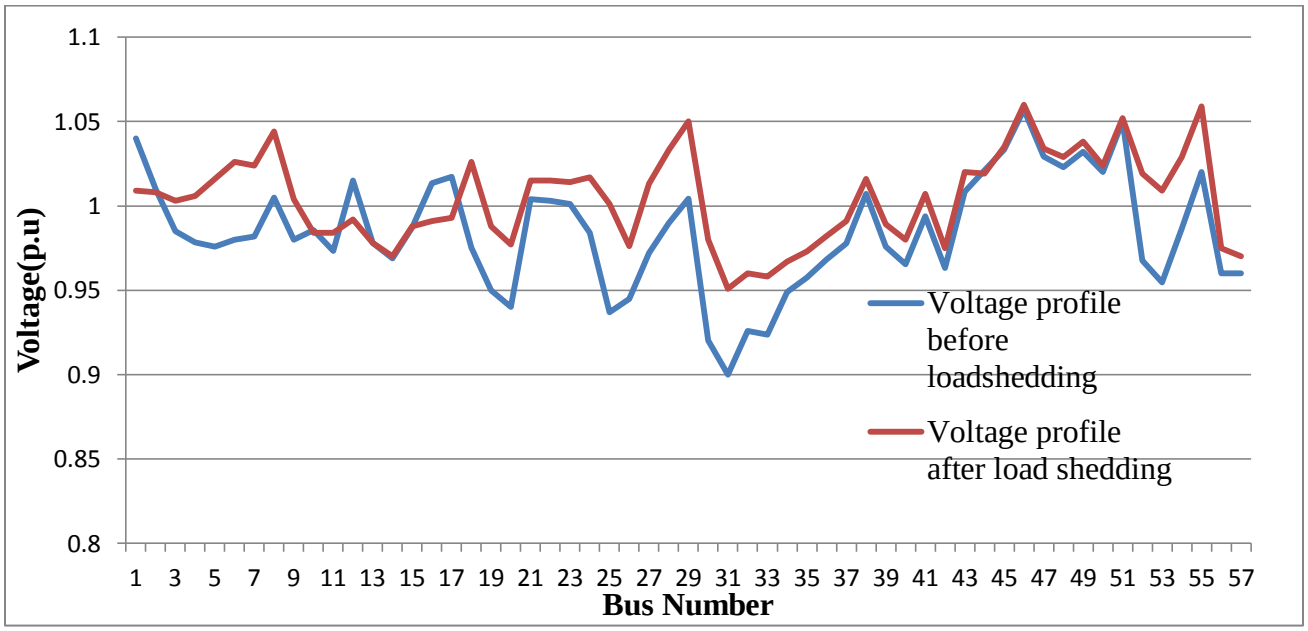

Figure 4.10: Voltage profiles of various buses before and after load shedding for case 2

4.10 Concluding Remarks

The main attribute of the proposed work is that the incursion of load management objective in the overall congestion management cost function has increased the reliability of the approach for all types of contingencies. Implementation of URCT algorithm for exact determination of participating generators for rescheduling process has remarkably reduced the efforts of a system operator as it requires very less generator information. Furthermore, the implementation of ITM-CPSO algorithm has substantially improved the profile of the congestion management in terms of reduced rescheduling, load shedding and net congestion management cost. The key facts like robustness to initial conditions, best searching quality and superior efficiency of proposed algorithm has confined the results to the best optimal ones. There is a substantial reduction in overall system losses after congestion relieve for each contingency case. Moreover, the voltage profiles of both the test systems have improved after load shedding, which ensures the secure operation of power system after CM using this technique.

Chapter 5: Implementation of ITM-CPSO for Optimal Placement of UPFC for Stability and Reliability Enhancement

5.1 Introduction

Security and reliability of power system are big challenges for a system operator under deregulated environment. Generally, power systems are designed on the basis of $N-1$ security criterion, which is an expensive and conservative process. $N-1$ represents first contingency, which means tripping of a line. To increase the stability and security of the power system under contingency, the concept of FACT devices was introduced by Hingorani ***et al.*** (2000). Among various FACT devices, UPFC is the most resourceful device as it can simultaneously control many parameters as well as can also regulate power flows of connecting buses effectively. In order to achieve the full benefits, it should be optimally located. The choice of UPFC location and parameter setting include some of the important factors such as improvement in stability and security margins, improvement in bus voltage profiles, ATC increment and prevention of power cut off. In the proposed work; two main factors, which are improvement in voltage profile of buses and increase in security and stability margins, have been chosen for the optimal allocation of UPFC.

This chapter presents an optimized approach for attaining the exemplary position and parametric settings of UPFC for enhancing system security and reliable operation of power system under contingency conditions. Initially, the severe outage line contingencies have been evaluated using performance index based ranking process and then the ITM-CPSO algorithm (detailed in Chapter 4) has been implemented to optimally allocate UPFC under each chosen outage line contingency. ITM-CPSO is a hybrid evolutionary algorithm, whose search procedure performs with in a normalized plane of search space for all the chosen optimization variables for population based procedures. The dual and full benefits of the characteristics of chaotic variables (i.e., periodicity and randomness) and Tent map (i.e., more flat distribution than logistic maps) have been taken while formulating the problem.

5.2 Mathematical Formulation for UPFC Power Equations

The following subsections explain the equivalent circuit of UPFC and its power injection model. Mathematical formulation of objective functions and its governing constraints have been done and are also presented.

5.2.1 Equivalent Circuit of UPFC and its Power Injection Model

UPFC is the most resourceful FACT device, which incorporates a combination of a shunt controller and a series controller interconnected through a common link. Figure 5.1 shows the equivalent circuit of UPFC. There are two ideal voltage source sources, shunt and series impedances connecting the transformers. Mathematical equations for ideal voltage source converters of UPFC can be represented by Eq. (5.1) and Eq. (5.2).

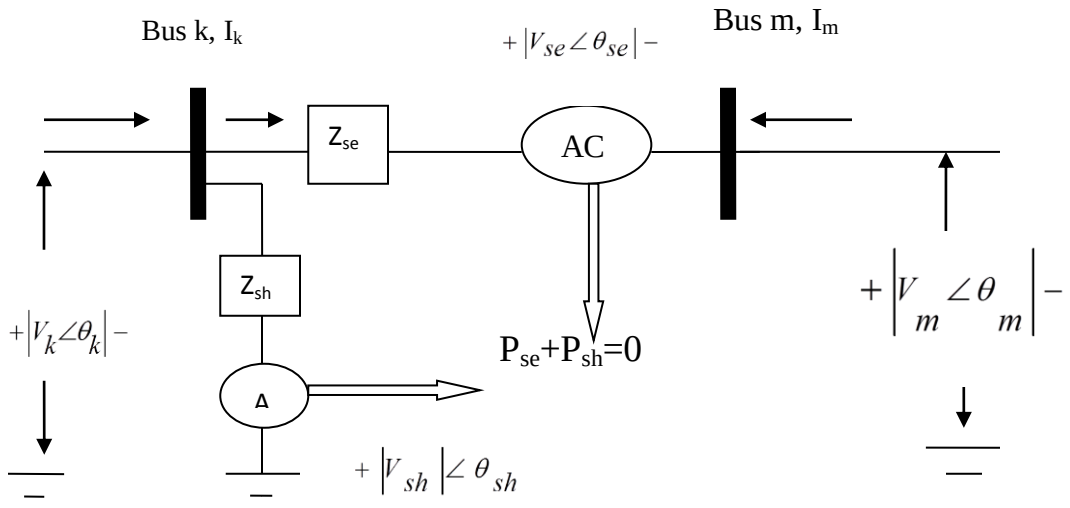

Figure 5.1: Equivalent circuit of UPFC **(**Zahid ***et al.,*** 2017)

$$E_{sh} = V_{sh}(\cos\theta_{sh} + j\sin\theta_{sh}) \tag{5.1}$$

$$E_{se} = V_{se}(\cos\theta_{se} + j\sin\theta_{se}) \tag{5.2}$$

The power injection at bus k and m can be found using power flow equations from Eq. (5.3) to Eq. (5.10).

At Bus k

$$P_k = V_k^2 G_{kk} + V_k V_m \left[G_{km} \cos(\theta_k - \theta_m) + B_{km} \sin(\theta_k - \theta_m)\right] + V_k V_{se} [G_{km} \cos(\theta_k - \theta_{se}) + B_{km} \sin(\theta_k - \theta_{se})] + V_k V_{sh} [G_{sh} \cos(\theta_k - \theta_{sh}) + B_{sh} \sin(\theta_k - \theta_{sh})] \quad (5.3)$$

$$Q_k = -V_k^2 B_{kk} - V_k V_m \left[G_{km} \sin(\theta_k - \theta_m) - B_{km} \cos(\theta_k - \theta_m)\right] + V_k V_{se} [G_{km} \sin(\theta_k - \theta_{se}) - B_{km} \cos(\theta_k - \theta_{se})] + V_k V_{sh} [G_{sh} \sin(\theta_k - \theta_{sh}) - B_{sh} \cos(\theta_k - \theta_{sh})] \quad (5.4)$$

At Bus m

$$P_m = V_m^2 G_{mm} + V_m V_k \left[G_{mk} \cos(\theta_m - \theta_k) + B_{mk} \sin(\theta_m - \theta_k)\right] + V_m V_{se} [G_{mm} \cos(\theta_m - \theta_{se}) + B_{mm} \sin(\theta_m - \theta_{se})] \quad (5.5)$$

$$Q_m = -V_m^2 B_{mm} + V_m V_k \left[G_{mk} \sin(\theta_m - \theta_k) - B_{mk} \cos(\theta_m - \theta_k)\right] + V_m V_{se} [G_{mm} \sin(\theta_m - \theta_{se}) - B_{mm} \cos(\theta_m - \theta_{se})] \quad (5.6)$$

Power flow equations of series converter

$$P_{se} = V_{se}^2 G_{mm} + V_{se} V_k \left[G_{km} \cos(\theta_{se} - \theta_k) + B_{km} \sin(\theta_{se} - \theta_k)\right] + V_{se} V_m [G_{mm} \cos(\theta_{se} - \theta_m) + B_{mm} \sin(\theta_{se} - \theta_m)] \quad (5.7)$$

$$Q_{se} = -V_{se}^2 B_{mm} + V_{se} V_k \left[G_{km} \sin(\theta_{se} - \theta_k) - B_{km} \cos(\theta_{se} - \theta_k)\right] + V_{se} V_m [G_{mm} \sin(\theta_{se} - \theta_m) - B_{mm} \cos(\theta_{se} - \theta_m)] \quad (5.8)$$

Power flow equations of shunt converter

$$P_{sh} = -V_{sh}^2 G_{sh} + V_{sh} V_k \left[G_{sh} \cos(\theta_{sh} - \theta_k) + B_{sh} \sin(\theta_{sh} - \theta_k)\right] \quad (5.9)$$

$$Q_{sh} = V_{sh}^2 B_{sh} + V_{sh} V_k \left[G_{sh} \sin(\theta_{sh} - \theta_k) - B_{sh} \cos(\theta_{sh} - \theta_k)\right] \quad (5.10)$$

Real power delivered to shunt converter P_{sh} is assumed to be equivalent to the real power required by the series converter P_{se} as represented by Eq. (5.11).

$$P_{sh} + P_{se} = 0 \quad (5.11)$$

5.2.2 UPFC Jacobian Equations

Linearized power flow equations with UPFC integrated with the existing system, can be represented as Eq. (5.12) and Eq. (5.13).

$$\begin{bmatrix} \Delta P_k \\ \Delta P_m \\ \Delta Q_k \\ \Delta Q_m \\ \Delta P_{mk} \\ \Delta Q_{mk} \\ \Delta P_g \end{bmatrix} = \begin{bmatrix} \frac{\partial P_k}{\partial \theta_k} & \frac{\partial P_k}{\partial \theta_m} & \frac{\partial P_k}{\partial V_{sh}} V_{sh} & \frac{\partial P_k}{\partial V_m} V_m & \frac{\partial P_k}{\partial \theta_{se}} & \frac{\partial P_k}{\partial V_{se}} V_{se} & \frac{\partial P_k}{\partial \theta_{sh}} \\ \frac{\partial P_m}{\partial \theta_k} & \frac{\partial P_m}{\partial \theta_m} & 0 & \frac{\partial P_m}{\partial V_m} V_m & \frac{\partial P_m}{\partial \theta_{se}} & \frac{\partial P_m}{\partial V_{se}} V_{se} & 0 \\ \frac{\partial Q_k}{\partial \theta_k} & \frac{\partial Q_k}{\partial \theta_m} & \frac{\partial Q_k}{\partial V_{sh}} V_{sh} & \frac{\partial Q_k}{\partial V_m} V_m & \frac{\partial Q_k}{\partial \theta_{se}} & \frac{\partial Q_k}{\partial V_{se}} V_{se} & \frac{\partial Q_k}{\partial Q_{sh}} \\ \frac{\partial Q_m}{\partial \theta_k} & \frac{\partial Q_m}{\partial \theta_m} & 0 & \frac{\partial Q_m}{\partial V_m} V_m & \frac{\partial Q_m}{\partial \theta_{se}} & \frac{\partial Q_m}{\partial V_{se}} V_{se} & 0 \\ \frac{\partial P_{mk}}{\partial \theta_k} & \frac{\partial P_{mk}}{\partial \theta_m} & 0 & \frac{\partial P_{mk}}{\partial V_m} V_m & \frac{\partial P_{mk}}{\partial \theta_{se}} & \frac{\partial P_{mk}}{\partial V_{se}} V_{se} & 0 \\ \frac{\partial Q_{mk}}{\partial \theta_k} & \frac{\partial Q_{mk}}{\partial \theta_m} & 0 & \frac{\partial Q_{mk}}{\partial V_m} V_m & \frac{\partial Q_{mk}}{\partial \theta_{se}} & \frac{\partial Q_{mk}}{\partial V_{se}} V_{se} & 0 \\ \frac{\partial P_g}{\partial \theta_k} & \frac{\partial P_g}{\partial \theta_m} & \frac{\partial P_g}{\partial V_{sh}} V_{sh} & \frac{\partial P_g}{\partial V_m} V_m & \frac{\partial P_g}{\partial \theta_{se}} & \frac{\partial P_g}{\partial V_{se}} V_{se} & \frac{\partial P_g}{\partial \theta_{sh}} \end{bmatrix} \begin{bmatrix} \Delta \theta_k \\ \Delta \theta_m \\ \frac{\Delta V_{sh}}{V_{sh}} \\ \frac{\Delta V_m}{V_m} \\ \Delta \theta_{se} \\ \frac{\Delta V_{se}}{V_{se}} \\ \Delta \theta_{sh} \end{bmatrix} \tag{5.12}$$

ΔP_g is the power mismatch between the shunt and series converters.

Linearized power flow equations can be modified as Eq. (5.13) if k and m are taken as PQ buses.

$$\begin{bmatrix} \Delta P_k \\ \Delta P_m \\ \Delta Q_k \\ \Delta Q_m \\ \Delta P_{mk} \\ \Delta Q_{mk} \\ \Delta P_g \end{bmatrix} = \begin{bmatrix} \frac{\partial P_k}{\partial \theta_k} & \frac{\partial P_k}{\partial \theta_m} & \frac{\partial P_k}{\partial V_k} V_k & \frac{\partial P_k}{\partial V_m} V_m & \frac{\partial P_k}{\partial \theta_{se}} & \frac{\partial P_k}{\partial V_{se}} V_{se} & \frac{\partial P_k}{\partial \theta_{sh}} \\ \frac{\partial P_m}{\partial \theta_k} & \frac{\partial P_m}{\partial \theta_m} & \frac{\partial P_m}{\partial V_k} V_k & \frac{\partial P_m}{\partial V_m} V_m & \frac{\partial P_m}{\partial \theta_{se}} & \frac{\partial P_m}{\partial V_{se}} V_{se} & 0 \\ \frac{\partial Q_k}{\partial \theta_k} & \frac{\partial Q_k}{\partial \theta_m} & \frac{\partial Q_k}{\partial V_k} V_k & \frac{\partial Q_k}{\partial V_m} V_m & \frac{\partial Q_k}{\partial \theta_{se}} & \frac{\partial Q_k}{\partial V_{se}} V_{se} & \frac{\partial Q_k}{\partial Q_{sh}} \\ \frac{\partial Q_m}{\partial \theta_k} & \frac{\partial Q_m}{\partial \theta_m} & \frac{\partial Q_m}{\partial V_k} V_k & \frac{\partial Q_m}{\partial V_m} V_m & \frac{\partial Q_m}{\partial \theta_{se}} & \frac{\partial Q_m}{\partial V_{se}} V_{se} & 0 \\ \frac{\partial P_{mk}}{\partial \theta_k} & \frac{\partial P_{mk}}{\partial \theta_m} & \frac{\partial P_{mk}}{\partial V_k} V_k & \frac{\partial P_{mk}}{\partial V_m} V_m & \frac{\partial P_{mk}}{\partial \theta_{se}} & \frac{\partial P_{mk}}{\partial V_{se}} V_{se} & 0 \\ \frac{\partial Q_{mk}}{\partial \theta_k} & \frac{\partial Q_{mk}}{\partial \theta_m} & \frac{\partial Q_{mk}}{\partial V_k} V_k & \frac{\partial Q_{mk}}{\partial V_m} V_m & \frac{\partial Q_{mk}}{\partial \theta_{se}} & \frac{\partial Q_{mk}}{\partial V_{se}} V_{se} & 0 \\ \frac{\partial P_g}{\partial \theta_k} & \frac{\partial P_g}{\partial \theta_m} & \frac{\partial P_g}{\partial V_k} V_k & \frac{\partial P_g}{\partial V_m} V_m & \frac{\partial P_g}{\partial \theta_{se}} & \frac{\partial P_g}{\partial V_{se}} V_{se} & \frac{\partial P_g}{\partial \theta_{sh}} \end{bmatrix} \begin{bmatrix} \Delta \theta_k \\ \Delta \theta_m \\ \frac{\Delta V_{sh}}{V_{sh}} \\ \frac{\Delta V_m}{V_m} \\ \Delta \theta_{se} \\ \frac{\Delta V_{se}}{V_{se}} \\ \Delta \theta_{sh} \end{bmatrix} \tag{5.13}$$

Here V_{sh} is assumed to be within the specified limits.

5.3 Contingency Ranking Procedure

Contingency analysis and ranking process should be performed by a system operator to ensure security and reliability power system. If the contingency exist for a long period, the system may become unstable. Here, the contingencies have been analyzed and ranked on the basis of "Performance Index" measurement. NOLL and NVVB are identified and the lines are ranked according to their severity index (NOLL + NVVB). This process is followed for the whole selected system and after this, the proposed algorithm is implemented for UPFC placement for various contingencies.

5.4 Objective Function

Elimination of line over loadings and bus over voltages is considered as the main criterion while formulating the objective function as expressed by Eq. (5.14).

$$OF = \sum_{l=1}^{Nl} w_l \left(\frac{S_l}{S_{l\max}} \right)^{2p} + \sum_{nb=1}^{NB} w_m \left(\frac{V_m^{ref} - V_m}{V_m^{ref}} \right)^{2q} \tag{5.14}$$

5.4.1 Equality Constraints

Power balance conditions must be satisfied, which are considered as the equality constraints as expressed by Eq. (5.15) to Eq. (5.18).

For bus k

$$P_k(V_k, \theta_k) + P_{dk} - P_{gk} = 0 \tag{5.15}$$

$$Q_k(V_k, \theta_k) + Q_{dk} - Q_{gk} = 0 \tag{5.16}$$

For bus m :

$$P_m(V_m, \theta_m) + P_{dm} - P_{gm} = 0 \tag{5.17}$$

$$Q_m(V_m, \theta_m) + Q_{dm} - Q_{gm} = 0 \tag{5.18}$$

5.4.2 Inequality Constraints

These constraints represent working parameter limits of generators, transformers and buses as expressed by Eq. (5.19) to Eq. (5.24).

$$P_{gk}^{\min} \le P_{gk} \le P_{gk}^{\max} .....k = 1,....., n_g \quad (5.19)$$

$$Q_{gk}^{\min} \le Q_{gk} \le Q_{gk}^{\max} .....k = 1,....., n_g \quad (5.20)$$

$$V_k^{\min} \le V_k \le V_k^{\max} .....k = 1,....., n_b \quad (5.21)$$

$$\theta_k^{\min} \le \theta_k \le \theta_k^{\max} \quad (5.22)$$

$$V_{sh}^{\min} \le V_{sh} \le V_{sh}^{\max} \quad (5.23)$$

$$V_{se}^{\min} \le V_{se} \le V_{se}^{\max} \quad (5.24)$$

Two variables namely series voltage source with operating range [0.001- 0.2] and shunt voltage source with range [0.9-1.1] of UPFC are simultaneously optimized.

5.5 Implementation of ITM-CPSO for Obtaining Optimal Positions and Parametric Settings of UPFC

Details of ITM-CPSO have been provided in Chapter 4. Newton-Raphson (N-R) method has been chosen for the load analysis of chosen bus systems and modified N-R method has been performed for contingency analysis procedure to identify Performance Index (PI). After this, ITM-CPSO algorithm has been implemented to evaluate the minimum objective function to allocate the UPFC at optimal positions. Parameters specification and execution procedure of the proposed algorithm has been detailed below in Table 5.1 and Table 5.2 respectively.

Table 5.1: Parameters initialization of proposed computational technique

Number of particles n_P	20
Maximum number of Generation $k_{\max}$	100
$w_{\max}$	0.9
$w_{\min}$	0.4
c_1	2
c_2	2

C_r	0.8
Termination Criterion	$k_{\max}$

Table 5.2: Execution procedure of ITM-CPSO algorithm

Step No	**Procedure**
1.	Initialize ITM-CPSO related parameters, data of power flow and UPFC parameters (V_{Se}, V_{Sh}).
2.	Initialize the population of swarm individuals in the feasible space.
3.	Set iteration count $(I_c) = 0$, Initialize the position and velocity of each particle and also the personal best position for each particle.
4.	Evaluate the objective function for each particle.
5.	Compare the evaluated values of the objective function for all the particles and obtain the best value of objective function.
6.	Obtain the global best solution among all the particles by comparing their fitness value.
7.	See stopping criterion, if it met, declare the output the current generation result otherwise update particles velocities and positions according to (4.35) and (4.36).
8.	Evaluate fitness of the updated particles and update P_{best} and G_{best}.
9.	Repeat the steps 1 to 6 from Table 4.1. Implement the mapping of chaotic variables to decision variables and update the best particle with variables $x^k_{best,i}, i = 1,2,3.....,n_P$.

Proposed algorithm's flow chart is shown in Figure 5.2.

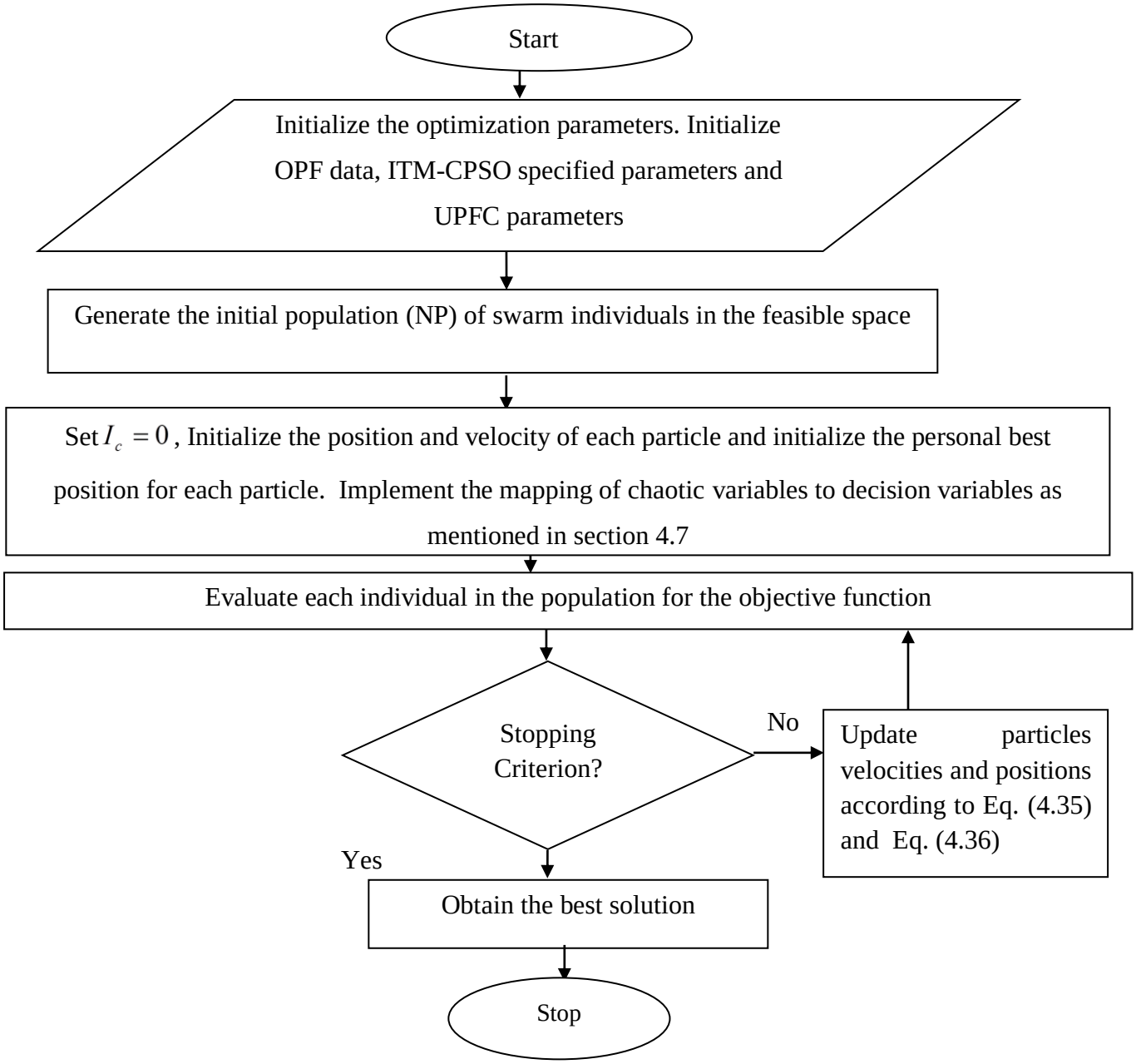

Figure 5.2: Flow chart of the proposed algorithm

5.6 Simulation Results and Discussions

For simulation purpose, MATLAB programming for both the ITM-CPSO and modified $N-R$ algorithm (incorporated with the UPFC parameters) has been done. Two test systems have been chosen for simulation purpose.

5.6.1 Test Case 1 (IEEE 14 Bus System)

This test system consists of 14 buses, 20 transmission lines, 5 generators and 11 loads. Line and bus data details of the test system are given in **Appendix 1**. As this system has 20 transmission lines so, 20 contingencies can be created for the system. NOLL and NOVB for each contingency case have been evaluated to measure the PI. 100% loading is considered as standard limit for % overloading measurement and bus voltage limit is taken from 0.9 p.u to 1.1 p.u to measure the voltage violation of buses. Main purpose of contingency analysis is to evaluate PI for each tripped line case, which further helps to rank the tripped lines. Level of severity for each tripped line case is identified using ranking operation. After performing contingency and ranking procedure for the system, 15 transmission lines are found to have maximum value of PI and the description of these 15 tripped line cases has been provided in Table 5.3.

Table 5.3: Description of contingency analysis and ranking operation procedure of IEEE 14 bus system

Tripped Line	**From Bus**	**To Bus**	**Number of overloaded lines (NOLL)**	**Number of voltage violated buses (NOVB)**	**Description of voltage violated buses (VVB)**	**Performance Index (NOLL+ NOVB)**	**Ranking**
1	1	2	5	7	2,4,5,6,7,13,14	12	1
3	2	3	4	5	3,9,10,12,14	9	2
2	1	5	2	6	9,10,11,12,13,14	8	3
10	5	6	1	5	6,11,12,13,14	6	4
4	2	4	3	2	10,14	5	5
14	7	8	0	3	9,10,14	3	6

15	7	9	0	3	9,10,14	3	7
13	6	13	1	2	13,14	3	8
5	2	5	1	1	14	2	9
7	5	4	0	1	14	1	10
8	4	7	0	1	14	1	11
9	4	9	0	1	14	1	12
16	9	10	0	1	10	1	13
17	9	14	0	1	14	1	14
20	13	14	0	1	14	1	15

From Table 5.3, it has been observed that tripping of line 1 is the most hazardous case as it involves overloading of 5 transmission lines and voltage violation of 7 buses. Complete description of % overloading of each transmission line and bus number of voltage violated buses corresponding to each contingency scenario without UPFC installation has been provided in Table 5.4.

Table 5.4: Description of % line overloading and voltage violated bus number of various contingency cases of IEEE 14 bus system (without UPFC installation)

Tripped Line	**From Bus**	**To Bus**	**Description of overloaded lines**	**% Over-loading**	**Number of voltage violated buses (NOVB)**	**Description of voltage violated buses (VVB)**
1	1	2	1-5 2-3 3-4 4-5 9-10	110.91 191.96 189.11 170.62 133.14	7	2,4,5,6,7,13,14
3	2	3	1-5 2-5 3-4 4-5	119.38 135.28 190.52 175.41	5	3,9,10,12,14
2	1	5	1-2	142.9	6	9,10,11,12,13,14

			2-5	163.7		
10	5	6	4-5	157.28	5	6,11,12,13,14
4	2	4	1-5 2-5 4-5	116.8 135.75 173.71	2	10,14
14	7	8	0	0	3	9,10,14
15	7	9	0	0	3	9,10,14
13	6	13	12-13	129.68	2	13,14
5	2	5	1-5	119.17	1	14
7	5	4	0	0	1	14
8	4	7	0	0	1	14
9	4	9	0	0	1	14
16	9	10	0	0	1	10
17	9	14	0	0	1	14
20	13	14	0	0	1	14

Table 5.4 clearly indicates that the tripping of transmission line numbers 1, 3, 2, 10, 4 are the most severe contingency cases as many lines with overloading and buses with over voltages are there with these tripping cases. To examine the utility of UPFC to alleviate all the contingencies, the steps of the proposed algorithm have been executed to find the most suitable line location of UPFC for each tripped line case. Details of line locations and the corresponding setting of UPFC parameters are shown in Table 5.6. After installing UPFC at the evaluated places using ITM-CPSO algorithm, the % overloading of lines and voltage violation details of various buses has been further evaluated and are shown in Table 5.5. It also shows the comparison of the proposed results with three other evolutionary algorithms namely AAA, DE and PSO, which are stated in literature. Deep analysis of results show that out of 15 contingency cases, 11 (outage of line 2, 14, 15, 13, 5, 7, 8, 9, 16, 17 and 20) are completed eradicated by installing UPFC at optimized locations and parameters acquired by ITM-CPSO approach corresponding to the contingency. While considering the most severe contingency case (tripping of line 1), the overloading of 3 transmission lines out of 5 has been completely vanished and overloading of rest two lines decreases from 191.96% to 102.23% (for line

2-3) and from 170.62% to 101.21% (for line 4-5) after installing UPFC at line number 6 with its parametric setting acquired by proposed algorithm.

Furthermore, all bus voltage violations are eliminated completely. While comparing the results with DE, the overloading of only two lines are completely removed and for rest three lines the overloading decreases from 191.96% to 110.42% (for line 2-3), 189.11% to 102.7 % (for line 3-4) and 170.62% to 110.76 (for line 4-5). While optimizing with PSO, the overloading % of three lines has been eliminated and overloading of line 1-5 is 108.65%, 2-4 is 112.23% and 4-5 is 138.98%. There is a generation of overloading of line 2-4; this is due to nonlinear power system structure and its system values. Analysis of results obtained with AAA, reveal that there is reduction in overloading from to 191.96% to 103.09% (for line 2-3) and 170.62% to 102.4% (for line 4-5). Also, for other line outage cases, % reduction in overloading of individual lines is highest in case of optimizing with ITM-CPSO. Statistical results of optimal line location and parametric setting of UPFC obtained after 100 independent runs of the proposed algorithm have been exposed in Table 5.6. The results are also compared with DE, PSO and AAA. Proposed algorithm outperforms for the defined objective function. Power system security and reliability are enhanced considerably as maximum relieving of % overloading and over voltages is possible while optimizing the objective function with proposed algorithm. The most severe line outage case (tripping of line 1) has been considered as the reference case for showing the voltage profiles at various buses as well as for generating convergence characteristics of objective function after installing UPFC using proposed approach. Figure 5.3 shows the distribution of voltage among various buses after placing UPFC acquired with its optimized settings at proposed optimal positions as determined by DE, PSO, AAA and ITM-CPSO. Voltage profile of the test system without UPFC is also shown in Fig. 5.3. Comparison of voltage profiles of proposed approach with three other comparative algorithms, clearly indicate that the proposed voltage profile have most uniform characteristics among all the algorithms.

Table 5.5: Description of % overloading of lines and voltage violations after using UPFC (at optimized location as shown in Table 5.6) by proposed algorithm and their comparison with AAA, DE and PSO

Tripped Line	**From Bus**	**To Bus**	**Description of overloaded lines and their (% Overloading after UPFC placement) using (DE) (Shaheen *et al.*, 2011)**	**Buses with voltage violation (DE) (Shaheen *et al.*, 2011)**	**Description of overloaded lines and their (% Overloading after UPFC placement) using (PSO) (Shaheen *et al.*, 2011)**	**Buses with voltage violation (PSO) (**Shaheen *et al.*, 2011**)**	**Description of overloaded lines and their (% Overloading after UPFC placement) using (AAA) (**Zahid ***et al.,*** 2017)	**Buses with voltage violation (AAA) (**Zahid ***et al.,*** 2017)	**Description of overloaded lines and their (% Overloading after UPFC placement) using ITM-CPSO (Proposed Algorithm)**	**Buses with voltage violation (Proposed)**
1	1	2	1-5 (0) 2-3 (110.42) 3-4 (102.7) 4-5 (110.76) 9-10 (0)	-	1-5 (108.65) 2-3 (0) 2-4 (112.23) 3-4 (0) 4-5 (138.98) 9-10 (0)	-	1-5 (0) 2-3 (103.09) 3-4 (0) 4-5 (102.4) 9-10 (0)	-	1-5 (0) 2-3 (102.23) 3-4 (0) 4-5 (101.21) 9-10 (0)	-
3	2	3	1-5 (0) 2-5 (0)	-	1-5 (0) 2-5 (0)		1-5 (0) 2-5 (0)	-	1-5 (0) 2-5 (0)	-

			3-4 (158.37) 4-5 (0)		3-4 (164.58) 4-5 (0)		3-4 (119.12) 4-5 (0)		3-4 (114.67) 4-5 (0)	
2	1	5	4-5 (102.96)	-	1-2 (0) 2-5 (0)		1-2 (0) 2-5 (0)	-	1-2 (0) 2-5 (0)	-
10	5	6	4-5 109.16	-	4-5 (114.88)	-	4-5 (101.03)	-	4-5 (101.01)	-
4	2	4	1-5 (0) 2-5 (0) 4-5 (123.18)	-	1-5 (0) 2-5 (0) 4-5 (132.26)	-	1-5 (0) 2-5 (0) 4-5 (106.05)	-	1-5 (0) 2-5 (0) 4-5 (105.12)	-
14	7	8	-	-	-	-	-	-	-	-
15	7	9	-	-	-	-	-	-	-	-
13	6	13	12-13 (0)	-	12-13 (0)	-	12-13 (0)	-	12-13 (0)	-
5	2	5	1-5 (0)	-	1-5 (0)	-	1-5 (0)	-	1-5 (0)	-
7	5	4	-	-	-	-	-	-	-	-
8	4	7	-	-	-	-	-	-	-	-
9	4	9	-	-	-	-	-	-	-	-
16	9	10	-	-	-	-	-	-	-	-
17	9	14	-	-	-	-	-	-	-	-
20	13	14	-	-	-	-	-	-	-	-

Table 5.6: Statistical results of line locations and parametric settings of UPFC by ITM-CPSO and their comparison with AAA, DE and PSO for various contingencies of IEEE 14 bus system

Tripped Line	**UPFC Line Location**				**DE (Shaheen *et al*., 2011)**		**PSO (Shaheen *et al*., 2011)**		**AAA (Zahid *et al*.,2017)**		**ITM-CPSO (proposed)**	
	Shaheen *et al*., 2011		**AAA (Zahid *et al*., 2017)**	**ITM-CPSO (Proposed)**	V_{se}	V_{sh}	V_{se}	V_{sh}	V_{se}	V_{sh}	V_{se}	V_{sh}
	DE	**PSO**										
1	6	6	3-4	6	0.173	0.900	0.089	1.094	0.1126	1.0073	0.087	1.095
3	6	6	2-5	6	0.092	0.997	0.107	1.086	0.1154	1.050	0.106	1.083
2	7	7	1-2	7	0.128	1.027	0.029	1.059	0.1233	1.0119	0.025	1.060
10	19	13	4-5	19	0.045	1.019	1.121	0.962	0.0246	0.9873	0.121	0.968
4	6	6	1-5	6	0.139	0.9756	0.119	1.082	0.1136	1.0246	0.115	1.082
14	6	6	3-4	6	0.108	1.065	0.028	1.100	0.0974	1.0231	0.024	1.100
15	17	17	10-14	17	0.026	1.055	0.045	0.927	0.1400	1.0318	0.048	0.928
13	20	20	12-13	20	0.061	1.018	0.090	1.012	0.1166	1.0162	0.078	1.011
5	20	6	1-5	6	0.036	0.927	0.109	0.900	0.1075	1.0215	0.105	0.900
7	20	6	13-14	6	0.084	0.901	0.091	0.900	0.0011	1.0409	0.094	0.900
8	20	6	3-4	6	0.037	0.987	0.046	0.950	0.1139	1.0135	0.044	0.950
9	6	20	13-14	20	0.086	0.918	0.100	0.900	0.1588	1.0078	0.102	0.900
16	6	6	3-4	6	0.101	0.90	0.079	0.900	0.1140	1.0135	0.075	0.900
17	6	6	3-4	6	0.056	1.022	0.104	0.992	0.1494	0.9095	0.100	0.994
20	6	6	3-4	6	0.077	1.033	0.089	1.094	0.1115	1.0250	0.087	1.097

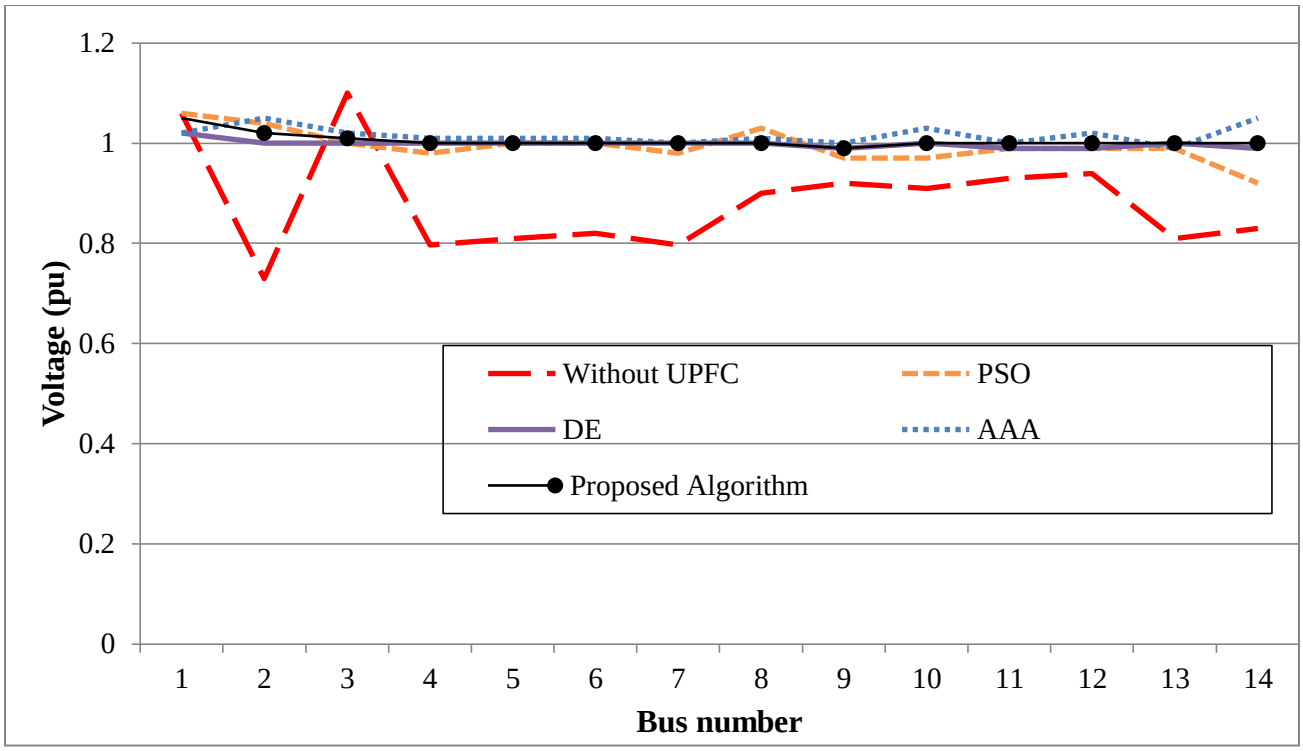

Figure 5.3: Comparison of voltage profile of IEEE 14 bus system using various optimization algorithms for most severe outage case (tripping of line 1)

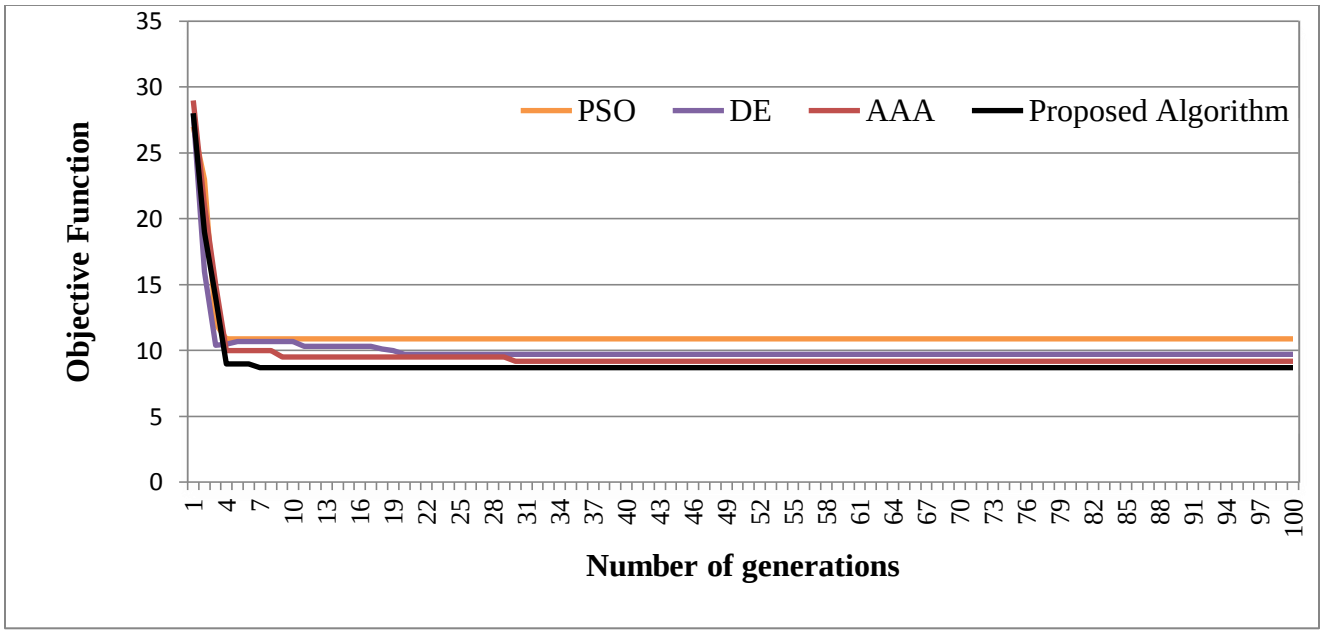

Figure 5.4: Convergence characteristics for the objective function using proposed algorithm ITM-CPSO and their comparison with DE, AAA and PSO for most severe line outage (line 1 tripped)

Furthermore, the convergence characteristics of the objective function have also been established using ITM-CPSO and are compared with convergence manners of AAA, DE and PSO optimization algorithms for the most severe line 1 outage case as shown in Fig. 5.4. Most consistent and balanced convergence characteristics are obtained using proposed technique as compared to other algorithms.

5.6.2 Test Case 2 (IEEE 30 Bus System)

This test system has 30 buses, 6 generators, 21 loads and 41 transmission lines. Bus and line data of the test system is detailed in **Appendix A1**. As this test system has 41 transmission lines so, there may be 41 contingency cases for the said system. Lines with PI $\geq$ 1 are the contingency lines. After performing contingency analysis for the test system, 23 cases have found to have higher values of PI and are chosen for the further ranking operation according to their level of severity as shown in Table 5.7.

Table 5.7: Description of contingency analysis and ranking operation procedure of IEEE 30 bus system

Tripped Line	From Bus	To Bus	Number of overloaded lines (NOLL)	Number of voltage violated buses (NOVB)	Description of voltage violated buses	Performance Index (NOLL + NOVB)	Ranking
1	1	2	9	10	2,3,4,6,7,9,12,13,14,15	19	1
14	9	10	4	10	10,16,17,18,20,21,19,22,24,26	14	2
18	12	15	1	8	14,15,18,19,20,23,24,26	9	3
10	6	8	2	4	25,26,29,30	6	4
2	1	3	4	1	3	5	5
3	2	4	5	0	0	5	6

22	15	18	2	3	18,19,20	5	7
6	2	6	4	0	0	4	8
8	5	7	3	1	7	4	9
5	2	5	3	0	0	3	10
11	6	9	3	0	0	3	11
20	14	15	2	1	14	3	12
25	10	20	0	3	18,19,20	3	13
35	25	27	1	2	25,26	3	14
36	27	28	0	3	26,29,30	3	15
4	3	4	2	0	0	2	16
29	21	22	2	0	0	2	17
37	27	29	0	2	29,30	2	18
38	27	30	1	1	30	2	19
19	12	16	1	0	0	1	20
21	16	17	1	0	0	1	21
23	18	19	0	1	19	1	22
24	19	20	0	1	19	1	23

Among 23 cases, 4 cases (outage of line: 1, 14, 18 and 10) are found to be severe and above them outage of line 1 is the most severe, with ranking 1. Outage of line 1 has resulted in overloading of 9 lines and overvoltage at 10 buses, which may result in cascade outages and failures if not prevented timely. Overloaded lines and their corresponding % overloading have also been evaluated during contingency analysis. Voltage violated buses have also been identified during the analysis. Complete description of overloaded lines, % overloading and buses with voltage violations has been revealed in Table 5.8.

Table 5.8: Description of % line over loadings with voltage violated bus number of various contingency cases of IEEE 30 bus system

Tripped Line	**From Bus**	**To Bus**	**Description of overloaded lines**	**% Overloading**	**Description of voltage violated buses**
	1	2	1-3 2-4 3-4 2-5 2-6 4-6 5-7 6-8 8-28	179.2 162.8 176.2 146.9 142.3 137.5 158.1 119.4 107.8	2,3,4,6,7,9,12,13,14,15
14	9	10	6-10 4-12 10-17 25-26	117.67 125.97 119.53 153.49	10,16,17,18,20,21,19,22,24,26
18	12	15	10-17	157.48	14,15,18,19,20,23,24,26
10	6	8	6-28 8-28	182.85 175.4	25,26,29,30
2	1	3	1-2 2-4 2-6 5-7	143.65 135.07 114.37 105.30	3
3	2	4	1-3 3-4 2-6 4-6 5-7	137.14 122.10 157.09 111.73 123.41	0
22	15	18	19-20	105.09	18,19,20

			10-20	123.41	
6	2	6	1-3 2-4 4-6 5-7	116.72 146.94 158 118.95	0
8	5	7	1-3 2-4 2-6	120.22 111.38 103.56	7
5	2	5	1-3 2-4 2-6	139.61 136.13 108.97	0
11	6	9	6-10 4-12 10-17	125.49 118.10 114.03	0
20	14	15	15-23 10-17	129.27 131.99	14
25	10	20	0	0	18,19,20
35	25	27	6-28	139.52	25,26
36	27	28	0	0	26,29,30
4	3	4	1-2 2-4	127.03 121.20	0
29	21	22	10-21 10-22	147.33 176.58	0
37	27	29	0	0	29,30
38	27	30	29-30	119.75	30
19	12	16	10-17	139.98	0
21	16	17	10-17	144.92	0
23	18	19	0	0	19
24	19	20	0	0	19

In order to alleviate these over loadings and over voltages, incorporation of UPFC at optimized line locations and parameter setting as determined from proposed algorithm has been done for each contingency case. Simulation results of the proposed algorithm for the most suitable line locations of UPFC and its parametric settings for each contingency case have been detailed in Table 5.10. After placing UPFC at evaluated optimal line locations for the each contingency case, the corresponding results of % overloading, violation of bus voltages have been summarized in Table 5.9 after 100 independent runs of proposed algorithm. From the results, it is clear that all the violations of bus voltages for 23 contingency cases are fully eradicated. Furthermore, 18 contingency cases are fully resolved for overloading and overvoltage issues by placing UPFC at their optimized locations. While analyzing the case of most severe contingency case (outage of line 1), 7 overloaded lines out of 9 are working under normal operating conditions after placing UPFC in line 7 (as determined by proposed algorithm). There is a remarkable improvement in voltage profiles of each bus after UPFC placement. Overloading of line 2-4 has been declined to 105.98 % from 162.8 % and for line 8-28 reduction in overloading is reduced from 107.8 % to 101.7%. With DE, only 6 overloaded lines are eradicated and overloading of 1-3 is reduced to 103.2%, 2-4 is declined to 129.63% and 6-7 has reduced to 1227.21%. Optimization with PSO has eliminated the overloading of only 5 lines completely. With AAA, overloading of line 2-4 is declined to 108.08% and for line 3-4 the reduction is 103.08%. After comparison the proposed results with DE, PSO and AAA, it can be stated that the % reduction in overloading of lines is found to be maximum for each contingency scenario using proposed approach.

Most severe line contingency case (outage of line 1) has been considered for comparison purpose of voltage profiles of buses after UPFC placement using proposed approach with other three evolutionary algorithms namely DE, PSO and AAA, which is shown in Fig. 5.5. For the proposed algorithm, the distribution of voltages among various buses is the most uniform indicating efficient overvoltage reduction capability. Furthermore, convergence characterization for the overall objective function has also been developed and compared with convergence manner of other algorithms as shown in Fig. 5.6. Proposed convergence is most rapid and consistent among all comparative convergences. Complete impact of UPFC placement using proposed approach on performance parameters of overall test system for ease contingency case has been detailed in Table 5.9. The comparison of results symbolizes the outperformance of UPFC (placed at proposed positions) as

compared to UPFC positions (obtained with DE, PSO and AAA) algorithms. For the most severe line outage case, there were 9 transmission lines with overloading and 10 buses with voltage violations before installing UPFC. After locating UPFC at line 7 (line location of proposed algorithm), overloading of 7 transmission lines are fully removed and voltage violations on all 10 buses were completely eliminated. Furthermore, the overloading of line 2 to 4 has reduced to 105.98% from 162.8% and of line 6 to 7 % overloading has decreased to 102.65% from 116.62%, and is shown in Table 5.10. Remaining overloaded transmission lines completely working under normal conditions. The voltage violations of buses (2, 3, 4, 6, 7, 9, 12, 13, 14 and 15) have been completely eliminated.

Table 5.9: Description of % overloading of lines and voltage violations after using UPFC (at optimized location as shown in Table 5.10) by proposed algorithm and their comparison with AAA, DE and PSO

Tripped Line	**From Bus**	**To Bus**	**Description of overloaded lines and their (% Overloading after UPFC placement using (DE) (**Shaheen ***et al***., 2011**)**	**Buses with voltage violation (DE) (**Shaheen ***et al***., 2011**)**	**Description of overloaded lines and their % Overloading after UPFC placement using (PSO) (**Shaheen ***et al***., 2011**)**	**Buses with voltage violation (PSO) (**Shaheen ***et al***., 2011**)**	**Description of overloaded lines and their % Overloading after UPFC placement using (AAA) (**Zahid ***et al.,*** 2017)	**Buses with voltage violation (AAA) (**Zahid ***et al.,*** 2017)	**Description of overloaded lines and their % Overloading after UPFC placement using ITM-CPSO (Proposed algorithm)**	**Buses with voltage violation (proposed)**
1	1	2	1-3 (103.2) 2-4 (129.63) 6-7 (127.21) 2-5 (0) 2-6 (0) 4-6 (0) 5-7 (0) 6-8 (0) 8-28 (0)	-	1-3 (0) 2-4 (148.62) 6-7 (116.32) 2-5 (0) 2-6 (109.51) 4-6 (0) 6-8 (0) 6-28 (112.2) 8-28 (0)	-	1-3 (0) 2-4 (108.08) 3-4 (103.08) 2-5 (0) 2-6 (0) 4-6 (0) 5-7 (0) 6-8 (0) 8-28 (0)	-	1-3 (0) 2-4 (105.98) 6-7 (0) 2-5 (0) 2-6 (0) 4-6 (0) 5-7 (0) 6-8 (0) 8-28 (101.74)	-

									8-28 (0)	
14	9	10	6-10 (0) 2-6 (115.97) 10-20 (127.7) 25-26 (0)	-	6-10 (0) 10-17 (109.01) 23-24 (116.8) 25-26 (107.2)	-	6-10 (0) 4-12 (0) 10-17 (0) 25-26 (113.04)	-	6-10 (0) 4-12 (0) 10-17 (0) 25-26 (102.01)	-
18	12	15	10-17 (0)	-	10-17 (0)	-	10-17 (0)	-	10-17 (0)	-
10	6	8	8-28 (0) 6-28 (0)	-	8-28 (0) 6-28 (0)	-	8-28 (0) 6-28 (0)	-	8-28 (0) 6-28 (0)	-
2	1	3	1-2 (101.02) 2-4 (0) 2-6 (0) 5-7 (0)	-	1-2 (0) 2-4 (103.4) 2-6 (0) 5-7 (0)	-	1-2 (0) 2-4 (125.46) 2-6 (0) 5-7 (0)	-	1-2 (0) 2-4 (100.45) 2-6 (0) 5-7 (0)	-
3	2	4	1-3 (107.77) 3-4 (0) 2-6 (109.37) 4-6 (0) 5-7 (0)	-	1-3 (106.53) 3-4 (0) 2-6 (127.17) 4-6 (0) 5-7 (0)	-	1-3 (0) 3-4 (0) 2-6 (102.7) 4-6 (0) 5-7 (0)	-	1-3 (0) 3-4 (0) 2-6 (104.01) 4-6 (0) 5-7 (0)	-
22	15	18	19-20 (0) 10-20 (0)	-	19-20 (0) 10-20 (0)	-	19-20 (0) 10-20 (0)	-	19-20 (0) 10-20 (0)	-
6	2	6	1-3 (107) 2-4 (0) 4-6 (0)	-	1-3 (107.82) 2-4 (0) 2-6 (110.45)	-	1-3 (0) 2-4 (0) 4-6 (104.5)	-	1-3 (0) 2-4 (0) 2-6 (108.98)	-

			5-7 (0)		5-7 (0)		5-7 (0)		5-7 (0)	
8	5	7	1-3 (0) 2-4 (0) 2-6 (0)	-	1-3 (0) 2-4 (0) 2-6 (0)	-	1-3 (0) 2-4 (0) 2-6 (0)	-	1-3 (0) 2-4 (0) 2-6 (0)	-
5	2	5	1-3 (0) 2-4 (0) 2-6 (0)	-	1-3 (0) 2-4 (0) 2-6 (0)	-	1-3 (0) 2-4 (0) 2-6 (0)	-	1-3 (0) 2-4 (0) 2-6 (0)	-
11	6	9	6-10 (0) 4-12 (0) 10-17 (0)	-	6-10 (0) 4-12 (0) 10-17 (0)	-	6-10 (0) 4-12 (0) 10-17 (0)	-	6-10 (0) 4-12 (0) 10-17 (0)	-
20	14	15	15-23 (0) 10-17 (0)	-	15-23 (0) 10-17 (0)	-	15-23 (0) 10-17 (0)	-	15-23 (0) 10-17 (0)	-
25	10	20	-	-	-	-	-	-	-	-
35	25	27	6-28 (0)	-	6-28 (0)	-	6-28 (0)	-	6-28 (0)	-
36	27	28	-	-	-	-	-	-	-	-
4	3	4	1-2 (0) 2-4 (0)	-	1-2 (0) 2-4 (0)	-	1-2 (0) 2-4 (0)	-	1-2 (0) 2-4 (0)	-
29	21	22	10-21 (0) 10-22 (0)	-	10-21 (0) 10-22 (0)	-	10-21 (0) 10-22 (0)	-	10-21 (0) 10-22 (0)	-
37	27	29	-	-	-	-	-	-	-	-
38	27	30	29-30 (0)	-	29-30 (0)	-	29-30 (0)	-	29-30 (0)	-
19	12	16	10-17 (0)	-	10-17 (0)	-	10-17 (0)	-	10-17 (0)	-

21	16	17	10-17 (0)	-	10-17 (0)	-	10-17 (0)	-	10-17 (0)	-
23	18	19	-	-	-	-	-	-	-	-
24	19	20	-	-	-	-	-	-	-	-

Table 5.10: Statistical results of line locations and parametric settings of UPFC by ITM-CPSO and their comparison with AAA, DE and PSO for various contingencies of IEEE 30 bus system

Tripped Line	**UPFC Line Location**				**DE (Shaheen *et al.*, 2011)**		**PSO (Shaheen *et al.*, 2011)**		**AAA (Zahid *et al.*, 2017)**		**ITM-CPSO (proposed)**	
	ITM-CPSO	**DE (**Shaheen ***et al.***,2011**)**	**PSO (**Shaheen ***et al.***, 2011**)**	**AAA**	V_{se}	V_{sh}	V_{se}	V_{sh}	V_{se}	V_{sh}	V_{se}	V_{sh}
1	7	7	7	2-5	0.0986	0.9893	0.120	0.946	0.0986	0.9893	0.0976	0.9876
14	25	25	25	6-10	0.0349	0.9305	0.007	1.010	0.0349	0.9305	0.0356	0.9345
18	7	7	7	4-6	0.154	0.937	0.079	1.034	0.0010	1.0468	0.076	1.0345
10	27	27	27	10-17	0.118	0.969	0.046	0.978	0.0191	1.0283	0.0196	1.012
2	4	4	4	5-7	0.088	1.082	0.104	1.034	0.0026	1.0295	0.167	1.023
3	4	4	4	4-6	0.123	1.007	0.087	0.991	0.0460	0.9988	0.089	0.9978

22	9	9	9	6-7	0.061	1.077	0.127	0.996	0.0210	1.0188	0.126	0..967
6	7	7	7	2-4	0.091	0.948	0.035	1.022	0.0184	1.0842	0.045	0.9978
8	32	32	32	2-4	0.105	1.077	0.106	0.998	0.0157	1.0263	0.105	0.997
5	4	4	4	4-6	0.049	1.022	0.054	0.957	0.0286	1.0807	0.068	0.076
11	27	27	27	10-17	0.127	0.965	0.107	1.048	0.0436	0.9934	0.045	0.9986
20	7	7	7	6-7	0.077	1.015	0.066	0.976	0.0543	1.0183	0.0578	1.0234
25	7	7	7	4-6	0.104	0.998	0.028	0.998	0.0393	0.9420	0.087	0.956
35	30	30	30	10-21	0.022	0.948	0.0063	0.948	0.0361	0.9745	0.0325	0.965
36	20	20	20	14-15	0.048	0.911	0.119	1.066	0.0145	0.9866	0.0187	0.9765
4	17	17	17	4-12	0.107	1.054	0.124	0.939	0.0407	1.1000	0.0345	1.1098
29	23	23	23	10-20	0.066	0.927	0.098	0.922	0.0697	0.9557	0.0678	0.9876
37	7	7	7	4-6	0.091	0.920	0.106	1.038	0.0468	1.0461	0.0567	1.0218
38	25	25	25	23-24	0.146	0.952	0.047	0.996	0.0011	1.0522	0.046	1.023
19	21	21	21	10-17	0.027	1.019	0.059	1.042	0.0312	0.9403	0.0432	0.9234

21	30	30	30	15-23	0.125	0.993	0.107	0.968	0.0108	1.0217	0.0108	1.0245
23	9	9	9	6-7	0.113	0.987	0.146	1.059	0.1607	0.9345	0.157	0.9567
24	9	9	9	6-7	0.098	0.984	0.076	0.997	0.0879	1.0303	0.076	0.9967

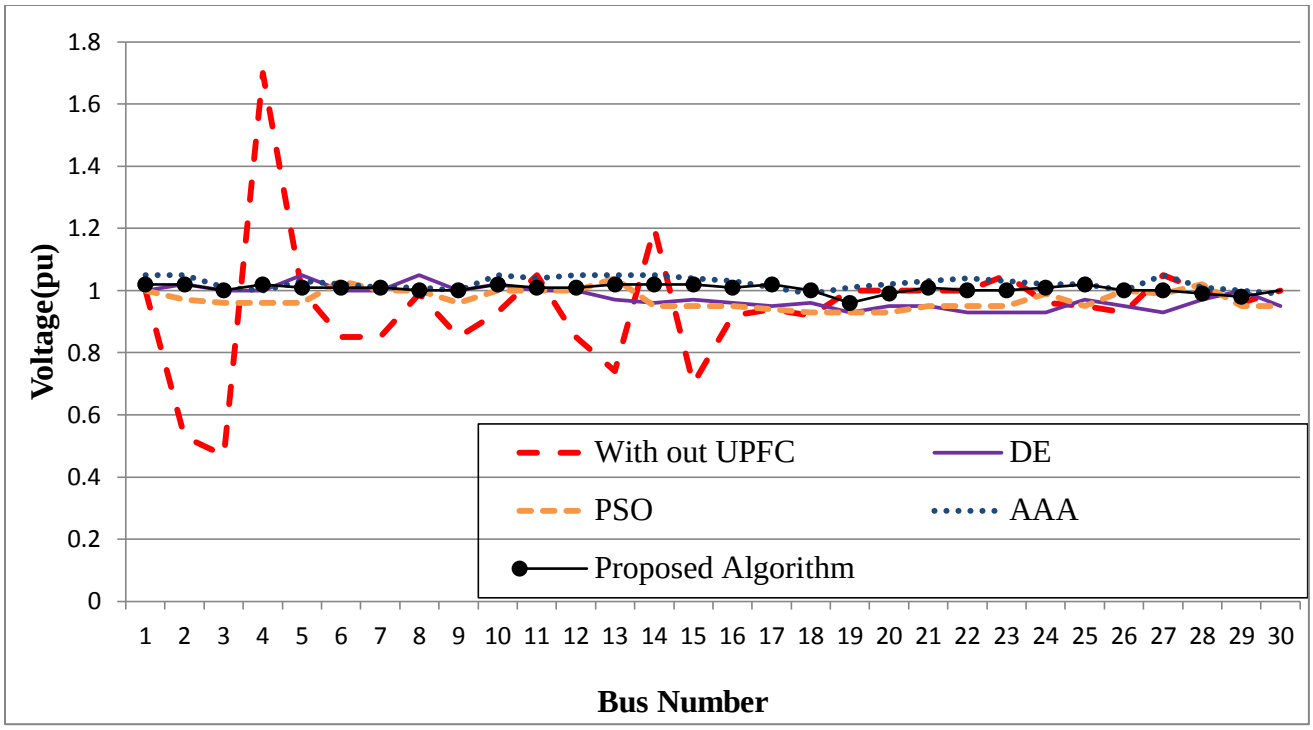

Figure 5.5: Comparison of voltage profile of various buses of IEEE 30 bus system using various optimization algorithms for most severe outage case (tripping of line 1)

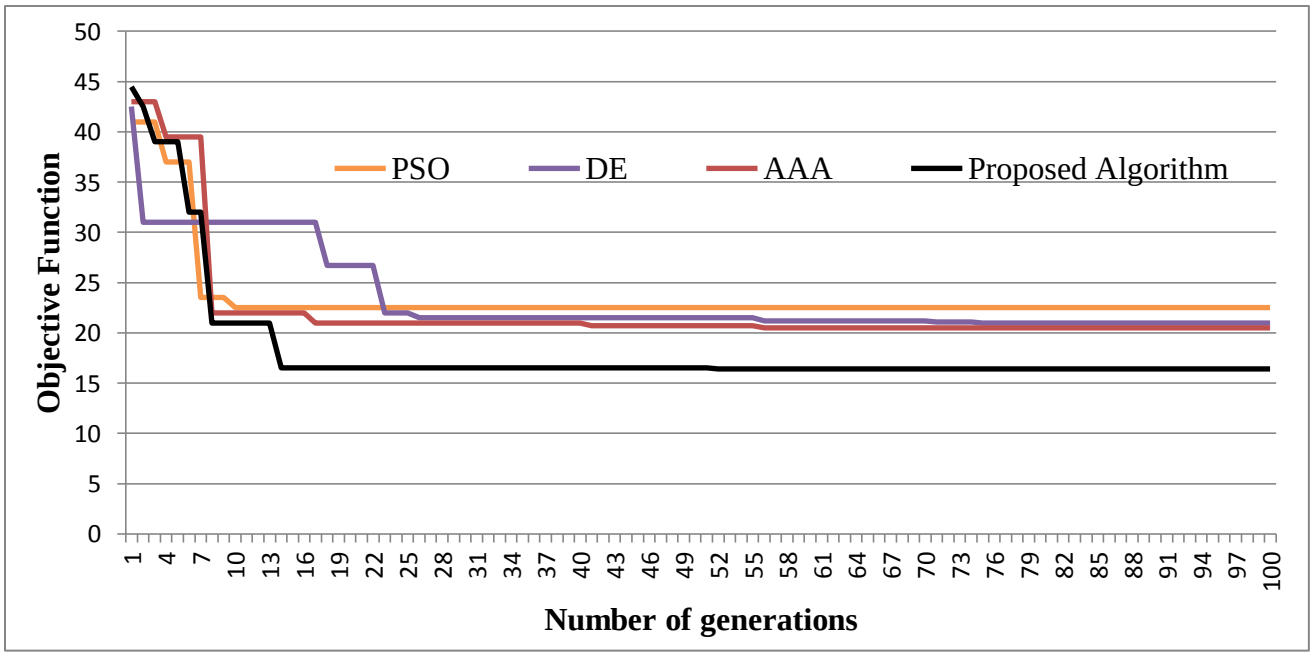

Figure 5.6: Convergence characteristics for the objective function using proposed algorithm ITM-CPSO and their comparison with DE, AAA and PSO for most severe line outage (line 1 tripped)

The convergence characterizations of the objective function using ITM-CPSO have been established and compared with the convergence manners of AAA, DE and PSO optimization techniques as shown in Fig. 5.6. Convergence characteristics of proposed algorithm are found to be the most consistent and rapid and converge to better solution as compared to rest comparative optimization algorithms.

5.7 Concluding Remarks

Contingency selection and ranking process performed in the first phase of the algorithm has made it easy for system operator to evaluate the performance index of severe contingency scenarios. Moreover, minimization of the performance index using ITM-CPSO has remarkably increased the reliability and security of the power systems. Efficacy of the results for allocating the UPFC in most suitable locations and optimal parameter settlings has been deeply analyzed and compared with other three comparative algorithms for the power quality validation. Comparison of results for each line outage case depicts the outperformance of the proposed technique with rest comparative algorithms in terms of rapid and consistent convergence, improved voltage profile, increased computational proficiency and best quality solutions.

Chapter 6: Optimal Feasible Solutions of Rescheduled Generation Cost using Novel Hybrid Chaotic Particle Swarm Optimization

6.1 Introduction

This chapter addresses the introduction and implementation of an advanced Twin Extremity Chaotic Map adaptive Particle Swarm Optimization (TECM-PSO) algorithm to optimize the rescheduled generation cost function for CM. The goal of proposed approach is twofold; firstly, to identify accurate number of participating generators for rescheduling process using Upstream Real Capacity Tracing (URCT) method (detailed in Chapter 4) requiring less information of generator units and secondly, to achieve minimum possible Rescheduled Generation Cost (RGC) using TECM-PSO algorithm while alleviating all the line overloads. Furthermore, to preserve the diversity of the algorithm and to increase its near global searching capability, the incursion of dynamic constraint handling has been done in the algorithm to retrieve the feasible solutions in the entire search space. The objective function is solved for near global optima using proposed algorithm. Twin extremity chaotic maps have been generated by updating the equations governing the PSO algorithm in order to prevent the particle swarm optimization plugging into local minima with less convergence rate at later stages of iterations. The feasibility of the proposed algorithm is validated on various line outage cases of both the small and large test systems. Simulation results show a considerable reduction in net rescheduled generation cost, power losses and rescheduled generation amount as compared to other comparative algorithms available in literature.

6.2 Problem Formulation

Minimization of real power rescheduling cost has been taken as the main objective function as expressed by Eq. (6.1).

$$\text{Main objective function } (MOF) = \text{RGCF } (\delta/\text{h}) = \min \sum_{i_p=1}^{Npg} (C_g^+ + C_g^-) * \Delta P_{gi_p} \qquad (6.1)$$

The various constraints governing the above objective function are stated in following sections.

6.2.1 Equality Constraints

These constraints are governed by Eq. (6.2) to Eq. (6.5).

(i) Power Equilibrium Constraint

This constraint is based on the principle of equilibrium between total generation and total loads as represented by Eq. (6.2).

$$\sum_{i_p=1}^{Npg}(P^0_{gi_p} + \Delta P_{gi_p}) + \sum_{k_g, k_g \neq i_p}^{Ng} P_{gk_g} = \sum_{m_{lb}=1}^{Nd} P^0_{Dm_{lb}} + P_L \quad (6.2)$$

Equation (6.2) can be rewritten as

$$\sum_{i_p=1}^{Npg} P^{resh}_{gi_p} + \sum_{k_g, k_g \neq i_p}^{Ng} P_{gk_g} = \sum_{m_{lb}}^{Nd} P^0_{Dm_{lb}} + P_L \quad (6.3)$$

where $P_{gi_p}^{resh} = P_{gi_p}^{0} + \Delta P_{gi_p}$

Active power loss P_L has been calculated based on the basic loss coefficients formulas.

(ii) Real and Reactive Power Balance Equations

Constraints governing the real and reactive power balance equations can be formulated as Eq. (6.4) and Eq. (6.5).

$$P_i - V_i \sum_{j=1}^{N_B} V_j (G_{ij} Cos\theta_{ij} + B_{ij} Sin\theta_{ij}) = 0, i = 1,2,\ldots N_{B-1} \quad (6.4)$$

$$Q_i - V_i \sum_{j=1}^{N_B} V_j (G_{ij} Sin\theta_{ij} - B_{ij} Cos\theta_{ij}) = 0, i = 1,2,\ldots N_{PQ} \quad (6.5)$$

6.2.2 Inequality Constraints

These constraints are stated from Eq. (6.6) to Eq. (6.10).

(i) Transmission Line Apparent Power Flow Limits

$$S_L \leq S_{L\max} \quad (6.6)$$

(ii) PQ Bus Voltage Limit Constraints

$$V_{Li\min} \le V_{Li} \le V_{Li\max},\ Li \in N_{PQ} \quad (6.7)$$

(iii) Generation Reactive Power Constraints

$$Q_{Gi\min} \le Q_{Gi} \le Q_{Gi\max} \quad (6.8)$$

(iv) Generation Real Power Limit Constraints

$$P_{Gi\min} \le P_{Gi} \le P_{Gi\max},\ G_i \in N_{PV} \quad (6.9)$$

(v) Generation Voltage Limit Constraints

$$V_{Gi\min} \le V_{Gi} \le V_{Gi\max}, G_i \in N_{PV} \quad (6.10)$$

6.3 Constraint Handling

Dynamic constraint handling approach (Iwan ***et al.,*** 2012) has been used in the algorithm by defining an auxiliary function *AF* due to which the proposed problem has been converted into dual-objective optimization problem, stated as min (*AF* , *MOF*). Where *AF* is considered as the first objective function and *MOF* is treated as the second objective function. The concept of incorporation of *AF* is to check whether an individual is within the feasible region or not and how close a particle is to the feasible region. *If* an individual lies outside the feasible region, *then* the individual will take *AF* as its optimization objective, *else MOF* will be optimized. Illustration of feasible and infeasible regions is shown in Fig. 6.1.

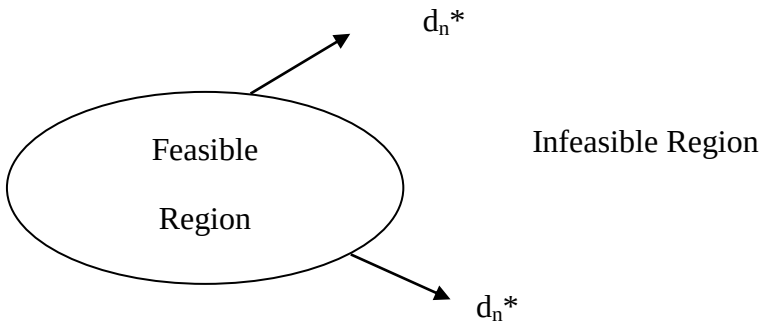

Figure 6.1: Feasible and infeasible region (Iwan ***et al.,*** 2012)

Where

$$AF = \sum_{n=1}^{n_D} \max(0, d_n) \tag{6.11}$$

In the Fig. 6.1, d_n represents the distance of an individual (candidate solution), represented by '*' marks to the constraint violation boundary.

Pseudo-code of dynamic constraint handling

If $AF = 0$ (constraints are satisfied)

Then OF(x) = *MOF*

Else OF(x) = *AF*

End

6.4 Proposed Methodology

Various PSO algorithms and the proposed PSO have been illustrated in the following section.

6.4.1 Standard Particle Swarm Optimization (S-PSO)

The equations for computing the velocity and position of the population can be given by Eq. (6.12) and Eq. (6.13) respectively.

$$V_i^{k+1} = wV_i^k + c_1 * r_1 * (P_{besti} - P_i^k) + c_2 * r_2 * (G_{best} - P_i^k) \tag{6.12}$$

$$P_i^{K+1} = P_i^K + V_i^{K+1} \tag{6.13}$$

To prevent algorithm divergence, the final value of velocity for each particle is limited, which is given by Eq. (6.14).

$$V_F \in [-V_{\max}, V_{\min}] \tag{6.14}$$

Fast convergence is achieved by properly selecting the inertia weight (w), which is defined by Eq. (6.15).

$$w = w_{\max} - \frac{w_{\max} - w_{\min}}{k_{\max}} \times k \tag{6.15}$$

6.4.2 Chaotic Particle Swarm Optimization (C-PSO)

In PSO, the parameters w, r_1, r_2 are the key factors affecting the convergence behavior of PSO. The main feature of chaotic sequences is that they can be quickly generated and stored easily and there is no need of storage of long sequences.

6.4.3 Proposed Twin Extremity Chaotic Mapped PSO (TECM-PSO) Algorithm

In this subsection overview of TECM-PSO has been illustrated.

- **Rationale**

Twin extremity chaotic mapping of PSO is proposed in the present work. These maps can give high frequencies in three regions of time mainly: 0.0, 0.5 and 1.0.In standard PSO, r_1 and r_2 effect the search capabilities of exploration and exploitation independently which further influence the convergence rate. From the frequency spectrum of logistic maps and twin extremity maps which occur near 0.0, 0.5 and 1.0 as shown in Fig. 6.2, it is clear that these maps can be adjusted by the variable n to control the frequencies near 0.0, 0.5 and 1.0. Even though the logistic maps can successfully replace the parameters r_1 and r_2 of PSO over the entire space due to its periodicity, but their distribution is not flat as shown in Fig. 6.2. Twin extremity chaotic maps raise the possibility near 0.5 to compensate for this drawback of logistic maps; the possibility near 0.5 can be adjusted by the variable n as shown in Fig. 6.3, Fig. 6.4, Fig.6.5 and Fig.6.6. If we choose $n = 2$, there is a best possibility of flat distribution near 0.5. Therefore, $n = 2$ has been chosen for the entire simulation.

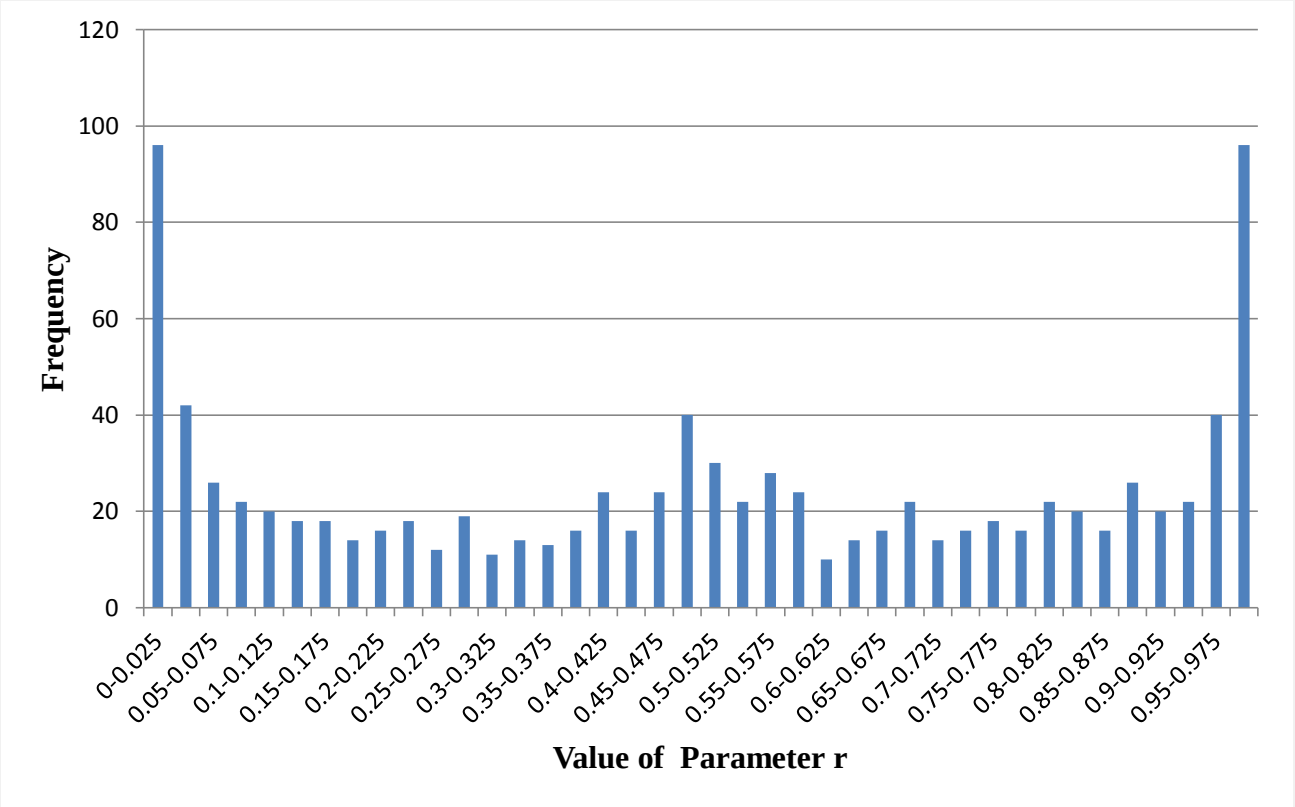

Figure 6.2: Frequency spectrum of logistic map

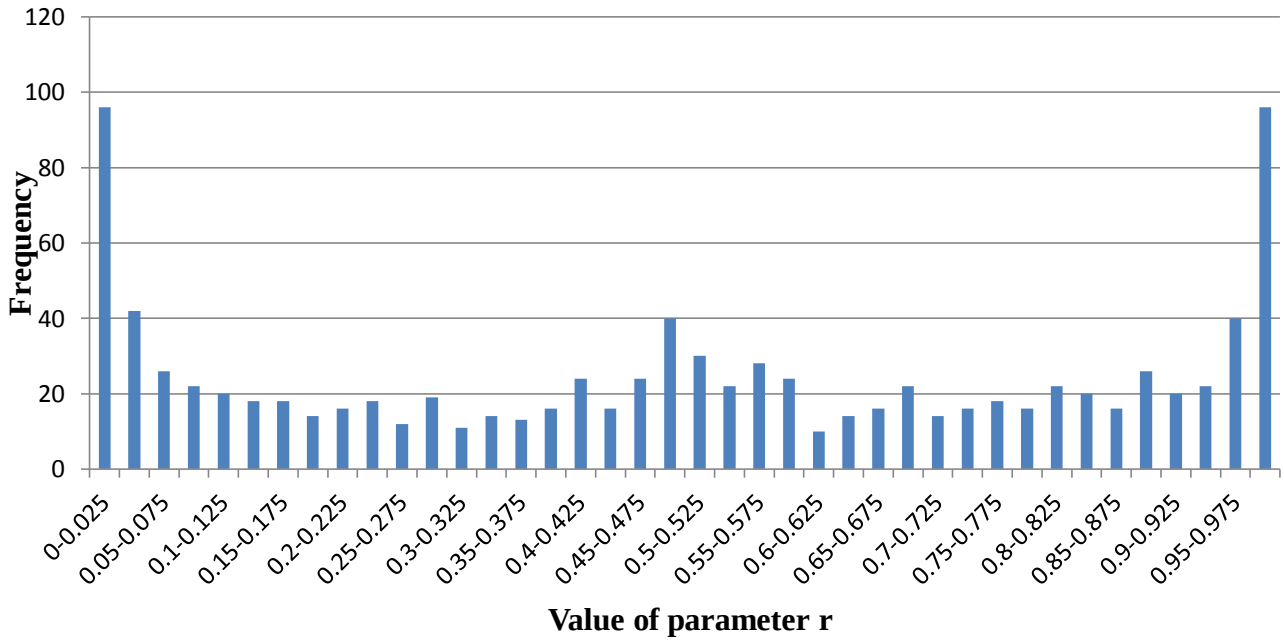

Figure 6.3: Frequency spectrum of twin-extremity map with $n = 1$ $(2n\Pi = 2\Pi)$

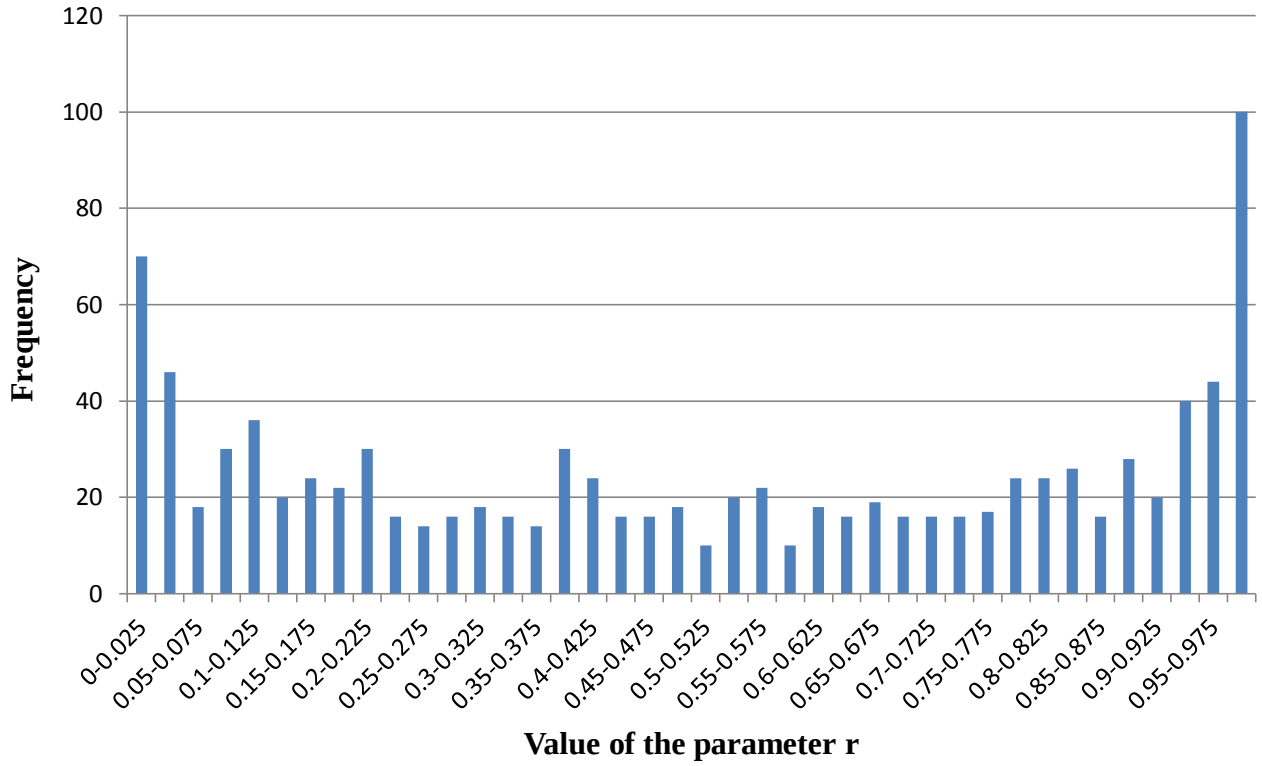

Figure 6.4: Frequency spectrum of twin-extremity map with $n = 2$ $(2n\Pi = 4\Pi)$

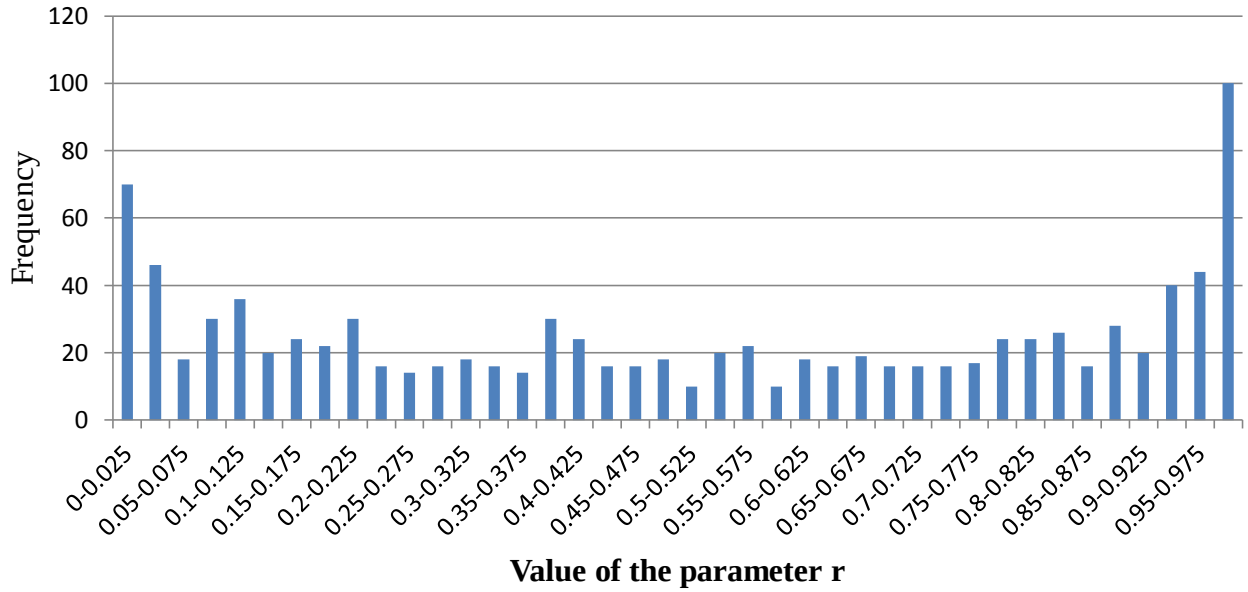

Figure 6.5: Frequency spectrum of twin-extremity map with $n = 4$ $(2n\Pi = 8\Pi)$

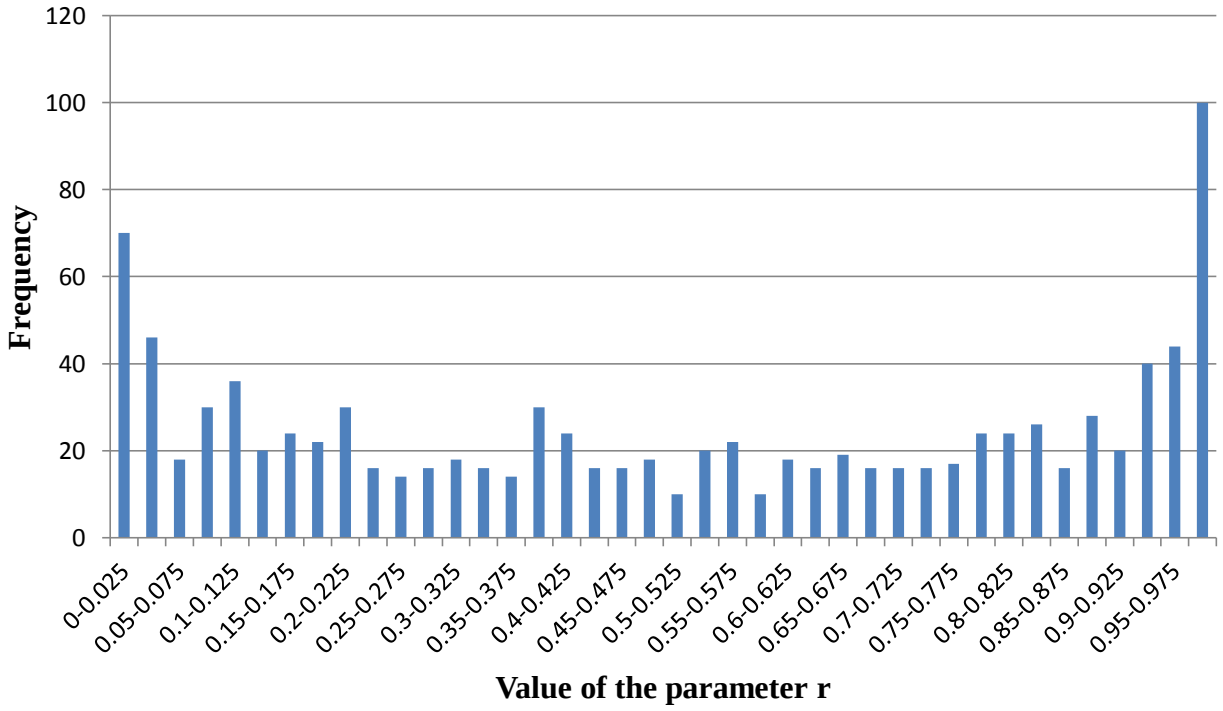

Figure 6.6: Frequency spectrum of twin-extremity map with $n = 8$ $(2n\Pi = 16\Pi)$

6.5 Mathematical Modeling of Generating TECM-PSO Sequences

In TECM-PSO, the sequences generated by twin extremity map substitute the random parameters r_1 and r_2 in PSO. The random parameters are modified by the twin extremity map based on the Eq. (6.16)

$$TECMr^{k+1} = [\sin(2n\Pi TECMr^{k}) + 1]/2 \qquad (6.16)$$

The initial range of $TECMr^{0}$ is [0, 1], but $TECMr^{0} \neq (0,0.25,0.5,1)$ when n is an integer.

The velocity update equation of TECM-PSO can be rewritten as Eq. (6.17)

$$V_i^{k+1} = w * V_i^{k} + c_1 * TECM_r^{k} * (P_{besti} - P_i^{k}) + c_2 * TECM_r^{k} * (G_{best} - P_i^{k}) \qquad (6.17)$$

In the above expression $TECM_r$ is a function based on the results of twin extremity map with values between 0 and 1.

6.5.1 Time Series Plot of TECM Sequence

Generally the system is initiated by vector with some initial value to observe how the system evolves. Here, we used $n=1$ and initial value $TECMr^0 = 0.777$ in the twin-extremity map to test and the corresponding Cr values have been generated. From Fig. 6.7, it has been observed that the Cr values show variance throughout the achievable space which proves the sequence as chaotic. Therefore, the twin extremity maps are indeed chaotic.

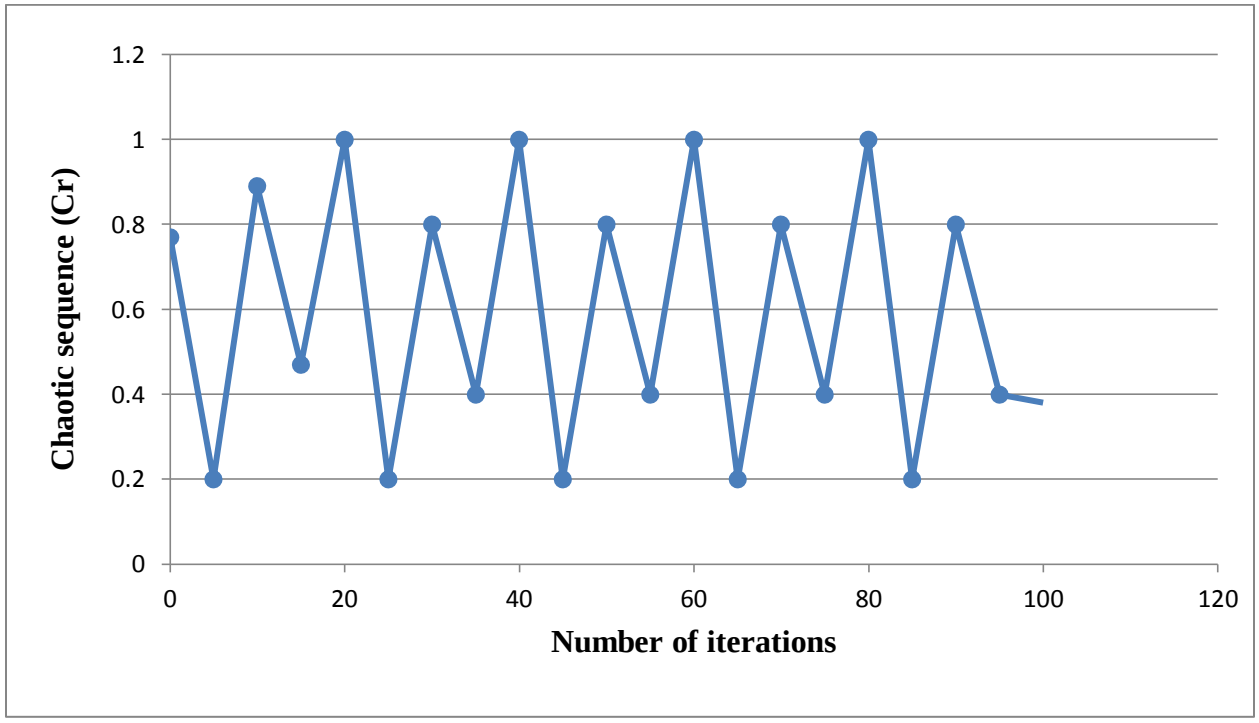

Figure 6.7: Time series plot of twin extremity map for 100 generations of Cr value with 0.777 as initial value

6.6 Stopping Criterion

In this study, standard deviation (σ_d) of populations is used as the stopping criterion. If the standard deviation is below a threshold (small predefined number, $\in_T$), the optimization stops. It can be formulated as expressed by Eq. (6.18).

$$\sigma_d = \sqrt{\frac{1}{\eta}\sum_{k=1}^{\eta}(x_{best,d}^{k} - \bar{x}_{best,d})^2} \prec \in_T \left(\max\left(x_{best,d}\right) - \min\left(x_{best,d}\right)\right); \text{ For d} = n_D \qquad (6.18)$$

6.7 Execution Procedure

Proposed TWCM-PSO Algorithm

Define Objective function $Of(X), X = (x_1, x_2, \ldots\ldots\ldots, x_{n_D})$ % n_D is the number of dimensions

Initialize the particle swarm and $TECMr^0$ randomly within the limits

while $\in_T$ <1% and η = 40

Evaluate the fitness of the particle swarm

for n =1: n_P % n_P is the number of particles

Find personal best P_{best} and Global best G_{best}

for d =1: n_D % n_D is the number of dimensions

Update the velocity and position of the particle using Eq. (6.17) and Eq. (6.13)

Update the inertia weight of the updated particle using Eq. (6.15)

Update the value of $TECMr$ by Eq. (6.16)

Find the updated particle's fitness evaluation taking into consideration dynamic objective constraint handling procedure. If the fitness of the current solution is better than the previous populations' global best's fitness, set the current solution as the new global best

end for

end for

Update the current best global solution

end while

Retrieve the best optimal solution

6.8 Implementation of Proposed Algorithm to Rescheduling Generation Cost Problem

In this section the steps and flow chart of the proposed algorithm have been unveiled.

1. Select a contingency from optimal power flow solution and evaluate RPCF values of each generator using URCT algorithm (as detailed in Chapter 4).
2. Identify the participating generator(s) for the rescheduling process to relieve contingency.

3. Execute the steps of TECM-PSO algorithm as explained in section 6.7 to evaluate the best optimal solution of the objective function and also to finally relieve the non-dominated near global optimum solution.

Figure 6.8 shows the flow chart of the proposed algorithm. This flow chart presents the description of stepwise execution of the proposed algorithm. Firstly we have to obtain the optimal Power Flow solution then to select a contingency and run the line flow. If power flow violations exist, then we have to evaluate the RPCF values of the generators to select the participating generators.

Once the numbers of participating generators are identified the next step is to execute the proposed algorithm to relieve the congestion. Firstly the iteration count and control parameters are initialized to evaluate the fitness of particle swarm.

Next step is to compute the minimum rescheduled generation cost of each individual in the population in order to obtain the best feasible solution over the entire convergence range by dynamic constraint handling method.

Next step is to check for the stopping criterion. If it is met, we will obtain the best near global optimal solution and dispatch the best minimum rescheduled generation cost and if it does not met, we have to modify the position and velocity of each particle and then the step by step execution of proposed algorithm is carried out again to obtain the near global best optimal solution.

In this way the step by step execution of proposed algorithm is carried out by keeping an eye on all the constraint handling procedures to obtain the best optimal near global solution.

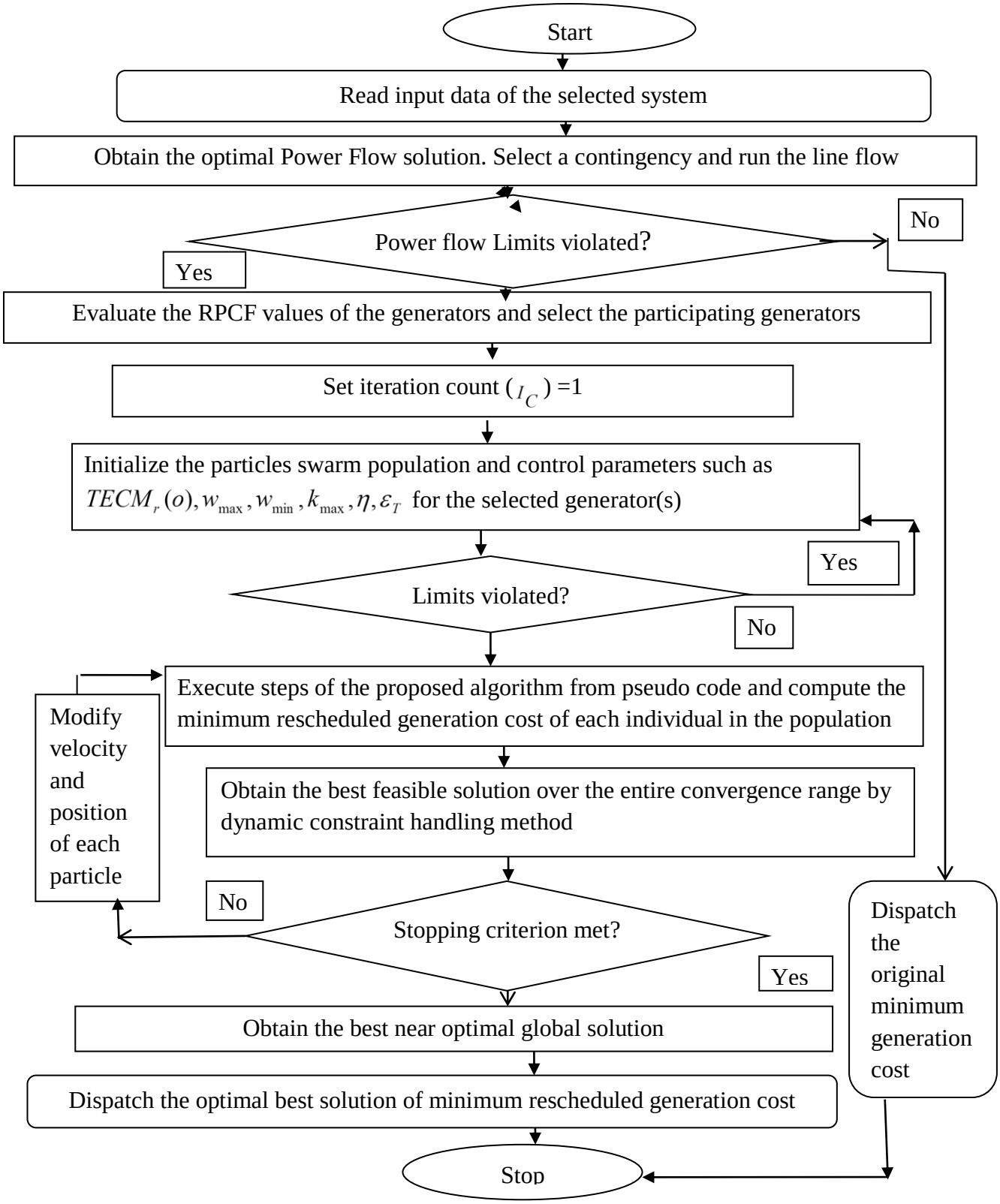

Figure 6.8: Flow chart of the proposed approach

The selection parameter of the proposed algorithm and the corresponding criterion has been described in Table 6.1.

Table 6.1: Selection parameters and their criterion

Specification	**Value**	**Selection Criterion**
$w_{\max}$, $w_{\min}$	0.9,0.4	A large weight factor facilitates global exploration while small weight factor facilitates local exploration. To make a balance between the two, choice has been made between its maximum and minimum range.
Cognitive parameter (c_1) , Social parameter (c_2)	2,2	Both values have been chosen 2 since this will make the weights for social and cognition parts to be 1.
Total number of iterations	150 (IEEE 30 & IEEE 57 bus systems), 250 (IEEE 118 bus system)	Numbers of iterations have been selected according to the size of the test systems.
Population Size	40	Based on trails, it has been found that population size of 40 is sufficient for solving the congestion management cost problem using the present approach.
$TECMr^0$	0.777	The initial values of TECM sequences can be chosen like 0.77, 0.777, 0.7777, 0.77777. Here, for the entire simulation 0.777 initial values has been chosen.
$\in_T$	<1%	This is the threshold value for the feasible region.
η	40	This value is decided on the basis of trial and independent runs.

6.9 Simulation Results and Discussions

The proposed algorithm has been tested on three main test systems. The description of the test cases of the three selected test systems has been shown in Table 6.2.

Table 6.2: Description of simulated test line outage cases of IEEE 30 bus, IEEE 57 bus and IEEE 118 bus systems

Test System	**Test Case**	**Contingency Considered**
IEEE 30 bus	Case A	Tripping of line 1-2
	Case B	Tripping of lines 1–7 with increase in load at all buses by 50%
IEEE 57 bus	Case C	Capacity reduction of lines 5–6 and 6–12 from 200 MW to 175 MW and 50 MW to 35 MW respectively
	Case D	Capacity reduction of line 2–3 from 85 MW to 20 MW
IEEE 118 bus	Case E	Tripping of line 8-5 with increase in load at buses 11–20 by 57%

Complete description of congested lines, line flows before CM and line limits corresponding to each contingency case have been shown in Table 6.3.

Table 6.3: Details of the congested lines flow for different test cases

Test Case	**Congested Lines**	**Line Flow (MW) During contingency**	**Specified Line Limit (MW)**	**Line Flow (MW) After rescheduling**
Case A	1-7 7-8	147.463 140.292	130 130	129.98 123.87
Case B	1-2 2-8	312.98 98.34	130 65	129.987 61.78

	2-9	106.56	65	64.23
Case C	5-6 6-12	195.956 49.45	175 35	174.56 34.78
Case D	2-3	37.048	20	19.98
Case E	16–17 30–17 8–30	208.98 581.17 367.297	175 500 175	145.89 497.89 154.78

6.9.1 IEEE 30 Bus System

IEEE 30 bus system consisting of 6 generator buses, 24 load buses and 41 transmission lines has been chosen for the test purpose. System line and bus data have been shown in **Appendix A1.** The total testing network real-power is 283.5 MW and reactive-power is 126.25 MVAR. Congestion has occurred in the test system due to outage of the line connected between the buses 1 and 2 (case A) and outage of the line between the buses 1 and 7 along with the 50% increase in the load at all the buses (case B) as shown in Table 6.2. Due to these outages there is an adverse effect on certain transmission lines of the system which have become congested as described in Table 3. If this congestion persists for a long time, the security and reliability of the transmission system will be in risk. Details of incremented and decremented bids submitted by generator companies are given in **Appendix A2.**

For alleviating contingency of case A, firstly the number of participating generators for the rescheduling process has been decided using URCT algorithm. URCT algorithm has yielded Real Power Contribution Factors (RPCF) of all the generators and the distribution of RPCF values of generators among various lines of the system have been plotted in Fig. 6.9. The bars indicated with red color indicate the distribution of RPCF values of generators among congested lines and the corresponding generators are the participating generators for rescheduling process of CM. From Fig. 6.9, it has been clear that only two generators G1and G2 are participating in rescheduling process to relieve the congestion for the case A.

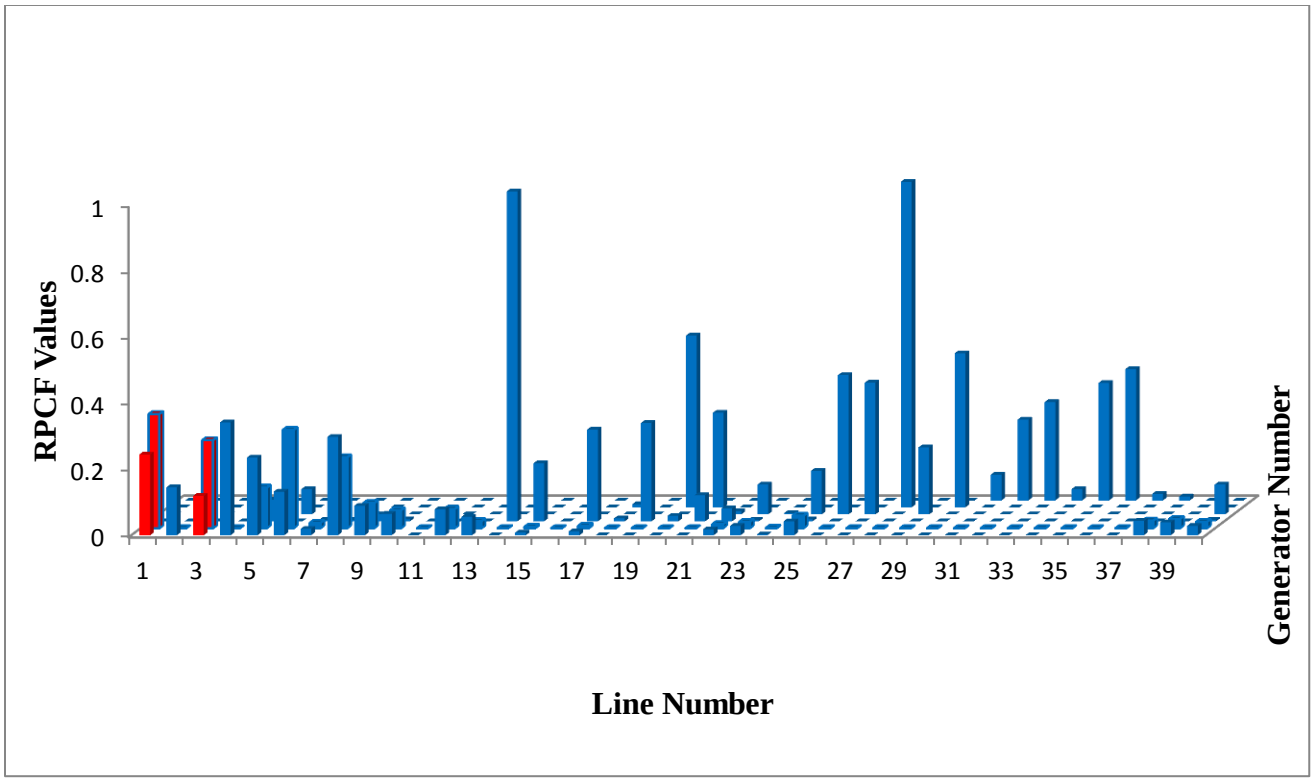

Figure 6.9: Distribution of generators contribution factors among various lines for line contingency case A (IEEE 30 bus system)

After determination of the exact number of participating generators, next step is to execute the procedure of the proposed algorithm as illustrated in section 6.7 to retrieve the best minimum rescheduled generation cost for the mentioned line outage case A. Proposed algorithm has been executed for 30 independent runs and the corresponding obtained statistical results of the individual generators adjustments, Net Generation Rescheduled (NGR), overall Rescheduled Generation Cost (RGC) and % Convergence Mobility Rate (CMR) of the proposed approach have been illustrated and compared with six other evolutionary comparative algorithms namely Particle Swarm Optimization (PSO), Firefly Algorithm (FFA), Flower Pollination Algorithm (FPA), Ant Lion Optimization (ALO), Symbiotic Organisms Search (SOS), Satin Bowerbird Optimization (SBO), which are shown in Table 6.4. NGR amount for the proposed algorithm is found to be 16.236 MW, which is minimum as compared to PSO with 22.93 MW, FPA with 24.703 MW, FFA with 24.742 MW, ALO with 24.1552 MW, SOS with 23.169 MW, SBO with 18.707 MW. Analysis the results of best global optimal solution for RGC, it is clear that the proposed algorithm converges to best global solution of 410.756 $/h as compared to PSO (538.95 $/h), FPA (519.62 $/h), FFA (511.873 $/h),

ALO (480.043 $/h), SOS (460.827 $/h) and SBO (421.58 $/h). Moreover, taking in terms of computational proficiency, % CMR of the proposed algorithm is evaluated by the expression given in Eq. (6.20). % CMR of proposed algorithm is 80.23 and is highest as compared to FPA with 54.4, FFA with 61.2, ALO with 70.4 and SBO with 78.1, which further depicts its fastest convergence rate.

Table 6.4: Simulated statistical results of contingency cases of IEEE 30 bus system using proposed algorithm and their comparison

Case A	**Optimization Algorithm**						
Variables	**PSO (Balaraman, 2011)**	**FPA (Verma and Mukherjee, 2016c)**	**FFA (Verma and Mukherjee, 2016a)**	**ALO (Verma and Mukherjee, 2016b)**	**SOS (Verma et al., 2017)**	**SBO (Chintam and Daniel, 2018)**	**TECM-PSO (Proposed)**
ΔPG1 (MW)	−8.61	−9.1278	−8.778	−9.0880	−8.588	-8.596	−8.456
ΔPG2 (MW)	10.40	14.14	15	15.0668	14.581	7.57	7.78
ΔPG3 (MW)	3.03	−0.206	0.106	0	0	0.3524	NP*
ΔPG4 (MW)	0.02	−0.0188	0.065	0.0001	0	1.096	NP*
ΔPG5 (MW)	0.85	0.189	0.173	0.0002	0	0.56891	NP*
ΔPG6 (MW)	−0.01	1.013	−0.618	0.00010	0	0.52286	NP*
NGR (MW)	22.93	24.703	24.742	24.1552	23.169	18.707	16.236
Best RGC	538.95	519.62	511.873	480.043	460.827	421.58	410.756

($/h)							
% CMR	NR	54.4	61.2	70.4	NR	78.1	80.23
Case B	**Optimization Algorithm**						
Variables	**PSO (Balaraman, 2011)**	**FPA (Verma and Mukherjee, 2016c)**	**FFA (Verma and Mukherjee, 2016a)**	**ALO (Verma and Mukherjee, 2016b)**	**SOS (Verma et al., 2017)**	**SBO (Chintam and Daniel, 2018)**	**TECM-PSO (Proposed)**
ΔPG1 (MW)	NR*	−8.589	−8.579	−8.588	−8.587	-9.00148	−8.271
ΔPG2 (MW)	NR*	74.024	75.995	76.4	76.459	62.90304	65.23
ΔPG3 (MW)	NR*	0	0.057	0.056	0.0005	34.24745	NP*
ΔPG4 (MW)	NR*	13.5174	42.994	42.844	41.083	2.05959	40.98
ΔPG5 (MW)	NR*	43.865	23.832	24.571	30.226	29.45485	22.781
ΔPG6 (MW)	NR*	27.89	16.5144	15.525	11.617	23.47373	10.243
NGR (MW)	168	167.896	167.974	167.98	167.975	161.1401	147.505
Best RGC ($/h)	5335.5	5320.8	5304.40	5296.75	5303	5238.93	5154.97
% CMR	NR	70.4	54.8	73.2	NR	78.4	82.3

NP* - Not Participating, NR* -Not reported

Also, the total system loss has been decreased to 10.929 MW after CM from 16.023 MW during congestion. Power flow in line 1-7 has been reduced to 129.98 MW after CM from 147.463 MW during congestion and in line 7-8, power flow has also come under specified limits from 140.292

MW during congestion to 123.87 MW after CM. A comparative graphical representation of individual generator adjustment to compensate for the congestion has been shown in Fig. 6.10. Comparison of change in overall real power generation show that minimum change in generation is required for the proposed algorithm which further has reduced the operator efforts. Furthermore, the convergence characteristics of the proposed approach have been established and compared with other algorithms in Fig. 6.11. From the results, it has been cleared that the proposed algorithm converges to near global optimal solution in least convergence time and iteration due to its rapid decreasing, uniform and consistent response. Number of feasible solutions are found to be 47, 342 for 30 independent runs and the best near global optimum solution for MOF has been found to be 410.756 $/h for case A. This indicates the proposed algorithm converges with fastest rate as compared to other algorithms.

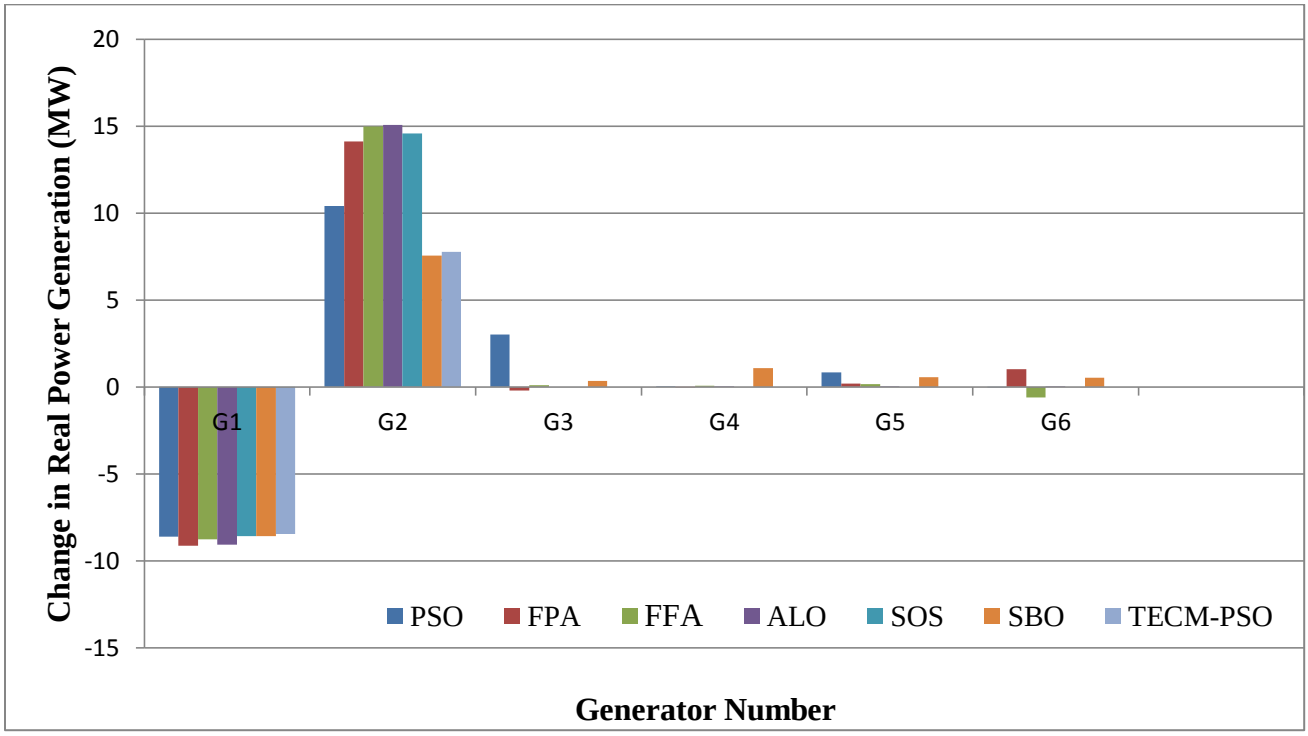

Figure 6.10: Change in real power generation of individual participating generator in MW for congestion relieving of case A (IEEE 30 bus system)

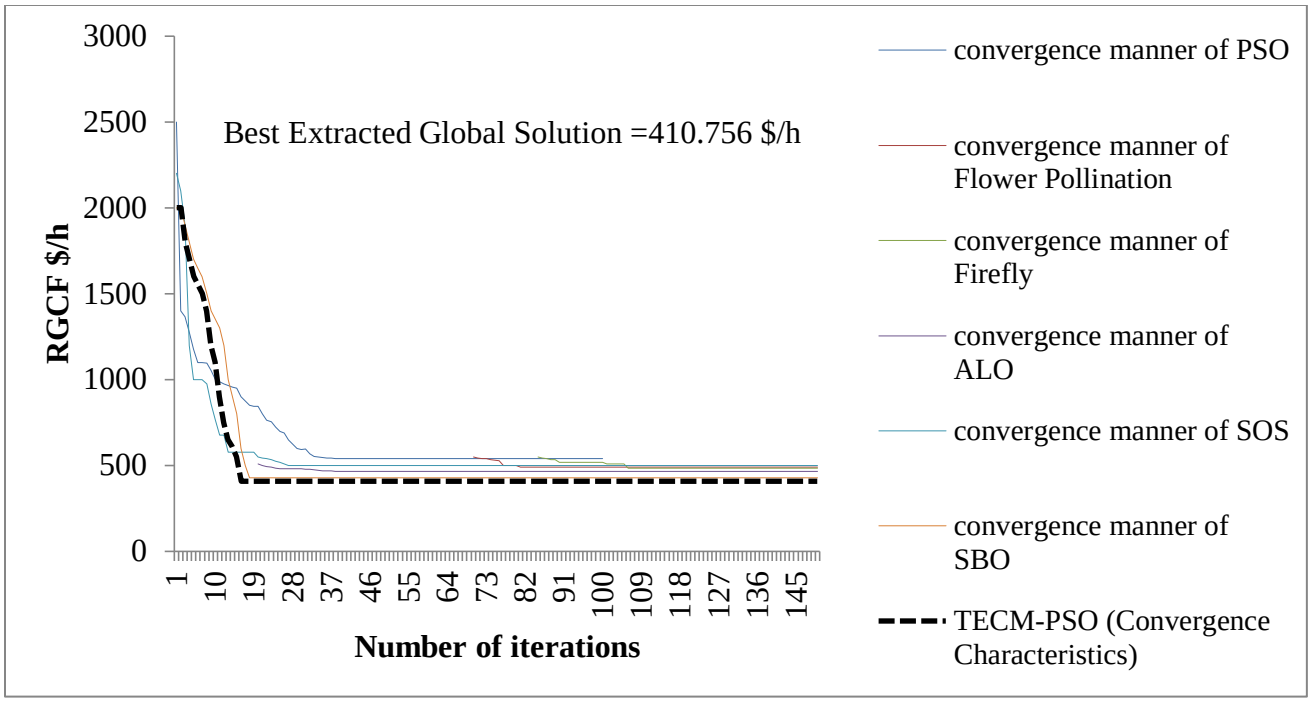

Figure 6.11: Comparison of convergence characteristics of different evolutionary algorithms for line outage case A (IEEE 30 bus system)

For congestion removal of case B, the RPCF values (obtained using URCT algorithm) of all the generators have been evaluated and their bar graph distribution among various lines of the system has been shown in Fig. 6.12. The bars indicated in red show the RPCF values of the participating generators for the rescheduling process as these RPCF values correspond to the congested lines. From Fig. 6.12, it can be easily analyzed that G1, G2, G4, G5 and G6 are the contributing generators for the rescheduling process to alleviate the said overloads. The outputs of the participating generators have been optimized using proposed algorithm to attain NGR and RGC. Statistical results of NGR, RGC, individual generator adjustments and % CMR have been revealed in Table 6.4. NGR amount has been found to be 147.505 MW and the overall CM cost is 5154.97 $/h for proposed algorithm, which are again the best solutions among all the comparative algorithms. The total system loss found to be 11.91 MW after simulation which was 37.8 MW during congestion.

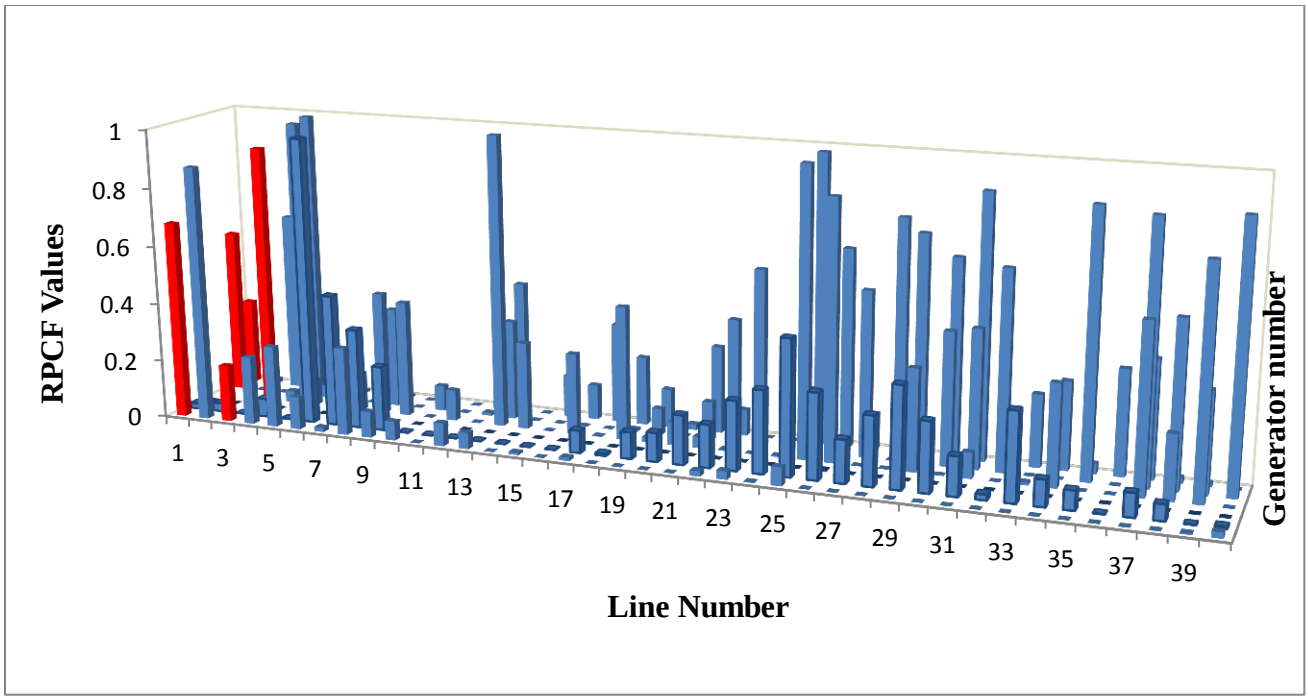

Figure 6.12: Distribution of generators contribution factors among various lines for line contingency case B (IEEE 30 bus system)

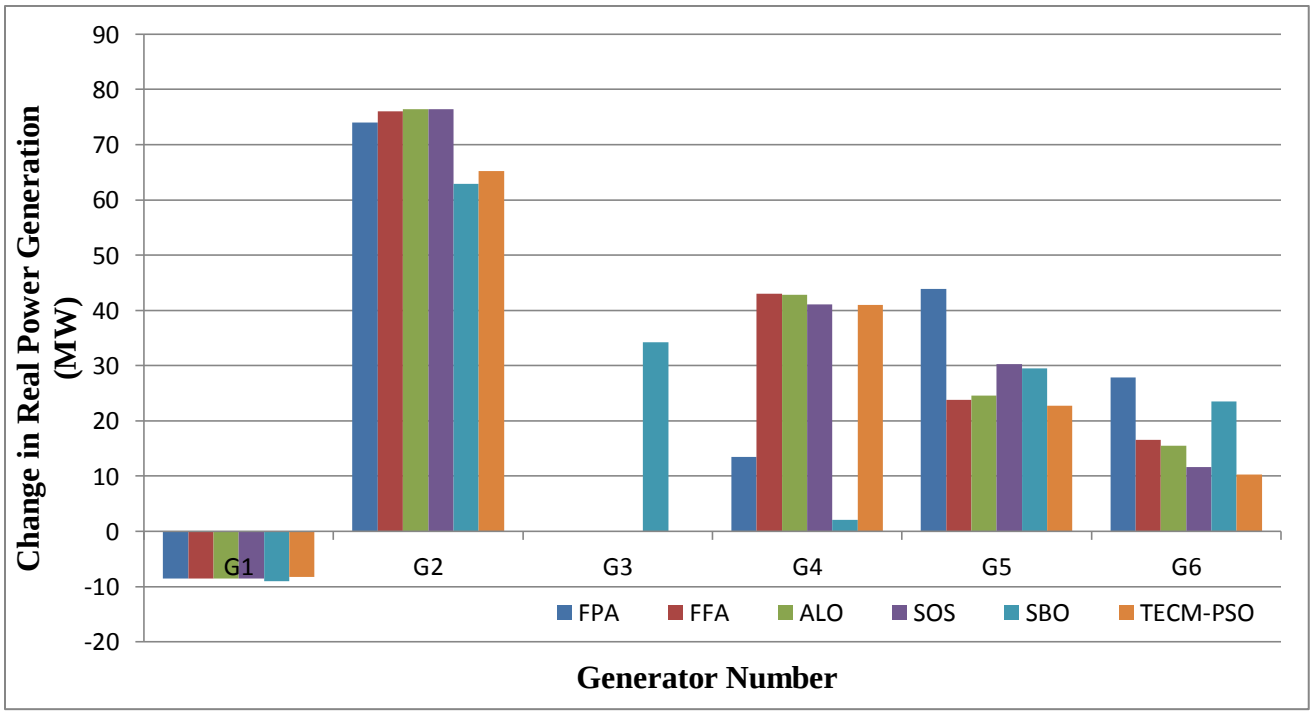

Figure 6.13: Change in real power generation of individual participating generator in MW for congestion relieving of case B (IEEE 30 bus system)

A comparative graphical representation of change in real power generation of the individual generators using proposed algorithm and six other evolutionary algorithms has been shown in Fig. 6.13. It has been observed that there is a remarkable reduction in NGR for the proposed algorithm. % CMR of proposed algorithm is highest (82.3) amongst all comparative algorithms and proves the computational proficiency of the algorithm. Overflow in line 1-2 has been reduced to 129.987 MW after CM from 312.98 MW before CM. For line 2-8 this decrease is from 98.34 MW (before CM) to 61.78 MW (after CM) for 2-9 it is from 106.56 MW (before CM) to 64.23 MW (after CM). Total feasible solutions are 47,789 for 30 independent runs of the proposed algorithm for the said case. The convergence characteristics of the proposed approach have been obtained and are shown in Fig. 6.14. Comparison of proposed convergence characteristics with the convergence manner of six other optimization algorithms namely PSO, FPA, FFA, ALO, SOS and SBO has also been done. From comparison it is clear that the proposed characteristics are the most consistent, balanced and optimized among all indicating the superiority of the approach.

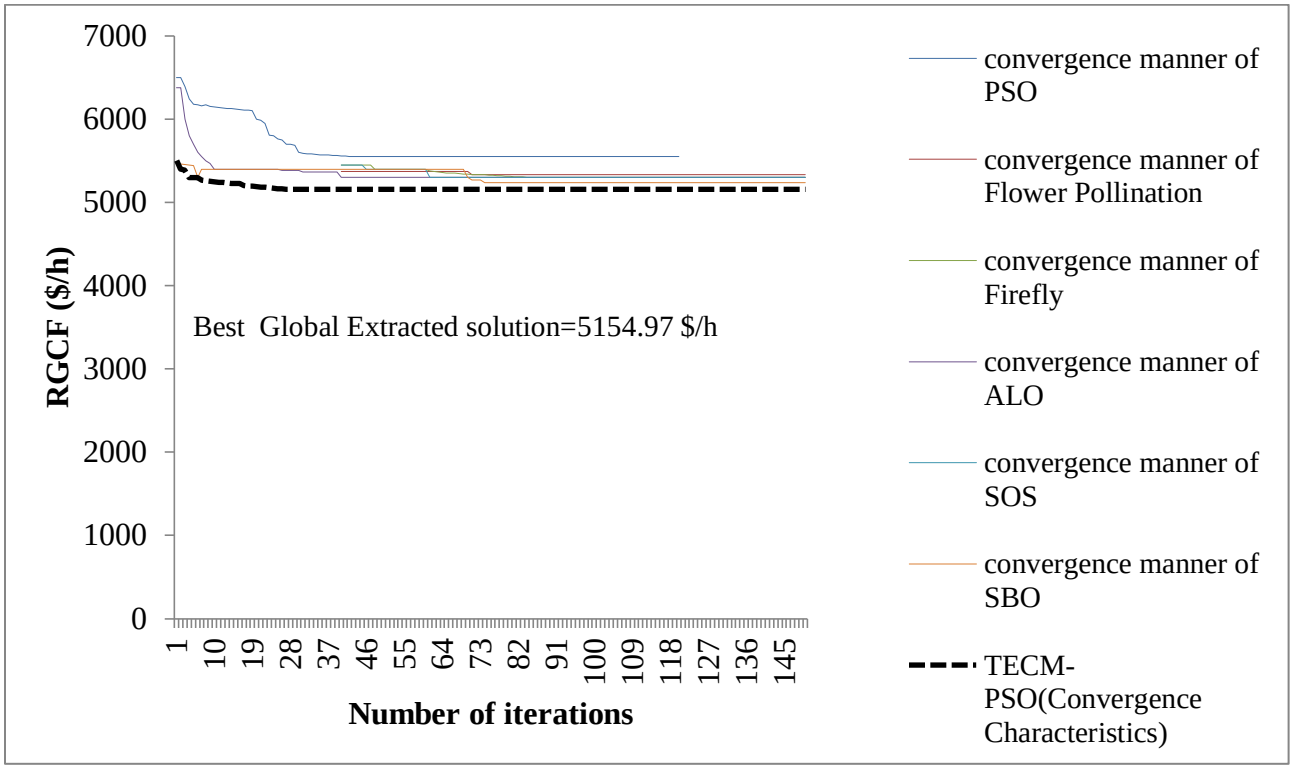

Figure 6.14: Comparison of convergence characteristics of different evolutionary algorithms for line outage case B (IEEE 30 bus system)

6.9.2 IEEE 57 Bus System

IEEE 57-bus test system comprising of seven generator buses, fifty load buses and eighty transmission lines has been chosen for the test purpose. The system line and bus data have been specified in **Appendix A1**. Details of incremented and decremented bids submitted by generator companies are given in **Appendix A2.**

The details of the selected test line outage cases (case C and case D) and the corresponding congested lines has been shown in Table 6.2 and Table 6.3 respectively. For alleviating congestion of both case C and case D, the first step in procedure is to evaluate RPCF values of all the generators which is been done by URCT algorithm and correspondingly the RPCF values have been plotted against each line and for all the generators in Fig. 6.15 and Fig. 6.18. From this distribution, it has been found that 3 generators (G1, G5 and G6), out of 7 for case C and 2 generators (G2 and G3), out of 7 for case D are actually participating in rescheduling process. This number is quite accurate as compared to the sensitivity approach stated in art of literature. This exact determination of the number of participating generator has reduced the efforts of a system operator with an ease of generator data handling.

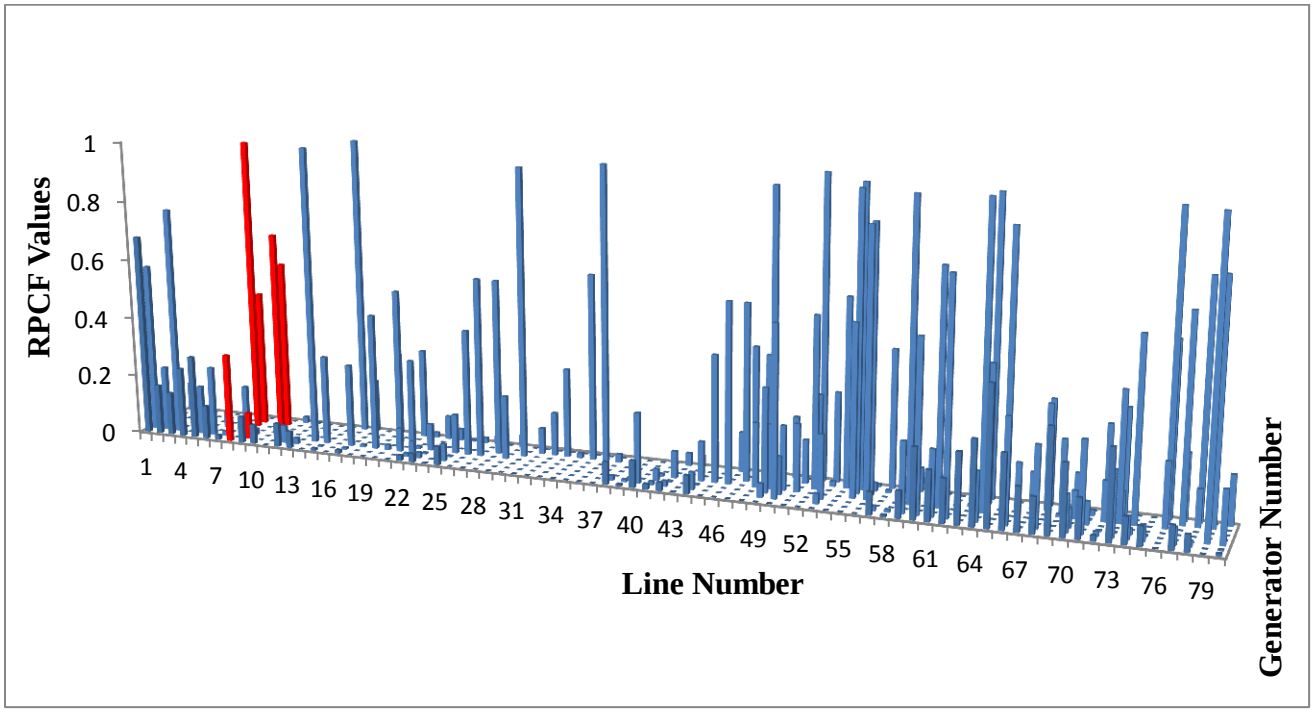

Figure 6.15: Distribution of generators contribution factors among various lines for line contingency case C (IEEE 57 bus system)

The next step is to execute the steps of TECM-PSO algorithm to find out the net amount of NGR and RGC cost to relieve the congestion for both the test cases. The statistical results of the proposed algorithm after 30 trial simulations have been evaluated and compared for mean values of generation adjustment of individual generators, total generation change and overall rescheduling cost with various evolutionary algorithms as shown in Table 6.5.

Table 6.5: Simulated statistical results of contingency cases of IEEE 57 bus system using proposed algorithm and their comparison

Case C	**Optimization Algorithm**						
Variables	**PSO (Balaraman, 2011)**	**FPA (Verma and Mukherjee, 2016c)**	**FFA (Verma and Mukherjee, 2016a)**	**ALO (Verma and Mukherjee, 2016b)**	**SOS (Verma et al., 2017)**	**SBO (Chintam and Daniel, 2018)**	**TECM-PSO (Proposed)**
ΔPG1 (MW)	23.13	0.876	5.635	34.367	70.001	-0.05437	67.54
ΔPG2 (MW)	12.44	0	2.523	1.609	0.0008	-11.72790	NP*
ΔPG3 (MW)	7.49	9.247	0.509	0	0.0003	-5.81154	NP*
ΔPG4 (MW)	−5.38	−1.362	0.107	−1.867	0	-45.26118	NP*
ΔPG5 (MW)	−81.21	−52.479	−39.151	−42.254	−44.222	-51.32093	−31.67
ΔPG6 (MW)	0	−24.548	−35.112	−31.596	−27.149	-34.86761	−34.167
ΔPG7 (MW)	39.03	64.334	62.193	30.327	.0002	-0.53486	NP*
NGR	168.70	152.849	145.227	142.02	141.385	144.5783	133.377

(MW)						9	
Best RGC ($/h)	6951.9	6340.8	6050.1	5896.548	5895	5773.27	5238.9
% CMR	NR	46.4	43.6	49.6	NR	89	90.02
Case D							
Variables	**PSO (Balaraman, 2011)**	**FPA (Verma and Mukherjee, 2016c)**	**FFA (Verma and Mukherjee, 2016a)**	**ALO (Verma and Mukherjee, 2016b)**	**SOS (Verma et al., 2017)**	**SBO (Chintam and Daniel, 2018)**	**TECM-PSO (Proposed)**
ΔPG1 (MW)	NR*	−0.006	0.370	−0.1074	0	0.76179	NP*
ΔPG2 (MW)	NR*	−35.623	−27.508	−28.2907	−28.35	0.08662	−20.567
ΔPG3 (MW)	NR*	20.097	31.629	28.593	28.59	22.04924	26.75
ΔPG4 (MW)	NR*	0.028	0.330	0.1338	0	0.17019	NP*
ΔPG5 (MW)	NR*	1.429	−2.254	−0.0503	0	-10.50832	NP*
ΔPG6 (MW)	NR*	−0.030	−1.935	−0.0088	0	-0.0000	NP*
ΔPG7 (MW)	NR*	13.965	−0.510	−0.0218	0	16.00743	NP*
NGR (MW)	76.314	71.181	64.539	57.2590	56.945	49.5859	47.137
Best RGC ($/h)	3117.6	2912.6	2618.1	2317.6	2307.1	2084.78	2012.89
% CMR	NR	36.8	34.4	42.8	NR	56	64.67

NP* - Not Participating, NR* - Not reported

From the statistical result it is cleared that the individual generator adjustment as well as net generation re-scheduled are found to be least for the proposed algorithm among all comparative algorithms for both the test cases. For case C, NGR has been found to be 133.377 MW, which is the least evaluated amount as compared to PSO with 168.70 MW, FPA with 152.849 MW, FFA with 145.227 MW, ALO with 142.02 MW, SOS with 141.385 MW and SBO with 144.578 MW. Moreover, there is a substantial decrease in RGC. RGC for proposed algorithm has been found to be 5238.9 $/h for the outage case C, which is again least as compared to results obtained with PSO (6951.9 $/h), FPA (6340.8 $/h), FFA (6050.1 $/h), ALO (5896.548 $/h), SOS (5895 $/h) and SBO (5773.27 $/h).Comparative graph governing the participation of individual generators of the proposed algorithm and six other comparative algorithms has been shown in Fig. 6.16.

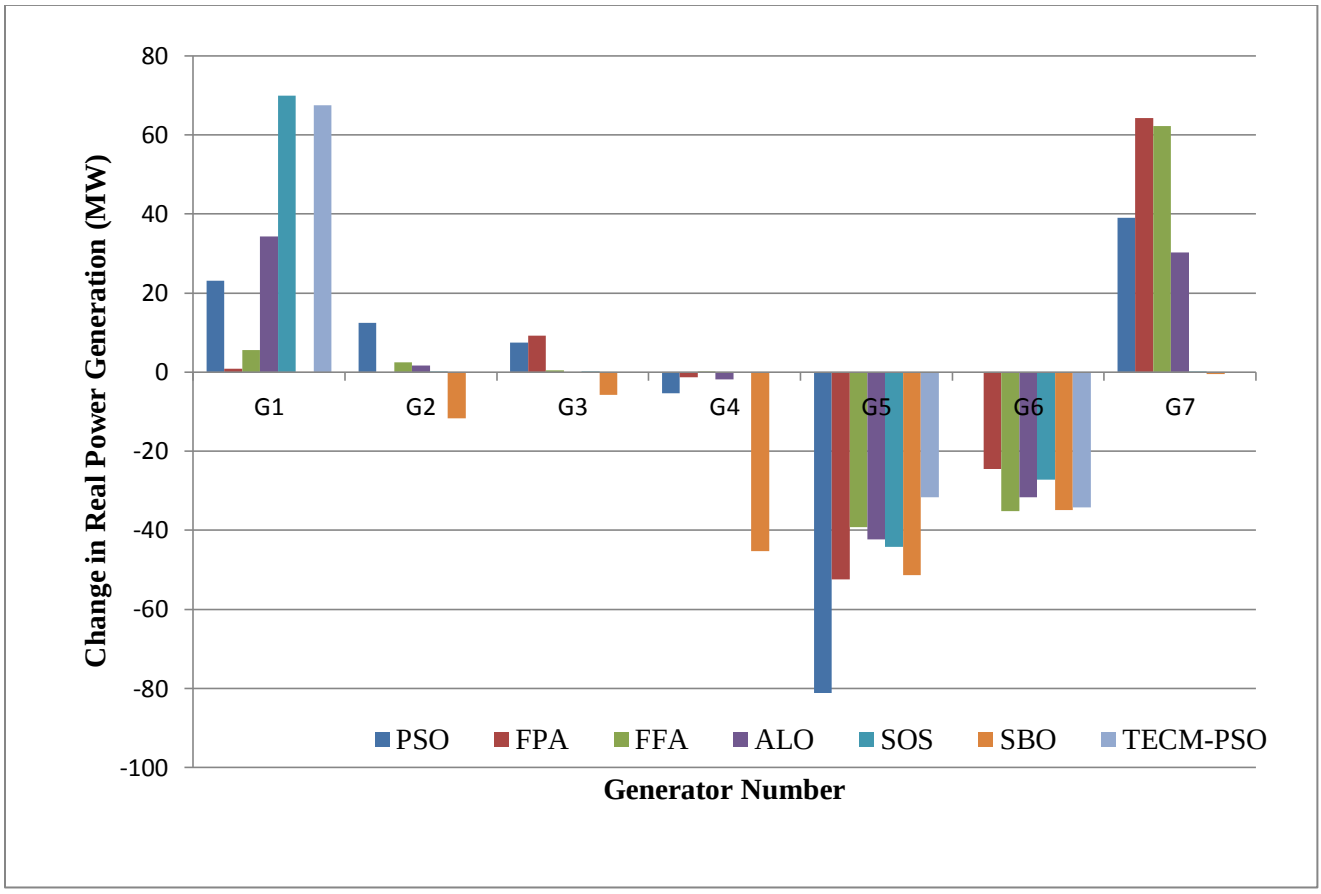

Figure 6.16: Change in real power generation of individual participating generator in MW for congestion relieving of case C (IEEE 57 bus system)

The total system loss during congestion was 61.598 MW during congestion, which has been decreased to 17.234 MW after simulating through proposed approach for the said case. Line flows in

the congested lines have come under their specified limits after rescheduling process. Line flow in line 5-6 has decreased to 174.56 MW after rescheduling from 195.956 MW before rescheduling and for line 6-12 line flow has reduced to 34.78 MW after rescheduling from 49.45 MW before rescheduling. Furthermore, the convergence precision and fast rate of convergence of proposed algorithm has improved the profile of CM considerably as shown in Fig. 6.17. MOF has been executed for 46, 897 times for 30 independent runs.

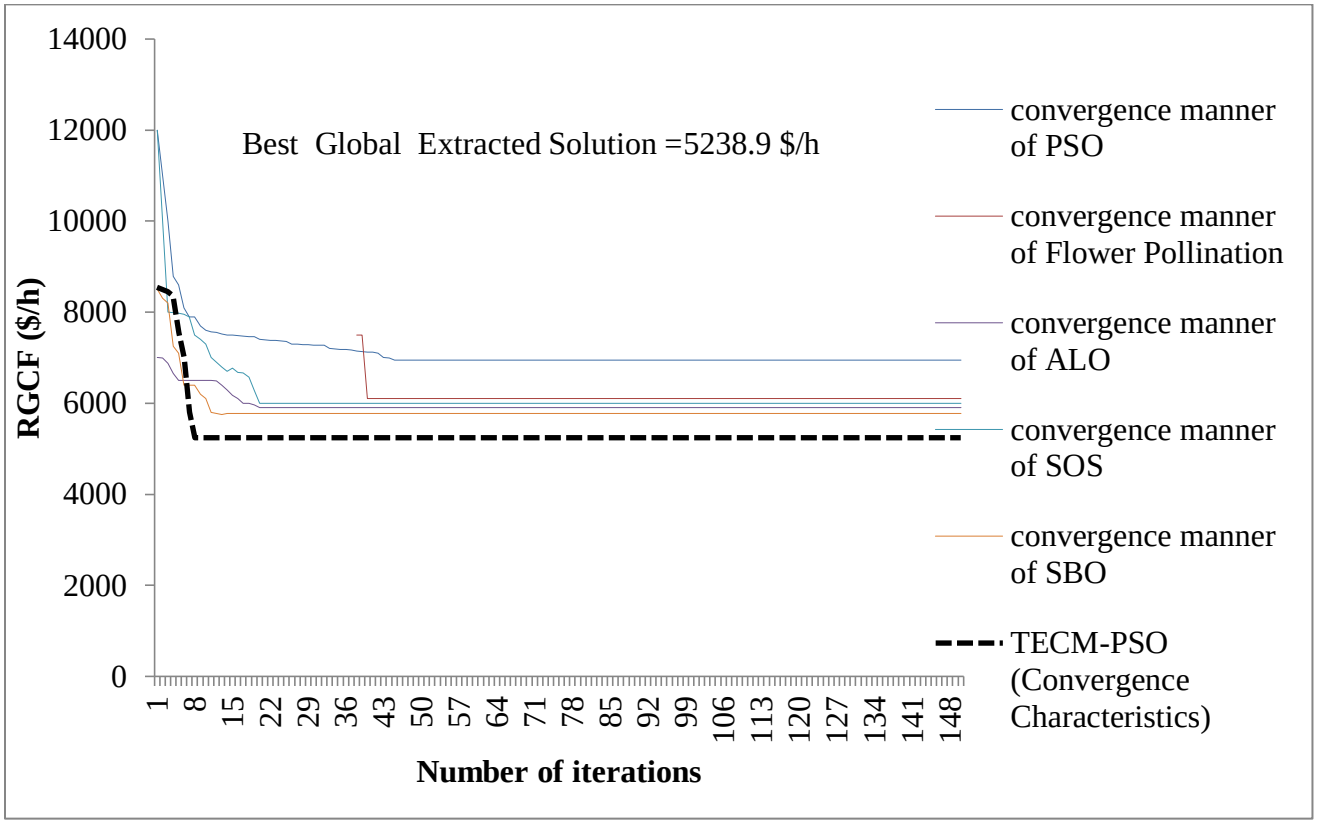

Figure 6.17: Comparison of convergence characteristics of different evolutionary algorithms for line outage case C (IEEE 57 bus system)

For case D, two generators are participating in rescheduling process as shown in Fig. 6.18 and as explained before. Participation of each generator in terms of the change in their real power outputs for the proposed algorithm and six other evolutionary algorithms have been revealed in Fig. 6.19.

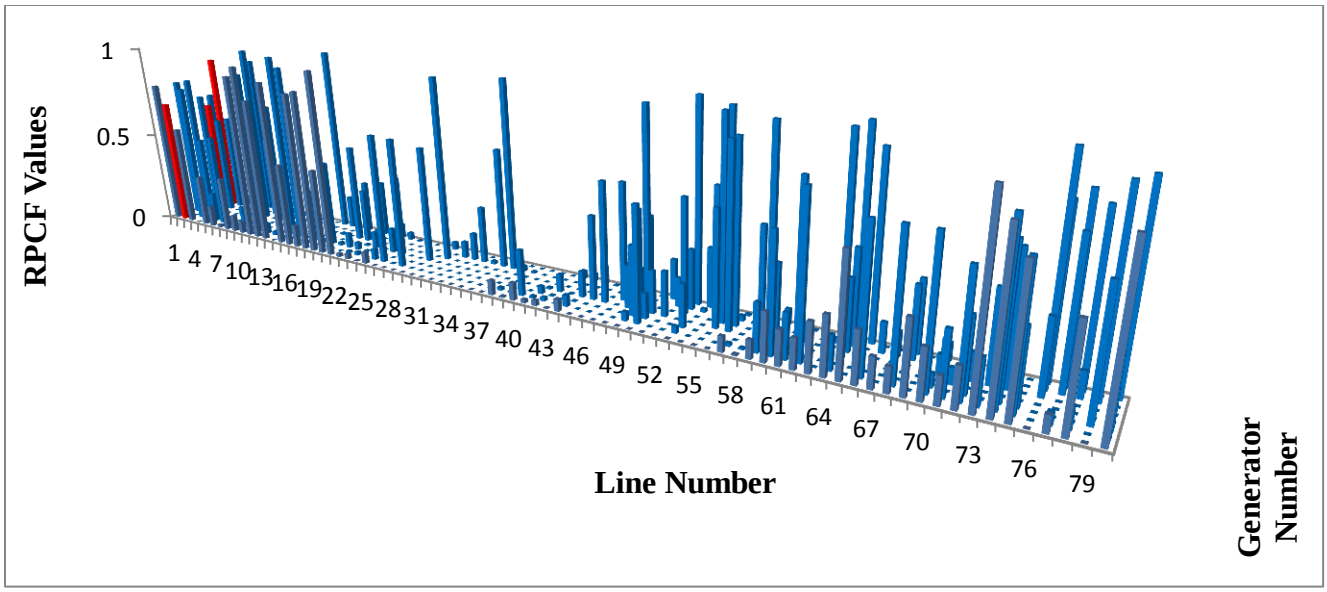

Figure 6.18: Distribution of generators contribution factors among various lines for line contingency case D (IEEE 57 bus system)

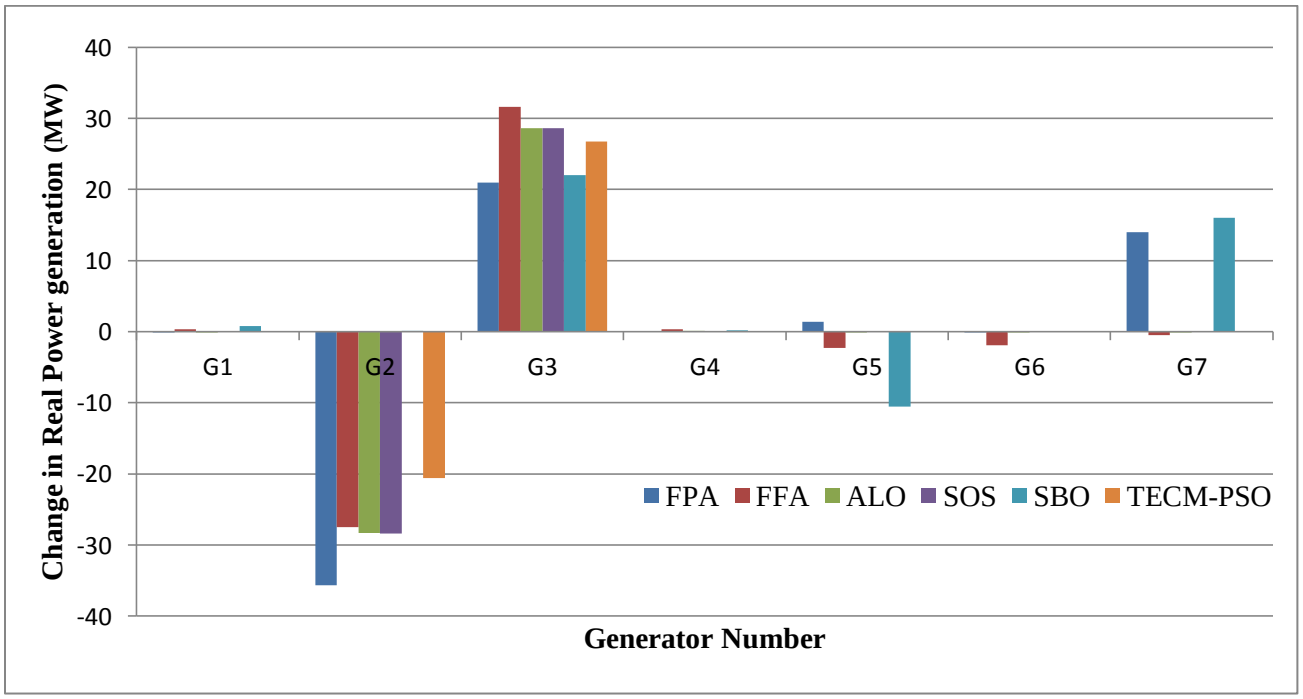

Figure 6.19: Change in real power generation of individual participating generator in MW for congestion relieving of case D (IEEE 57 bus system)

The bar graph distribution in Fig. 6.19 clearly shows the least change in outputs of participating generators for rescheduling purpose in case of proposed algorithm. Furthermore, analyzing the

statistical results for case D, NGR, RGC and % CMR have been found to be 47.137 MW, 2012.89 $/h and 64.67 respectively for the proposed technique. While NGR values for PSO, FPA, FFA, ALO, SOS and SBO are 76.314 MW, 71.181 MW, 64.539 MW, 57.2590 MW, 56.945 MW and 49.5859 MW respectively. Simulation results of RGC for PSO, FPA, FFA, ALO, SOS and SBO are respectively the 3117.6 $/h, 2912.6 $/h, 2618.1 $/h, 2317.6 $/h, 2307.1 $/h and 2084.78 $/h. These results clearly indicate that the proposed algorithm outperforms among all in terms of significant reduction of NGR and RGC. Overloading of line 2-3 has also been eliminated completely. The convergence characteristics of the proposed and comparative algorithms have been shown in Fig. 6.20. Numbers of feasible solutions have been found to be 46, 678 out of 48, 000.The comparison of % CMR values as shown in Table 6.5 indicate that the convergence mobility of proposed approach is highest with precise and accurate control of governing parameters of CM. Most consistent and balanced characteristics have been obtained for the proposed algorithm.

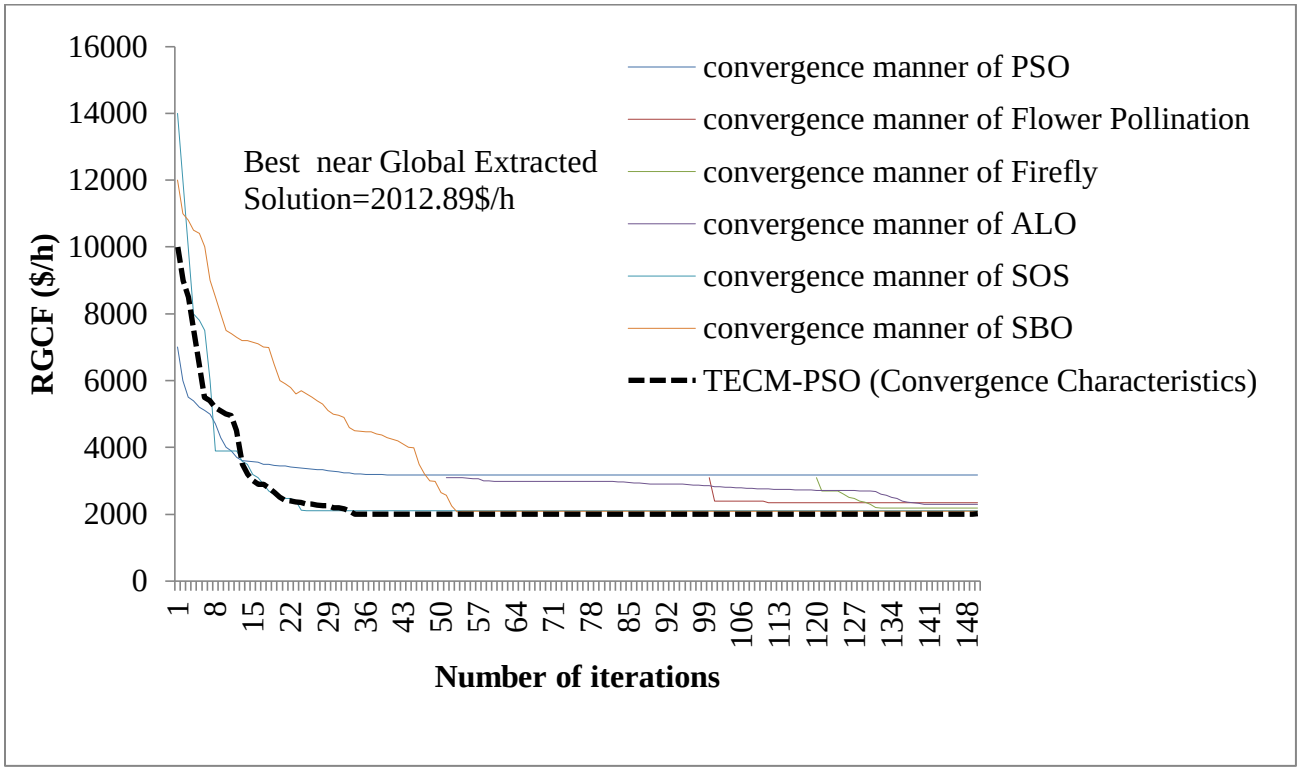

Figure 6.20: Comparison of convergence characteristics of different evolutionary algorithms for line outage case D (IEEE 57 bus system)

6.9.3 IEEE 118 Bus System

IEEE 118 bus system with 54 generator buses, 64 load buses and 186 transmission lines has been considered here for test purpose. Details of bus data and line data are shown in **Appendix A1.** Details of incremented and decremented bids submitted by generator companies are given in **Appendix A2.**

Description of the outage case and the identified congested lines from the load flow solution has been depicted in Table 6.3. The number of participating generators for the said contingency has been evaluated from RPCF of generators using URCT algorithm and the RPCF distribution of all the individual and participating generators among various lines of the test system have been shown in Fig. 6.21. From distribution of RPCF values this has been cleared that out of 54 generators, only 17 generators (G1, G5, G6, G11, G12, G14, G15, G17, G19, G21, G25, G26, G28, G34, G37, G47, G51) are participating in generation rescheduling process which is quite lesser in number as compared to sensitivity based method of identifying the participating generators mentioned in literature. Furthermore, the active power of these participating generators has been rescheduled using the proposed algorithm.

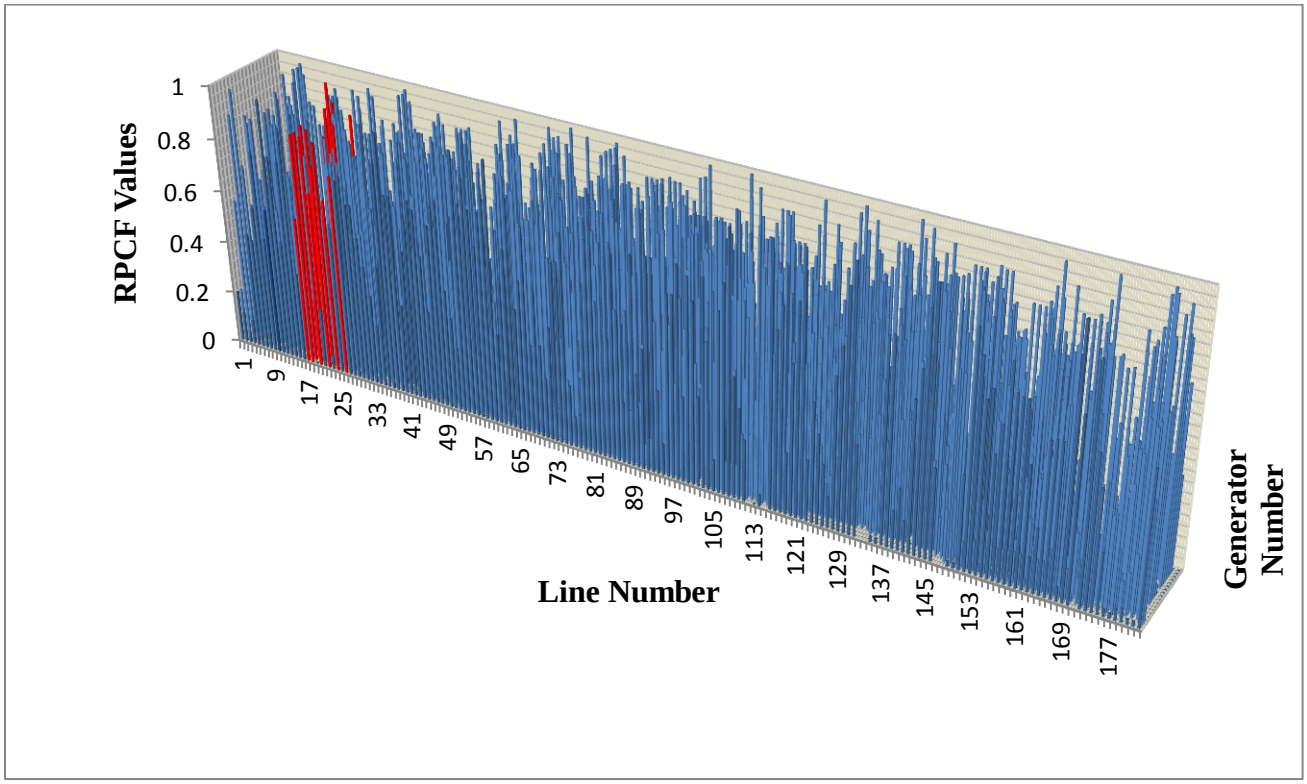

Figure 6.21: Distribution of generators contribution factors among various lines for line contingency case E (IEEE 118 bus system)

The statistical results of individual generator adjustment, NGR, RGC and % CMR obtained after 30 trials of simulation for the individual generator adjustments, net NGR and overall congestion management cost have been shown in Table 6.6. Comparison of results has also been done with five other algorithms.

Table 6.6: Simulation statistical results of contingency case of IEEE 118 bus system using proposed algorithm and their comparison

Case E	**Optimization Algorithm**					
Variables	**PSO (Balaraman, 2011)**	**FPA (Verma and Mukherjee, 2016c)**	**FFA (Verma and Mukherjee, 2016a)**	**ALO (Verma and Mukherjee, 2016b)**	**SBO (Chintam and Daniel, 2018)**	**TECM-PSO (Proposed)**
ΔPG1 (MW)	24.502	2.7636	10.223	8.7247	6.3506	6.5467
ΔPG2 (MW)	0	0.1765	4.7701	0.0005	3.45815	NP*
ΔPG3 (MW)	1.0259	4.8005	11.165	0.0015	5.01763	NP*
ΔPG4 (MW)	1.3148	0	−0.5718	−0.0782	8.99506	NP*
ΔPG5 (MW)	−21.82	−207.8	−207.3	−207.7	-203.28939	−187.89
ΔPG6 (MW)	105.32	105.32	104.93	105.22	8.81232	100.87
ΔPG7 (MW)	0	0	0.8256	0.123	22.22845	NP*
ΔPG8 (MW)	16.815	0.0023	4.6322	0.0011	0.61579	NP*

ΔPG9 (MW)	23.665	0	1.6977	0.0675	6.78422	NP*
ΔPG10 (MW)	0	0	2.1221	0.0355	2.32609	NP*
ΔPG11 (MW)	121.51	18.689	8.3874	2.3777	-0.2996	0.9865
ΔPG12 (MW)	116.31	12.302	13.317	116.12	1.06873	25.45
ΔPG13 (MW)	3.0092	0	0.0087	0.0001	0.62895	NP*
ΔPG14 (MW)	0.0177	0	0.7567	0.2949	4.24786	0.7856
ΔPG15 (MW)	8.8665	78.737	83.455	69.115	12.42693	55.868
ΔPG16 (MW)	7.1475	0	−0.2312	0.0140	0.2169	NP*
ΔPG17 (MW)	0.4916	0	1.4716	−0.027	0.49255	−0.045
ΔPG18 (MW)	0	0	5.777	−0.0004	1.48727	NP*
ΔPG19 (MW)	0	0	3.8414	0.9068	0.46018	0.5678
ΔPG20 (MW)	6.0792	−11.934	0.7992	0.0748	-0.34758	NP*
ΔPG21 (MW)	19.359	9.6558	10.422	42.198	-1.09116	32.14
ΔPG22 (MW)	36.798	1.665	11.756	0.0004	-0.24492	NP*
ΔPG23 (MW)	0	0	−0.2571	0.0052	0.36291	NP*

ΔPG24 (MW)	0	0	0.3293	0.0001	0.25945	NP*
ΔPG25 (MW)	0	113.40	6.8269	104.53	1.53135	72.15
ΔPG26 (MW)	0	101.12	2.5788	0.1359	-5.89327	0.1236
ΔPG27 (MW)	0	0	0.9488	0.0413	0.3658	NP*
ΔPG28 (MW)	0	4.409	14.5599	1.2427	-112.363	1.1987
ΔPG29 (MW)	0	15.742	11.042	0.0021	-6.58455	NP*
ΔPG30 (MW)	10.702	0	0.8295	0.0006	-4.10322	NP*
ΔPG31(MW)	0	0	0.4552	0.0018	0.90951	NP*
ΔPG32 (MW)	0	−10.03	0.3774	0.0001	0.40333	NP*
ΔPG33 (MW)	0	0	0.7425	0.0005	0.17212	NP*
ΔPG34 (MW)	0	0	3.9674	0.2010	0.78747	0.1234
ΔPG35 (MW)	0	0	−0.049	−0.0004	0.14819	NP*
ΔPG36 (MW)	0	0	0.6654	0.0006	0.18178	NP*
ΔPG37 (MW)	0	8.51	118.22	4.8963	-3.22489	0.1789
ΔPG38 (MW)	0	0	−0.319	0.0051	0.32378	NP*

ΔPG39 (MW)	0	1.1382	4.9421	0.0035	-0.80088	NP*
ΔPG40 (MW)	0	0	1.938	−0.0005	-74.35625	NP*
ΔPG41 (MW)	0	0	0.9656	0.0237	0.19709	NP*
ΔPG42 (MW)	0	0	−0.092	0.0001	0.15209	NP*
ΔPG43 (MW)	0	0	1.53	0.0452	1.21754	NP*
ΔPG44 (MW)	0	0	1.1018	0.0023	0.13011	NP*
ΔPG45 (MW)	0	0	0.3837	0.2974	-0.54271	NP*
ΔPG46 (MW)	0	6.0703	22.78	0.0223	-3.72569	NP*
ΔPG47 (MW)	0	0	−0.125	0.2498	1.82584	0.2167
ΔPG48 (MW)	0	0	3.0727	0.0276	0.36729	NP*
ΔPG49 (MW)	0	0	1.5325	0.1654	0.15896	NP*
ΔPG50 (MW)	0	0	2.5903	0.2261	0.99087	NP*
ΔPG51 (MW)	0	46.354	3.7627	46.1738	-0.90559	6.89
ΔPG52 (MW)	0	0	12.6412	0.0002	0.27131	NP*
ΔPG53 (MW)	0	0	0.4368	0.0006	0.78541	NP*

ΔPG54 (MW)	0	0	0.4615	−0.0002	1.05513	NP*
NGR (MW)	717.7839	760.69	709.01	711.46	515.9883	492.0309
Best RGC ($/h)	17, 742	17, 189	17, 041	15, 448	12,336.05	11,978.867
% CMR	NR	40.2	41.6	75.5	83.2	85.67

NP*- Not Participating, NR*- Not reported, SOS (NR in literature)

From the results, it has been clear that total amount of NGR and net RGC to relieve the congestion are found to be 492.0309 MW and 11,978.86 $/h respectively for the proposed algorithm, which are least among all the mentioned comparative algorithms. The total system loss has been found to be 164.878 MW after alleviating congestion which was 257.968 MW during congestion. Total feasible solutions are 47, 234 for 30 independent runs of proposed algorithm. Significant decrease in NGR and RGC can be seen in results for proposed algorithm. Figure 6.22 represents the comparative representation of individual generator adjustments of participating generators to relieve congestion.

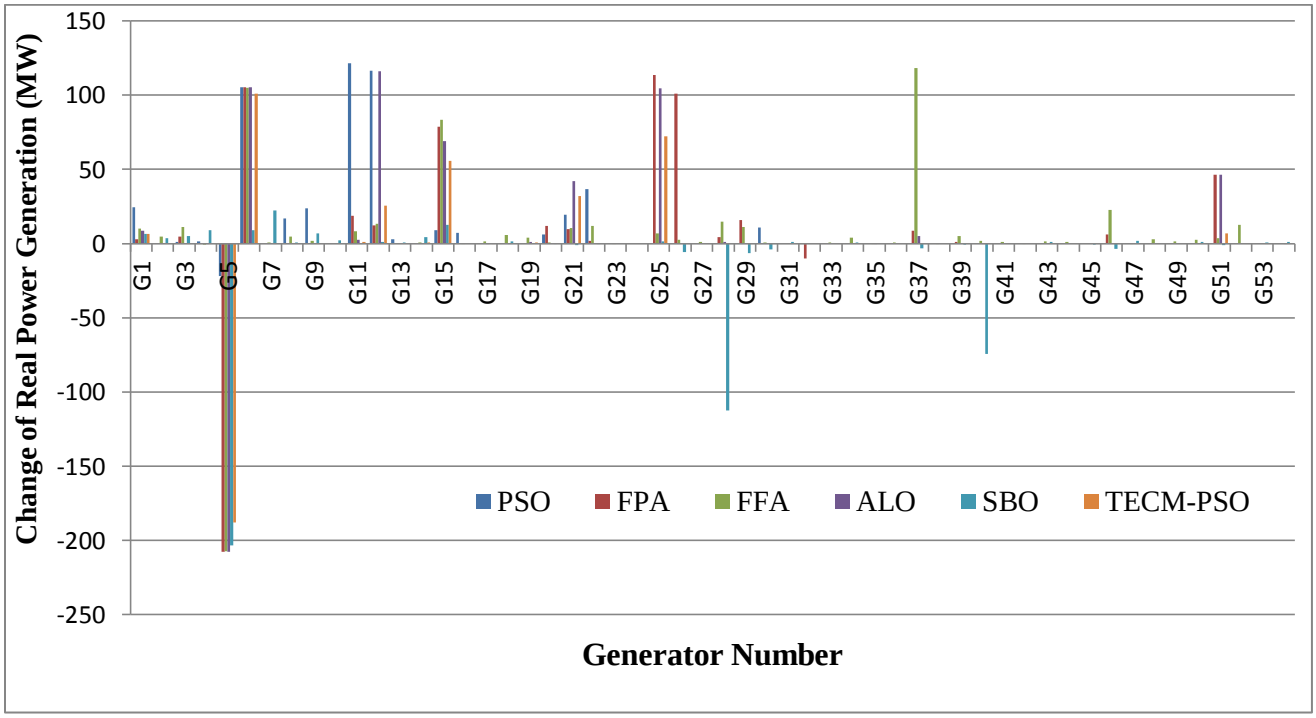

Figure 6.22: Change in real power generation of individual participating generator in MW for congestion relieving of case E (IEEE 118 bus system)

From Fig. 6.22, it is clear that the net amount of overall rescheduled generation power is also optimized using proposed approach. From the results, it has also been endowed that throughout the tests that the proposed algorithm provides near global optimum solution among all the mentioned comparative algorithms in every independent trial run and it remains consistent even for large system as well. Line flows in congested lines have also come under specified limits after rescheduling. Line flow in 16-17 has been decreased to 145.89 MW after rescheduling from 208.98 MW during contingency. Similarly, line flows of line 30-17 has been found to be 497.89 MW after rescheduling and of 8-30 lime has reduced to 154.78 MW after CM as compared to 367.297 MW before CM. Furthermore, the convergence characteristics of the proposed algorithm have been established as well as compared with convergence manner of four other evolutionary techniques (namely FPA, FFA, ALO and SBO) as shown in Fig. 6.23.

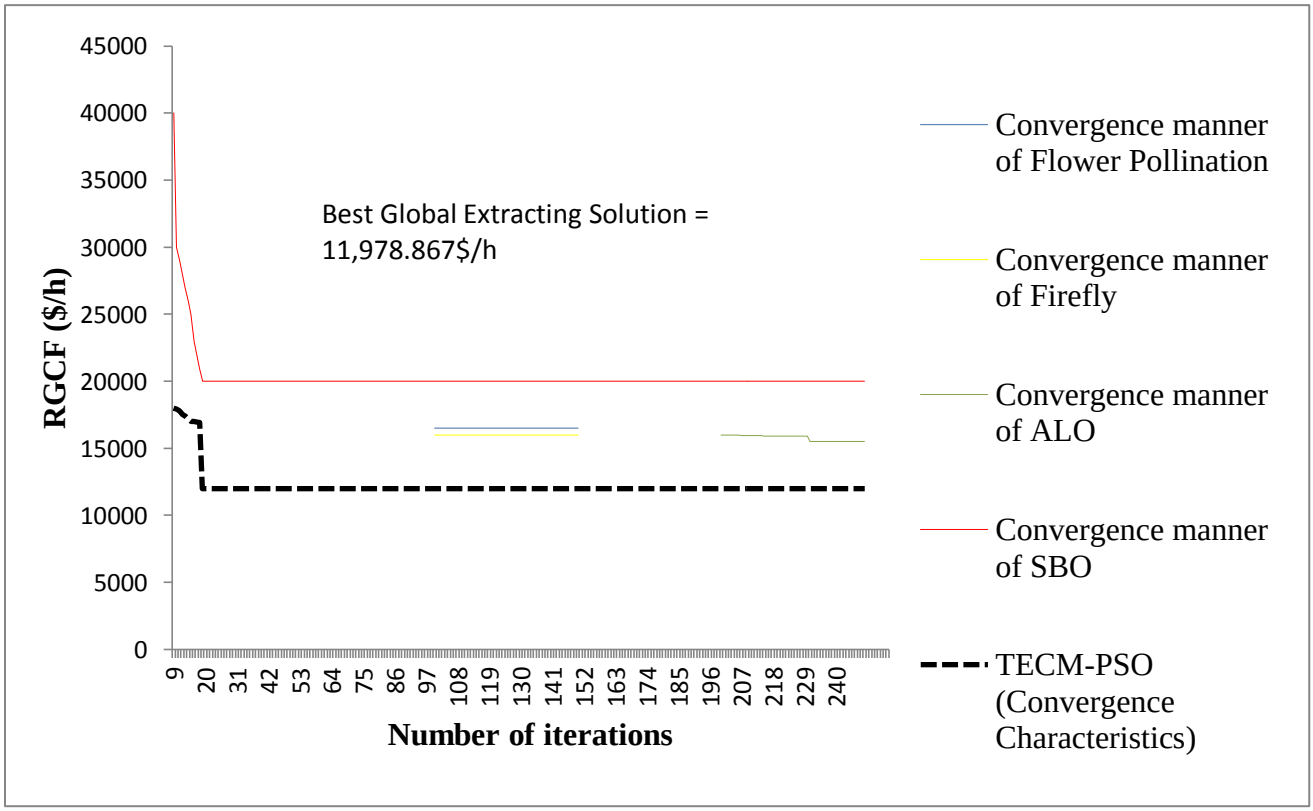

Figure 6.23: Comparison of convergence characteristics of different evolutionary algorithms for line outage case E (IEEE 118 bus system)

TECM-PSO offers the most optimized characteristics as the convergence mobility of it is fastest among all algorithms.

6.10 Computational Effectualness and Convergence Mobility Range of Proposed Approach

The use of vigorous power flow tracing algorithm has emerged the exact and accurate number of participating generators for each contingency case with less generator data information as compared to sensitivity based approach stated in art of literary. This has reduced the deed of system operator. The sequences generated by the twin extremity map have replaced the random numbers for different PSO parameters and hence the convergence speed and precision has been increased. Also, there is no need of tuning the penalty coefficients for each generation and hence the particles have been guided to their feasible and optimal search space quickly resulting in less computational time for attaining next position for each particle. Table 6.7 clearly indicates the statistical results and computational effectualness of the proposed approach for all test cases.

Table 6.7: Statistical results of proposed algorithm in terms of best, mean and worst RGC, standard deviation and MFE (Main Function Evaluations) for 30 independent runs

Statistic	**Case A**	**Case B**	**Case C**	**Case D**	**Case E**
Mean RGC	460.827	5296.754	5473.276	2212.789	12,023.35
Best RGC	410.756	5154.978	5238.96	2012.898	11,978.867
Worst RGC	490.875	5309.788	5521.892	2287.676	12,768.456
Standard deviation	0.098	0.087	0.1245	0.2346	0.2643
Number of times main Function Evaluations Occurs (MFE)	47,342	47,789	46,897	46,678	47,234

Furthermore, to judge the convergence speed, convergence mobility rate (CMR) is evaluated for all the prescribed cases. Following procedure is followed to evaluate CMR.

CMR Evaluation Procedure

1. Execute the algorithms up to the maximum of number of main objective evaluations($NMOF^{\max}$)
2. Based on convergence, determine minimum objective value found and determine in which number of main objective evaluations this value has come. Set this as $NMOF^{R}$.
3. Compute the percentage CMR of the algorithm using Eq. (6.20)

$$CMR(\%) = \left(1 - \frac{NMOF^{R}}{NMOF^{\max}}\right) \times 100 \quad , \quad \text{where} \quad CMR \in (0,1) \tag{6.20}$$

If for an algorithm CMR = 1, it indicates best convergence rate and CMR = 0, depicts the worst convergence rate of the considered algorithm. The average percentage CMR of the proposed method for all the test cases has been evaluated and compared with other evolutionary algorithms, which are shown in Table 6.4, Table 6.5 and Table 6.6.The average percentage CMR of the proposed algorithm is highest among all for all the test cases, which reveals the effectiveness of proposed approach. Figure 6.24 shows the bar comparison of % CMR values of various comparative optimization algorithms and proposed algorithm. This comparison indicates the highest % CMR of the proposed algorithm.

Figure 6.24: Comparison of % CMR values of various evolutionary algorithms for selected test cases

6.11 Concluding Remarks

Novel TECM-PSO optimized robust and effective method of rescheduled cost management has been analyzed and explored quantitatively and qualitatively in this chapter. The proposed framework has been designed for two main criterions of optimization. First criterion incorporates URCT methodology in the algorithm to evaluate exact number of participating generators for rescheduling process and second criterion implements dynamic constraint optimized TECM-PSO algorithm to the outputs of participating generators to achieve near global optimal solution of re-scheduled generation cost function for all types of contingencies. The main attribute of proposed algorithm is that it always evolves global optimum solutions in every independent trial run which remain consistent even for large system as well. Decrease in NGR using proposed approach lies in the scale range of 1.15 to 1.56 for case A, 1.092 to 1.138 for case B, 1.06 to 1.25 for case C, 1.05 to 1.61 for case D and 1.04 to 1.45 for case E. Moreover, the percentage decrease in RGC is in the range of 3% to 23.78 % for case A, 2 % to 33.8% for case B, 9.25% to 24.64 % for case C, 3.4% to 34.5 % for case D and 2.8% to 32.4 % for case E respectively. Also, % CMR is found to be the highest among all comparative algorithms for each case. Outcomes of proposed approach and their comparison with other evolutionary algorithms clearly claim, “TECM-PSO” as a powerful optimization approach for CM.

Chapter 7 Concluding Remarks and Future Scope

The chapter aims to illustrate the overall conclusion of the thesis and possible future scope. Optimal findings, research contributions and their real time utilization for congestion management have been detailed in this chapter.

Analysis of results has been done both quantitatively and qualitatively. Introduction to deregulated power system and its structure is presented in the thesis, which will help researchers to understand the difference between traditional vertical utility system and deregulated power system. Detailed literature analysis and the corresponding research gaps are also mentioned. Interrelation of research gaps and contribution of the proposed research has made it easy to understand the requirement of proposed work in the present deregulated scenario.

Incorporation of dual features of OPF and AC PTCDF has led to extract the exact and accurate static and dynamic ATC values with faster convergence rate. The dynamic attribute of the proposed methodology is that the distribution of sensitivity factors among various line for different types of transactions have been further utilized for finding the optimal location of UPFC for respective transactions, which has not been done so far in previous research work.

Implementation of modified power flow tracing algorithm has considerably reduced the efforts of the system operator to estimate the number of participating generators for the rescheduling process. Implementation of the novel ITM-CPSO algorithm to evaluate the overall CM cost has substantially improved the profile of the congestion management in terms of least congestion management cost, minimum generation adjustments and the overall system losses. Further, the incorporation of load management procedure in the same algorithm has turned the proposed technique security ensured and most reliable for complete congestion relieve for all types of contingencies.

ITM-CPSO algorithm has been further designed to optimally allocate UPFC in case of $N-1$ contingency scenarios of IEEE 14 and IEEE 30 bus systems. Improvement in voltage profile of the system using the proposed approach is also dynamic. Obtained convergence characteristics of the

proposed algorithm are found to be the most consistent, rapid and converge to a better solution as compared to rest comparative optimization algorithms.

Moreover a novel hybrid chaotic algorithm (TECM-PSO) has also been introduced and designed to evaluate rescheduled generation cost function for the most severe outage cases of three test systems namely IEEE 30, IEEE 57 and IEEE 118 bus systems. Quantitative analysis of the results clearly indicates that the proposed approach has outperformed among all comparative algorithms mentioned in literature. Also, the CMR is also found to be highest among all. Furthermore, the established convergence characteristics have found to be most consistent, rapid and precise. Quantitative and qualitative analysis of results proves that the proposed approach has the ability to converge to the best global solution in minimum computation time.

Future Scope

After carrying out the extensive research work and deep analyses of the results, it has been observed that the present research work can be extended in following directions.

- The evaluated ATC results can be further utilized to find better generation locations for alleviating congestion.
- The optimal line locations for UPFC placement using sensitivity curves can further enhance the ATC values for all types of transactions by inserting the UPFC to the evaluated line locations.
- In the proposed work of minimization of overall CMC, the load management has been achieved through load shedding procedure. CMC can be further evaluated by considering other load management methodologies.
- In the thesis optimal location of UPFC has been identified using a robust, dynamic and effective ITM-CPSO algorithm. Furthermore, ITM-CPSO can be explored to find the optimal location of other FACT devices.
- Design of novel model using TECM-PSO has been proven to be best suited for evaluating the feasible solutions over the entire searching range. So, the aforesaid model can be applied to another real time test systems with the same objective function.
- Both proposed dynamic chaotic PSO algorithms can be explored for different objective functions in later research.

List of SCI Publications

1. Indu Batra, Smarajit Ghosh (2018), "An Improved Tent Map-Adaptive Chaotic Particle Swarm Optimization (ITM-CPSO) Based Novel Approach toward Security Constraint Optimal Congestion Management", Iranian Journal of Science and Technology, Transactions of Electrical Engineering. (**Springer Nature)** Volume 42, Issue 3, pp. 261–289. https://doi.org/10.1007/s40998-018-0072-6. Impact Factor : **0.519**
2. Indu Batra, Smarajit Ghosh (2018), "A Novel Approach of Congestion Management in Deregulated Power System Using an Advanced and Intelligently Trained Twin Extremity Chaotic Map Adaptive Particle Swarm Optimization Algorithm", Arabian Journal for Science and Engineering. (**Springer Nature**) Volume 44, Issue 8, pp. 6861-6886. https://doi.org/10.1007/s13369-018-3675-3. Impact Factor: **1.092**
3. Indu Batra, Smarajit Ghosh (2017), "A Novel Approach of Congestion Management using an Advanced Intelligently Trained Chaotic-Catfish Particle Swarm Optimization Algorithm", Romanian Journal of Information Science and Technology. (Communicated).
4. Indu Batra, Smarajit Ghosh (2021), "A Novel Approach towards Optimal Congestion Management using Advanced Chaotic Particle Swarm Optimization", IETE Journal of Research, **(Taylor and Francis)** (Communicated).

References

Aggarwal, S.K., Saini, L.M., Kumar, A. (2009), "Electricity Price Forecasting in Deregulated Markets: A Review and Evaluation", International Journal of Electrical Power & Energy System, Vol. 31, Issue 1, pp. 13–22. Doi:10.1016/j.ijepes.2008.09.003

Alamelu, S., Baskar, S., Babulal, C.K., Jeyadevi, S. (2015), "Optimal Sitting and Sizing of UPFC using Evolutionary Algorithms", International Journal of Electrical Power & Energy System, Vol. 69, pp. 222–231. Doi:10.1016/j.ijepes.2014.12.081

Alomoush, M. I. (2005), "Performance Indices to Measure and Compare System Utilization and Congestion Severity of Different Dispatch Scenarios", Electric Power System Research, Vol. 74, Issue 2, pp. 223–230. Doi:10.1016/j.epsr.2004.10.012

Androulidakis, E.A., Alexandridis, A.T., Psillakis, H.E., Agoris, D.P. (2005), "Challenges and Trends of Restructuring Power Systems due to Deregulation", Proceedings of the 5th WSEAS International Conference on Power Systems and Electromagnetic Compatibility, pp. 49–54, Corfu, Greece, 23-25th August, 2005.

Arabkhaburi, D., Kazemi, A., Yari, M., Aghaei, J. (2006), "Optimal Placement of UPFC in Power Systems using Genetic Algorithm", IEEE International Conference on Industrial Technology, pp.1694–1699. Doi: 10.1109/ICIT.2006.372474

Arrillaga, J., Bollen, M. H. J., Watson, N. R. (2000), "Power Quality Following Deregulation", Proceedings of the IEEE Conference, Vol. 88, Issue 2, pp. 246–261. Doi:10.1109/5.824002

Balaraman, S, Kamaraj, N. (2011), "Transmission congestion management using particle swarm optimization", Journal of Electrical System, Vol. 7, Issue 1, pp. 54–70.

Balaraman, S. (2013), "Applications of evolutionary algorithms and neural network for congestion management in power systems", Ph.D. dissertation, Anna University, India. http://hdl.handle.net/10603/10314

Balaraman, S., Kamaraj, N. (2010), "Congestion Management in Deregulated Power System using Real Coded Genetic Algorithm", International Journal of Engineering Science and Technology, Vol. 2, Issue 11, pp. 6681–6690.

Baskar, G., Mohan, M.R. (2009), "Contingency Constrained Economic Load Dispatch using Improved Particle Swarm Optimization for Security Enhancement", Electric Power System Research, Vol. 79, Issue 4, pp.615–621. Doi:10.1016/j.epsr.2008.08.013

Behera Saswati K and Mohanty, M. (2019), "Congestion management using Thyristor Controlled Series Compensator Employing Improved Grey Wolf Optimization Technique", International Journal of Electrical Engineering Education.Doi:10.1177/0020720918822730

Besharat, H., Taher, S.A. (2008), "Congestion Management by Determining Optimal Location of TCSC in Deregulated Power Systems", International Journal of Electrical Power & Energy System, Vol. 30, Issue10, pp. 563–568. Doi:10.1016/j.ijepes.2008.08.007

Bhattacharya, K., Bollen, Math, H. J., Daalder, Jaap, E. (2001), "Operation of Restructured Power Systems", link.springer.com/book/10.1007/978-1-4615-1465-7.

Bialek, J. (1996), "Tracing the Flow of Electricity", IEE Proceeding of Generation Transmission and Distribution, Vol. 143, Issue 4, pp. 313–320. Doi:10.1049/ip-gtd:19960461

Blanco, G., Olsina, F., Garces, F., Rehtanz, C. (2011), "Real Option Valuation of FACTS Investments based on the Least Square Monte Carlo Method", IEEE Transactions on Power System, Vol. 26, Issue 3, pp.1389–1398. Doi:10.1109/TPWRS.2010.2094211

Bompard, E., Correia, P., Gross, G., Amelin, M. (2003), "Congestion Management Schemes: A Comparative Analysis under a Unified Framework", IEEE Transactions on Power System, Vol. 18, Issue 1, pp.346–352. Doi: 10.1109/TPWRS.2002.807077

Boonyaritdachochai, P., Boonchuay, C., Ongsakul, W. (2010), "Optimal Congestion Management in an Electricity Market using Particle Swarm Optimization with Time-Varying Acceleration Coefficients", Computers and Mathematics with Applications, Vol. 60, Issue 4, pp. 1068–1077. Doi:10.1016/j.camwa.2010.03.064

Campbell, M. K. (2001), "Power System Deregulation", IEEE Potentials, Vol. 20, Issue 4, pp. 8-9. Doi:10.1109/45.983331

Chanda, S., De, A. (2011), "Application of Particle Swarm Optimization for Relieving Congestion in Deregulated Power System", IEEE Conference on Recent Advances in Intelligent Computational Systems, 03 November 2011 , Trivandrum, India, pp. 837–840. Doi: 0.1109/RAICS.2011.6069427

Chandwani M., Chaudhari, N.S. (1993), "Decision making as a Fuzzy logic process", International Journal of Management and Systems (IJOMAS), Vol.9, pp. 105-116.

Chen, L., Lilan, S., Yangwei, P.D. (2014), "Chaotic Improved PSO-based Multi objective Optimization for Minimization of Power Losses and L Index in Power Systems", Energy

Conversation and Management, Vol. 86, pp. 548–560. Doi:10.1016/j.enconman.2014.06.003

Chintam, J.R., Daniel, M. (2018),"Real Power Rescheduling of Generators for Congestion Management using a Novel Satin Bowerbird Optimization Algorithm", Energies, Vol. 11, Issue 1, pp. 1–16. Doi: 10.3390/en11010183

Christie, R.D., Wollenberg, B.F., Wangensteen, I. (2000), "Transmission management in the Deregulated Environment", Proceedings of IEEE, Vol. 88, Issue 2, pp.170–195. Doi: 10.1109/5.823997

Chung, C. Y., Lei, W., Howell, F. Kundur, P. (2004), "Generation Rescheduling Methods to Improve Power Transfer Capability Constrained by Small-Signal Stability", IEEE Transaction on Power System, Vol. 19, Issue.1, pp. 524–530. Doi: 10.1109/TPWRS.2003.820700

Conejo A.J. and Bertrand, R.G. (2006), "Congestion Management Ensuring Voltage Stability", IEEE Transaction on Power System, Vol. 21, Issue 1, pp.357–364. Doi :10.1109/TPWRS.2005.860910

Dhanalakshmi, S., Kananan, S., Mahadevan, K. (2011), "Market modes for Deregulated Environment — A Review," IEEE International Conference on Emerging Trends in Electrical and Computer Technology, pp. 82–87, 23-24th March 2011, Nagercoil, India. Doi:10.1109/ICETECT.2011.5760096

Donde, V., Pai, M. A., Hiskens, I. A. (2001), "Simulation and Optimization in an AGC System after Deregulation", IEEE Transactions on Power System, Vol. 16, Issue 3, pp. 481–489. Doi:10.1109/59.932285

Dutta, S. and Singh, S.P. (2008), "Optimal Rescheduling of Generator for Congestion Management based on Particle Swarm Optimization", IEEE Transactions on Power System, Vol. 23, Issue 4, pp.1560–1569. Doi:10.1109/TPWRS.2008.922647

Ejebe, G. C., Tong, J., Waight, J.G. (1998), "Available Transfer Capability Calculations", IEEE Transactions on Power System, Vol. 13, Issue 4, pp. 481–487. Doi:10.1109/59.736300

Esmaili M, Ebadi F, Shayanfar HA, Jadid S (2013), "Congestion Management in Hybrid Power Markets using Modified Benders Decomposition", Applied Energy Vol. 102, pp. 1004–1012. Doi:10.1016/j.apenergy.2012.06.019

Fang, X., Chow, J.H., Jiang, X., Fardanesh, B., Uzunovic, E., Edris, A. (2009), "Sensitivity Methods in the Dispatch and Sitting of FACTS Controllers", IEEE Transaction on Power System, Vol. 24, Issue 2, pp.713–720. Doi:10.1109/TPWRS.2009.2016531

Fernandez, E. Saini, R.P. and Devadas, V., "Socio-economic factors: Effect on energy consumption pattern in rural hilly area", Nigerian Journal of Renewable Energy, Vol 10, Issue 1, 2002, pp.126-133.

Ferrero R.W, Shahidehpour S.M., Ramesh V.C. (1997), "Transaction Analysis in Deregulated Power Systems using Game Theory", IEEE Transaction on Power System, Vol. 12, Issue 3, pp. 1340–1347. Doi: 10.1109/59.630479

Flueck, A. J., Chiang, H. D., Shah, K. S. (1996), "Investigation the Installed Real Power Transfer Capability of a Large Scale Power System under a Proposed Multi Area Interchange Schedule using CPFLOW", IEEE Transaction on Power Systems, Vol. 11, Issue 2, pp. 883–889. Doi:10.1109/59.496170

Georgilakis, P. S. and Vernados, P.G. (2011), "Flexible AC Transmission System Controllers: An Evaluation", Materials Science Forum, Trans Tech Publications, Vol. 670, pp. 399–406. Doi:10.4028/www.scientific.net/MSF.670.399

Ghahremani and Kamwa, I. (2013), "Optimal Placement of Multiple-Type FACTS Devices to Maximize Power System Loadability using a Generic Graphical User Interface", IEEE Transactions on Power Systems. Vol. 28, Issue 2, pp. 764–778. Doi:10.1109/TPWRS.2012.2210253

Guan, X. and Luh, P.B. (1999), "Integrated Resource Scheduling and Bidding in the Deregulated Electric Power Market: New Challenges", Discrete Event Dynamic Systems, Vol. 9, Issue 4, pp. 331–350. Doi:10.1023/A:1008398332406

Gultom, M.L Yohanna. (2019), "Governance Structures and Efficiency in the U.S. Electricity Sector after the Market Restructuring and Deregulation", Energy Policy, Vol. 129, pp. 1008–1019. Doi:10.1016/j.enpol.2019.02.005

Hagh, M.T., Alipour, M., Teimourzadeh, S. (2014), "Application of HGSO to Security Based Optimal Placement and Parameter Setting of UPFC", Energy Conversion and Management, Vol. 86, pp. 873–885. Doi:10.1016/j.enconman.2014.06.057

Hamound G. (2000), "Assessment of available transfer capacity of transmission systems", IEEE Trans. Power Systems, Vol. 15, Issue 1, pp. 27-32.

Hazara J., Sinha A.K. (2008), "Congestion Management using Multi Objective Particle Swarm Optimization", IEEE Power and Energy Society General Meeting - Conversion and Delivery of Electrical Energy in the 21st Century, Pittsburgh, PA, USA, 20–24 July 2008. Doi: 10.1109/PES.2008.4596019

Hingorani N.G., Gyugyi, L. (2000) "Understanding FACTS: Concepts and Technology of Flexible AC Transmission Systems," IEEE Press, Vol. 2, New York,445 Hoes Lane, Piscataway.

Hira, A., Huxtable, D., Leger, A. (2005), "Deregulation and Participation: An International Survey of Participation in Electricity Regulation", Governance An International Journal of Policy, Administration and Institutions, Vol. 18, Issue 1, pp. 53–88. Doi:10.1111/j.1468-0491.2004.00266.x.

Hosseini, S.A., Amjady, N., ShafieKhah, M., Catalao, J.P.S. (2016), "A new multi objective solution approach to solve transmission congestion management problem of energy markets", Applied Energy, Vol. 165, pp.462–471.

Hota, P. K. and Nail, A. P. (2016), "Analytical Review of Power Flow Tracing in Deregulated Power System", American Journal of Electrical and Electronic Engineering", Vol. 4 Issue 3, pp. 92–101. Doi: 10.12691/ajeee-4-3-4

Hur, D. and Kim, B. (2003), "Application of Distributed Optimal Power Flow to Power System Security Assessment" Electrical Power Components Systems, Vol. 31, Issue 1, pp 71–80, 2003. Doi:10.1080/15325000390112080

Ilic, M., Yoon, Y., Zobian, A. (1997), "Available Transmission Capacity (ATC) and its Value under Open Access", IEEE Transaction on Power Systems, Vol. 12, Issue 2, pp. 636–645. 10.1109/59.589630

Iqbal, F., Siddiqui, A. S., Deb, T., Khan, M.T., Rana, A. S. (2018), " Power Systems Reliability- A Bibliographical Survey, Smart Science, Vol. 6, Issue 1, pp. 80–93. Doi:10.1080/23080477.2017.1407985

Iwan, M., Akmeliawati, R., Faisal, T., Al-Assadi, H.M.A.A. (2012), "Performance Comparison of Differential Evolution and Particle Swarm Optimization in Constrained Optimization," Procedia Engineering. Vol. 41, pp. 1323–1328. Doi:10.1016/j.proeng.2012.07.317

Jiang, S., Annakkage, U.D., Gole, A. M. (2006), "A Platform for Validation of FACTS Models", IEEE Transactions on Power Delivery, Vol. 21, Issue 1, pp. 484-491. Doi:10.1109/TPWRD.2005.852301

Jiao, B., Lian, Z. Gu, X.S. (2008), "A Dynamic Inertia Weight Particle Swarm Optimization Algorithm", Chaos, Solitons & Fractals, Vol. 37, Issue 3, pp. 698–705. Doi:10.1016/j.chaos.2006.09.063

Kanimozhi R, Selvi K, Balaji KM (2014), "Multi objective approach for load shedding based on voltage stability index consideration", Alexandra Engineering Journal. Vol. 53, pp. 817–825.

Karthikeyan, P. S., Raglend, I. J., Kothari , D. P. (2013), " A Review on Market Power in Deregulated Electricity Market," International Journal of Electrical Power & Energy Systems, Vol. 48, pp. 139–147. Doi:10.1016/j.ijepes.2012.11.024

Kennedy, J. and Eberhart, R (1995). " Particle swarm optimization," *Proceedings of ICNN'95* - International Conference on Neural Networks", Perth, WA, Australia, Vol.4, pp. 1942-1948,27 Nov-1 Dec,1995. Doi:10.1109/ICNN.1995.488968

Kumar A., Srivastava, S.C., Singh, S. N. (2004), "A Zonal Congestion Management Approach using Real and Reactive Power Rescheduling", IEEE Transactions of Power System, Vol. 19. Issue 1, pp. 554–562. Doi:10.1109/TPWRS.2003.821448

Kumar, A., Srivastava, S. C., Singh, S.N. (2004), "Available Transfer Capacity (ATC) Determination in a competitive Electric Market using AC distribution factors", Electric Power Components and Systems, Vol. 32, Issue 9, pp 927–939. Doi:10.1080/15325000490253623

Kumar, B.V. and Srikanth, N.V. (2017), " A Hybrid Approach for Optimal Location and Capacity of UPFC to Improve the Dynamic Stability of the Power System," Applied Soft Computing, Vol. 52, pp. 974–986. Doi:10.1016/j.asoc.2016.09.031

Kumar, G.N. and Kalavathi, M.S, (2014), " Cat Swarm Optimization for Optimal Placement of Multiple UPFC's in Voltage Stability Enhancement Under Contingency", International Journal of Electrical Power & Energy System, Vol. 57, pp. 97–104. Doi:10.1016/j.ijepes.2013.11.050

Kumar, T. A. and Ramana, N. (2013), "A Review on Control Strategies for LFC in Deregulated Scenario", i-manager's Journal on Circuits and Systems, Vol. 1, Issue 1, pp. 27–36. Doi:10.26634/jcir.1.1.2197

Lal, L.L., (2001), “Power System Restricting and Deregulation: Trading, Performance and Information Technology”, John Wiley & Sons, Ltd., New York. Doi:10.1002/0470846119

Lashkar, A., Kazemi, A., Nabavi, A. (2012), “ Multi objective Optimal Location of FACTS Shunt-Series Controllers for Power System Operation Planning”, IEEE Transactions on Power Delivery, Vol. 27, Issue 2, pp. 481–490. Doi:10.1109/TPWRD.2011.2176559

Liu, B., Kang, J., Jiang, N. Jing, Y. (2011), “ Cost Control of the Transmission congestion Management in Electricity Systems Based on Ant Colony Algorithm”, Energy and Power Engineering, Vol. 3, Issue 1, pp. 17–23.Doi:10.4236/epe.2011.31003

Liu, B., Wang, L., Jin Y.H., Tang Fang, Huang De-Xian (2005), “Improved Particle Swarm Optimization Combined with Chaos”, Chaos, Solitons and Fractals, Vol. 25, Issue 5, pp. 1261–1271.Doi:10.1016/j.chaos.2004.11.095

Liu, Kai, Ni, Yixin, F. Wu, Felix, Bi, T.S. (2007), “Decentralized Congestion Management for Multilateral Transactions Based on Optimal Resource Allocation”, IEEE Transactions on Power Systems, Vol. 22, Issue 4, pp. 1835–1842. Doi:10.1109/TPWRS.2007.907540

Lu, H. and Chen, W. (2006), "Dynamic-objective Particle Swarm Optimization for Constrained Optimization Problems", Journal of Combinatorial Optimization, Vol. 12, Issue 4, pp. 409–419. Doi:10.1007/s10878-006-9004-x

Luo, X., Patton, A. D., Singh, C. (2000), “Real Power Transfer Capability Calculations using Multi Layer Feed Forward Neural Network”, IEEE Transactions on Power Systems, Vol. 15, Issue 2, pp. 903–908.Doi:10.1109/59.867192

Malaki, M., Shirani, R., Siahkali, H. (2001), “New approach for determination of the energy and connection cost at the power grid nodes” In: IEEE power engineering society summer meeting, pp 1489–1494.

Milano, F., Canizares, C.A., Invernizzi, M. (2003), “Multi objective Optimization for Pricing System Security in Electricity Markets”, IEEE Transaction on Power System, Vol. 18, Issue 2, pp. 596–604. Doi:10.1109/TPWRS.2003.810897

Mukherjee, A. and Mukherjee, V. (2016), “Solution of Optimal Power Flow with FACTS Devices using a Novel oppositional Krill Herd Algorithm”, International Journal of Electrical Power & Energy System, Vol. 78, pp.700–714. Doi:10.1016/j.ijepes.2015.12.001

Mustafa M. W. and Bawazir R. O. (2013), "Optimal Location of FACTS for ATC Enhancement", International Journal of Engineering and Advanced Technology, Vol. 3, Issue 1, pp. 80–85.

Ni, E., Luh, P. B., Rourke, S. (2004), "Optimal Integrated Generation Bidding and Scheduling with Risk Management under a Deregulated Power Market", IEEE Transactions on Power Systems, Vol. 19, Issue 1, pp. 600–609. Doi:10.1109/TPWRS.2003.818695

Niimura, T., Niioka, S., Yokoyama, R. (2003), "Transmission loading relief solutions for congestion management", Electrical Power System Research. Vol. 67, pp.73–78.

Orfanogianni, T. and Gross, G (2007), "A General Formulation for LMP Evaluation", IEEE Transactions on Power Systems, Vol. 22, Issue 3, pp. 1163–1173. Doi:10.1109/TPWRS.2007.901297

Ou, Y. and Singh, C. (2002), "Assessment of Available Transfer Capability and Margins", IEEE Transactions on Power Systems, Vol. 17, Issue 2, pp. 463–468. Doi:10.1109/TPWRS.2002.1007919

Overbye, T. J., Cheng, X., Sun, Y. (2004), "A Comparison of the AC and DC Power Flow MODELS for LMP Calculations", Proceedings of 37th Annual Hawaii IEEE International Conference on System Sciences, pp. 1–9, 5–8th January, 2004, Hawaii, USA. Doi:10.1109/HICSS.2004.1265164

Pal, N.K., Ifeanyi, B.J., Obaro, O.J. (2016), "Deregulation of Electric Power in a Developing Economy: Prospects for Nigeria", International Research Journal of Engineering and Technology, Vol. 3, Issue 11, pp. 1235–1241.

Pandey, S. N., Pandey, N. K., Shashikala, T. (2010), "Neural Network based Approach for ATC Estimation using Distributed Computing", IEEE Transactions on Power Systems, Vol. 25, Issue 3, pp. 1291–1300. Doi:10.1109/TPWRS.2010.2042978

Pandiarajan, K., and Babulal, C.K. (2014), "Transmission Line Management using Hybrid Differential Evolution with Particle Swarm Optimization", Journal of Electrical Systems, Vol. 10, Issue 1, pp. 21–35.

Panida, B., Chanwit, B., Weerakorn, O. (2010), "Optimal Congestion Management in an Electricity Market using Particle Swarm Optimization with Time-Varying Acceleration Coefficients", Computers & Mathematics with Applications, Vol. 60, Issue 4, pp. 1068–1077. Doi:10.1016/j.camwa.2010.03.064

Patel Adarsh, Trivedi Aditya, (2010) “Particle-Swarm-Optimization-Based Multiuser Detector for Multicarrier CDMA Communications” IEEE International Conference on Computational Intelligence and Communication Networks, 26-28 Nov. 2010, Bhopal, India, pp. 534-538, 2010. Doi:10.1109/CICN.2010.105

Phadke, A.R. Fozdar, M.Niazi, K.R. (2012), “A New Multi objective Fuzzy-GA Formulation for Optimal Placement and Sizing of Shunt FACTS Controller”, International Journal of Electrical Power & Energy System, Vol. 40, Issue 1, pp. 46–53.Doi:10.1016/j.ijepes.2012.02.004

Pillay, A., Karthikeyan, S.P., Kothari, D.P. (2015), “Congestion Management in Power Systems – A Review”, International Journal of Electrical Power & Energy System, Vol. 70, pp. 83–90. Doi:10.1016/j.ijepes.2015.01.022

Price, J. E. (2007), “Market-Based Price Differentials in Zonal and LMP Market Designs”, IEEE Transactions on Power Systems, Vol. 22, Issue 4, pp. 1486–1494. Doi:10.1109/TPWRS.2007.907136

Rahimi, A.F. and Sheffrin, A.Y. (2003), "Effective market monitoring in deregulated electricity markets," IEEE Transactions on Power Systems, Vol. 18, no. 2, pp. 486-493, Doi: 10.1109/TPWRS.2003.810680

Rao, M.V., Sivanagaraju, S., Suresh Chintalapudi, V. (2016), “Available Transfer Capability Evaluation and Enhancement using various FACTS Controllers: Special Focus on System Security”, Ain Shams Engineering Journal, Vol. 7, Issue 1, pp. 191-207. Doi:10.1016/j.asej.2015.11.006

Rashidi-Nejad, M., Song, Y. H., Javidi-Dasht-Bayaz, M. H. (2002), “Operating Reserve Provision in Deregulated Power Markets”, IEEE Power Engineering Society Winter Meeting, Conference Proceedings, 1305–1310, New York. Doi:10.1109/PESW.2002.985226

Reddy, K. R. S., Padhy, N. P., Patel, R.N. (2006), "Congestion Management in Deregulated Power System using FACTS Devices", IEEE Power India Conference, pp. 1–8, 1-12 April, 2006, New Delhi, India.Doi:10.1109/POWERI.2006.1632541

Roselyn, J.P., Devaraj, D., Dash, S.S. (2013) Multi objective differential evolution for voltage security constraint optimal power flow in deregulated power systems. International Journal of Emerging Electrical Power. Doi:10.1515/ijeeps-2013-0086

Salehizadeh, M.R., Rahimi-Kian, A., Oloomi-Buygi, M. (2014), "A Multi Attribute Congestion-Driven Approach for Evaluation of Power Generation Plans" International Transactions on Electrical Energy Systems. Vol. 25, Issue 3, pp. 482–497. Doi: 10.1002/etep.1861

Saravanan, M.R.Slochanal , S. Venkatensh, P. Abraham, P.S. (2007), "Application of Particle Swarm Optimization Technique for Optimal Location of Fact Devices Considering Cost of Installation and System Load Ability, "Electrical Power Systems Research, Vol. 77, Issue 3, pp.276–283. Doi:0.1016/j.epsr.2006.03.006

Sarker, J. and Goswami, S.K. (2014),"Solution of Multiple UPFC Placement Problems using Gravitational Search Algorithm", International Journal of Electrical Power & Energy System, Vol. 55, pp. 531–541. Doi:10.1016/j.ijepes.2013.10.008

Sarwar, M.D. and Siddiqui, A.S. (2015),"An Efficient Particle Swarm Optimizer for Congestion Management in Deregulated Electricity Market", Journal of Electrical Systems and Information Technology, Vol. 2, Issue 3, pp. 269–282. Doi:10.1016/j.jesit.2015.08.002

Selvi, K. Ramaraj, N. Bhavani, M. (2007), "Total Transfer Capability Evaluation using Genetic Algorithms", Journal of the Institution of Engineers, Vol. 88, pp. 60–64.

Shaheen, H. I. Rashed, G.I. Cheng, S.J. (2011), "Optimal Location and Parameter Setting of UPFC for Enhancing Power System Security based on Differential Evolution Algorithm", International Journal of Electrical Power & Energy System, Vol. 33, Issue 1, pp. 94–105. Doi:10.1016/j.ijepes.2010.06.023

Shahidehpour, M., Yamin, H., ZY, Li. (2002)," Market Operations in Electric Power Systems", John Wiley& Sons, New York. Doi: 10.1002/etep.1861

Shayesteh, E., Yousefi, A. Parsa Moghaddam M., Sheikh-El-Eslami, M. K. (2009), "ATC Enhancement using Emergency Demand Response Program", IEEEIEEE/PES Power Systems Conference and Exposition, pp. 1–7, 15–18th March 2009, Seattle, WA, USA. Doi:10.1109/PSCE.2009.4840037

Shikoski J., Katic, V., Rechkoski, R. (2003), "New Infra Technologies in the Deregulated Power Sector", Turkish Journal of Electrical Engineering, Vol. 11, Issue 2, pp. 131–141.

Shukla, U. K. and Tampy, A. (2011), "Analysis of Competition and Market Power in the Wholesale Electricity Market in India", Energy Policy, Vol. 39, Issue 5, pp. 2699–2710. Doi: 10.1016/j.enpol.2011.02.039

Singh S. N. and David A. K. (2001), "Optimal Location of FACTS Devices for Congestion Management", Electrical Power Systems Research, Vol. 58, Issue 2, pp. 71–79. Doi:10.1016/S0378-7796(01)00087-6

Singh, H.K. Srivastava, S.C., Sharma, A.K. (2006), "Sensitivity Based Approach for Transmission Congestion Management Utilizing Bids for Generation Rescheduling and Load Curtailment", International Journal of Emerging Electric Power Systems, Vol. 7, Issue 4, pp. 1–23. Doi:10.2202/1553-779X.1357

Song, Sung-Hwan., Lim Jung-Uk, Moon Seung-II. (2004), "Installation and Operation of FACTS Devices for Enhancing Steady-State Security", Electrical Power Systems Research, Vol. 70, Issue 1, pp. 7–15. Doi:10.1016/j.epsr.2003.11.009

Sood, Y.R., Padhy, N.P., Gupta, H.O. (2007),"Deregulated Model and Locational Marginal Pricing", Electrical Power Systems Research, Vol. 77, Issue 5, pp. 574–582. Doi:10.1016/j.epsr.2006.05.009

Soto, D. and Green, T. C. (2002), "A Comparison of High-Power Converter Topologies for the Implementation of FACTS Controllers" IEEE Transactions on Industrial Electronics, Vol. 49, Issue 5, pp. 1072–1080. Doi:10.1109/TIE.2002.803217

Surender, R. S.Kumari,S. M, and Sydulu, M. (2010), "Congestion management in Deregulated Power System by Optimal Choice and Allocation of FACTS Controllers using Multi objective Genetic Algorithm", Journal of Electrical Engineering and Technology, Vol. 4, Issue 4, pp. 1–7.

Taher A.S. and Amooshahi, M.K. (2012), "New Approach for Optimal UPFC Placement using Hybrid Immune Algorithm in Electric Power Systems", International Journal of Electrical Power & Energy System, Vol. 43, Issue 1, pp. 899–909. Doi:10.1016/j.ijepes.2012.05.064

Tanweer, M.R., Suresh, S., Sundararajan, N. (2015),"Mentoring based Particle Swarm Optimization Algorithm for Faster Convergence", IEEE Congress on Evolutionary Computation,25-28th May 2015, Sendai, Japan. pp. 196–203. Doi:10.1109/CEC.2015.7256892

Tekchandani, P., Trivedi, A. (2011), "Clock Drift Management using Particle Swarm Optimization" International Conference on Intelligent Computing, Bio-Inspired Computing and Applications, pp. 386-393, 2011, Springer, Zhengzhou,china,11-14th August ,2011.

Thampi SM, El-Alfy ESM, Mitra S, Trajkovic L. (2018), "Soft computing and intelligent systems: Techniques and applications", Journal of Intelligent & Fuzzy Systems, Vol. 34, Issue 3, pp. 1237-1241, 2018.

Thomas Jaya, Chaudhari Narendra S. (2013), "Hybrid Approach for 2D Strip Packing Problem Using Genetic Algorithm", International Work Conference on Artificial Neural Network (IWANN13), Tenerife, Spain, 12 -14 June, 2013.

Tuglie, E. D. Dicorato, M.Scala, M. L.Scarpellini, P. (2000), "A Static Optimization Approach to Access Dynamic Available Transfer Capability", IEEE Transactions on Power Systems, Vol. 15, Issue 3, pp. 1069–1076. Doi:10.1109/59.871735

Uriarte, A. Particia, M. Fevrier, V. (2016), "An Improved Particle Swarm Optimization Algorithm Applied to Benchmark Functions", IEEE International Conference on Intelligent Systems, 4–6th September 2016, Sofia, Bulgaria, pp. 120–128. Doi:10.1109/IS.2016.7737410

Venkaiah, Ch. Kumar D. M. V. (2011), "Fuzzy Adaptive Bacterial Foraging Congestion Management using Sensitivity based Optimal Active Power Rescheduling of Generators", Applied Soft Computing, Vol. 11, Issue 8, pp. 4921–4930.Doi:10.1016/j.asoc.2011.06.007

Verma, K.S. and Gupta, H.O. (2006), "Impact on Real and Reactive Power Pricing in Open Power Market Using Unified Power Flow Controller", IEEE Transactions on Power Systems Vol. 21, Issue 1, pp. 365–371. Doi:10.1109/TPWRS.2005.857829

Verma, K.S., Singh, S.N. and Gupta, H. O. (2001), "Location of Unified Power Flow Controller for Congestion Management", Electric Power Systems Research, Vol. 58, Issue 2, pp. 89–96. Doi:10.1016/S0378-7796(01)00123-7

Verma, S. and Mukherjee, V. (2016a), "Firefly Algorithm for Congestion Management in Deregulated Environment", Engineering Science and Technology, an International Journal, Vol. 19, Issue 3, pp. 1254–1265. Doi:10.1016/j.jestch.2016.02.001

Verma, S. and Mukherjee, V. (2016b), "Optimal Real Power Rescheduling of Generators for Congestion Management using a Novel Ant Lion Optimizer", IET Generation, Transmission & Distribution, Vol. 10, Issue 10, pp. 2548–2561. Doi:10.1049/iet-gtd.2015.1555

Verma, S. Mukherjee, V. (2016c), "A Novel Flower Pollination Algorithm for Congestion Management in Electricity Market", Proceedings of 3rd International Conference on Recent Advances in Information Technology, pp. 1–6, 3–5th March, 2016, Dhanbad, India. Doi:10.1109/RAIT.2016.7507902

Verma, S. Saha, S. Mukherjee, V. (2017), "A Novel Symbiotic Organisms Search Algorithm for Congestion Management in Deregulated Environment", Journal of Experimental & Theoretical Artificial Intelligence, Vol. 29, Issue 1, pp. 59–71. Doi: 10.1080/0952813X.2015.1116141

Vijay , V. and Verma, A.K. (2010), "Reliability of electric power systems: challenges in the deregulated environment — a research perspective", International Journal of System Assurance Engineering and Management, Vol. 1, Issue, 1, pp. 24–31. Doi:10.1007/s13198-010-0013-x

Wibowo, R. S., Yorino, N.Eghbal, M., Zoka, Y. Sasaki, Y. (2011), "FACTS Devices Allocation with Control Coordination Considering Congestion Relief and Voltage Stability", IEEE Transactions on Power Systems, Vol. 26, Issue 4, pp. 2302–2310. Doi:10.1109/TPWRS.2011.2106806

Xiang, T. Liao, X. Wong, K.W. (2007), "An Improved Particle Swarm Optimization Algorithm Combined with Piecewise Linear Chaotic Map", Applied Mathematics Computation, Vol. 190, Issue 2, pp. 1637–1645. Doi:10.1016/j.amc.2007.02.103

Xiao, Ying., Song, YH., Liu, Chen-Ching, Sun Y. Z. (2003), "Available Transfer Capacity Enhancement using FACT Devices", IEEE Transactions on Power Systems, Vol. 18, Issue 1, pp. 305–312.Doi:10.1109/TPWRS.2002.807073

Yadav, K.N., Sharma, P. (2013), "Available Transfer Capability Calculation using DCPTDF Incorporating Multiple Line Contingencies and Generator Addition under Deregulated Environment", International Journal of Advanced Research in Electrical, Electronics and Instrumentation Engineering", Vol. 2, Issue 6, pp. 2297–2307.

Yamin H.Y. and Shahidehpour S.M. (2003), "Transmission Congestion and Voltage Profile Management Coordination in Competitive Electricity Markets", International Journal of Electrical Power and Energy System, Vol. 25, Issue 10, pp. 849–861.Doi:10.1016/S0142-0615(03)00070-X

Yang Chien-Feng, Gordon G.Lai, Chia-Hau Lee, Ching-Tzong Su, Gary W.Chang, (2012), "Optimal Setting of Reactive Compensation Devices with an Improved Voltage Stability Index for Voltage Stability Enhancement", International Journal of Electrical Power and Energy Systems, Vol. 37, Issue 1, pp. 50–57. Doi:10.1016/j.ijepes.2011.12.003

Yang, C.H., Tsai, S.W., Chuang, L.Y., Yang, C.H. (2012), "An Improved Particle Swarm Optimization with Double-Bottom Chaotic Maps for Numerical Optimization", Applied Mathematics Computing Vol. 219, Issue 1, pp. 260–279. Doi:10.1016/j.amc.2012.06.015

Yaoyao, He., Zhou, J., Li, C., Yang, J, Li, Q. (2008), "A Precise Chaotic Particle Swarm Optimization Algorithm based on Improved Tent Map", International Conference on Natural Computation, Jinan, China, pp. 569–573, 18-20th October 2008. Doi:10.1109/ICNC.2008.588

Yesuratnam G and Thukaram D. (2007), "Congestion Management in Open Access Based on Relative Electrical Distances using Voltage Stability Criteria", Electric Power Systems Research, Vol. 77, Issue 12, pp. 1608–1618. Doi:10.1016/j.epsr.2006.11.007.

Yu, C.W., Chung, T. S., Tse, C. T., Chung, C. Y. (2003), "Energy transaction Scheduling with Interchange Capability Assessment under Open Transmission Access", Electric Power Systems Research, Vol. 67, Issue 1, pp. 59–66. Doi:10.1016/S0378-7796(03)00046-4.

Yuan-Kang,wu. (2007), "A novel algorithm for ATC calculations and applications in deregulated electricity markets", International Journal of Electrical Power and Energy Systems. 29. 810-821. Doi:10.1016/j.ijepes.2007.06.014.

Yusoff, N.I., Zin, A. A. M., Khairuddin, A.B. (2017), "Congestion Management in Power System—A Review", Proceedings of 3rd IEEE International Conference on Power Generation Systems and Renewable Energy Technologies (PGSRET), pp. 22–27, 4–6th April 2017, Johor Bahru, Malaysia. Doi:10.1109/PGSRET.2017.8251795.

Zahid M, Chen J, Li Y, Duan , Lei, Bo, Mohy-ud-din G, Waqar, A. (2017), "New Approach for Optimal Location and Parameters Setting of UPFC for Enhancing Power Systems Stability under Contingency Analysis", Energies, Vol. 10. Doi: 10.3390/en10111738.

Zeraatzade, M. (2010), "Transmission Congestion Management by Optimal Placement of FACTS Devices", PhD Thesis, School of Engineering and Design Brunel University, West London, UK.

Appendices

Line data and bus data of IEEE 14, IEEE 30, IEEE 57 and IEEE 118 bus systems have been mentioned in Appendix A1 and Appendix A2 shows details of incremented and decremented power bids submitted by individual generators for IEEE 30 bus, IEEE57 bus and IEEE 118 bus systems.

Appendix A1

Line Data –IEEE 14 Bus System

Line Number	From Bus	To Bus	Resistance (pu)	Reactance (pu)	Half line charging Susceptance (pu)	MVA rating
1	1	2	0.01938	0.05917	0.02640	120
2	1	5	0.05403	0.22304	0.02190	65
3	2	3	0.04699	0.19797	0.01870	36
4	2	4	0.05811	0.17632	0.02460	65
5	2	5	0.05695	0.17388	0.01700	50
6	3	4	0.06701	0.17103	0.01730	65
7	4	5	0.01335	0.04211	0.00640	45
8	4	7	0	0.20912	0	55
9	4	9	0	0.55618	0	32
10	5	6	0	0.25202	0	45
11	6	11	0.09498	0.1989	0	18
12	6	12	0.12291	0.25581	0	32
13	6	13	0.06615	0.13027	0	32
14	7	8	0	0.17615	0	32
15	7	9	0	0.11001	0	32
16	9	10	0.03181	0.0845	0	32
17	9	14	0.12711	0.27038	0	32
18	10	11	0.08205	0.19207	0	12
19	12	13	0.22092	0.19988	0	12
20	13	14	0.17093	0.34802	0	12

Bus Data –IEEE 14 Bus System

Bus Number	Voltage	Angle	Generation Real Power (MW)	Generation Reactive Power (MVAR)	Load Real Power (MW)	Load Reactive Power (MVAR)	Reactive power limits Q_{min} (MVAR)	Reactive Power Limits Q_{max} (MVAR)
1	1.060	0	114.17	-16.9	0	0	0	10
2	1.045	0	40	0	21.7	12.7	-42	50
3	1.010	0	0	0	94.2	19.1	23.4	40
4	1	0	0	0	47.8	-3.9	0	0
5	1	0	0	0	7.6	1.6	0	0
6	1	0	0	0	11.2	7.5	0	0
7	1	0	0	0	0	0	0	0
8	1	0	0	0	0	0	0	0
9	1	0	0	0	29.5	16.6	0	0
10	1	0	0	0	9	5.8	0	0
11	1	0	0	0	3.5	1.8	0	0
12	1	0	0	0	6.1	1.6	0	0
13	1	0	0	0	13.8	5.8	0	0
14	1	0	0	0	14.9	5.0	0	0

Line Data- IEEE 30 Bus System

Line no	From bus	To bus	Resistance (pu)	Reactance (pu)	Susceptance(pu)	Rating
1	1	2	0.01920	0.05750	0.02640	130
2	1	3	0.04520	0.18520	0.02040	130
3	2	4	0.05700	0.17370	0.01840	65
4	3	4	0.01320	0.03790	0.00420	130
5	2	5	0.04720	0.19830	0.02090	130
6	2	6	0.05810	0.17630	0.01870	65

7	4	6	0.01190	0.04140	0.00450	90
8	5	7	0.04600	0.11600	0.01020	70
9	6	7	0.02670	0.08200	0.00850	130
10	6	8	0.01200	0.04200	0.00450	32
11	6	9	0.00000	0.20800	0.00000	65
12	6	10	0.00000	0.55600	0.00000	32
13	9	11	0.00000	0.20800	0.00000	65
14	9	10	0.00000	0.11000	0.00000	65
15	4	12	0.00000	0.25600	0.00000	65
16	12	13	0.00000	0.14000	0.00000	32
17	12	14	0.12310	0.25590	0.00000	32
18	12	15	0.06620	0.13040	0.00000	32
19	12	16	0.09450	0.19870	0.00000	16
20	14	15	0.22100	0.19970	0.00000	16
21	16	17	0.08240	0.19320	0.00000	16
22	15	18	0.10700	0.21850	0.00000	16
23	18	19	0.06390	0.12920	0.00000	32
24	19	20	0.03400	0.06800	0.00000	32
25	10	20	0.09360	0.20900	0.00000	32
26	10	17	0.03240	0.08450	0.00000	32
27	10	21	0.03480	0.07490	0.00000	32
28	10	22	0.07270	0.14990	0.00000	32
29	21	22	0.01160	0.02360	0.00000	32
30	15	23	0.10000	0.20200	0.00000	16
31	22	24	0.11500	0.17900	0.00000	16
32	23	24	0.13200	0.27000	0.00000	16
33	24	25	0.18850	0.32920	0.00000	16
34	25	26	0.25440	0.38000	0.00000	16
35	25	27	0.10930	0.20870	0.00000	16
36	28	27	0.00000	0.39600	0.00000	65

37	27	29	0.21980	0.41530	0.00000	16
38	27	30	0.32020	0.60270	0.00000	16
39	29	30	0.23990	0.45330	0.00000	16
40	8	28	0.06360	.020000	0.02140	32
41	6	28	0.01690	0.05990	0.00650	32

Bus Data –IEEE 30 Bus System

Bus Number	Generation power		Load power		Voltage	Q_{min}	Q_{max}	V_{min}	V_{max}
	Real (MW)	Reactive (MVAR)	Real (MW)	Reactive (MVAR)					
1	0	0	0	0	1.06	0	0	0.9	1.1
2	0.4	0.5	0.217	0.127	1.043	-0.20	1	0.9	1.1
3	0	0	0.024	0.012	1.0	0	0	0.9	1.1
4	0	0	0.076	0.016	1.06	0	0	0.9	1.1
5	0	0.37	0.942	0.19	1.01	-0.15	0.8	0.9	1.1
6	0	0	0	0	1.0	0	0	0.9	1.1
7	0	0	0.228	0.109	1.01	0	0	0.9	1.1
8	0	0.373	0.3	0.03	1.01	-0.15	0.6	0.9	1.1
9	0	0	0	0	1	0	0	0.9	1.1
10	0	0.19	0.058	0.02	1	0	0	0.9	1.1
11	0	0.162	0	0	1.082	-0.1	0.5	0.9	1.1
12	0	0	0.112	0.075	1	0	0	0.9	1.1
13	0	0.106	0	0	1.071	-0.15	0.6	0.9	1.1
14	0	0	0.062	0.016	1	0	0	0.9	1.1
15	0	0	0.082	0.025	1	0	0	0.9	1.1
16	0	0	0.035	0.018	1	0	0	0.9	1.1
17	0	0	0.09	0.058	1	0	0	0.9	1.1
18	0	0	0.032	0.009	1	0	0	0.9	1.1

19	0	0	0.095	0.034	1	0	0	0.9	1.1
20	0	0	0.022	0.007	1	0	0	0.9	1.1
21	0	0	0.175	0.112	1	0	0	0.9	1.1
22	0	0	0	0	1	0	0	0.9	1.1
23	0	0	0.032	0.016	1	0	0	0.9	1.1
24	0	0.043	0.087	0.067	1	0	0	0.9	1.1
25	0	0	0	0	1	0	0	0.9	1.1
26	0	0	0.035	0.023	1	0	0	0.9	1.1
27	0	0	0	0	1	0	0	0.9	1.1
28	0	0	0	0	1	0	0	0.9	1.1
29	0	0	0.024	0.009	1	0	0	0.9	1.1
30	0	0	0.106	0.019	1	0	0	0.9	1.1

Line Data-IEEE 118 Bus System

Line No.	From Bus	To Bus	Resistance (pu)	Reactance (pu)	Susceptance (pu)	Flow Limit (MW)
1	1	2	0.0303	0.0999	0.0254	175
2	1	3	0.0129	0.0424	0.01082	175
3	4	5	0.00176	0.00798	0.0021	500
4	3	5	0.0241	0.108	0.0284	175
5	5	6	0.0119	0.054	0.01426	175
6	6	7	0.00459	0.0208	0.0055	175
7	8	9	0.00244	0.0305	1.162	500
8	8	5	0	0.0267	0	500
9	9	10	0.00258	0.0322	1.23	500
10	4	11	0.0209	0.0688	0.01748	175
11	5	11	0.0203	0.0682	0.01738	175
12	11	12	0.00595	0.0196	0.00502	175
13	2	12	0.0187	0.0616	0.01572	175
14	3	12	0.0484	0.16	0.0406	175

15	7	12	0.00862	0.034	0.00874	175
16	11	13	0.02225	0.0731	0.01876	175
17	12	14	0.0215	0.0707	0.01816	175
18	13	15	0.0744	0.2444	0.06268	175
19	14	15	0.0595	0.195	0.0502	175
20	12	16	0.0212	0.0834	0.0214	175
21	15	17	0.0132	0.0437	0.0444	500
22	16	17	0.0454	0.1801	0.0466	175
23	17	18	0.0123	0.0505	0.01298	175
24	18	19	0.01119	0.0493	0.01142	175
25	19	20	0.0252	0.117	0.0298	175
26	15	19	0.012	0.0394	0.0101	175
27	20	21	0.0183	0.0849	0.0216	175
28	21	22	0.0209	0.097	0.0246	175
29	22	23	0.0342	0.159	0.0404	175
30	23	24	0.0135	0.0492	0.0498	175
31	23	25	0.0156	0.08	0.0864	500
32	26	25	0	0.0382	0	500
33	25	27	0.0318	0.163	0.1764	500
34	27	28	0.01913	0.0855	0.0216	175
35	28	29	0.0237	0.0943	0.0238	175
36	30	17	0	0.0388	0	500
37	8	30	0.00431	0.0504	0.514	175
38	26	30	0.00799	0.086	0.908	500
39	17	31	0.0474	0.1563	0.0399	175
40	29	31	0.0108	0.0331	0.0083	175
41	23	32	0.0317	0.1153	0.1173	140
42	31	32	0.0298	0.0985	0.0251	175
43	27	32	0.0229	0.0755	0.01926	175
44	15	33	0.038	0.1244	0.03194	175

45	19	34	0.0752	0.247	0.0632	175
46	35	36	0.00224	0.0102	0.00268	175
47	35	37	0.011	0.0497	0.01318	175
48	33	37	0.0415	0.142	0.0366	175
49	34	36	0.00871	0.0268	0.00568	175
50	34	37	0.00256	0.0094	0.00984	500
51	38	37	0	0.0375	0	500
52	37	39	0.0321	0.106	0.027	175
53	37	40	0.0593	0.168	0.042	175
54	30	38	0.00464	0.054	0.422	175
55	39	40	0.0184	0.0605	0.01552	175
56	40	41	0.0145	0.0487	0.01222	175
57	40	42	0.0555	0.183	0.0466	175
58	41	42	0.041	0.135	0.0344	175
59	43	44	0.0608	0.2454	0.06068	175
60	34	43	0.0413	0.1681	0.04226	175
61	44	45	0.0224	0.0901	0.0224	175
62	45	46	0.04	0.1356	0.0332	175
63	46	47	0.038	0.127	0.0316	175
64	46	48	0.0601	0.189	0.0472	175
65	47	49	0.0191	0.0625	0.01604	175
66	42	49	0.0715	0.323	0.086	175
67	42	49	0.0715	0.323	0.086	175
68	45	49	0.0684	0.186	0.0444	175
69	48	49	0.0179	0.0505	0.01258	175
70	49	50	0.0267	0.0752	0.01874	175
71	49	51	0.0486	0.137	0.0342	175
72	51	52	0.0203	0.0588	0.01396	175
73	52	53	0.0405	0.1635	0.04058	175
74	53	54	0.0263	0.122	0.031	175

75	49	54	0.073	0.289	0.0738	175
76	49	54	0.0869	0.291	0.073	175
77	54	55	0.0169	0.0707	0.0202	175
78	54	56	0.00275	0.00955	0.00732	175
79	55	56	0.00488	0.0151	0.00374	175
80	56	57	0.0343	0.0966	0.0242	175
81	50	57	0.0474	0.134	0.0332	175
82	56	58	0.0343	0.0966	0.0242	175
83	51	58	0.0255	0.0719	0.01788	175
84	54	59	0.0503	0.2293	0.0598	175
85	56	59	0.0825	0.251	0.0569	175
86	56	59	0.0803	0.239	0.0536	175
87	55	59	0.04739	0.2158	0.05646	175
88	59	60	0.0317	0.145	0.0376	175
89	59	61	0.0328	0.15	0.0388	175
90	60	61	0.00264	0.0135	0.01456	500
91	60	62	0.0123	0.0561	0.01468	175
92	61	62	0.00824	0.0376	0.0098	175
93	63	59	0	0.0386	0	500
94	63	64	0.00172	0.02	0.216	500
95	64	61	0	0.0268	0	500
96	38	65	0.00901	0.0986	1.046	500
97	64	65	0.00269	0.0302	0.38	500
98	49	66	0.018	0.0919	0.0248	500
99	49	66	0.018	0.0919	0.0248	500
100	62	66	0.0482	0.218	0.0578	175
101	62	67	0.0258	0.117	0.031	175
102	65	66	0	0.037	0	500
103	66	67	0.0224	0.1015	0.02682	175
104	65	68	0.00138	0.016	0.638	500

105	47	69	0.0844	0.2778	0.07092	175
106	49	69	0.0985	0.324	0.0828	175
107	68	69	0	0.037	0	500
108	69	70	0.03	0.127	0.122	500
109	24	70	0.00221	0.4115	0.10198	175
110	70	71	0.00882	0.0355	0.00878	175
111	24	72	0.0488	0.196	0.0488	175
112	71	72	0.0446	0.18	0.04444	175
113	71	73	0.00866	0.0454	0.01178	175
114	70	74	0.0401	0.1323	0.03368	175
115	70	75	0.0428	0.141	0.036	175
116	69	75	0.0405	0.122	0.124	500
117	74	75	0.0123	0.0406	0.01034	175
118	76	77	0.0444	0.148	0.0368	175
119	69	77	0.0309	0.101	0.1038	175
120	75	77	0.0601	0.1999	0.04978	175
121	77	78	0.00376	0.0124	0.01264	175
122	78	79	0.00546	0.0244	0.00648	175
123	77	80	0.017	0.0485	0.0472	500
124	77	80	0.0294	0.105	0.0228	500
125	79	80	0.0156	0.0704	0.0187	175
126	68	81	0.00175	0.0202	0.808	500
127	81	80	0	0.037	0	500
128	77	82	0.0298	0.0853	0.08174	200
129	82	83	0.0112	0.03665	0.03796	200
130	83	84	0.0625	0.132	0.0258	175
131	83	85	0.043	0.148	0.0348	175
132	84	85	0.0302	0.0641	0.01234	175
133	85	86	0.035	0.123	0.0276	500
134	86	87	0.02828	0.2074	0.0445	500

135	85	88	0.02	0.102	0.0276	175
136	85	89	0.0239	0.173	0.047	175
137	88	89	0.0139	0.0712	0.01934	500
138	89	90	0.0518	0.188	0.0528	500
139	89	90	0.0238	0.0997	0.106	500
140	90	91	0.0254	0.0836	0.0214	175
141	89	92	0.0099	0.0505	0.0548	500
142	89	92	0.0393	0.1581	0.0414	500
143	91	92	0.0387	0.1272	0.03268	175
144	92	93	0.0258	0.0848	0.0218	175
145	92	94	0.0481	0.158	0.0406	175
146	93	94	0.0223	0.0732	0.01876	175
147	94	95	0.0132	0.0434	0.0111	175
148	80	96	0.0356	0.182	0.0494	175
149	82	96	0.0162	0.053	0.0544	175
150	94	96	0.0269	0.0869	0.023	175
151	80	97	0.0183	0.0934	0.0254	175
152	80	98	0.0238	0.108	0.0286	175
153	80	99	0.0454	0.206	0.0546	200
154	92	100	0.0648	0.295	0.0472	175
155	94	100	0.0178	0.058	0.0604	175
156	95	96	0.0171	0.0547	0.01474	175
157	96	97	0.0173	0.0885	0.024	175
158	98	100	0.0397	0.179	0.0476	175
159	99	100	0.018	0.0813	0.0216	175
160	100	101	0.0277	0.1262	0.0328	175
161	92	102	0.0123	0.0559	0.01464	175
162	101	102	0.0246	0.112	0.0294	175
163	100	103	0.016	0.0525	0.0536	500
164	100	104	0.0451	0.204	0.0541	175

165	103	104	0.0466	0.1584	0.0407	175
166	103	105	0.0535	0.1625	0.0408	175
167	100	106	0.0605	0.229	0.062	175
168	104	105	0.00994	0.0378	0.00986	175
169	105	106	0.014	0.0547	0.01434	175
170	105	107	0.053	0.183	0.0472	175
171	105	108	0.0261	0.0703	0.01844	175
172	106	107	0.053	0.183	0.0472	175
173	108	109	0.0105	0.0288	0.0076	175
174	103	110	0.03906	0.1813	0.0461	175
175	109	110	0.0278	0.0762	0.0202	175
176	110	111	0.022	0.0755	0.02	175
177	110	112	0.0247	0.064	0.062	175
178	17	113	0.00913	0.0301	0.00768	175
179	32	113	0.0615	0.203	0.0518	500
180	32	114	0.0135	0.0612	0.01628	175
181	27	115	0.0164	0.0741	0.01972	175
182	114	115	0.0023	0.0104	0.00276	175
183	68	116	0.00034	0.00405	0.164	500
184	12	117	0.0329	0.14	0.0358	175
185	75	118	0.0145	0.0481	0.01198	175
186	76	118	0.0164	0.0544	0.01356	175

Bus Data –IEEE 118 Bus System

Bus No.	Voltage Max (pu)	Voltage Min (pu)	Generation P_{max} (MW)	Generation P_{min} (MW)	Generation Q_{max} (MVAR)	Generation Q_{min} (MVAR)	Load P_d (MW)	Load Q_d (MVAR)
1	1.05	0.94	0	0	0	0	54.14	8.66
2	1.06	0.95	0	0	0	0	21.23	9.55

3	1.06	0.95	0	0	0	0	41.4	10.62
4	1.09	0.99	30	5	300	-300	31.85	12.74
5	1.09	0.99	0	0	0	0	55.2	23.35
6	1.09	0.97	30	50	50	-13	20.17	2.12
7	1.09	0.97	0	0	0	0	74.31	24.42
8	1.09	0.98	30	5	300	-300	49.89	10.62
9	1.09	0.98	0	0	0	0	36.09	16.99
10	1.09	0.98	300	150	200	-147	14.86	1.06
11	1.08	0.97	0	0	0	0	95.54	31.85
12	1.09	0.98	300	100	120	-35	26.54	10.62
13	1.05	0.95	0	0	0	0	11.68	3.18
14	1.07	0.98	0	0	0	0	63.69	36.09
15	1.05	0.98	30	10	30	-10	47.77	26.54
16	1.07	0.98	0	0	0	0	19.11	3.18
17	1.09	0.98	0	0	0	0	14.86	8.49
18	1.07	0.98	100	25	50	-16	10.62	5.31
19	1.06	0.98	30	5	24	-8	7.43	3.18
20	1.04	0.96	0	0	0	0	65.82	13.8
21	1.03	0.95	0	0	0	0	18.05	7.43
22	1.04	0.97	0	0	0	0	25.48	4.25
23	1.09	0.98	0	0	0	0	45.65	28.66
24	1.09	0.98	300	5	300	-300	62.63	24.42
25	1.09	0.98	300	100	140	-47	24.42	9.55
26	1.09	0.98	350	100	1000	-1000	62.63	27.6
27	1.09	0.96	30	8	300	-300	35.03	9.55
28	1.08	0.94	0	0	0	0	32.91	18.05
29	1.08	0.93	0	0	0	0	27	11
30	1.06	0.98	0	0	0	0	20	23
31	1.09	0.94	300	8	300	-300	37	10
32	1.08	0.97	100	25	42	-14	37	23

33	1.04	0.96	0	0	0	0	18	7
34	1.08	0.97	30	8	24	-8	16	8
35	1.08	0.96	0	0	0	0	53	22
36	1.08	0.96	100	25	24	-8	28	10
37	1.09	0.98	0	0	0	0	34	0
38	1.04	0.95	0	0	0	0	20	11
39	1.09	0.93	0	0	0	0	87	30
40	1.09	0.93	30	8	300	-300	17	4
41	1.09	0.93	0	0	0	0	17	8
42	1.09	0.92	30	8	300	-300	18	5
43	1.06	0.96	0	0	0	0	23	11
44	1.06	0.97	0	0	0	0	113	32
45	1.06	0.98	0	0	0	0	63	22
46	1.09	0.98	100	25	100	-100	84	18
47	1.09	0.98	0	0	0	0	12	3
48	1.09	0.98	0	0	0	0	12	3
49	1.09	0.98	250	50	210	-85	277	113
50	1.09	0.99	0	0	0	0	78	3
51	1.07	0.97	0	0	0	0	77	14
52	1.06	0.97	0	0	0	0	39	18
53	1.06	0.96	0	0	0	0	28	7
54	1.09	0.97	0	0	0	0	66	20
55	1.09	0.97	0	0	0	0	68	27
56	1.09	0.97	250	50	300	-300	47	11
57	1.08	0.98	100	25	23	-8	68	36
58	1.07	0.97	100	25	15	-8	61	28
59	1.09	0.98	0	0	0	0	71	26
60	1.09	0.99	0	0	0	0	39	32
61	1.09	0.99	200	50	300	-100	130	26
62	1.09	0.98	100	25	20	-20	54	27

63	1.06	0.96	0	0	0	0	20	10
64	1.07	0.98	0	0	0	0	11	7
65	1.07	0.98	420	100	200	-67	24	15
66	1.09	0.98	420	100	200	-67	21	10
67	1.09	0.98	0	0	0	0	48	10
68	1.08	0.98	0	0	0	0	78	42
69	1.09	0.98	300	80	99999	-99999	65	10
70	1.06	0.98	80	30	32	-10	12	7
71	1.06	0.99	0	0	0	0	30	16
72	1.09	0.99	30	10	100	-100	42	31
73	1.06	0.99	30	5	100	-100	38	15
74	1.03	0.93	20	5	9	-6	15	9
75	1.04	0.94	0	0	0	0	34	8
76	1.02	0.93	100	25	23	-8	37	18
77	1.08	0.98	100	25	70	-20	22	15
78	1.07	0.99	0	0	0	0	5	3
79	1.07	0.99	0	0	0	0	23	16
80	1.09	0.99	300	150	280	-165	38	25
81	1.07	0.98	0	0	0	0	31	26
82	1.09	0.98	100	25	9900	-9900	43	16
83	1.07	0.99	0	0	0	0	28	12
84	1.03	0.96	0	0	0	0	2	1
85	1.02	0.96	30	10	23	-8	8	3
86	0.96	0.93	0	0	0	0	39	30
87	1.09	0.98	300	100	1000	-100	25	13
88	1.06	0.98	0	0	0	0	8.49	3.18
89	1.09	0.98	200	50	300	-210	23.35	7.43
90	1.09	0.98	20	8	300	-300	21.23	8.49
91	1.09	0.98	50	20	100	-100	33	15
92	1.09	0.98	300	100	9	-3	54.14	8.66

93	1.08	0.98	0	0	0	0	21.23	9.55
94	1.07	0.98	0	0	0	0	41.4	10.62
95	1.05	0.98	0	0	0	0	31.85	12.74
96	1.07	0.98	0	0	0	0	55.2	23.35
97	1.08	0.98	0	0	0	0	20.17	2.12
98	1.08	0.98	0	0	0	0	74.31	24.42
99	1.09	0.98	300	100	100	-100	49.89	10.62
100	1.09	0.98	300	100	155	-50	36.09	16.99
101	1.08	0.98	0	0	0	0	14.86	1.06
102	1.09	0.98	0	0	0	0	95.54	31.85
103	1.09	0.98	20	8	40	-15	26.54	10.62
104	1.08	0.99	100	25	23	-8	11.68	3.18
105	1.08	0.98	100	25	23	-8	63.69	36.09
106	1.07	0.96	0	0	0	0	47.77	26.54
107	1.06	0.94	20	8	200	-200	19.11	3.18
108	1.08	0.98	0	0	0	0	14.86	8.49
109	1.08	0.98	0	0	0	0	10.62	5.31
110	1.09	0.97	50	25	23	-8	7.43	3.18
111	1.09	0.97	100	25	1000	-100	65.82	13.8
112	1.09	0.97	100	25	1000	-100	18.05	7.43
113	1.09	0.98	100	25	200	-100	25.48	4.25
114	1.08	0.96	0	0	0	0	45.65	28.66
115	1.08	0.96	0	0	0	0	62.63	24.42
116	1.09	0.98	0	0	0	0	24.42	9.55
117	1.06	0.95	0	0	0	0	62.63	27.6
118	1.03	0.93	0	0	0	0	35.03	9.55

Bus Data for IEEE 57 Bus System

Bus Number	Voltage	Angle	Generation data (MW)	(MVAR)	Load data (MW)	(MVAR)	Generation	
1	1.04	0	146.39	0	55	17	-140	200
2	1.01	0	87.55	0	3	88	-40	50
3	0.99	0	41.97	0	41	21	-40	60
4	0.98	0	89.67	0	75	2	-30	25
5	1.01	0	461.21	0	150	22	-140	200
6	0.98	0	100	0	121	26	-30	9
7	1.02	0	344.95	0	377	24	-150	155
8	1	0	0	0	0	0	0	0
9	1	0	0	0	13	4	0	0
10	1	0	0	0	0	0	0	0
11	1	0	0	0	5	2	0	0
12	1	0	0	0	0	0	0	0
13	1	0	0	0	18	2.3	0	0
14	1	0	0	0	10.5	5.3	0	0
15	1	0	0	0	22	5	0	0
16	1	0	0	0	43	3	0	0
17	1	0	0	0	42	8	0	0
18	1	0	0	0	27.2	9.8	0	0
19	1	0	0	0	3.3	0.6	0	0
20	1	0	0	0	2.3	1	0	0
21	1	0	0	0	0	0	0	0
22	1	0	0	0	0	0	0	0
23	1	0	0	0	6.3	2.1	0	0
24	1	0	0	0	0	0	0	0
25	1	0	0	0	6.3	3.2	0	0
26	1	0	0	0	0	0	0	0
27	1	0	0	0	9.3	0.5	0	0

28	1	0	0	0	4.6	2.3	0	0
29	1	0	0	0	17	2.6	0	0
30	1	0	0	0	3.6	1.8	0	0
31	1	0	0	0	5.8	2.9	0	0
32	1	0	0	0	1.6	0.8	0	0
33	1	0	0	0	3.8	1.9	0	0
34	1	0	0	0	0	0	0	0
35	1	0	0	0	6.0	3	0	0
36	1	0	0	0	0	0	0	0
37	1	0	0	0	0	0	0	0
38	1	0	0	0	14	7	0	0
39	1	0	0	0	0	0	0	0
40	1	0	0	0	0	0	0	0
41	1	0	0	0	6.3	3	0	0
42	1	0	0	0	7.1	4	0	0
43	1	0	0	0	2	1	0	0
44	1	0	0	0	12	1.8	0	0
45	1	0	0	0	0	0	0	0
46	1	0	0	0	0	0	0	0
47	1	0	0	0	29.7	11.6	0	0
48	1	0	0	0	0	0	0	0
49	1	0	0	0	18	8.5	0	0
50	1	0	0	0	21	10.5	0	0
51	1	0	0	0	18	5.3	0	0
52	1	0	0	0	4.9	2.2	0	0
53	1	0	0	0	20	10	0	0
54	1	0	0	0	4.1	1.4	0	0
55	1	0	0	0	6.8	3.4	0	0
56	1	0	0	0	7.6	2.2	0	0
57	1	0	0	0	6.7	2.0	0	0

Line Data for IEEE 57 Bus System

Start Bus	End Bus	R(pu)	X(pu)	B/2	Line Limit	Start Bus	End Bus	R(pu)	X(pu)	B/2	Line Limit
1	2	0.0083	0.0280	0.0645	150	10	29	0.0	0.0648	0.0	100
2	3	0.0298	0.0850	0.0409	85	25	30	0.1350	0.2020	0.0	100
3	8	0.0112	0.0366	0.0190	100	30	31	0.3260	0.4970	0.0	100
8	9	0.0625	0.132	0.0129	100	31	32	0.5070	0.7550	0.0	100
8	4	0.0430	0.148	0.0174	50	32	33	0.0392	0.0360	0.0	100
4	10	0.0200	0.102	0.0138	40	34	32	0.0	0.9530	0.0	100
4	5	0.0339	0.173	0.0235	100	34	35	0.0520	0.0780	0.0016	100
5	6	0.0099	0.050	0.0274	200	35	36	0.0430	0.0537	0.0008	100
6	11	0.0369	0.167	0.0220	50	36	37	0.0290	0.0366	0.0	100
6	12	0.0258	0.0848	0.0109	50	37	38	0.0300	0.1009	0.0010	100
6	7	0.0648	0.0295	0.0386	50	37	39	0.0192	0.0379	0.0	100
6	13	0.0481	0.158	0.0203	50	36	40	0.0	0.0466	0.0	100
13	14	0.0132	0.0434	0.0055	50	22	38	0.2070	0.0295	0.0	100
13	15	0.0269	0.0869	0.0115	100	12	41	0.0	0.7490	0.0	100
1	15	0.0178	0.0910	0.0494	200	41	42	0.0289	0.3520	0.0	100
1	16	0.0454	0.2060	0.0273	100	41	43	0.0	0.4120	0.0	100
1	17	0.0238	0.1080	0.0143	100	38	44	0.0	0.0585	0.0010	100
3	15	0.0162	0.0530	0.0272	100	15	45	0.0230	0.1042	0.0	100
8	18	0.0	0.5550	0.0	100	14	46	0.0182	0.0735	0.0	100
8	18	0.0	0.4300	0.0	100	46	47	0.0834	0.0680	0.0016	100
9	4	0.0302	0.0641	0.0062	100	47	48	0.0801	0.0233	0.0	100
10	5	0.0139	0.0712	0.0097	100	48	49	0.1386	0.1290	0.0024	100
11	7	0.0277	0.1262	0.0164	100	49	50	0.0	0.1280	0.0	100
12	13	0.0223	0.0732	0.0094	100	50	51	0.0	0.2200	0.0	100
7	13	0.0178	0.0580	0.0302	100	11	51	0.1442	0.0712	0.0	100
7	16	0.0180	0.0813	0.0108	100	13	49	0.0762	0.1910	0.0	100
7	17	0.0397	0.1790	0.0238	100	29	52	0.1878	0.1870	0.0	100

14	15	0.0171	0.0547	0.0074	100	52	53	0.1732	0.0984	0.0	100
18	19	0.4610	0.6850	0.0	100	53	54	0.0 0	0.2320	0.0	100
19	20	0.2830	0.4340	0.0	100	54	55	0.0624	0.2265	0.0	100
21	20	0.0	0.7767	0.0	100	12	43	0.0	0.1530	0.0	100
21	22	0.0736	0.1170	0.0	100	44	45	0.5530	0.1242	0.0020	100
22	23	0.0099	0.0152	0.0	100	40	56	0.2125	1.1950	0.0	100
23	24	0.1660	0.2560	0.0042	100	56	41	0.0	0.5490	0.0	100
24	25	0.0	1.23	0.0	100	56	42	0.1740	0.3540	0.0	100
24	25	0.0	1.1820	0.0	100	39	57	0.1150	1.3550	0.0	100
24	26	0.0	0.4300	0.0	100	57	56	0.0312	0.2600	0.0	100
26	27	0.1650	0.2540	0.0	100	38	49	0.0 0	0.1770	0.003	100
27	28	0.0618	0.0954	0.0	100	38	48	0.0	0.0482	0.0	100
28	29	0.0418	0.0587	0.0	100	6	55	0.0	0.1205	0.0	100

Appendix A2

Details of incremented and decremented power bids submitted by individual generators for IEEE 30 bus, IEEE57 bus and IEEE 118 bus systems have been listed in table A21, Table A22 and Table A23 respectively.

Table A21: Price bids submitted by GENCOs for IEEE 30 bus system

Generator Bus Number (i)	**Price bids submitted by GENCO**	
	Incremented $C_{g_i}^{+}$ ($/MWh)	**Decremented $C_{g_i}^{-}$ ($/MWh)**
1	22	18
2	21	19
3	42	38
4	43	37
5	43	35
6	41	39

Table A22: Price bids submitted by GENCOs for IEEE 57 bus system

Generator Bus Number (i)	**Price bids submitted by GENCO**	
	Incremented $C_{g_i}^{+}$ ($/MWh)	**Decremented $C_{g_i}^{-}$ ($/MWh)**
1	44	41
2	43	39
3	42	38
6	43	37
8	42	39
9	44	40
12	44	41

Table A23: Price bids submitted by GENCOs for IEEE 118 bus system

Generator Bus	**Price bids submitted by GENCO**	**Generator Bus**	**Price bids submitted by GENCO**

Number (i)	**Incremented** $C_{g_i}^{+}$ **($/MWh)**	**Decremented** $C_{g_i}^{-}$ **($/MWh)**	**Number**	**Incremented** $C_{g_i}^{+}$ **($/MWh)**	**Decremented** $C_{g_i}^{-}$ **($/MWh)**
1	40	38	65	25	17
4	43	35	66	26	18
6	41	38	69	28	15
8	44	39	70	43	39
10	22	17	72	47	38
12	23	18	73	44	36
15	45	35	74	43	39
18	41	38	76	44	36
19	44	36	77	47	38
24	45	35	80	23	15
25	27	18	85	43	39
26	23	18	87	25	17
27	41	39	89	44	36
31	45	35	90	42	38
32	24	18	91	41	38
34	43	37	92	44	36
36	44	36	99	43	37
40	43	35	100	42	36
42	47	38	103	24	17
46	45	35	104	44	38
49	25	18	105	43	39
54	32	30	107	42	38
55	42	36	110	43	37
56	43	37	111	22	18
59	23	17	112	42	38
61	26	16	113	47	33
62	24	36	116	45	35

Bibliography

Indu Batra: Born in Ambala city, Haryana, India on 5th May, 1981. She did her B. Tech in Electrical Engineering, from Jind Institute of Engineering and Technology, affiliated to Kurukshetra Universtity, Kurukshetra in 2003. She did M. Tech in Power Engineering from Baba Banda Singh Bahadur Engineering College, affiliated to Punjab Technical University, Jalandhar, India in 2011. She is presently pursuing Ph.D from Thapar Institute of Engineering and Technology, Patiala on regular basis. Her research areas include power system analysis, modern power system optimization, and soft computation techniques towards optimal congestion management in deregulated power system. She has above 12 year of academic and research experience.

Contact email: indu.batra@thapar.edu
Contact email: indubatra5@gmail.com

Smarajit Ghosh: Born in Ghatal, West Bengal, India on 16 August, 1967. He did his B. Tech. and M. Tech. in Electrical Machines and Power Systems from Calcutta University in 1994 and 1996 respectively. He pursued his Ph.D. from Indian Institute of Technology, Kharagpur, India in 2000. His research areas include load flow study, network reconfigurations, optimum capacitor allocation, application of soft computing in Electrical Power Distribution Systems, data-security. He has already served REC (Durgapur), BITS Pilani and Sikkim Manipal University, as a lecturer, Assistant Professor and Professor respectively. He has authored a number of books published by Prentice Hall of India Private Limited and Pearson Education as a single author.

Smarajit Ghosh is presently serving as a Professor at Thapar Institute of Engineering and Technology (Deemed to be University), Patiala in Department of Electrical and Instrumentation Engineering from 2007.

Contact email: sghosh@thapar.edu
Contact email: smarajitg@hotmail.com